

Brownian dynamics of active and passive anisotropic colloidal particles

INAUGURAL-DISSERTATION

zur Erlangung des Doktorgrades der
Mathematisch-Naturwissenschaftlichen Fakultät der
Heinrich-Heine-Universität Düsseldorf

vorgelegt von

Raphael Wittkowski
aus Düsseldorf

Düsseldorf, Dezember 2011

Aus dem Institut für Theoretische Physik II (Weiche Materie)
der Heinrich-Heine-Universität Düsseldorf

Gedruckt mit der Genehmigung der
Mathematisch-Naturwissenschaftlichen Fakultät der
Heinrich-Heine-Universität Düsseldorf

Referent: Prof. Dr. rer. nat. Hartmut Löwen
1. Korreferent: Prof. Dr. rer. nat. Helmut Brand
2. Korreferent: Prof. Dr. rer. nat. Holger Stark

Tag der mündlichen Prüfung: 27. März 2012

Vorwort

Die vorliegende Arbeit entstand im Zeitraum von Herbst 2010 bis Ende 2011 am Institut für Theoretische Physik II (Weiche Materie) der Heinrich-Heine-Universität Düsseldorf. Ein Teil der in dieser Arbeit vorgestellten Ergebnisse wurde bereits in den Artikeln [WLB10, AWL11, HWL11, WL11, WLB11a, WLB11b, WL12] veröffentlicht. Im Einzelnen basieren die Kapitel in dieser Arbeit wie folgt auf bereits veröffentlichten oder zur Veröffentlichung bestimmten Artikeln:

Kapitel 2:

- Raphael Wittkowski und Hartmut Löwen:
Dynamical density functional theory for colloidal particles with arbitrary shape.
Molecular Physics **109**, 2935-2943 (2011)

Kapitel 3:

- Borge ten Hagen, Raphael Wittkowski und Hartmut Löwen:
Brownian dynamics of a self-propelled particle in shear flow.
Physical Review E **84**, 031105 (2011)
- Raphael Wittkowski und Hartmut Löwen:
Self-propelled Brownian spinning top: dynamics of a biaxial swimmer at low Reynolds numbers.
Physical Review E **85**, 021406 (2012)

Kapitel 4:

- Raphael Wittkowski und Hartmut Löwen:
Dynamical density functional theory for colloidal particles with arbitrary shape.
Molecular Physics **109**, 2935-2943 (2011)

Kapitel 5:

- Cristian Vasile Achim, Raphael Wittkowski und Hartmut Löwen:
Stability of liquid crystalline phases in the phase-field-crystal model.
Physical Review E **83**, 061712 (2011)
- Raphael Wittkowski, Hartmut Löwen und Helmut Rainer Brand:
Polar liquid crystals in two spatial dimensions: the bridge from microscopic to macroscopic modeling.
Physical Review E **83**, 061706 (2011)

- Raphael Wittkowski, Hartmut Löwen und Helmut Rainer Brand:
Microscopic and macroscopic theories for the dynamics of polar liquid crystals.
Physical Review E **84**, 041708 (2011)
- Heike Emmerich, Hartmut Löwen, Raphael Wittkowski, Thomas Gruhn, Gyula I. Tóth, György Tegze und László Gránásy:
Phase-field-crystal models for condensed matter dynamics on atomic length and diffusive time scales: an overview.
Advances in Physics (in Vorbereitung)

Auf Grundlage dieser Arbeit sind zurzeit noch weitere Projekte in Arbeit. Diese betreffen flüssigkristalline Phasen auf gekrümmten zweidimensionalen Riemannschen Mannigfaltigkeiten, Phasenfeldkristall-Modelle in beschränkter Geometrie und das in Unterkapitel 4.3 angegebene Dissipationsfunktional der dynamischen Dichtefunktionaltheorie.

Danksagung

An dieser Stelle danke ich allen, die mich im Zusammenhang mit dieser Arbeit über das übliche Maß hinaus unterstützt haben. Als erstes und mit besonderem Ausdruck danke ich deshalb meinem Betreuer Herrn Prof. Dr. Hartmut Löwen, der mir die Möglichkeit gegeben hat, an seinem Lehrstuhl an einigen interessanten Projekten zu arbeiten, und der mich in der gesamten Zeit hervorragend betreut hat.

Ebenso danke ich Herrn Prof. Dr. Helmut Brand für die lange und überaus produktive Zusammenarbeit. Aus seinen sehr ausführlichen Antworten auf diverse Fragen meinerseits habe ich viel gelernt. Zusammen mit meinem Betreuer hat er entscheidend zum schnellen Erfolg meiner Promotion beigetragen.

Abschließend danke ich den Mitarbeitern des Instituts für Theoretische Physik II der Heinrich-Heine-Universität Düsseldorf für hilfreiche Diskussionen. Dies sind insbesondere Borge ten Hagen, Andreas Härtel, Dr. Andreas Menzel, Tim Neuhaus, Dr. Michael Schmiedeberg, Joachim Wenk und Dr. Henricus Wensink.

Kurzfassung

Die Beschreibung der statischen Eigenschaften und des dynamischen Verhaltens von Vielteilchensystemen gehört zu den ältesten Problemen der theoretischen Physik. Dieses sehr allgemeine Problem tritt in unterschiedlicher Gestalt in fast allen Bereichen der Physik auf. In der vorliegenden Arbeit werden einzelne Spezialfälle dieses Problems aus dem Bereich der Physik der weichen kondensierten Materie untersucht. Diese Spezialfälle betreffen die Brownsche Dynamik wechselwirkender anisotroper kolloidaler Teilchen und schließen sowohl passive Teilchen (kolloidale Flüssigkristalle) als auch aktive Teilchen (selbstangetriebene Mikroschwimmer) ein.

Der Hauptteil dieser Arbeit besteht aus drei Kapiteln. Im ersten Kapitel wird die Brownsche Dynamik eines einzelnen aktiven kolloidalen Teilchens mit beliebiger Form untersucht. Zunächst wird die dazugehörige Langevin-Gleichung aufgestellt. Anschließend werden für einige interessante Spezialfälle dieser Gleichung analytische Lösungen hergeleitet. Für allgemeinere und nicht analytisch lösbare Fälle werden numerische Lösungen präsentiert. Der Einfluss einer Scherströmung auf die Bewegung des aktiven Teilchens wird anhand des analytisch lösbaren Spezialfalls eines aktiven kugelförmigen Teilchens in einer ebenen Couette-Strömung diskutiert.

Das zweite Kapitel geht auf die kollektive Dynamik eines Systems wechselwirkender kolloidaler Teilchen mit beliebiger Form ein. Ausgehend von der entsprechenden Smoluchowski-Gleichung wird die klassische dynamische Dichtefunktionaltheorie auf den Fall beliebig geformter aktiver oder passiver kolloidaler Teilchen verallgemeinert. Es wird gezeigt, dass diese neue verallgemeinerte dynamische Dichtefunktionaltheorie auch als Variationsproblem für ein Dissipationsfunktional formuliert werden kann. Diese alternative Formulierung der dynamischen Dichtefunktionaltheorie ermöglicht es, die dynamischen Gleichungen von Phasenfeldkristall-Modellen mit mehreren Ordnungsparameterfeldern einfacher und sehr viel schneller herzuleiten, als dies mit der bisherigen Formulierung der dynamischen Dichtefunktionaltheorie möglich ist. Die neue Darstellung mithilfe eines Dissipationsfunktionals schafft darüber hinaus eine Grundlage für die Interpretation der dynamischen Dichtefunktionaltheorie im Rahmen der linear irreversiblen Thermodynamik.

Im dritten Kapitel werden schließlich die Statik und die Dynamik kolloidaler Flüssigkristalle mit Hilfe mikroskopischer, mesoskopischer und makroskopischer klassischer Molekularfeldtheorien beschrieben. Aus der statischen und dynamischen Dichtefunktionaltheorie (mikroskopisch) werden Phasenfeldkristall-Modelle (mesoskopisch) für a-polare und polare kolloidale Flüssigkristalle im zwei- und dreidimensionalen Raum hergeleitet. Diese werden anschließend mit statischen und dynamischen symmetriebasierten Modellen (makroskopisch) auf Grundlage der klassischen Ginzburg-Landau-Theorie und der verallgemeinerten Hydrodynamik verglichen.

Die in dieser Arbeit erzielten Resultate können unter anderem auf kolloidale Flüssigkristalle angewendet werden, um deren Gleichgewichtsphasendiagramm zu untersuchen. Sie können aber auch zur Beschreibung der dissipativen Dynamik von Flüssigkristall-Phasenübergängen und topologischen Defekten in flüssigkristallinen Phasen sowie zur Untersuchung des Schwarmverhaltens künstlicher Mikroschwimmer und lebender Mikroorganismen verwendet werden. Die Ergebnisse dieser Arbeit sind auch von grundlegender Bedeutung und helfen zum Beispiel beim Verständnis der Zusammenhänge zwischen klassischer Dichtefunktionaltheorie, Phasenfeldkristall-Modellen und symmetriebasierten makroskopischen Modellen.

Abstract

The proper description of the static equilibrium properties and the dynamic behavior of many-particle systems is one of the oldest problems in theoretical physics. This very general problem is highly relevant for most fields of physics. In the present work, several aspects in the context of this problem are investigated. These aspects concern the Brownian dynamics of interacting anisotropic colloidal particles that can be passive (colloidal liquid crystals) or active (self-propelled microswimmers).

The main part of this work is subdivided into three chapters. In the first chapter, the Brownian dynamics of an individual active colloidal particle with arbitrary shape is investigated. After the formulation of the corresponding Langevin equation, analytical solutions for some special cases are derived and numerical solutions for more general situations are presented. Taking the example of a spherical colloidal particle, the effect of an imposed shear flow is discussed also. The second chapter considers the collective dynamics of a large set of interacting active colloidal particles with arbitrary shape. Starting from the appropriate many-particle Smoluchowski equation, classical dynamical density functional theory is generalized to arbitrarily shaped active or passive colloidal particles. It is proved that this new and generalized dynamical density functional theory can be reformulated in terms of the variational optimization of a dissipation functional. This alternative representation of dynamical density functional theory allows an easier and much faster derivation of the dynamic equations of phase field crystal models with various order-parameter fields than the traditional formulation of dynamical density functional theory. The reformulation with a dissipation functional additionally establishes a basis for the interpretation of dynamical density functional theory out of linear irreversible thermodynamics. The third chapter finally treats the statics and dynamics of colloidal liquid crystals by means of microscopic, mesoscopic, and macroscopic classical mean-field theories. Using static and dynamical density functional theory (microscopic), phase field crystal models (mesoscopic) for apolar and polar colloidal liquid crystals in two and three spatial dimensions are derived and compared with static and dynamic symmetry-based approaches (macroscopic) on the basis of classical Ginzburg-Landau theory and generalized hydrodynamics.

The results obtained in this work can, for example, be applied to colloidal liquid crystals in order to explore their equilibrium phase diagram and phase transition dynamics as well as to the dissipative dynamics of topological defects in liquid crystalline phases and to artificial microswimmers or living microorganisms in order to describe their non-equilibrium swarming behavior. The results are also of more fundamental interest, since they help to clarify the relationship between classical density functional theory, phase field crystal models, and symmetry-based macroscopic approaches.

Contents

Vorwort	v
Danksagung	vii
Kurzfassung	ix
Abstract	xi
1 Introduction	1
2 Active and passive soft matter	7
2.1 Geometric classification of rigid colloidal particles	7
2.2 Active colloidal particles in nature and science	10
3 Individual dynamics of an active colloidal particle	13
3.1 Langevin equations for active colloidal particles	13
3.2 LE for an active colloidal particle with arbitrary shape	15
3.2.1 Special analytical solutions of the Langevin equation	18
3.2.1.1 Three spatial dimensions	19
3.2.1.2 Two spatial dimensions	19
3.2.1.3 Orthotropic particles	22
3.2.2 Numerical solutions of the Langevin equation	24
3.2.2.1 Three spatial dimensions	24
3.2.2.2 Two spatial dimensions	26
3.2.2.3 Orthotropic particles	29
3.3 Motion of an active colloidal particle in shear flow	32
3.3.1 Fluctuation-averaged trajectories	33
3.3.1.1 Analytical results for zero temperature	33
3.3.1.2 Analytical results for positive temperature	34
3.3.2 Mean square displacement	36
3.4 Applications and generalized Langevin equations	37
4 Collective dynamics of interacting colloidal particles	39
4.1 Dynamical density functional theory for colloidal particles	39
4.2 DDFT for active colloidal particles with arbitrary shape	41
4.2.1 Smoluchowski equation	42

4.2.2	DDFT equation	45
4.2.3	Special cases	47
4.3	Reformulation of DDFT using a dissipation functional	48
4.4	Applications and further development of DDFT	50
5	Statics and dynamics of colloidal liquid crystals	53
5.1	Classical mean-field theories for the modeling of liquid crystals	53
5.1.1	Density functional theory	57
5.1.1.1	Static density functional theory	58
5.1.1.2	Dynamical density functional theory	62
5.1.2	Phase field crystal models	67
5.1.2.1	Static phase field crystal models	68
5.1.2.2	Dynamic phase field crystal models	73
5.1.3	Ginzburg-Landau theory	75
5.1.3.1	Static Ginzburg-Landau theory	76
5.1.3.2	Dynamic Ginzburg-Landau theory	79
5.1.4	Generalized hydrodynamics	80
5.1.4.1	Generalized hydrostatics	83
5.1.4.2	Generalized hydrodynamics	83
5.2	Derivation of phase field crystal models from DFT	87
5.3	Static phase field crystal models for liquid crystals	87
5.3.1	Two spatial dimensions	90
5.3.1.1	Static free-energy functional	91
5.3.1.2	Special cases of the PFC model	96
5.3.1.3	Equilibrium bulk phase diagram	97
5.3.2	Three spatial dimensions	106
5.3.2.1	Static free-energy functional	106
5.3.2.2	Special cases of the PFC model	109
5.4	Dynamic phase field crystal models for liquid crystals	110
5.4.1	Two spatial dimensions	110
5.4.1.1	Dynamic equations	112
5.4.1.2	Dissipation functional	114
5.4.2	Three spatial dimensions	115
5.5	Comparison with macroscopic models	115
5.5.1	Static macroscopic models	116
5.5.1.1	Static Ginzburg-Landau theory	116
5.5.1.2	Generalized hydrostatics	117
5.5.2	Dynamic macroscopic models	119
5.5.2.1	Dynamic Ginzburg-Landau theory	119
5.5.2.2	Generalized hydrodynamics	120
5.6	Applications and enhanced models	121
6	Summary	123

Appendix	129
A Gradient expansion of a multiple convolution integral	131
B Numerical solution of stochastic differential equations	133
Bibliography	139
Index	171
List of symbols	175

1 Introduction

The precise and suitable description of interacting many-particle systems in their static equilibrium state and with respect to their non-equilibrium dynamics belongs to the oldest problems in theoretical physics and has not been entirely solved up to now. In different manifestations, this very general problem arises in many fields of current physics. Beyond classical physics, the problem appears, for example, as quantum mechanical many-body problem in the theoretical description of Bose-Einstein condensates and superfluids [LL92, WF03]. Also in relativistic systems like hot cosmic plasmas [Som00], a lot of interacting particles have to be described.

In this work, only classical many-particle systems are considered. For these systems the various methods of classical statistical physics [LL08] are available. Furthermore, the considerations in this work are restricted to non-deformable solid *colloidal particles*¹, i. e., particles with a size between 1 nm and 1000 nm, that are suspended in a viscous liquid² and classified as *soft condensed matter* [CL95, BH03], so that molecular fluids [Ach90, LL91b, Bat00] and granular materials [HW04] are excluded. Due to their size, colloidal particles are classical Brownian particles that move under the influence of thermal fluctuations. Their overdamped *Brownian dynamics* is purely dissipative (irreversible), while reversible³ dynamics is not considered throughout this work. Although colloidal particles are clearly larger than atoms and – except for macromolecules – also exceed the size of usual molecules, colloidal systems share many properties with atomic and molecular materials. For example, colloidal particles can constitute *colloidal liquid crystals* that are very similar to molecular liquid crystals [GP95]. Colloidal particles are often used to study fundamental physical phenomena like self-organization, pattern formation, phase transitions, and critical phenomena.

The traditional artificial colloidal particle that is considered in soft condensed matter physics is a spherical, i. e., isotropic, particle [HM06], but with the technological advance in the processing of nanomaterials in the last few years, also *anisotropic* colloidal particles with diverse shapes became producible. Aside from difficulties in the production of anisotropic colloidal particles, their theoretical description is also much more complicated than is the case for isotropic particles, since their interaction depends on their orientation. Depending on the symmetry properties of the colloidal particles

¹The more general term *colloid* includes aside from solid particles also small liquid or gaseous systems, but such colloids with a variable shape are neglected in this work.

²In general, colloidal particles could also be dispersed in a solid, in a gas, and even in a plasma. In the case of a plasma, the colloidal dispersion would be called a *complex* or *dusty plasma* [Bou99].

³An *irreversible* process increases the entropy of a thermodynamic system, while the total entropy remains constant for *reversible* processes.

considered, they have up to three non-trivial orientational degrees of freedom in addition to their three translational degrees of freedom⁴ (see figure 1.1). While *isotropic*

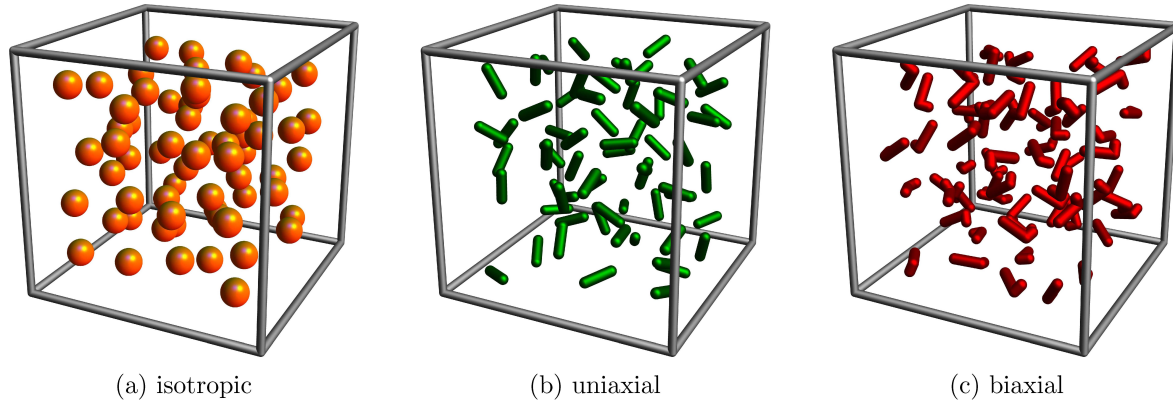


Figure 1.1: (a) Isotropic (spherical) particles are entirely described by their center-of-mass positions \vec{r}_i with $i = 1, \dots, N$, while (b) for uniaxial (rod-like) particles like spherocylinders the direction $\hat{u} = (\sin(\theta) \cos(\phi), \sin(\theta) \sin(\phi), \cos(\theta))$ of their axis of symmetry, where θ and ϕ are the usual polar and azimuthal angles in spherical coordinates, respectively, has to be considered also. (c) In the general case of biaxial or arbitrarily shaped particles, Eulerian angles $\vec{\varpi} = (\phi, \theta, \chi)$ are used to describe their orientations. The plot shows L-shaped particles as an example.

particles have only trivial orientational degrees of freedom⁵, *uniaxial* particles that possess rotational symmetry about a certain axis have two non-trivial orientational degrees of freedom. Colloidal particles without rotational symmetry are called *biaxial* and even have three non-trivial orientational degrees of freedom. To address this problem, the colloidal particles that are considered throughout this work are assumed to be anisotropic⁶, while isotropic particles are always included as a special case.

Colloidal particles appear in very different forms both in nature and in technological processing. Even microorganisms like diatoms, whose silica frustules exhibit multifarious shapes, can be considered as anisotropic colloidal particles. The colloidal particles that are investigated in soft condensed matter physics are usually *passive*, i. e., they move only under the influence of thermal fluctuations and external forces and torques. In recent years, however, *active* colloidal particles that are self-propelled by an internal drive also became the focus of attention in a relatively new subfield of soft condensed matter physics that treats the so-called *active soft matter*. Swimming microorganisms

⁴The non-deformable rigid colloidal particles, that are considered in this work, have only translational and orientational but no additional internal degrees of freedom in contrast to, for example, flexible polymers [DE07].

⁵A sphere has three *rotational* degrees of freedom, but only trivial *orientational* degrees of freedom. Such trivial orientational degrees of freedom are not counted here.

⁶In the context of anisotropy, it is necessary to distinguish between the shape and the interaction of a particle. While, for example, a polarized sphere has an isotropic shape, its interaction with other particles is anisotropic.

are probably the best example for active particles, since their diversity and prevalence are tremendous. Against this, there are only a few technological concepts for artificial microswimmers. Neither the motion of an individual active colloidal particle nor their collective dynamics have been completely investigated up to now. Therefore, this work deals with both active and passive anisotropic colloidal particles.

This work is structured into six chapters. After the general introduction on hand, which constitutes chapter 1, an introduction to active and passive soft matter is given in chapter 2. This chapter contains a classification of technologically producible colloidal particles with respect to their shape and a section about active colloidal particles, where examples for artificial microswimmers and swimming microorganisms are given and their methods of propulsion are discussed.

Chapter 3 investigates the dynamics of an individual active colloidal particle with arbitrary shape. The considerations also include particles with a hydrodynamic translational-rotational coupling [HB91]. For the mathematical description of the stochastic motion of an active colloidal particle under the influence of thermal fluctuations and internal and external forces and torques, a Langevin equation [CKW04] is constructed. In principle, it is also possible to describe the stochastic dynamics equivalently by a Fokker-Planck equation [Ris96] or by a path integral [Gra78, Kle09], but here the usage of a Langevin equation is more convenient, since deterministic trajectories for a vanishing absolute temperature $T = 0$ and mean (fluctuation-averaged) trajectories for $T > 0$ are mainly discussed. The chapter starts with a short section about Langevin equations for active colloidal particles and continues with the formulation of the general Langevin equation for an active colloidal particle with arbitrary shape in a viscous liquid at rest at infinity with a low Reynolds number. From this Langevin equation, some analytical solutions for special cases are derived and discussed. For more general situations, where analytical solutions are not available, numerical solutions are presented.

It turns out that even at $T = 0$ the trajectories of the active colloidal particle in three spatial dimensions are very complicated, thus inhibiting a simple classification. When the motion of the particle is restricted to two spatial dimensions, however, a classification of the noise-free trajectories becomes possible. This classification is discussed for arbitrarily shaped particles as well as for particles with inflection symmetry or rotational symmetry. With respect to the trajectories in three spatial dimensions, a few special cases are investigated. Orthotropic particles⁷ in the absence of thermal fluctuations and external forces and torques are analytically found to move on a circular helix. The noise average of this circular helix is a generalized *conchospiral* for $T > 0$. For colloidal particles with an arbitrary shape at $T = 0$, *superhelical* trajectories are observed when there is no external force. Furthermore, also the effect of an imposed shear flow is discussed by the example of a spherical active colloidal particle in two-dimensional Couette flow.

Chapter 4 considers the collective dynamics of a large set of interacting active colloidal particles with arbitrary shape using *classical dynamical density functional theory* (DDFT), which provides a dynamic equation for the one-particle density field that is

⁷A body is called *orthotropic*, if it possesses three mutually perpendicular planes of symmetry.

proportional to the probability to find a colloidal particle at a certain position with a certain orientation. After a historic overview about the development of DDFT, a generalization of current DDFT is derived from an appropriate many-particle Smoluchowski equation. This generalized DDFT describes active and passive colloidal particles with arbitrary shape. Before that, DDFT was only applicable to spherical and uniaxial particles with no hydrodynamic translational-rotational coupling. The previous versions of DDFT appear as special cases of the new generalization. Furthermore, it is proved that the new and generalized DDFT can be reformulated as a variational optimization problem for a dissipation functional. This alternative representation of DDFT corresponds to the formalism of linear irreversible thermodynamics and allows an easier and much faster derivation of the dynamic equations of phase field crystal models with various order-parameter fields than the traditional formulation of DDFT. The reformulation in terms of a dissipation functional additionally establishes a basis for the interpretation of DDFT out of linear irreversible thermodynamics, where dissipation functionals are used to derive the dynamic equations for irreversible processes.

Thereafter, chapter 5 deals with the statics and dynamics of colloidal liquid crystals composed of uniaxial colloidal particles that are *apolar* or *polar*⁸. When polar particles arrange their orientations collectively, a liquid crystalline phase with a local macroscopic polarization can arise. Such a spontaneous polarization has been observed for banana-shaped bent-core molecules [BCP92] as well as for rod-like molecules in a Langmuir monolayer [TYN⁺03]. To model the statics and dynamics of apolar and polar colloidal liquid crystals in two and three spatial dimensions, microscopic, mesoscopic, and macroscopic *classical mean-field theories* are used. These mean-field theories are either derived from fundamental microscopic equations or with the help of general symmetry considerations and basic laws of thermodynamics. The derivation of a symmetry-based model is usually much faster and can be performed more generally than the corresponding microscopic derivation, but symmetry-based macroscopic theories have the disadvantage that they involve a number of unknown coefficients that cannot be determined within the respective theory. In a microscopically derived model, the same coefficients are by contrast given in terms of microscopic expressions as, for example, generalized moments of a microscopic correlation function.

In the first section of the chapter, an overview on the four classical mean-field theories used is given. The first of these mean-field theories is the microscopic *classical density functional theory* (DFT). Static DFT yields an approximation for the free-energy functional that corresponds to the considered system in terms of the one-particle density field. This free-energy functional is strongly connected with the microscopic n -particle direct correlation functions with $1 \leq n \leq N$. DDFT, on the other hand, provides a dynamic equation for the time-evolution of the one-particle density field. From DFT it is possible to derive mesoscopic *phase field crystal* (PFC) *models* that are a further development of the traditional *phase field* (PF) *models*. Different from PF models, which have a spatially uniform ground state, the equilibrium state of PFC models can be non-uniform and periodic so that these models are more appropriate for the mod-

⁸A colloidal particle is called *polar*, if it has no head-tail symmetry, and *apolar* otherwise.

eling of crystallization processes. Both PF and PFC models consist of an expansion of the free-energy density in terms of relevant order-parameter fields and their gradients. In this gradient expansion, PF models take only second-order derivatives into account, while PFC models achieve stable periodic states through the consideration of gradients up to the fourth order. The dynamic equations for the order-parameter fields in a PFC model can be derived from DDFT. However, it is also possible to derive PFC models on the basis of general symmetry considerations.

Similar symmetry considerations are the basis for the remaining two macroscopic mean-field theories. The first of them is *classical Ginzburg-Landau theory*, which describes the statics of a thermodynamic system in the vicinity of a phase transition by a symmetry-based gradient expansion of a generalized energy density in terms of the order-parameter fields that define the phase transition regarded. Corresponding dynamic equations for the order-parameter fields can be derived from a dissipation functional that is constructed on the basis of symmetry considerations as well. The second macroscopic theory is *generalized hydrodynamics*, which is used to describe a thermodynamic system in the bulk of a phase. Its static variant is termed *generalized hydrostatics* and leads to an expansion of a generalized energy density in terms of hydrodynamic variables and their gradients. If it is necessary, additional slowly relaxing non-hydrodynamic variables can also be taken into account. On the basis of the gradient expansion of the generalized energy density, dynamic equations for the hydrodynamic and slowly relaxing non-hydrodynamic variables can be derived within the framework of *generalized hydrodynamics*.

In the remaining sections of the chapter, microscopic static DFT and DDFT are used to derive mesoscopic static and dynamic PFC models for apolar and polar colloidal liquid crystals in two and three spatial dimensions. In the context of the dynamics, the corresponding dissipation functionals are also derived. Several special cases of the PFC models known from the literature are identified. The PFC models are also compared with static and dynamic symmetry-based approaches on the basis of Ginzburg-Landau theory and of generalized hydrodynamics. Furthermore, some phase diagrams for apolar colloidal liquid crystals in two spatial dimensions are calculated numerically and the arising liquid crystalline phases are discussed. Among the stable liquid crystalline phases are isotropic, nematic, columnar, smectic A, and plastic crystalline phases. The plastic crystals can have triangular, honeycomb, and square lattices. They exhibit orientational patterns with a complex topology involving a sublattice with topological defects. Finally, in chapter 6, a summary and an outlook for this work are given.

In the appendix of this work, two additional sections address special mathematical topics with relevance for the previous chapters in more detail. Appendix A treats gradient expansions of multiple convolution integrals and can be used as formulary for gradient expansions like those that go along with the derivation of PFC models from DFT. This part of the appendix serves as a supplement for chapter 5. In appendix B, numerical methods for the solution of stochastic differential equations are discussed. The necessary background information on stochastic calculus is summarized and a stochastic Runge-Kutta scheme of weak order 2.0 is presented. This stochastic

Runge-Kutta scheme is appropriate for the simultaneous numerical solution of coupled stochastic differential equations and is applied to the nonlinear Langevin equations in chapter 3 in order to solve them numerically.

2 Active and passive soft matter

Soft matter includes a huge set of different types of colloidal particles that can be characterized by their shape, size, and mechanical and chemical properties. All these colloidal particles can be distinguished into two basic classes. The first one contains *passive particles* that move only as a consequence of external forces and torques. This so-called *passive soft matter* includes particles made out of various materials and non-motile living microorganisms. Suspensions of passive anisotropic colloidal particles constitute colloidal liquid crystals and can exhibit various liquid crystalline phases¹.

All particles that are self-propelled by an internal propulsion mechanism are called *active particles* instead and constitute *active soft matter*, which is the complementary class to passive soft matter. Active particles are wide-spread in nature, since all motile microorganisms belong to this class, but there are also several realizations of artificial active particles. In recent years, different strategies have been developed to produce colloidal particles with a constant internal drive. Therefore, active particles can be further distinguished with respect to the type of their self-propulsion mechanism.

The shape of both active and passive colloidal particles can be arbitrary. It is already possible to produce colloidal particles with a very complicated shape. To give an overview about the different shapes that can be realized, section 2.1 classifies these shapes and presents examples. Of course, the shape of a colloidal particle can also be variable. This is the case for particles that are made out of a deformable material. Especially living microorganisms such as, for example, amoebae are able to change their shape and for some of them modulations of their shape are the origin of their drive. Such deformable colloidal particles, however, are not considered in this work. After the geometric classification, section 2.2 treats active colloidal particles in more detail.

2.1 Geometric classification of rigid colloidal particles

Induced by technological advance in the processing of nanomaterials, a large number of differently shaped colloidal particles have become synthetizable during recent years. The different shapes of these colloidal particles can be classified by means of their geometric properties. Figure 2.1 on page 9 shows a detailed classification of colloidal shapes with respect to symmetry and convexity. Such a classification is of big importance, since anisotropic colloidal particles may form a huge set of mesotropic phases

¹For example, suspensions of the tobacco-mosaic virus have already been known since 1936 to exhibit liquid crystalline order [BPBF36].

(mesophases) [Cha92, Boy08] that result from different states of translational and orientational order. The possible states of translational and orientational order depend strongly on the shapes of the particles. Therefore, a classification of their shapes is also a classification of the possible phases that these particles may exhibit.

The most simple and at once completely symmetric, i. e., *isotropic*, shape is the sphere. This is the traditional shape for colloidal particles in soft matter physics, because it is simple to produce and due to a lack of non-trivial orientational degrees of freedom it is relatively simple to describe theoretically. Since spheres possess only (non-trivial) translational degrees of freedom, they solely appear in the completely disordered isotropic phase and in the crystalline state [HM06]. The shape of a sphere is globally convex and there is no non-convex analog with full symmetry. All other colloidal particle shapes are *anisotropic* and either uniaxial or biaxial. The characteristic property of *uniaxial* particles is an axis of symmetry, whose orientation is denoted by the unit vector \hat{u} below. These particles have rotational symmetry and possess one non-trivial orientational degree of freedom in two spatial dimensions and two non-trivial orientational degrees of freedom in three spatial dimensions. Uniaxial particles are further distinguished into apolar and polar particles. A uniaxial particle is called *apolar*, if it has head-tail symmetry, and polar otherwise. Rod-like particles [RDP⁺04, HAN⁺06] like spherocylinders and spheroids are uniaxial and the most simple anisotropic colloidal particles. They are convex and apolar and of big importance, since they may evolve the industrially important nematic phase and serve as excellent model systems for many liquid crystals [WDCK90, THT09, LLRC10].

A further member of convex and apolar particles are the platelets [WLP98, BHD05, BRS⁺06, BDW⁺08, LHMS10]. Their phase diagram is similar to the one of rod-like particles with a strong affinity to form columnar stacks [MPVL10]. Systems of such disk-like particles are realized in nature, for example, by clay suspensions [DHM95, MDL⁺95, DHM97]. Examples for non-convex apolar particles are dumbbells (dimers) [JKB05, MD08, DJK⁺10], which are produced by mergence of two spheres of equal size, and rings [YLW⁺06, Tha08], which can be made by etching from colloidal spheres that are partially embedded in a metal layer. The complement of apolar particles is built by the *polar* particles that have no head-tail symmetry. A famous member of this particle class are the Janus particles [HCLG06, HCS⁺08, WM08]. They are spheres with a different coating on one half of the surface. The original Janus particles had a hydrophilic and a hydrophobic coating. Nowadays, one coating is often reactive like a platinic coating that decomposes hydrogen peroxide catalytically. Such particles are immersed into a hydrogen peroxide solution to realize active particles (microswimmers) that are driven by an intrinsic drive [PCYB10]. Cones are a further member of uniaxial polar particles. Carbon nanocones appear naturally in graphite [KDT⁺97, JRDG03, NEHK09] and do not need to be produced by an elaborate method.

By the mergence of two spheres with different diameters, one obtains a pear-like particle [KBEP06, HJL⁺09]. Pears and also bowls [JIC⁺07, MKD⁺10] are non-convex particles that are uniaxial and polar. The latter particles often stack into each other and form columnar structures [MD10].



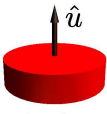
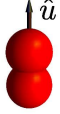

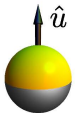
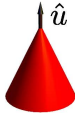

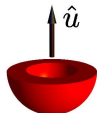










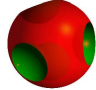

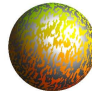
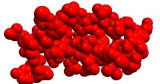
	symmetry	convex particles	non-convex particles			
isotropic	full symmetry	 spheres				
anisotropic	rotational symmetry around axis \hat{u}	apolar  rods	 platelets	 dumbbells	 rings	
		polar  Janus particles	 cones	 pears	 bowls	
	discrete rotational or inflection symmetry	 cubes	 tetrahedra	 trimers	 chiral particles special colloidal molecules	
		 boards	 pyramides	 tetrapods	 octapods multipods	 stars
		 regular patchy particles		 lock-and-key particles		
	no symmetry	 irregular patchy particles		 general colloidal molecules		

Figure 2.1: Classification of synthesizable colloidal particles with respect to their shape. Geometric properties used to classify the different shapes are symmetry and convexity.

Particles with less symmetry are *biaxial*. They are the complement to the uniaxial particles in the class of the anisotropic particles. Biaxial particles have either only discrete symmetries, like discrete rotational symmetry and inflection symmetry, or are completely asymmetric. In both cases, the biaxial particles have three orientational degrees of freedom² and a unit vector is no longer sufficient to describe their orientation. Instead, two perpendicular unit vectors or Eulerian angles have to be used [DE07]. Due to the additional orientational degree of freedom, the phase diagrams of biaxial colloidal particles are much richer than those for uniaxial particles [SLW10]. Convex colloidal particles with discrete rotational or inflection symmetry are, for example, polyhedra like cubes [CM97, MC99, ZLX⁺06, SGM08] and tetrahedra [YW97, HEK⁺09], boards [PPT⁺09], pyramids [GKC04, Hel05, FTO08], and regular patchy particles [ZG04, BLT⁺06, CYK⁺07, Sci08]. The latter differ from Janus particles by a patchy coating with a regular, for example, tetrahedral, arrangement.

Non-convex particles with discrete rotational symmetry or inflection symmetry include special colloidal molecules that are realized by more than two spheres merged in a regular arrangement. Examples for such colloidal molecules include trimers [LS03] consisting of three equal spheres and chiral particles [ZBP⁺08, WJ09] consisting of many equal spheres in a helical arrangement. Further non-convex particles with discrete rotational symmetry are multipod-shaped nanocrystals [NW07, DMD⁺10], stars [ZLX⁺06, WCH09], and some lock-and-key particles [SICP10]. Patchy particles may also belong to the class of colloidal particles without any kind of symmetry. This is the case, if the patches are arranged or sized in an irregular way. Irregular patchy particles made by coating of spherical particles are always convex. Colloidal molecules with arbitrary shape and size belong on the other hand to the completely asymmetric non-convex colloidal particles [MEP03, QZR⁺08, KVK⁺09, SZO⁺10].

2.2 Active colloidal particles in nature and science

Active colloidal particles are the constituents of *active soft matter*³ and a rather new field of interest in soft condensed matter physics. They are small self-propelled particles that move under the influence of internal, external, hydrodynamic, and random forces and torques through a viscous liquid. External forces and torques can, for example, result from external electromagnetic or gravitational fields, while hydrodynamic forces and torques are caused by the liquid flow around the particle, and random forces and torques are always present for $T > 0$ due to thermal fluctuations, with the internal forces and torques as the special feature of active particles in contrast to passive particles. These internal forces and torques are caused by internal self-propulsion mechanisms of the active colloidal particles. Due to their small size, active colloidal particles

²In two spatial dimensions, anisotropic particles have always only one orientational degree of freedom and are uniaxial. Biaxial particles do no more exist in two spatial dimensions than triaxial particles in three spatial dimensions.

³The more general term *active matter* includes also self-propelled macroscopic objects such as, for example, shoals of fish.

move at low Reynolds numbers, where inertia is unimportant and the dynamics is overdamped and Brownian. At low Reynolds numbers, the liquid flow around the colloidal particle is kinematically reversible and described by the quasistationary creeping-flow equations [HB91], which are invariant against time reversal. This has an important consequence for the kind, in which these particles propel themselves. To generate a directed force or torque with a non-vanishing time-average, the propulsion mechanism must break time reversal symmetry [Pur77, Sta07]. This is realized in a variety of ways for natural and artificial active particles. In nature, active colloidal particles appear in the form of swimming microorganisms, but they can also be produced artificially. Both swimming microorganisms and artificial microswimmers use a couple of very different techniques for propulsion [MK06, EZB⁺08, LP09]. Nevertheless, in theoretical descriptions of the dynamics of an active particle, it is often possible to neglect the details of the propulsion mechanism and to model it simply by a force and a torque that are permanently connected with the particle⁴. Up to a certain extent, it is also possible to model a deformable colloidal swimmer, which changes its shape for propulsion, as rigid non-deformable particle with a particular internal force and torque.

Swimming microorganisms include various procaryotic and eucaryotic motile cells such as protozoa and many bacteria and use different techniques for swimming. Their mechanisms for locomotion contain protoplasmic flow, deformations of the shape involving traveling waves, cilia, and flagella [JV72]. Protoplasmic flow is especially used by amoebae for locomotion and goes along with strong shape deformations, but it does not allow high velocities. An example for a microorganism that swims fast through deformations of its shape in combination with a flagellum is the parasitic protozoon *Trypanosoma brucei*, which causes the African sleeping sickness⁵ (*African trypanosomiasis*). Flagella are also used by the rod-shaped bacterium *Bacillus subtilis*, which is heavily flagellated and can move fast in liquids, and by the green alga *Chlamydomonas reinhardtii*, that has two flagella and is known for its ability to resist external torques. In a shear flow, it retains its orientation [RJP10, Sta10] and swims constantly upward in the gravitational field of the earth. This phenomenon is also called *negative gravitaxis*. Very different is the drive of the harmless protozoon *Paramecium aurelia* that is studded by a large number of cilia. More details on swimming microorganisms and their locomotion can be found in reference [LP09].

The variety of artificial microswimmers is much smaller, since there are not so many different strategies for their realization. For the construction of an artificial microswimmer two problems have to be solved. At first, one needs a suitable self-propulsion mechanism [EZB⁺08, EH10], and secondly, the microswimmer has to be supplied with energy. Propulsion mechanisms for artificial microswimmers were at first discussed by Purcell in 1977 [Pur77, Sta07]. Like the three-sphere swimmer in reference [DZ09], such microswimmers change their shapes in a non-reciprocal way in order to generate

⁴Of course, a swimmer is in principle force-free and torque-free [Dho96], but the internal forces and torques are meant to be effective quantities, which govern the propulsion mechanism of the particle.

⁵For a short review, see reference [KJM04]. A theoretical modeling of the dynamics of trypanosomes and a comparison with experimental observations are presented in reference [ZUP⁺11].

a net motion [Sta07]. Alternative concepts are the propulsion by electroosmotic flow [LPB96], magnetically actuated cilia [DS09, GDS09], the magnetically driven artificial flagellum [DBR⁺05], and flexible ferromagnetic swimmers that are exposed to an alternating magnetic field [BC09]. For the latter microswimmers, the necessary breaking of time reversal symmetry is achieved by the buckling instability.

A similar idea are colloidal rotors that are composed of paramagnetic colloidal particles in a suitable time-dependent magnetic field [TGPS08]. Simpler and for the realization of a dense suspension of active particles more appropriate are catalytically driven particles. Such particles are partly coated with a chemically reactive layer as, for example, Janus particles and swim in a suitable chemical reactive medium. The chemically reactive coating can be made out of platinum. When a particle like this is immersed in a hydrogen peroxide solution, the platinum acts as catalyst and cleaves the hydrogen peroxide into water and oxygen. The pressure of the released oxygen drives the microswimmers [PKO⁺04, DFW⁺06]. Also nanorotors [QBX⁺07] can be driven catalytically.

However, catalytically driven particles have the drawback that the hydrogen peroxide is gradually used up with time and has to be replaced. But for active suspensions with a high concentration of active particles, it is not possible to exchange the hydrogen peroxide without disturbing the small microswimmers. In this respect, different concepts for the energy supply based on microwave radiation or light are better. One of these ideas is that of Volpe et al. [VBV⁺11], who use Janus particles with a half gold covering. These Janus particles swim due to self-diffusiophoresis in a critical binary liquid mixture when they are illuminated, since the incident light heats one of the two caps of the Janus particles and this causes a local asymmetric demixing of the binary mixture. Further examples for artificial microswimmers can be found in references [LP09, EH10, Ram10].

While active particles move, they dissipate energy so that they are always out of thermodynamic equilibrium. This dissipative non-equilibrium dynamics of active particles is very interesting and includes individual and collective motion. The collective dynamics [KS11] of active particles is complex and the rheological behavior [HRRS04] of active particle suspensions is different from passive suspensions both in bulk and in confinement [PDO09]. Among the observable effects of collective motion are self-organization with pattern formation [SS08], clustering [WL08], flocking [TTR05], swarming [WL08, EG09], laning, turbulence, and jamming [PDB06, LGG⁺09]. Furthermore, some instabilities can be investigated in active suspensions. Although active particles have been studied in experiments [HJR⁺07], by simulation [GS06, CFM⁺08, OO09, KS11], and theoretically [MRR07, TL08, HTL09, TZL09, ZUP⁺11], there are still many open questions. Furthermore, the dynamics of active particles is not only interesting with respect to biology and for fundamental theoretical reasons. It is also relevant for medicine, since parasitic motile protozoa and bacteria are the cause for many serious diseases such as, for example, the *African trypanosomiasis*, *leishmaniasis*, and *salmonellosis*. There are technological applications as well, like the enhancing of fluid mixing [KB04] in industrial processes.

3 Individual dynamics of an active colloidal particle

In this chapter, the dynamics of an individual active colloidal particle is considered. After an introductory section about Langevin equations for active colloidal particles in previous work, the Langevin equation for an active colloidal particle with arbitrary shape is presented and analytical solutions for various special cases are discussed. The very complicated trajectories of the general Langevin equation are investigated numerically. In a further section of this chapter, the influence of shear flow on the motion of an active colloidal particle is also addressed. Applications of the obtained results and possible generalizations are discussed at the end of this chapter.

3.1 Langevin equations for active colloidal particles

Langevin equations [CKW04] are stochastic differential equations that describe the time evolution of slowly changing variables in a thermodynamic system with a large number of fast fluctuating microscopic variables that influence the time evolution of the slow variables. Such slowly changing variables are, for example, position, orientation, momentum, and angular momentum of a colloidal particle in a viscous liquid. In this example, the quickly changing microscopic variables characterize the liquid molecules and relax much faster to local thermodynamic equilibrium than the few slow variables of the colloidal particle. If several colloidal particles have to be described simultaneously, especially the densities of conserved quantities like momentum density and energy density are variables that relax slowly to local thermodynamic equilibrium.

Such a *separation of time scales* between a few slow and many fast relaxing variables is an important and justified assumption in the statistical description of colloidal particles and allows the consideration of the thermodynamic system on the large time scale of the slow variables, where the many microscopic degrees of freedom do not have to be described directly. For the overdamped Brownian motion of a colloidal particle there is a further separation of times scales between the position and orientation of the colloidal particle on the one hand and its momentum and angular momentum on the other hand. The dynamics can therefore also be described on a still larger time scale, where the inertia of the colloidal particle is unimportant and the Langevin equation¹ does not depend on momentum and angular momentum, but only on position and orientation of the colloidal particle.

¹In the case of an overdamped Brownian particle, the corresponding Fokker-Planck equation is independent of momentum variables and often called a *Smoluchowski equation*.

Langevin equations consist of two contributions that describe the slow variables directly and model the influence of the fast variables on the dynamics of the slow variables, respectively. The first contribution is deterministic and describes the time evolution of the undisturbed slow variables. With the second contribution, which is a stochastic noise term, all microscopic variables are taken into account and their influence on the dynamic equations of the slow variables is modeled. The stochastic noise can usually be assumed to be Gaussian and white, since the microscopic variables are locally in thermodynamic equilibrium on the time scale of the slow variables. The construction of a Langevin equation is one possibility of three equivalent ways to describe stochastic processes. In general, the stochastic dynamics can alternatively also be described by a Fokker-Planck equation [Ris96] or by a path integral² [Gra78, Kle09]. While a Langevin equation describes particular realizations of the stochastic time evolution of the slow variables, the other methods involve deterministic equations for these variables. A Fokker-Planck equation describes the probability for the variables to attain certain values at a certain time and path integral methods assign a probability to each possible realization for the time evolution of the slow variables. All these three methods have different advantages and disadvantages, but for the description of the trajectories of individual Brownian particles in this chapter, Langevin equations are most convenient.

Historically, the first Langevin equation was proposed by Langevin in 1908 [Lan08] and describes the Brownian motion of a passive spherical colloidal particle under the influence of thermal fluctuations. In this chapter, a much more complicated Langevin equation is presented. On the one hand, it takes not only spherical but generally arbitrarily shaped colloidal particles into account, and on the other hand, the colloidal particles are assumed to be active. While the theory of the Brownian dynamics of spherical and uniaxial colloidal particles is quite advanced [Dho96], much less is known for biaxial particles, since their additional non-trivial degrees of freedom complicate the description of Brownian motion considerably [CFW04]. Very general Langevin equations that respect also biaxial particles have been studied in references [FT02, MD04], but these references take only passive colloidal particles into account. For active particles, there have been only a few studies yet and they prefer to describe colloidal particles with a simple symmetric shape. A few years ago, it was shown by van Teeffelen and Löwen that the simultaneous action of an internal force and an internal torque on a colloidal particle in two spatial dimensions leads to circle-swimming [TL08]. The considerations in this reference were carried out for rod-like particles and later supplemented with numerical solutions³ in a confined system [TZL09]. About the same time, the Langevin equations for a spherical active particle in a linear channel, that restricts the particle to one spatial and one orientational degree of freedom, were discussed [HTL09]. Recently, the Brownian motion of spherical and rod-like active particles in two and three spatial dimensions was also addressed using Langevin equations [ES11, HTL11].

²To avoid mistaking the term *path integral* with the vector analytic path integrals, the alternative name *functional integral* is often used.

³See appendix B for numerical methods for the solution of stochastic differential equations.

In the following, the Langevin equation for the much more general case of an active colloidal particle with arbitrary shape, that moves in three spatial dimensions under the influence of internal, external, hydrodynamic, and random forces and torques, is formulated and discussed. While the internal forces and torques control the translational and angular propulsion velocity of the particle and are constant in a body-fixed frame, the external forces and torques are constant in a space-fixed laboratory frame. The consideration of arbitrary shapes includes all biaxial particles and also particles with a hydrodynamic translational-rotational coupling [Bre65, Bre67] as, for example, screw-like particles. This is important for many applications, since real active particles are in general biaxial. Furthermore, the effect of shear flow is discussed. While the equations of motion for passive anisotropic particles in a flowing liquid have already been known since the 1920s [Jef22], active Brownian particles were at this time not considered at all. Nevertheless, the flow field of the liquid has a big influence on the dynamics of an active colloidal particle and there are many situations in which it cannot be neglected. Especially swimming microorganisms in natural systems frequently live in flowing water.

3.2 Langevin equation for an active colloidal particle with arbitrary shape

The Langevin equation for the Brownian motion of an active biaxial particle suspended in an unbounded viscous liquid at rest at infinity can be derived using low Reynolds number hydrodynamics [HB91]. It is assumed that the colloidal particle is rigid and that it has a constant mass density. The motion of such a particle is characterized by the translational center-of-mass velocity $\vec{r}(t) = d\vec{r}/dt$ with the center-of-mass position $\vec{r}(t)$ and the time variable t as well as by the instantaneous angular velocity $\vec{\omega}(t)$. The Brownian motion of colloidal particles with arbitrary shape involves a hydrodynamic coupling between the translational and the rotational degrees of freedom, that was described theoretically, for example, by Brenner [Bre65, Bre67] in the 1960s. In 2002, Fernandes and de la Torre [FT02] proposed a corresponding Brownian dynamics simulation algorithm for the motion of a passive rigid particle with arbitrary shape. The underlying equations of motion have been generalized toward an imposed external flow field for the surrounding liquid by Makino and Doi [MD04] in 2004. Their description is appropriately generalized here toward an active biaxial particle that experiences an internal effective force \vec{F}_0 and torque \vec{T}_0 both of which are constant in a body-fixed coordinate system. Using a compact notation that is explained below, the basic completely overdamped *Langevin equation for three spatial dimensions*

$$\boxed{\vec{v} = \vec{\mathcal{B}}(\vec{r}) + \beta \mathcal{D}(\vec{r}) (\mathcal{R}^{-1}(\vec{r}) \vec{K}_0 - \vec{\nabla}_{\vec{r}} U(\vec{r}) + \mathcal{R}^{-1}(\vec{r}) \vec{k})} \quad (3.1)$$

for an active Brownian particle with arbitrary shape is given here in a rather short form. The biaxial particle has the position $\vec{r}(t) = (x_1, x_2, x_3)$ and the orientation

$\vec{\omega}(t) = (\phi, \theta, \chi)$ given in Eulerian angles⁴. For abbreviation, the translational and orientational degrees of freedom are summarized by a compact 6-dimensional vector $\vec{\mathbf{r}} = (\vec{r}, \vec{\omega})$ that obviously involves a generalized velocity $\vec{\mathbf{v}} = (\dot{\vec{r}}, \dot{\vec{\omega}})$ and a generalized gradient $\vec{\nabla}_{\vec{\mathbf{r}}} = (\vec{\nabla}_{\vec{r}}, \vec{\nabla}_{\vec{\omega}})$. This gradient operator is composed of the usual translational gradient operator $\vec{\nabla}_{\vec{r}} \equiv \partial_{\vec{r}} = (\partial_1, \partial_2, \partial_3)$ acting on the Cartesian coordinates of \vec{r} and of the rotational gradient operator $\vec{\nabla}_{\vec{\omega}} = i\hat{L}$ [GG84] that is given by the product of the imaginary unit i and the angular momentum operator \hat{L} in Eulerian angles⁵. In a space-fixed coordinate system, the rotational gradient operator $\vec{\nabla}_{\vec{\omega}}$ is given by [GG84] $\vec{\nabla}_{\vec{\omega}} = M^{-T}(\vec{\omega})\partial_{\vec{\omega}}$ with the matrix [Sch76]

$$M(\vec{\omega}) = \begin{pmatrix} 0 & -\sin(\phi) & \cos(\phi) \sin(\theta) \\ 0 & \cos(\phi) & \sin(\phi) \sin(\theta) \\ 1 & 0 & \cos(\theta) \end{pmatrix}, \quad (3.2)$$

$$M^{-1}(\vec{\omega}) = \begin{pmatrix} -\cos(\phi) \cot(\theta) & -\sin(\phi) \cot(\theta) & 1 \\ -\sin(\phi) & \cos(\phi) & 0 \\ \cos(\phi) \csc(\theta) & \sin(\phi) \csc(\theta) & 0 \end{pmatrix} \quad (3.3)$$

and the angular derivation operator $\partial_{\vec{\omega}} = (\partial_\phi, \partial_\theta, \partial_\chi)$ acting on the Eulerian angles $\vec{\omega}$. The angular velocity $\dot{\vec{\omega}}(t)$, on the other hand, can be expressed as $\dot{\vec{\omega}} = M(\vec{\omega})\dot{\vec{\omega}}$ with the time derivative $\dot{\vec{\omega}}(t) = d\vec{\omega}/dt$ of the Eulerian angles $\vec{\omega}(t)$. Furthermore, in equation (3.1) the compact notation $\vec{K}_0 = (\vec{F}_0, \vec{T}_0)$ for the generalized propulsion force \vec{K}_0 is used. It combines the effective propulsion force \vec{F}_0 and torque \vec{T}_0 . In general, the biaxial particle is exposed to an external potential $U(\vec{\mathbf{r}})$ giving rise to an external force $\vec{F}_{\text{ext}} = -\vec{\nabla}_{\vec{r}}U$ and an external torque $\vec{T}_{\text{ext}} = -\vec{\nabla}_{\vec{\omega}}U$ that are both considered to be constant in the sequel in order to keep the model simple. The 6×6 -dimensional rotation matrix $\mathcal{R}^{-1}(\vec{\mathbf{r}})$ in equation (3.1) is associated with the geometric transformation from the body-fixed frame to the space-fixed laboratory frame. Its inverse $\mathcal{R}(\vec{\mathbf{r}})$ is the block diagonal rotation matrix

$$\mathcal{R}(\vec{\mathbf{r}}) = \text{diag}(\mathbf{R}(\vec{\omega}), \mathbf{R}(\vec{\omega})) \quad (3.4)$$

with the rotation submatrices

$$\begin{aligned} \mathbf{R}(\vec{\omega}) &= \mathbf{R}_3(\chi) \mathbf{R}_2(\theta) \mathbf{R}_3(\phi), \\ \mathbf{R}^{-1}(\vec{\omega}) &= \mathbf{R}^T(\vec{\omega}) = \mathbf{R}_3(-\phi) \mathbf{R}_2(-\theta) \mathbf{R}_3(-\chi), \end{aligned} \quad (3.5)$$

⁴Alternatively, the orientation of the particle could also be described by means of two perpendicular axes [CFW04], but here the use of Eulerian angles is more appropriate, since they do not involve additional geometric constraints and lead to simpler equations with a more compact notation.

⁵As there is no uniqueness in the definitions of the Eulerian angles $\vec{\omega} = (\phi, \theta, \chi)$, the popular convention of Gray and Gubbins [GG84], which is equivalent to the second convention of Schutte [Sch76], is used for convenience. This convention has the advantage that it is a direct generalization of the spherical coordinates (θ, ϕ) that are identical with the first two Eulerian angles ϕ and θ , while the third angle χ describes the rotation around the axis, which is defined by the polar angle θ and the azimuthal angle ϕ in the spherical coordinate system [GG84].

where the elementary rotation matrices $R_i(\varphi)$ describe a clockwise rotation (when looking down the axes) around the i th Cartesian axis by the angle φ for $i \in \{1, 2, 3\}$:

$$R_1(\varphi) = \begin{pmatrix} 1 & 0 & 0 \\ 0 & \cos(\varphi) & \sin(\varphi) \\ 0 & -\sin(\varphi) & \cos(\varphi) \end{pmatrix}, \quad (3.6)$$

$$R_2(\varphi) = \begin{pmatrix} \cos(\varphi) & 0 & -\sin(\varphi) \\ 0 & 1 & 0 \\ \sin(\varphi) & 0 & \cos(\varphi) \end{pmatrix}, \quad (3.7)$$

$$R_3(\varphi) = \begin{pmatrix} \cos(\varphi) & \sin(\varphi) & 0 \\ -\sin(\varphi) & \cos(\varphi) & 0 \\ 0 & 0 & 1 \end{pmatrix}. \quad (3.8)$$

The particle shape and its hydrodynamic properties enter the Langevin equation in the symmetric⁶ generalized short-time diffusion tensor⁷ $\mathcal{D}(\vec{\mathbf{r}})$. This tensor can be expressed by the 6×6 -dimensional matrix

$$\mathcal{D}(\vec{\mathbf{r}}) = \frac{1}{\beta\eta} \mathcal{R}^{-1}(\vec{\mathbf{r}}) \mathcal{H}^{-1} \mathcal{R}(\vec{\mathbf{r}}) = \begin{pmatrix} \mathbf{D}^{\text{TT}}(\vec{\omega}) & \mathbf{D}^{\text{TR}}(\vec{\omega}) \\ \mathbf{D}^{\text{RT}}(\vec{\omega}) & \mathbf{D}^{\text{RR}}(\vec{\omega}) \end{pmatrix}, \quad (3.9)$$

where $\mathbf{D}^{\text{TT}}(\vec{\omega})$, $\mathbf{D}^{\text{TR}}(\vec{\omega}) = (\mathbf{D}^{\text{RT}}(\vec{\omega}))^{\text{T}}$, and $\mathbf{D}^{\text{RR}}(\vec{\omega})$ are 3×3 -dimensional submatrices that correspond to pure translation, translational-rotational coupling, and pure rotation, respectively⁸. Here, η is the dynamic (shear) viscosity of the embedding liquid and $\beta = 1/(k_{\text{B}}T)$ with the Boltzmann constant k_{B} and the effective⁹ temperature T denotes the inverse thermal energy. The hydrodynamic matrix \mathcal{H} is constant. It only depends on the shape and the size of the Brownian particle and is independent of the viscosity of the liquid. This matrix \mathcal{H} is composed of the symmetric translation tensor \mathbf{K} , the not necessarily symmetric coupling tensor \mathbf{C}_{S} with the reference point¹⁰ S , and the symmetric rotation tensor Ω_{S} [Bre67, HB91]:

$$\mathcal{H} = \begin{pmatrix} \mathbf{K} & \mathbf{C}_{\text{S}}^{\text{T}} \\ \mathbf{C}_{\text{S}} & \Omega_{\text{S}} \end{pmatrix}. \quad (3.10)$$

The Langevin equation (3.1) thus involves altogether 21 shape-dependent parameters. Finally, $\vec{k}(t) = (\vec{f}_0, \vec{\tau}_0)$ summarizes the stochastic force $\vec{f}_0(t)$ and torque $\vec{\tau}_0(t)$ due to

⁶The reciprocity relation $\mathcal{D}(\vec{\mathbf{r}}) = (\mathcal{D}(\vec{\mathbf{r}}))^{\text{T}}$ is a consequence of *Onsager's principle* [LL08].

⁷The tensor $\mathcal{D}(\vec{\mathbf{r}})$ could also be called a *damping tensor* or *inverse friction tensor*.

⁸For experimental investigations of the three-dimensional translational and rotational diffusion of bi-axial colloidal particles, see, for example, references [HWHW09, HEEW11] and references therein.

⁹Since active particles are out of thermodynamic equilibrium, only an *effective* temperature can be assigned to active systems [PCYB10].

¹⁰The coupling tensor \mathbf{C}_{S} becomes symmetric, if one chooses the *center of hydrodynamic reaction* as reference point S [HB91]. In general, the center-of-mass position of the particle should be chosen as reference point.

thermal fluctuations, that act on the Brownian particle, in body-fixed coordinates for $T > 0$. This thermal noise $\vec{k}(t)$ is assumed to be Gaussian white noise with mean

$$\langle \vec{k}(t) \rangle = \vec{0} \quad (3.11)$$

and correlation

$$\langle \vec{k}(t_1) \otimes \vec{k}(t_2) \rangle = \mathcal{H} \frac{2\eta}{\beta} \delta(t_1 - t_2), \quad (3.12)$$

where $\langle \cdot \rangle$ denotes the noise average and \otimes is the dyadic product. Notice that the dynamics that is described by the Langevin equation (3.1) depends on the definition of the stochastic contribution $\propto \vec{k}(t)$. Depending on the particular type of stochastic calculus, that is chosen to handle the multiplicative noise in the Langevin equation, different expressions for the drift term $\vec{\mathcal{B}}(\vec{r})$ in equation (3.1) are appropriate (see appendix B or reference [Ris96] for details). In general, the drift term can be written as [Ris96, CKW04, LL07]

$$\mathcal{B}_i = \frac{1}{2} \mathcal{M}_{ij} \partial_{r_k} (b_{kl} b_{jl}) - \alpha \mathcal{M}_{ij} b_{kl} (\partial_{r_k} b_{jl}) \quad (3.13)$$

with the matrix $\mathcal{M} = \text{diag}(\mathbb{1}, \mathbf{M})$, the derivation operator $\partial_{\vec{r}} = (\partial_{\vec{r}}, \partial_{\vec{\alpha}})$, the expression

$$b_{ik} b_{jk} = 2 \mathcal{M}_{il}^{-1} \mathcal{D}_{lm} \mathcal{M}_{mj}^{-T}, \quad (3.14)$$

and the parameter α . Only if this parameter is chosen properly, the additive drift term $\vec{\mathcal{B}}(\vec{r})$ in the Langevin equation guarantees that the solutions of the Langevin equation respect the Boltzmann distribution, when the internal force and torque vanish and the system is in thermodynamic equilibrium at temperature T . In particular, one has to choose $\alpha = 0$ for the *Itô stochastic calculus*¹¹, $\alpha = 1/2$ for the *Stratonovich stochastic calculus*, and $\alpha = 1$ for the *Klimontovich stochastic calculus*. This circumstance is always relevant in the case of multiplicative noise, but the necessity of the adaptation of the Langevin equation to the type of stochastic calculus has been missed in previous work [FT02, MD04].

3.2.1 Special analytical solutions of the Langevin equation

The Langevin equation (3.1) represents a system of six coupled nonlinear stochastic differential equations [Has07] that cannot be solved analytically in general. There exist only a few analytical solutions for rather special situations. Several simple Langevin equations for active spherical or uniaxial particles in two or three spatial dimensions are known from the literature [TL08, HTL09, HTL11] and are special cases of the general Langevin equation (3.1). They are not as general and complicated as equation (3.1) and can be solved analytically. Other analytically solvable special cases of equation (3.1) are obtained for orthotropic particles in the absence of thermal fluctuations.

¹¹In the following, the Itô stochastic calculus is chosen for convenience.

3.2.1.1 Three spatial dimensions

In the general three-dimensional case, it is not even possible to solve the Langevin equation (3.1) analytically, if the stochastic noise is neglected. Further simplifications that reduce the number of the degrees of freedom or diagonalize the matrix \mathcal{H} are necessary in order to obtain soluble cases.

3.2.1.2 Two spatial dimensions

An obvious simplification of the general Langevin equation (3.1) is the restriction to two spatial dimensions. A two-dimensional analog of the general Langevin equation can be obtained by choosing the values $x_3 = 0$, $\theta = \pi/2$, and $\chi = 0$, leaving only a single azimuthal angle ϕ . In analogy to the notation in reference [TL08], the vectors $\mathcal{R}^{-1}(\vec{\mathbf{x}})\vec{K}_0 = (\vec{F}_A, 0, 0, 0, M)$, $\vec{k}(t) = (0, f_\perp, f_\parallel, -\tau, 0, 0)$, and $\mathcal{R}^{-1}(\vec{\mathbf{x}})\vec{k} = (\vec{f}, 0, 0, 0, \tau)$ with the internal driving force $\vec{F}_A = F_\parallel \hat{u}_\parallel + F_\perp \hat{u}_\perp$ and the internal driving torque M are defined. The orientation vector $\hat{u}_\parallel = (\cos(\phi), \sin(\phi))$ denotes the figure axis of the particle and $\hat{u}_\perp = (-\sin(\phi), \cos(\phi))$ is its orthogonal complement. Similarly, the vector $\vec{f}(t)$ denotes the stochastic force and $\tau(t)$ is the stochastic torque acting on the particle. The stochastic force vector $\vec{f}(t)$ is decomposed like the internal driving force: $\vec{f}(t) = f_\parallel \hat{u}_\parallel + f_\perp \hat{u}_\perp$. Moreover, the new two-dimensional position vector is $\vec{r} = (x_1, x_2)$, the corresponding gradient is $\vec{\nabla}_{\vec{r}} = (\partial_1, \partial_2)$, and the stochastic noise is characterized by the vector $\vec{\xi}(t) = (f_\perp, f_\parallel, -\tau)$ with mean

$$\langle \vec{\xi}(t) \rangle = \vec{0} \quad (3.15)$$

and correlation

$$\langle \vec{\xi}(t_1) \otimes \vec{\xi}(t_2) \rangle = \tilde{\mathcal{H}} \frac{2\eta}{\beta} \delta(t_1 - t_2), \quad (3.16)$$

where $\tilde{\mathcal{H}} = (\mathcal{H}_{ij})_{i,j=2,3,4}$ is a 3×3 -dimensional submatrix of \mathcal{H} . The *Langevin equations for two spatial dimensions* are then given by

$$\begin{aligned} \dot{\vec{r}} &= \vec{B}_T + \beta(D_T(\vec{F}_A - \vec{\nabla}_{\vec{r}}U + \vec{f}) - \vec{D}_C(M - \partial_\phi U + \tau)), \\ \dot{\phi} &= B_R + \beta(D_R(M - \partial_\phi U + \tau) - \vec{D}_C \cdot (\vec{F}_A - \vec{\nabla}_{\vec{r}}U + \vec{f})) \end{aligned} \quad (3.17)$$

with the translational drift vector

$$\vec{B}_T(\phi) = B_T^\parallel \hat{u}_\parallel + B_T^\perp \hat{u}_\perp, \quad (3.18)$$

which is in accordance with the interpretation of the solution of the Langevin equations as an Itô process [KP06], the translational short-time diffusion tensor

$$D_T(\phi) = D_1 \hat{u}_\parallel \otimes \hat{u}_\parallel + D_2 (\hat{u}_\parallel \otimes \hat{u}_\perp + \hat{u}_\perp \otimes \hat{u}_\parallel) + D_3 \hat{u}_\perp \otimes \hat{u}_\perp, \quad (3.19)$$

and the coupling vector

$$\vec{D}_C(\phi) = D_C^{\parallel} \hat{u}_{\parallel} + D_C^{\perp} \hat{u}_{\perp} . \quad (3.20)$$

They involve only 9 instead of 21 shape-dependent parameters. These are the translational drift coefficients

$$B_T^{\parallel} = \frac{1}{\beta\eta} \left((\mathcal{H}^{-1})_{24} - (\mathcal{H}^{-1})_{15} \right) , \quad (3.21)$$

$$B_T^{\perp} = \frac{1}{\beta\eta} \left((\mathcal{H}^{-1})_{16} - (\mathcal{H}^{-1})_{34} \right) , \quad (3.22)$$

the rotational drift coefficient

$$B_R = \frac{1}{\beta\eta} (\mathcal{H}^{-1})_{56} , \quad (3.23)$$

the translational diffusion coefficients

$$D_1 = \frac{1}{\beta\eta} (\mathcal{H}^{-1})_{33} = \frac{1}{\beta\eta} (\tilde{\mathcal{H}}^{-1})_{22} , \quad (3.24)$$

$$D_2 = \frac{1}{\beta\eta} (\mathcal{H}^{-1})_{23} = \frac{1}{\beta\eta} (\tilde{\mathcal{H}}^{-1})_{12} , \quad (3.25)$$

$$D_3 = \frac{1}{\beta\eta} (\mathcal{H}^{-1})_{22} = \frac{1}{\beta\eta} (\tilde{\mathcal{H}}^{-1})_{11} , \quad (3.26)$$

the coupling coefficients

$$D_C^{\parallel} = \frac{1}{\beta\eta} (\mathcal{H}^{-1})_{34} = \frac{1}{\beta\eta} (\tilde{\mathcal{H}}^{-1})_{23} , \quad (3.27)$$

$$D_C^{\perp} = \frac{1}{\beta\eta} (\mathcal{H}^{-1})_{24} = \frac{1}{\beta\eta} (\tilde{\mathcal{H}}^{-1})_{13} , \quad (3.28)$$

and the rotational diffusion coefficient

$$D_R = \frac{1}{\beta\eta} (\mathcal{H}^{-1})_{44} = \frac{1}{\beta\eta} (\tilde{\mathcal{H}}^{-1})_{33} . \quad (3.29)$$

Some of these nine coefficients are zero or equal, respectively, if the described Brownian particle is symmetric. Table 3.1 on the facing page gives an overview over possible symmetries of the shape of a particle and the corresponding properties of the shape-dependent coefficients (3.21)-(3.29).

Although the Langevin equations (3.17) for two spatial dimensions are much simpler than equation (3.1), they are still coupled nonlinear stochastic differential equations and thus not analytically solvable. However, if the external potential $U(\vec{r}, \phi)$ is set to zero, the Langevin equations can be solved analytically and depending on the temperature the center-of-mass trajectory becomes either a circle ($T = 0$) or a logarithmic spiral ($T > 0$) like in reference [TL08].

Table 3.1: Connection between the symmetry of the particle shape and the parameters (3.21)-(3.29) in the Langevin equations (3.17) for two spatial dimensions.

type of shape:	uniaxial	uniaxial	uniaxial	uniaxial	isotropic
symmetries:	no symmetry	inflection symmetry	inflection symmetry	inflection symmetry	rotational symmetry
invariance properties:	—	$x_1 \rightarrow -x_1$	$x_2 \rightarrow -x_2$	$x_1 \rightarrow -x_1,$ $x_2 \rightarrow -x_2$	$\phi \rightarrow \phi + \Delta\phi$ $\forall \Delta\phi \in [0, 2\pi)$
shape-dependent parameters: $D_1 \neq 0,$ $D_R \neq 0$	$B_T^\parallel \neq 0,$ $B_T^\perp \neq 0,$ $B_R \neq 0,$ $D_2 \neq 0,$ $D_3 \neq 0,$ $D_C^\parallel \neq 0,$ $D_C^\perp \neq 0$	$B_T^\parallel = 0,$ $B_T^\perp \neq 0,$ $B_R = 0,$ $D_2 = 0,$ $D_3 \neq 0,$ $D_C^\parallel \neq 0,$ $D_C^\perp = 0$	$B_T^\parallel \neq 0,$ $B_T^\perp = 0,$ $B_R = 0,$ $D_2 = 0,$ $D_3 \neq 0,$ $D_C^\parallel = 0,$ $D_C^\perp \neq 0$	$B_T^\parallel = 0,$ $B_T^\perp = 0,$ $B_R = 0,$ $D_2 = 0,$ $D_3 \neq 0,$ $D_C^\parallel = 0,$ $D_C^\perp = 0$	$B_T^\parallel = 0,$ $B_T^\perp = 0,$ $B_R = 0,$ $D_2 = 0,$ $D_3 = D_1,$ $D_C^\parallel = 0,$ $D_C^\perp = 0$

The analytical solution for $U(\vec{r}, \phi) = f_\parallel = f_\perp = \tau = 0$ is given by

$$\begin{aligned} \vec{r}(t) = \vec{r}_0 + \frac{\beta}{\omega} (F_\parallel D_2 + F_\perp D_3 - MD_C^\perp) (\hat{u}_\parallel(\phi_0 + \omega t) - \hat{u}_\parallel(\phi_0)) \\ - \frac{\beta}{\omega} (F_\parallel D_1 + F_\perp D_2 - MD_C^\parallel) (\hat{u}_\perp(\phi_0 + \omega t) - \hat{u}_\perp(\phi_0)), \end{aligned} \quad (3.30)$$

$$\phi(t) = \phi_0 + \omega t \quad (3.31)$$

with the scalar angular velocity

$$\omega = \beta(MD_R - D_C^\parallel F_\parallel - D_C^\perp F_\perp), \quad (3.32)$$

the initial position $\vec{r}_0 = \vec{r}(0)$, and the initial orientation $\phi_0 = \phi(0)$. If instead of $U(\vec{r}, \phi)$ the translational diffusion coefficient D_2 and the coupling coefficients D_C^\parallel and D_C^\perp vanish, as it is the case for a particle with double inflection symmetry, the Langevin equations (3.17) become similar to the Langevin equations for the Brownian circle swimmer in reference [TL08], but with a more general driving force \vec{F}_A that is not necessarily parallel to the figure axis. For $D_2 = D_C^\parallel = D_C^\perp = F_\perp = 0$, the Langevin equations (3.17) are equivalent to the Langevin equation in reference [TL08]. An additional constraint on spherical particles that are only able to move along the x_1 -axis leads to the Langevin equations for an active spherical particle on a substrate [HTL09]. With similar simplifications it is also possible to obtain the Langevin equations for spherical or uniaxial active particles in two spatial dimensions that are discussed in reference [HTL11] from equations (3.17).

3.2.1.3 Orthotropic particles

Another possibility to simplify the Langevin equation (3.1) considerably is the exclusive consideration of orthotropic particles. All geometric bodies with three pairwise orthogonal planes of symmetry such as spheres, spheroids (ellipsoids of revolution), biaxial ellipsoids, cylinders, cuboids, and some prisms belong to this important class. Orthotropic particles have no translational-rotational coupling so that the coupling tensor C_S vanishes. Furthermore, the translation tensor K and the rotation tensor Ω_S are diagonal for orthotropic particles. These properties of K , C_S , and Ω_S can be derived from the circumstance that the center of mass, which is chosen as reference point S , and the mutual point of intersection of the three planes of symmetry of an orthotropic particle coincide [HB91]. The vanishing of the coupling tensor C_S results from the fact that the point of intersection of the three pairwise perpendicular planes of symmetry of the particle is identical with the *center of hydrodynamic reaction* for orthotropic bodies. With these considerations, the Langevin equation (3.1) simplifies to the *Langevin equations for orthotropic particles*:

$$\begin{aligned}\dot{\vec{r}} &= \beta D^{TT}(\mathbf{R}^{-1}\vec{F}_0 - \vec{\nabla}_{\vec{r}}U + \mathbf{R}^{-1}\vec{k}_T), \\ \dot{\vec{\omega}} &= \vec{B}_R + \beta D^{RR}(\mathbf{R}^{-1}\vec{T}_0 - \vec{\nabla}_{\vec{\omega}}U + \mathbf{R}^{-1}\vec{k}_R).\end{aligned}\quad (3.33)$$

Here, the rotational drift vector \vec{B}_R is defined as the second part of the 6-dimensional drift vector $\vec{B}(\vec{r})$: $\vec{B}_R = (\vec{B}(\vec{r}))_{i=4,5,6}$. Similarly, the Gaussian white noises $\vec{k}_T(t)$ and $\vec{k}_R(t)$ are independent and defined as the first and second part of $\vec{k}(t) = (\vec{k}_T, \vec{k}_R)$, respectively. The Langevin equations for spherical or uniaxial particles, that are considered in reference [HTL11], are special cases of the more general Langevin equations (3.33) for biaxial orthotropic particles. To be able to solve these stochastic differential equations analytically, it is at first necessary to neglect \vec{k}_T and \vec{k}_R , i. e., to consider the case $T = 0$. A further negligence of the drive or the external potential leads to two special cases, which are analytically solvable.

a) Settling orthotropic passive particle

A particle without drive, i. e., with $\vec{F}_0 = \vec{T}_0 = \vec{0}$, at $T = 0$ moves only under the influence of the external potential $U(\vec{r}, \vec{\omega})$. In the case of a constant gravitational field, only the constant external force $\vec{F}_{\text{ext}} = -\vec{\nabla}_{\vec{r}}U$ acts on the particle and the external torque $\vec{T}_{\text{ext}} = -\vec{\nabla}_{\vec{\omega}}U$ vanishes. The motion of such a settling particle is well known from the literature [HB91]. It is characterized by a constant velocity $\dot{\vec{r}}$ and a constant orientation $\vec{\omega} = \vec{\omega}_0 = \vec{\omega}(0)$:

$$\dot{\vec{r}} = \beta D^{TT}(\vec{\omega}_0)\vec{F}_{\text{ext}} = \text{const.}, \quad \vec{\omega} = \vec{\omega}_0 = \text{const.}\quad (3.34)$$

b) Orthotropic active particle

If the external potential $U(\vec{r}, \vec{\omega})$ is neglected instead of the drive in equations (3.33) for $T = 0$, they describe the helical motion of an arbitrary orthotropic active particle

in the absence of external and random forces and torques:

$$\dot{\vec{r}} = \mathbf{R}^{-1}(\vec{\omega}) \mathbf{K}^{-1} \frac{1}{\eta} \vec{F}_0, \quad \dot{\vec{\omega}} = \mathbf{R}^{-1}(\vec{\omega}) \Omega_S^{-1} \frac{1}{\eta} \vec{T}_0. \quad (3.35)$$

These equations of motion are trivial in the body-fixed coordinate system, where the velocities $\dot{\vec{r}}$ and $\dot{\vec{\omega}}$ are constant. Since the angular velocity $\vec{\omega}$ is constant in body-fixed coordinates, it is also constant in the space-fixed system. This means that one expects a helix for the center-of-mass trajectory as it is known from the motion of protozoa like *Euglena gracilis* [JV72] and bacteria like *Thiovulum majus* [SJ01]. The analytical solution of equations (3.35) is in fact the circular helix

$$\vec{r}(t) = \vec{r}_0 + \frac{(\vec{\omega} \times \vec{v}_0) \times \vec{\omega}}{\|\vec{\omega}\|^3} \sin(\|\vec{\omega}\|t) + \frac{\vec{\omega} \times \vec{v}_0}{\|\vec{\omega}\|^2} (1 - \cos(\|\vec{\omega}\|t)) + \frac{\vec{\omega} \cdot \vec{v}_0}{\|\vec{\omega}\|^2} \vec{\omega} t \quad (3.36)$$

with axis

$$\mathbb{A} = \vec{r}_0 + \frac{\vec{\omega} \times \vec{v}_0}{\|\vec{\omega}\|^2} + \vec{\omega} \mathbb{R}, \quad (3.37)$$

radius

$$r = \frac{\|(\mathbf{K}^{-1} \vec{F}_0) \times (\Omega_S^{-1} \vec{T}_0)\|}{\eta^2 \|\vec{\omega}\|^2}, \quad (3.38)$$

and pitch

$$h = 2\pi \frac{|(\mathbf{K}^{-1} \vec{F}_0) \cdot (\Omega_S^{-1} \vec{T}_0)|}{\eta^2 \|\vec{\omega}\|^2}, \quad (3.39)$$

where $\vec{r}_0 = \vec{r}(0)$ is the initial position, $\vec{v}_0 = \dot{\vec{r}}(0) = \mathbf{R}^{-1}(\vec{\omega}_0) \mathbf{K}^{-1} \vec{F}_0 / \eta$ is the initial velocity, and $\|\vec{\omega}\| = \|\Omega_S^{-1} \vec{T}_0 / \eta\|$ is the modulus of the angular velocity. This helical trajectory is shown schematically in figure 3.1. When a constant gravitational field

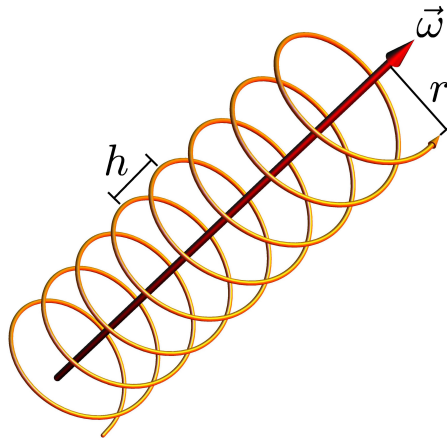


Figure 3.1: The center-of-mass trajectory of an orthotropic particle for a constant external potential and $T = 0$ is a circular helix with radius r and pitch h that evolves from the rotation of the orthotropic particle with the constant angular velocity $\vec{\omega}$.

is also taken into account, the helix becomes deformed and, for example, its cross section might become elliptic, but the axis of the helix remains a straight line. In the case $T > 0$, where the stochastic contributions in the Langevin equations (3.33) have to be considered, it is, however, no longer possible to find analytical solutions. This case requires the usage of appropriate numerical integrators for stochastic differential equations and is studied in the next section.

3.2.2 Numerical solutions of the Langevin equation

In general situations, where analytical solutions do not exist, the Langevin equation (3.1) can only be investigated with the help of numerical methods. Appropriate numerical methods in increasing order of the truncation error are the Euler-Maruyama method, the Milstein method, and stochastic Runge-Kutta methods [KP06], which have to be derived in the Itô sense in order to be compatible with the Itô stochastic calculus that has been chosen for the Langevin equations in this chapter (see appendix B for further information). If there are no thermal fluctuations ($T = 0$), the stochastic Langevin equation (3.1) becomes deterministic and a standard Runge-Kutta scheme of high order can be applied. The numerical results for $T = 0$ and $T > 0$ that are presented in what follows have been obtained by an explicit fourth-order deterministic Runge-Kutta scheme [AS72, PTVF92, AW05, But08] and by a multi-dimensional explicit stochastic Runge-Kutta scheme of weak order 2.0 for Itô stochastic differential equations [KP06], respectively. During the whole section, \vec{F}_0 , \vec{T}_0 , $\vec{F}_{\text{ext}} = -\vec{\nabla}_{\vec{r}}U$, and $\vec{T}_{\text{ext}} = -\vec{\nabla}_{\vec{\omega}}U$ are assumed to be constant vectors that do not depend on \vec{r} or $\vec{\omega}$. Furthermore, arbitrary Brownian particles with a hydrodynamic translational-rotational coupling and orthotropic particles without a translational-rotational coupling in two and three spatial dimensions are considered for $T = 0$ and $T > 0$. Parallel to the previous section, this section is divided into a first subsection about the general Langevin equation for three spatial dimensions, a second subsection about two spatial dimensions, and a third subsection about orthotropic particles.

3.2.2.1 Three spatial dimensions

For arbitrarily shaped particles in three spatial dimensions, various differently shaped trajectories are found as solutions of the Langevin equation (3.1). Figure 3.2 on the facing page gives a selection of typical trajectories that can be observed for arbitrarily shaped particles with an arbitrary drive at $T = 0$. In order to sample some typical solutions, random values have been chosen for the 21 shape-dependent parameters in the matrix \mathcal{H} , for the elements of the internal force \vec{F}_0 and torque \vec{T}_0 , for the elements of the external force \vec{F}_{ext} and torque \vec{T}_{ext} , and for the initial conditions. Altogether more than 100 random parameter combinations were considered. In doing so, four different cases with vanishing and non-vanishing vectors for \vec{F}_{ext} and \vec{T}_{ext} were distinguished (see figure 3.2 on the next page). Depending on the choice of \vec{F}_{ext} and \vec{T}_{ext} , the observed trajectories appeared to share common features and to be distinguishable into four

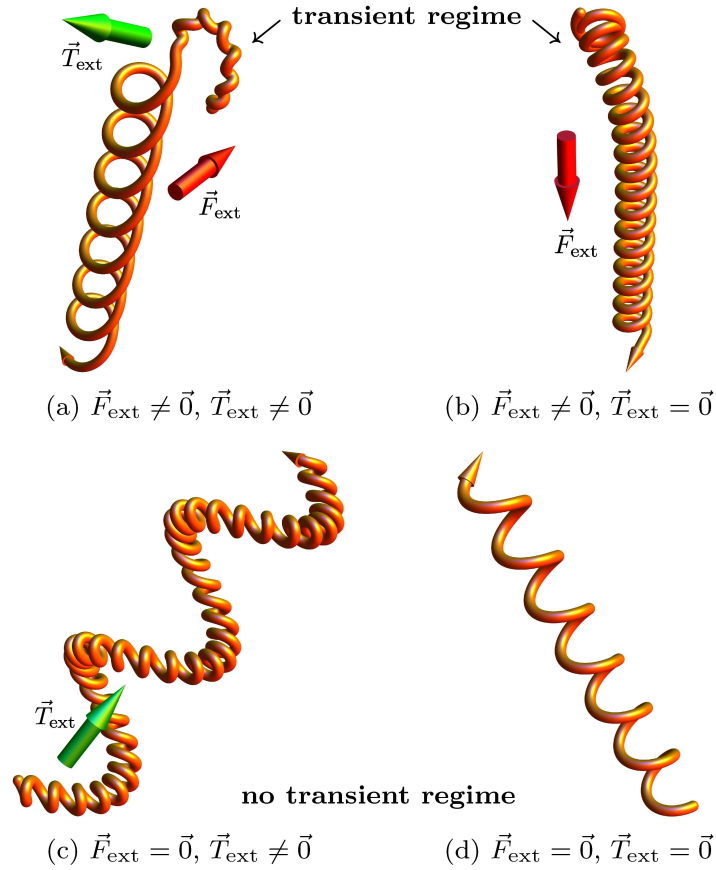


Figure 3.2: Typical trajectories of arbitrarily shaped active particles in three spatial dimensions for constant vectors $\vec{F}_0 \neq \vec{0}$, $\vec{T}_0 \neq \vec{0}$ and temperature $T = 0$ (schematic). The external force $\vec{F}_{\text{ext}} = -\vec{\nabla}_{\vec{r}}U$ and torque $\vec{T}_{\text{ext}} = -\vec{\nabla}_{\vec{\omega}}U$ are constant, too. For a non-vanishing external force, the particle's center-of-mass trajectory starts with an irregular transient regime and changes into a periodic motion, as it is shown in plots (a) and (b). The general periodic motion (a) that is observed, if there is also a non-vanishing external torque, reduces to a circular helix (b) parallel to the external force, if there is no external torque. The other two plots (c) and (d) show the situation for a vanishing external force, where a transient regime is not observed. There, the trajectory is either a *superhelix*-like curve (c) parallel to a non-vanishing external torque or a circular helix (d), if there is no external torque. However, the trajectories (a)-(c) can also be irregular. Straight trajectories, that are preceded by a transient regime for $\vec{F}_{\text{ext}} \neq \vec{0}$, can be observed, too.

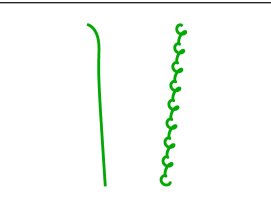
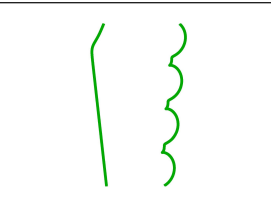
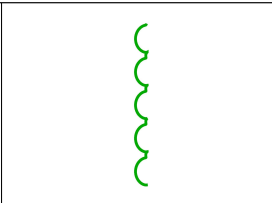
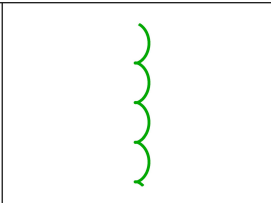
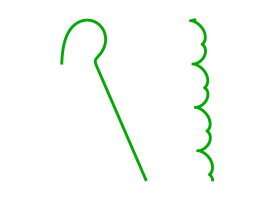

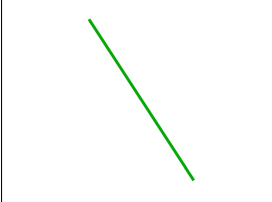
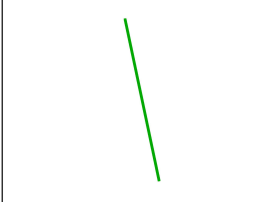
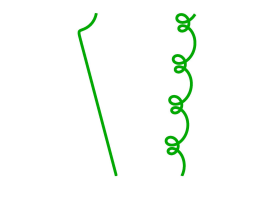
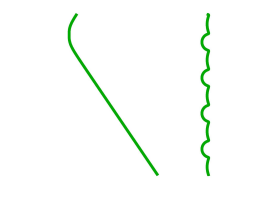

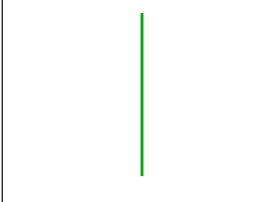
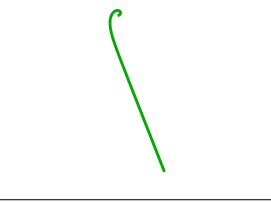
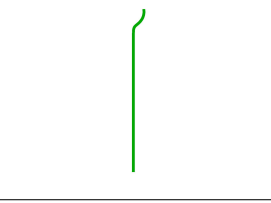
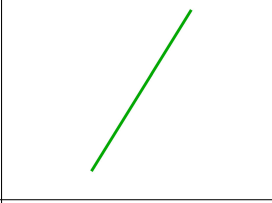
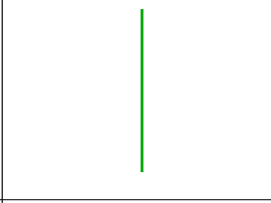
different classes. The four trajectories, that are shown in figure 3.2 on the preceding page, are representatives of these classes. They can be characterized as follows: if there are both an external force and an external torque, active particles that start with an irregular transient regime and end up in a simple periodic center-of-mass trajectory are usually observed [see figure 3.2(a)]. Notice that the length of the initial transient regime as well as the periodicity length of the final periodic motion depend on the particular parameters and can become rather big. In the case of no external torque, the periodic motion after the transient regime is a circular helix with its axis being parallel to the direction of the external force vector. This situation is illustrated in figure 3.2(b). The analogous case of an external torque but no external force is schematically shown in figure 3.2(c). There, a *superhelix*-like curve with the orientation parallel to the direction of the external torque vector and without a preceding transient regime is observed. In contrast to the trajectory in figure 3.2(a), the complicated superhelix-like curve does not turn into a simpler periodic curve after some time, since there is no transient regime for $\vec{F}_{\text{ext}} = \vec{0}$. As the fourth case, the motion in the absence of both external forces and torques is shown in figure 3.2(d). It appears to be a circular helix. Also in this case, a transient regime is not observed. In the situation of plots 3.2(a) and 3.2(b), completely irregular trajectories can appear, when the transient regime is very long. Even in the transient-free situation of figure 3.2(c), irregular trajectories are observed, when the rotational frequency ratio between the immanent rotation of the active particle and the rotation due to the external torque is irrational. Furthermore, straight trajectories appear as a special case. They are preceded by a transient regime, if $\vec{F}_{\text{ext}} \neq \vec{0}$. A complete and detailed classification of all trajectories that can be observed in three spatial dimensions is, however, not possible, since the number of the parameters defining the shape of the particle and all further relevant quantities like internal and external forces and torques is quite big. This number is much smaller, however, in two spatial dimensions, where a more detailed classification is possible.

3.2.2.2 Two spatial dimensions

The Langevin equations (3.17) for two spatial dimensions were solved analytically in section 3.2.1.2 for $U(\vec{r}, \phi) = 0$ and $T = 0$. Here, the case $T = 0$ is considered, too, but now for a constant non-vanishing external force $\vec{F}_{\text{ext}} = -\vec{\nabla}_{\vec{r}}U$, since this external force leads to various different non-trivial trajectories. The observed trajectories are classified with respect to the shape and the kind of self-propulsion of the particle in table 3.2 on page 28. Since the drift coefficients B_{T}^{\parallel} , B_{T}^{\perp} , and B_{R} can be neglected for $T = 0$, the shape of the particle is only described with the six parameters D_1 , D_2 , D_3 , D_{C}^{\parallel} , D_{C}^{\perp} , and D_{R} , where D_1 and D_{R} can be set to one by a suitable rescaling of the length and time scales. For the remaining parameters, particles with a translational-rotational coupling and particles without a translational-rotational coupling as well as asymmetric particles, particles with one axis of symmetry, particles with two mutually perpendicular axes of symmetry, and isotropic particles with rotational symmetry are distinguished. Moreover, the constant parameters F_{\parallel} , F_{\perp} , and $M_{\text{eff}} = M - \partial_{\phi}U$ are used to describe

the self-propulsion of the particle. Four situations of a non-vanishing internal force \vec{F}_A and torque M , a drive only by either an internal force or an internal torque, and a passive particle with a vanishing drive are considered. A further distinction with respect to the external force and torque is not necessary, because the external force can always be chosen to be bigger than zero, since the case of a vanishing external force has been proved to lead to a trivial circular trajectory in section 3.2.1.2, and the external torque $-\partial_\phi U$ is already included in the effective torque M_{eff} and can be neglected. In general, straight lines with an aperiodic transient regime, arbitrary periodic curves, cycloids, and simple straight lines were found as trajectories in two spatial dimensions by random choices of the parameters. These trajectories still have the basic features of their three-dimensional analogs, but are much simpler to describe. It is only for particles with translational-rotational coupling, i. e., particles where at least one of the coefficients D_C^{\parallel} and D_C^{\perp} does not vanish, that the straight trajectories are preceded by an initial transient regime. These trajectories are characterized by a monotonous rotation of the particle when it starts moving and an ensuing rotation-free straight motion. In the transient regime, the particle rotates until the internal torque, the external torque, and the additional torque due to the translational-rotational coupling compensate each other. For active particles with translational-rotational coupling, periodic trajectories are observed also, where a canceling of the total torque does not happen during the initial rotation. This is not the case for symmetric particles with a vanishing effective torque M_{eff} and for passive particles, for which a periodic trajectory is not observed. The motion of symmetric particles without translational-rotational coupling is always periodic or constant. In both cases the trajectory is parallel to the direction of the external force, if the effective torque M_{eff} is not zero. Without the effective torque, only straight trajectories are observed for these particles. Solely in the case of passive rotationally symmetric particles, the orientation of these straight trajectories is parallel to the external force.

Table 3.2: Detailed classification of the trajectories of arbitrarily shaped particles in two spatial dimensions for $T = 0$ with respect to the symmetries that are summarized in table 3.1 on page 21. An external force $\vec{F}_{\text{ext}} \neq \vec{0}$ is chosen, since all trajectories become circles otherwise. In the plots below, \vec{F}_{ext} is always oriented downwards in the negative x_2 -direction. Internal and external torques are combined to the effective torque $M_{\text{eff}} = M - \partial_\phi U$.

particle shape	no symmetry	x_1 -axis or x_2 -axis is axis of symmetry	x_1 -axis and x_2 -axis are axes of symmetry	rotational symmetry
	$D_2 \neq 0, D_3 \neq 0, D_C^\parallel \neq 0, D_C^\perp \neq 0$	$D_2 = 0, D_3 \neq 0, D_C^\parallel \neq 0 \vee D_C^\perp \neq 0$	$D_2 = 0, D_3 \neq 0, D_C^\parallel = 0, D_C^\perp = 0$	$D_2 = 0, D_3 = D_1, D_C^\parallel = 0, D_C^\perp = 0$
$F_\parallel \neq 0, F_\perp \neq 0, M_{\text{eff}} \neq 0$				
	straight line after transient regime ^a or periodic curve ^b	straight line after transient regime ^a or periodic curve ^b	periodic curve ^c $\parallel \vec{F}_{\text{ext}}$	cycloid ^c $\parallel \vec{F}_{\text{ext}}$
$F_\parallel \neq 0, F_\perp \neq 0, M_{\text{eff}} = 0$				
	straight line after transient regime ^a or periodic curve ^b	straight line after transient regime ^a	straight line ^d	straight line ^d
$F_\parallel = 0, F_\perp \neq 0, M_{\text{eff}} \neq 0$				
	straight line after transient regime ^a or periodic curve ^b	str. line after trans. regime ^a or periodic curve ^b $\parallel \vec{F}_{\text{ext}}$	cycloid ^c $\parallel \vec{F}_{\text{ext}}$	straight line ^c $\parallel \vec{F}_{\text{ext}}$
$F_\parallel = 0, F_\perp \neq 0, M_{\text{eff}} = 0$				
	straight line after transient regime ^a	straight line after transient regime ^a $\parallel \vec{F}_{\text{ext}}$	straight line ^d	straight line ^d $\parallel \vec{F}_{\text{ext}}$

^a The particle rotates monotonously until it reaches its final orientation. Then the angle $\phi(t)$ remains constant.

^b The angle $\phi(t)$ and the center of mass of the particle describe periodic curves with the same periodicity.

^c The particle rotates with a constant angular velocity, i. e., $\phi(t) \propto t$.

^d The orientation of the particle is constant: $\phi(t) = \text{const.}$

3.2.2.3 Orthotropic particles

To regard the influence of thermal fluctuations on the motion of an active biaxial Brownian particle, numerical solutions of the Langevin equations (3.33) for orthotropic particles are considered in this section for $T > 0$. For this purpose, first of all, characteristic quantities for the length scale, time scale, and force scale are chosen and the Langevin equations (3.33) are rescaled to dimensionless units. A suitable choice for the characteristic length l_c , the characteristic time t_c , and the characteristic force F_c is

$$l_c = \sqrt{\frac{\lambda_{\max}(\mathbf{D}^{\text{TT}})}{\lambda_{\max}(\mathbf{D}^{\text{RR}})}}, \quad t_c = \frac{1}{\lambda_{\max}(\mathbf{D}^{\text{RR}})}, \quad F_c = \frac{\eta l_c^2}{t_c} = \eta \lambda_{\max}(\mathbf{D}^{\text{TT}}), \quad (3.40)$$

where $\lambda_{\max}(\cdot)$ denotes the biggest eigenvalue of the respective matrix. These characteristic quantities are used to express the position $\vec{r} = \vec{r}' l_c$, time $t = t' t_c$, forces $\vec{F}_0 = \vec{F}'_0 F_c$, $\vec{F}_{\text{ext}} = \vec{F}'_{\text{ext}} F_c$, torques $\vec{T}_0 = \vec{T}'_0 F_c l_c$, $\vec{T}_{\text{ext}} = \vec{T}'_{\text{ext}} F_c l_c$, translation tensor $\mathbf{K} = \mathbf{K}' l_c$, and rotation tensor $\Omega_S = \Omega'_S l_c^3$ by the dimensionless position $\vec{r}' = (x'_1, x'_2, x'_3)$, time t' , forces \vec{F}'_0 , \vec{F}'_{ext} , torques \vec{T}'_0 , \vec{T}'_{ext} , translation tensor \mathbf{K}' , and rotation tensor Ω'_S , respectively. In the rescaled Langevin equations, the parameter

$$T' = \frac{2t_c}{\eta\beta l_c^3} = \frac{2}{\eta\beta} \sqrt{\frac{\lambda_{\max}(\mathbf{D}^{\text{RR}})}{\lambda_{\max}^3(\mathbf{D}^{\text{TT}})}} \propto T \quad (3.41)$$

appears as a dimensionless temperature. This parameter has been varied and fluctuation-averaged trajectories have been calculated for different temperatures with fixed initial conditions $\vec{r}'_0 = (x'_{1,0}, x'_{2,0}, x'_{3,0})$ and $\vec{\omega}'_0 \equiv \vec{\omega}_0$. The results for the case of vanishing external forces and torques, where the trajectory for $T' = T = 0$ is known from the analytical solution in section 3.2.1.3 to be a circular helix, are shown in figure 3.3 on the following page. For this figure, the dimensionless forces $\vec{F}'_0 = (-0.5, 0, 3)$, $\vec{F}'_{\text{ext}} = \vec{0}$, torques $\vec{T}'_0 = (-1, 0, 0)$, $\vec{T}'_{\text{ext}} = \vec{0}$, translation tensor $\mathbf{K}' = \text{diag}(1, 2, 3)$, rotation tensor $\Omega'_S = \text{diag}(1, 3, 4)$, initial conditions $\vec{r}'_0 = \vec{0}$, $\vec{\omega}'_0 = (0, \pi/2, 0)$, and temperatures $T' \in \{0, 0.05, 0.1, 0.3\}$ have been chosen. It is apparent that the center-of-mass trajectory for $T' = 0$ and the fluctuation-averaged center-of-mass trajectories for $T' > 0$ have no transient regime in figure 3.3 on the next page. This is also the case for non-vanishing constant external forces and torques and a general feature of orthotropic particles in contrast to less symmetric particles with a translational-rotational coupling. In the presence of thermal fluctuations, the helical motion of the active orthotropic particle is damped exponentially with time and the fluctuation-averaged center-of-mass trajectory becomes a *conchospiral* [Boy99], whose radius and pitch decay exponentially with time [see plots 3.4(a) and 3.4(b)]. This result was confirmed by a fit of the numerical solutions with the general parametrization of a conchospiral and agrees with the observation of a logarithmic spiral, also named *spira mirabilis* by Jacob Bernoulli, in the special case of two spatial dimensions of the Langevin equations (3.33) that is investigated in reference [TL08]. In the situation of figure 3.3 on the following page,

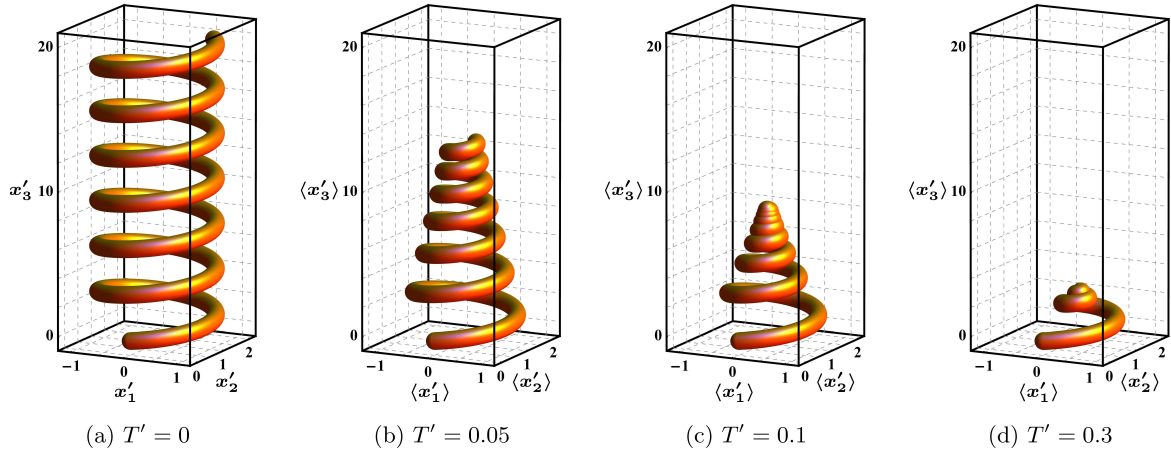


Figure 3.3: Mean trajectories of an active orthotropic particle in the absence of external forces and torques for the dimensionless temperatures $T' = 0$, $T' = 0.05$, $T' = 0.1$, and $T' = 0.3$. In the left two plots, the trajectories are shown for the time interval $0 \leq t' \leq 40$, while the right two plots show mean trajectories with $0 \leq t' \leq 80$.

the axes of the conchospirals are parallel to the x'_3 -axis and can be parametrized by [Boy99, TL08]

$$\begin{aligned} x'_1(t') &= x'_{1,0} + \alpha'_1 (\cos(\phi_0) - \cos(\phi(t'))e^{-\gamma'_1 t'}) \\ &\quad - \alpha'_2 (\sin(\phi_0) - \sin(\phi(t'))e^{-\gamma'_1 t'}) , \end{aligned} \quad (3.42)$$

$$\begin{aligned} x'_2(t') &= x'_{2,0} + \alpha'_1 (\sin(\phi_0) - \sin(\phi(t'))e^{-\gamma'_1 t'}) \\ &\quad + \alpha'_2 (\cos(\phi_0) - \cos(\phi(t'))e^{-\gamma'_1 t'}) , \end{aligned} \quad (3.43)$$

$$x'_3(t') = x'_{3,0} + H'_{\max} (1 - (1 - \varepsilon' t')e^{-\gamma'_2 t'}) , \quad (3.44)$$

$$\phi(t') = \phi_0 + \omega' t' \quad (3.45)$$

with the angular frequency $\omega' = \|\vec{\omega}'\| = \|\Omega_S^{-1} \vec{T}'_0\|$ [see equations (3.35)] and the dimensionless fit parameters α'_1 , α'_2 , γ'_1 , γ'_2 , H'_{\max} , and ε' . Equations (3.42), (3.43), and (3.45) describe a logarithmic spiral, which is the trajectory of the two-dimensional circle swimmer in reference [TL08], while the parametrization (3.44) of the third spatial variable $x'_3(t')$ is here more general than in reference [Boy99]. In equation (3.44), there is an additional term $\propto \varepsilon'$, which makes sure that a helix is obtained as special case of the conchospiral for $T' = 0$, i. e., for $\gamma'_1 = \gamma'_2 = 0$. This is, however, not the case for the parametrization in reference [Boy99]. Based on the parametrization (3.42)-(3.45), radius and pitch of the conchospirals can be derived. The fit parameters α'_1 , α'_2 , and γ'_1 determine the dimensionless radius $r'(t') = r(t)/l_c$ of the conchospirals:

$$r'(t') = r'_0 e^{-\gamma'_1 t'} , \quad (3.46)$$

$$r'(0) = r'_0 = \sqrt{\alpha'^2_1 + \alpha'^2_2} . \quad (3.47)$$

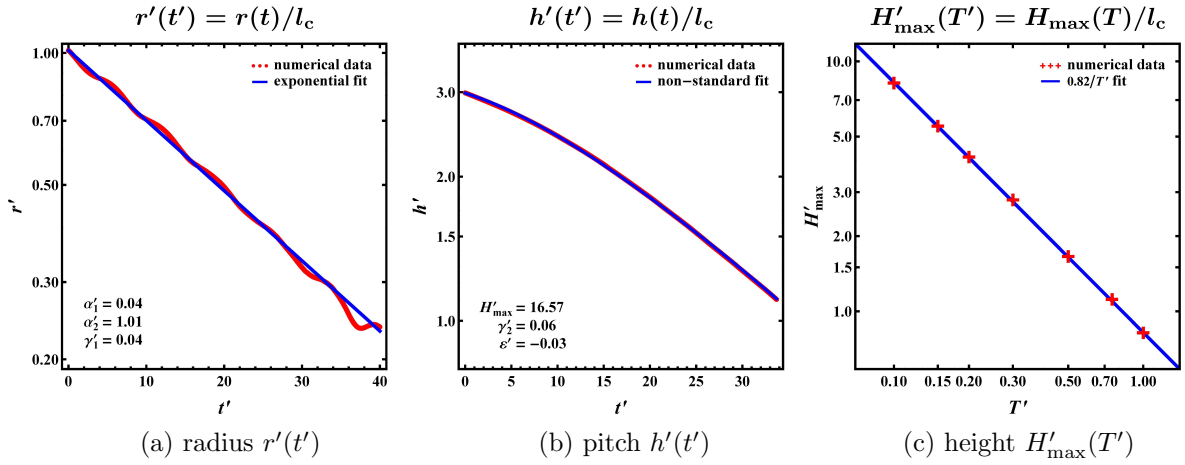


Figure 3.4: (a) Radius $r'(t')$ and (b) pitch $h'(t')$ of a trajectory that is shaped as a conchospiral decay exponentially with time t' . In the linear-logarithmic plots (a) and (b), the exponential decay is obvious for the radius, but not for the pitch, where the exponential function has a linear time-dependent prefactor [see equation (3.48)]. The numerical data (red dots following a curved line) for these plots were taken from the conchospiral in figure 3.3(b). (c) The height $H'_{\max}(T')$ of the conchospirals is inversely proportional to the temperature T' . The parameters for plot (c) are the same as for figure 3.3 on the preceding page, but with more and different values for T' . In each plot, a straight blue line corresponding to equations (3.46)-(3.49) was fitted to the numerical data.

Their dimensionless pitch $h'(t') = h(t)/l_c$ depends on the remaining fit parameters γ'_2 , H'_{\max} , and ϵ' :

$$h'(t') = H'_{\max} e^{-\gamma'_2 t'} \left((1 - \epsilon' t') (1 - e^{-\frac{2\pi}{\omega'} \gamma'_2}) + \epsilon' \frac{2\pi}{\omega'} e^{-\frac{2\pi}{\omega'} \gamma'_2} \right). \quad (3.48)$$

Some representative numerical values for radius and pitch are shown in plots 3.4(a) and 3.4(b). Furthermore, the height $H_{\max}(T)$ of the conchospiral and its dimensionless analog $H'_{\max}(T') = H_{\max}(T)/l_c$, defined as the distance from the initial position of the particle to its final position for $t' \rightarrow \infty$ measured along the axis of the conchospiral, are finite and decrease monotonously when the temperature is increased. For the numerical calculations that correspond to the results shown in figure 3.3 on the preceding page the inverse power law

$$H'_{\max}(T') \approx 0.82 T'^{-1} \quad (3.49)$$

was determined [see figure 3.4(c)]. When there is additionally a constant external force, the helix for $T' = 0$ as well as the conchospirals for $T' > 0$ are deformed and their cross-sections can become elliptic.

3.3 Motion of an active colloidal particle in shear flow

Following reference [MD04], the Langevin equation (3.1) can be easily generalized to also take a prescribed flow field of the liquid into account. The resulting Langevin equation is, however, not analytically solvable and its numerical solutions can be expected to be even more complicated than those for the flow-free case of a quiescent liquid that was described in the previous section. Therefore, only a special case of this generalized Langevin equation for a streaming liquid is discussed here. This special case treats a spherical active particle with radius R_s in two spatial dimensions. The active particle moves in the absence of any external potential in Couette shear flow with shear rate $\dot{\gamma}$ (see figure 3.5). Its drive is modeled by the internal force $\vec{F}_A = F\hat{u}$

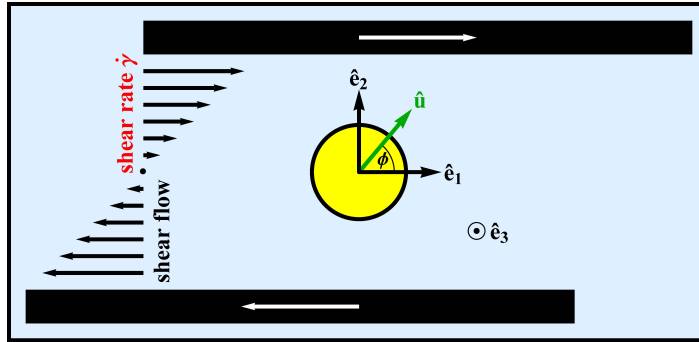


Figure 3.5: A spherical active colloidal particle with orientation \hat{u} moves in linear shear flow with shear rate $\dot{\gamma}$.

that is always parallel to the orientation $\hat{u} = (\cos(\phi), \sin(\phi))$ of the particle and by the constant internal or external torque M . The shear flow leads to the additional translational velocity $(\dot{\gamma}x_2, 0)$ and to the additional angular velocity $-\dot{\gamma}/2$. Moreover, thermal fluctuations cause a Gaussian white noise random force $\vec{f}(t) = (f_1, f_2)$ and a Gaussian white noise random torque $\tau(t)$ that act on the particle. The stochastic motion of the active particle is described by the Langevin equations

$$\begin{aligned}\dot{\vec{r}} &= \Gamma_s \vec{r} + \beta D_T (\vec{F}_A + \vec{f}) , \\ \dot{\phi} &= -\frac{\dot{\gamma}}{2} + \beta D_R (M + \tau)\end{aligned}\tag{3.50}$$

with the simple shear matrix [Dho96]

$$\Gamma_s = \begin{pmatrix} 0 & \dot{\gamma} \\ 0 & 0 \end{pmatrix},\tag{3.51}$$

the translational short-time diffusion coefficient $D_T \equiv D_1$, that is identical with the diffusion coefficient D_1 in section 3.2.1.2, and the rotational short-time diffusion coefficient D_R . For spherical particles, the relation $D_T/D_R = 4R_s^2/3$ holds between these two diffusion coefficients. The Gaussian white noise is characterized by the stochastic

vector $\tilde{\zeta}(t) = (f_1, f_2, \tau)$ with mean

$$\langle \tilde{\zeta}(t) \rangle = \vec{0} \quad (3.52)$$

and correlation

$$\langle \tilde{\zeta}(t_1) \otimes \tilde{\zeta}(t_2) \rangle = \frac{2}{\beta^2} \text{diag} (D_T^{-1}, D_T^{-1}, D_R^{-1}) \delta(t_1 - t_2). \quad (3.53)$$

The Langevin equations (3.50) contain two well-known special cases: when the shear rate $\dot{\gamma}$ is zero, the Langevin equation in reference [TL08] is obtained; if instead of the shear rate the self-propulsion vanishes, the traditional Brownian motion of a passive spherical particle in shear flow is described by the resulting Langevin equation [CV83, HBRZ10].

3.3.1 Fluctuation-averaged trajectories

The Langevin equations (3.50) are simple enough to be solved analytically. Some analytical results for the trajectories in the case of vanishing thermal fluctuations and equations for the mean trajectories in the case of non-vanishing thermal fluctuations are given in reference [HWL11], where the dimensionless variables $\vec{r}' = (x'_1, x'_2) = \vec{r}/R_s$, $t' = D_R t$ and the dimensionless quantities $F' = 4\beta R_s F/3$, $M' = \beta M$, $\dot{\gamma}' = \dot{\gamma}/(2D_R) = \text{Pe}_r/2$ with the rotational Péclet number $\text{Pe}_r = \dot{\gamma}/D_R$ are used to simplify the equations.

3.3.1.1 Analytical results for zero temperature

For $T = 0$, there are no thermal fluctuations and the Langevin equations (3.50) become deterministic and can be integrated easily. Depending on the value of the effective dimensionless torque $\omega' = M' - \dot{\gamma}'$, the cases $\omega' = 0$ and $\omega' \neq 0$ should be distinguished. The corresponding analytical solutions of the Langevin equations are given in the two following paragraphs.

a) Absence of an effective torque

If the torque M' , that results from the drive of the particle, and the additional dimensionless torque $\dot{\gamma}'$ due to the shear flow cancel each other, the effective torque $\omega' = 0$ is zero and the particle moves with constant orientation. The corresponding solution of the Langevin equations is given in dimensionless form by [HWL11]

$$\begin{aligned} x'_1(t') &= x'_{1,0} + \dot{\gamma}' F' \sin(\phi_0) t'^2 + (2\dot{\gamma}' x'_{2,0} + F' \cos(\phi_0)) t', \\ x'_2(t') &= x'_{2,0} + F' \sin(\phi_0) t', \\ \phi(t') &= \phi_0 \end{aligned} \quad (3.54)$$

with the initial conditions $x'_{1,0} = x'_1(0)$, $x'_{2,0} = x'_2(0)$, and $\phi_0 = \phi(0)$. Notice the quadratic time-dependence of the term $\dot{\gamma}' F' \sin(\phi_0) t'^2$ in the equation for $x'_1(t')$. This term results from the shear flow and is absent, if the liquid is quiescent.

b) Presence of an effective torque

In the complementary situation $\omega' \neq 0$, where M' and $\dot{\gamma}'$ do not compensate each other, the particle rotates with the constant angular velocity ω' . The analytical solution of the Langevin equations is for this case given by [HWL11]

$$\begin{aligned} x'_1(t') &= x'_{1,0} + 2\dot{\gamma}' \left(x'_{2,0} + \frac{F'}{\omega'} \cos(\phi_0) \right) t' + \frac{F'}{\omega'^2} (2\dot{\gamma}' - \omega') (\sin(\phi_0) - \sin(\phi_0 + \omega' t')) , \\ x'_2(t') &= x'_{2,0} + \frac{F'}{\omega'} (\cos(\phi_0) - \cos(\phi_0 + \omega' t')) , \\ \phi(t') &= \phi_0 + \omega' t' \end{aligned} \quad (3.55)$$

and describes cycloids in the (x_1, x_2) -plane. A cycloid for the initial conditions $x'_{1,0} = x'_{2,0} = \phi_0 = 0$ and parameters $F' = 10$, $\dot{\gamma}' = 5$, and $M' = 0$ is plotted as red dashed curve in figure 3.6 on the next page.

3.3.1.2 Analytical results for positive temperature

In the case of a non-vanishing temperature $T > 0$, thermal fluctuations lead to a damped motion of the active particle. The damping effect is obvious in the analytical solution [HWL11]

$$\begin{aligned} \langle x'_1(t') \rangle &= x'_{1,0} + 2\dot{\gamma}' (x'_{2,0} + \alpha_1) t' + \alpha_3 - \alpha_4(t') e^{-t'} , \\ \langle x'_2(t') \rangle &= x'_{2,0} + \alpha_1 - \alpha_2(t') e^{-t'} , \\ \langle \phi(t') \rangle &= \phi_0 + \omega' t' \end{aligned} \quad (3.56)$$

for the fluctuation-averaged mean trajectories that are described by the Langevin equations (3.50) for positive temperature. In this result, the abbreviations

$$\begin{aligned} \alpha_1 &= a_1 , \\ \alpha_2(t') &= b_1(t') , \\ \alpha_3 &= a_2 - \frac{2\dot{\gamma}'}{1 + \omega'^2} (a_1 + a_2 \omega') , \\ \alpha_4(t') &= b_2(t') - \frac{2\dot{\gamma}'}{1 + \omega'^2} (b_1(t') + b_2(t') \omega') , \end{aligned} \quad (3.57)$$

that in turn depend on the constants

$$a_1 = \frac{F'}{1 + \omega'^2} (\sin(\phi_0) + \omega' \cos(\phi_0)) , \quad (3.58)$$

$$a_2 = \frac{F'}{1 + \omega'^2} (\cos(\phi_0) - \omega' \sin(\phi_0)) \quad (3.59)$$

and on the functions

$$\begin{aligned} b_1(t') &= \frac{F'}{1 + \omega'^2} (\sin(\phi_0 + \omega' t') + \omega' \cos(\phi_0 + \omega' t')) , \\ b_2(t') &= \frac{F'}{1 + \omega'^2} (\cos(\phi_0 + \omega' t') - \omega' \sin(\phi_0 + \omega' t')) , \end{aligned} \quad (3.60)$$

are used to keep the presentation of the analytical solution clear. A representative example for these damped trajectories is shown as solid blue line in the main part of figure 3.6. The parameters are the same as for the red dashed cycloid. By comparison

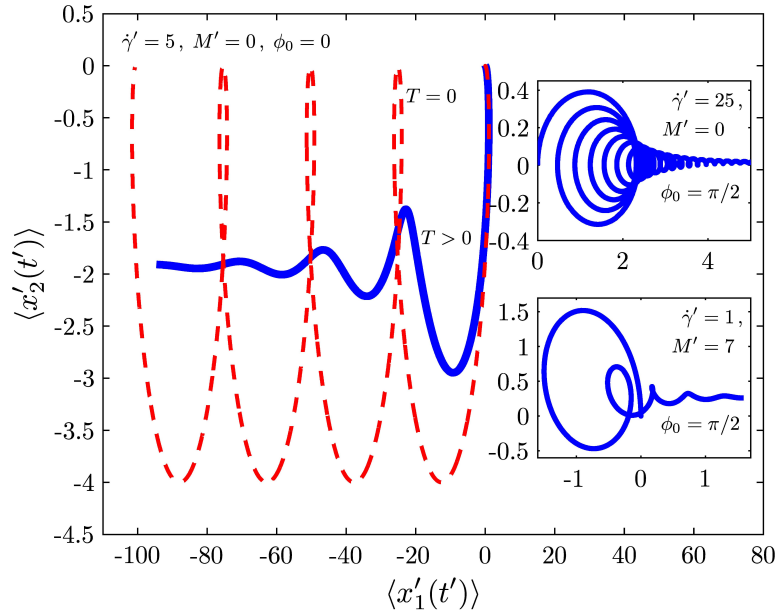


Figure 3.6: Cycloidal trajectory for $T = 0$ (red dashed line) and the corresponding damped mean trajectory for $T > 0$ (blue solid line). The insets show more complicated mean trajectories for $T > 0$. For all trajectories in this figure, the dimensionless force is $F' = 10$ and the initial conditions are $x'_{1,0} = x'_{2,0} = 0$.

of the two corresponding trajectories for $T = 0$ and for $T > 0$ in this figure, the effect of dissipative damping through thermal fluctuations is obvious. Although only a spherical active particle is considered in this section and the Langevin equations (3.50) that describe its stochastic motion are simple, rather complicated and very different trajectories can be observed due to the shear flow. The insets in figure 3.6 show two of these complicated trajectories. Further qualitatively different trajectories can be obtained for other parameter combinations.

3.3.2 Mean square displacement

The shear flow has considerable influence on the mean square displacement. This can also be derived analytically from the Langevin equations (3.50). However, the full analytical result is too complicated to be presented here (see reference [HWL11] for details). It turns out that five different dynamic regimes can be identified, where the mean square displacement scales with t^ν and the exponent is $\nu \in \{0, 1, 2, 3, 4\}$. The exponent $\nu = 0$ is observed for an active particle with non-vanishing effective torque ω' in the absence of shear flow at $T = 0$. This particle moves on a circular trajectory. The value $\nu = 1$ is the usual exponent for simple diffusion. This exponent appears in the diffusive motion of active and passive particles in a quiescent liquid for $T > 0$. Without shear flow, the exponent $\nu = 2$ can be established as well. This is the case, when the effective torque ω' and the temperature T vanish so that the particle moves ballistically. The exponent $\nu = 3$ can be observed in the absence of shear flow only for a short time in a transient regime [HTL11]. This exponent is not observed in the long-time limit, if the liquid is quiescent. In the presence of shear flow, the t^3 scaling is in contrast the most general situation for long times and can also be observed in the Taylor diffusion of passive particles [CV83]. Finally, the exponent $\nu = 4$ is realized for an active particle with $\omega' = T = 0$. If the colloidal particle starts with an initial orientation $\phi_0 \neq 0$, that is not perpendicular to the gradient direction of the shear flow, a term that is quadratic in t' is included in equations (3.54) and the mean square displacement has therefore a contribution proportional to t'^4 . For $\phi_0 = 0$ and $\phi_0 = \pi$, the mean square displacement is instead only a quadratic function in t' .

In sum, the mobility of the particle is hugely enhanced by shear flow. The increased mobility also becomes apparent in a faster broadening of the spatial probability distribution of the particle. Aside from the accelerated broadening, a further effect of the shear flow can be observed at the spatial probability distribution. In figure 3.7 on the facing page, the spatial probability distribution for an active particle with a vanishing effective torque ω' and an initial orientation in the positive x'_1 -direction is shown. The distributions presented are obtained from a Brownian dynamics simulation on the basis of the Langevin equations (3.50). As a result of rotational Brownian motion, the active particle can move in any direction although it starts parallel to the x'_1 -axis. In the x'_2 -direction, which is not influenced by the shear flow, the spatial probability distribution is symmetric and exhibits a transient double-peak structure [see figure 3.7(a)]. This double-peak structure is a result of the non-rotational active motion of the particle and vanishes with time, since thermal fluctuations decorrelate the orientation of the particle for larger times. With time, the spatial probability distribution broadens more and more and the double-peak structure finally disappears. In the long-time limit, the motion becomes diffusive and a Gaussian distribution emerges. The double-peak structure is also observed in the x'_1 -direction, but under the influence of shear flow the particle behaves differently in this direction. This situation is shown in figure 3.7(b). The spatial probability distribution is not symmetric anymore and the transient double-peak structure has two maxima of different height.

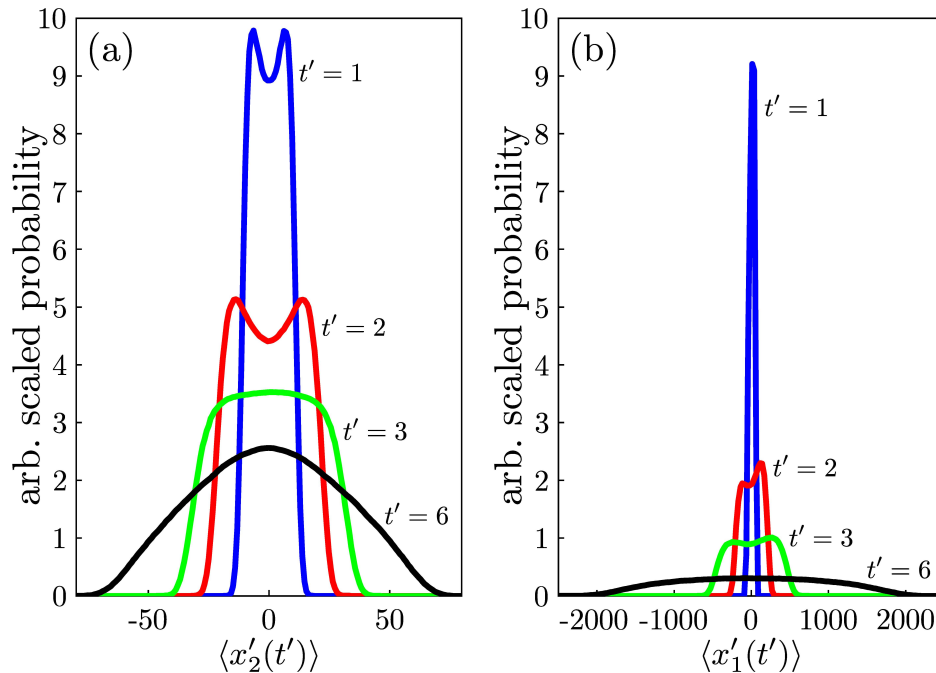


Figure 3.7: Time evolution of the spatial probability distribution of an active spherical particle at $T > 0$. While (a) in the x'_2 -direction a symmetric transient double-peak structure is observed, there is (b) an asymmetric transient double-peak structure due to the shear flow in the x'_1 -direction. The two plots correspond to the parameters $F' = 10$, $M' = 5$, and $\dot{\gamma}' = 5$ and to the initial conditions $x'_{1,0} = x'_{2,0} = \phi_0 = 0$.

3.4 Applications and generalized Langevin equations

The results of this chapter have various applications in the context of swimming microorganisms and artificial microswimmers. For example, the Langevin equation (3.1) for an active colloidal particle with arbitrary shape could be used to describe the motion of swimming microorganisms theoretically. The helical trajectory (3.36), that was derived from the Langevin equation, is indeed typical for swimming microorganisms [JV72, SJ01]. Also the solutions of the Langevin equations (3.50) for an active particle in shear flow should be similar to real trajectories of swimming microorganisms in shear flow [EZB⁺08, LGG⁺09]. With suitable microorganisms, it would also be possible to observe the accelerated regime in experiments, where the mean square displacement scales with t^4 . This regime was predicted for active particles with a certain internal torque that compensates the additional torque due to the shear flow so that the colloidal particles do not rotate. Although this behavior is very special, it can in fact be realized with the gravitactic green alga *Chlamydomonas reinhardtii* that swims upward in a gravitational field and retains its orientation unaffected by the flow of the surrounding liquid [RJP10, Sta10]. For the future, a comparison of the results in this chapter with experiments and with computer simulations [Sat10] would be desirable.

Additionally, some of the basic results could be further generalized to more complicated situations. With the help of references [Dho96, MD04] it is, for example, easy to add a term to the Langevin equation (3.1) that regards the influence of an arbitrary prescribed constant or time-dependent flow field of the liquid. It is further possible to generalize this Langevin equation by the consideration of system boundaries that confine the stochastic motion of the arbitrarily shaped active colloidal particle. Possible geometries for the confinement of the motion are channels between parallel walls [WL08] and cylindrical tubes [CWG10]. When there are geometric restrictions for the motion of the colloidal particle, the hydrodynamic interaction of the colloidal particle with the system boundaries has to be taken into account as well [LS05, Sta09, DPZY10]. Instead of an individual active particle, also a large ensemble of interacting active particles could be considered. These particles would interact with each other both directly by excluded volume interactions and indirectly through hydrodynamic interactions [Sta09]. Such an active suspension has interesting properties like an anomalous effective viscosity [Sta10] that deviate significantly from the properties of passive suspensions. Furthermore, this ensemble of interacting active particles could be described both in an unbounded domain and in confinement. The consideration of such an active ensemble is obviously very important, since especially swimming microorganisms often occur in swarms. Therefore, this topic is addressed in the following chapter.

4 Collective dynamics of interacting colloidal particles

After the description of the motion of individual active colloidal particles in the previous chapter, this chapter considers the collective dynamics of an ensemble of interacting colloidal particles that may be passive or active. The description of their collective Brownian dynamics is based on classical dynamical density functional theory (DDFT) that proved to be a very useful tool for the description of the collective Brownian motion of passive soft matter. The first section of this chapter gives an overview about the history of DDFT and further developments in recent years. After that, a generalized DDFT, that holds even for active and passive colloidal particles with arbitrary shape, is derived. This enhanced DDFT includes previous versions of DDFT as special cases and is, for example, highly relevant for the investigation of the dynamics of colloidal liquid crystals, which consist of arbitrarily shaped colloidal particles. In comparison with older versions of DDFT, the new generalization allows for the first time that biaxial particles are considered also, whose shapes may even give rise to a hydrodynamic translational-rotational coupling. The obtained generalization of DDFT is afterwards reformulated using a dissipation functional. This alternative formulation of DDFT leads to a better understanding of DDFT in the context of linear irreversible thermodynamics and provides a method to derive the dynamic equations for phase field crystal models with many order-parameter fields – like those derived in chapter 5 – much faster and much more easily than it would be possible otherwise. This chapter ends with a discussion of possible applications and further developments of the new and generalized DDFT.

4.1 Dynamical density functional theory for colloidal particles

DDFT is the time-dependent analog of static DFT¹. While static DFT can be used to construct a static Helmholtz free-energy functional $\mathcal{F}[\rho(\vec{\mathbf{r}})]$ of a colloidal system in terms of the equilibrium one-particle density field $\rho(\vec{\mathbf{r}}) \equiv \rho(\vec{r}, \vec{\omega})$, that is proportional to the probability density to find a colloidal particle at a certain position \vec{r} with a certain orientation $\vec{\omega}$, in order to describe the equilibrium state of this system, DDFT provides a dynamic equation, the so-called DDFT equation, for the time-

¹Necessary details about static DFT and DDFT are described in section 5.1.1.

dependent non-equilibrium one-particle density field $\rho(\vec{\mathbf{x}}, t)$. This dynamic equation describes the dissipative non-equilibrium relaxation dynamics of the colloidal system. The dynamics described by the DDFT equation is driven by the functional derivative of the time-dependent Helmholtz free-energy functional $\mathcal{F}[\rho(\vec{\mathbf{x}}, t)]$ with respect to the time-dependent one-particle density field $\rho(\vec{\mathbf{x}}, t)$.

After early suggestions of symmetry-based DDFT equations by Evans [Eva79] and Dieterich et al. [DFM90], DDFT was at first derived systematically by Marconi and Tarazona [MT99, MT00] in 1999 for spherical colloidal particles. Their derivation started from the Langevin equation for spherical particles [Dea96] that interact via a pair-interaction potential. Later, in 2004, DDFT was rederived by Archer and Evans [AE04] from the Smoluchowski equation that corresponds to the Langevin equation for interacting spherical particles. As a further alternative to the previous derivations of DDFT, Español and Löwen used a projection operator technique in 2009 in order to rederive DDFT in a more general context [EL09]. Up to now, several generalizations of this traditional DDFT have been proposed. In 2007, it was generalized by Rex, Wensink, and Löwen [RWL07] toward systems of colloidal particles with non-trivial orientational degrees of freedom. This generalization is based on the Smoluchowski equation for rigid rods [Dho96] and describes systems of anisotropic uniaxial particles without a hydrodynamic translational-rotational coupling in three spatial dimensions. It made DDFT applicable to the important class of uniaxial colloidal liquid crystals, but fails for colloidal particles with a more complicated shape. A special variant of this DDFT for uniaxial particles was later derived for colloidal systems with only two spatial dimensions and is given in reference [WL08]. In this reference, a possible self-propulsion of the colloidal particles was taken into account, too. Recently, rod-like active particles in a gravitational field were addressed by Enculescu and Stark in three spatial dimensions [ES11]. Situations with more complicated particle shapes have so far not been considered in the context of DDFT.

There are further attempts for other important generalizations of DDFT, but they are only valid for spherical particles and many of them are beyond that not satisfying. Among them are various attempts like those in references [Arc06, MTCM08, Arc09, MM09, MM10] for a generalization of DDFT toward molecular dynamics, where inertia is important and the dynamics is not overdamped, but up to now, none of these approaches is consistent with experimental observations. Such derivations usually fail, since a suitable closure relation cannot be found (see section 5.1.1.2 for details). The adiabatic approximation, that is used as closure relation in the derivation of the traditional DDFT for overdamped Brownian particles, is not appropriate for molecular dynamics. Further extensions of DDFT were proposed for mixtures of different species of colloidal particles. A first success in this regard was achieved by Archer [Arc05] through the consideration of a free-energy functional, that depends on the one-particle densities for the different kinds of colloidal particles, and a set of DDFT equations for the time-evolution of these one-particle densities. However, his approximation for the free-energy functional and his DDFT equations have to be improved. His dynamic equations contain only diagonal dissipative terms and should also contain non-diagonal dissipative coupling terms. The consideration of hydrodynamic interactions between

the colloidal particles is another important possibility to enhance current DDFT. At least for spherical particles, a DDFT equation with hydrodynamic interactions was derived by Rex and Löwen [RL08, RL09]. Only valid for spherical particles is also the DDFT equation of Rauscher and co-workers [RDKP07] for colloidal particles in a flowing liquid. Their DDFT equation was later applied to spherical particles in shear flow by Brader and Krüger [BK11], but it does not yet regard the influence of the colloidal particles back on the liquid. In a different effort, DDFT was generalized by Rauscher toward confinement and hydrodynamic interactions with system boundaries [Rau10]. Nevertheless, this reference, too, confines itself to spherical particles, although anisotropic particles prevail.

Nowadays, it is already possible to produce colloidal particles with rather complicated shapes including biaxial particles with or without a hydrodynamic translational-rotational coupling [HB91] (see section 2.1 for examples). Although static DFT has very powerful tools presently available such as fundamental measure theory [HM09] that allow to consider also such complicated colloidal particles in the context of static DFT, the dynamics of these biaxial particles could up to now not be investigated on the basis of DDFT. For these reasons, the development of DDFT is pushed forward with this chapter through a further generalization of DDFT, which is now also applicable to active and passive biaxial particles with an arbitrary shape.

4.2 Dynamical density functional theory for active colloidal particles with arbitrary shape

The new DDFT is designated to describe the collective Brownian motion of N interacting biaxial active colloidal particles that are suspended in a viscous liquid. As in the previous chapter, the particles are again assumed to be rigid and to have an arbitrary shape. The positions and orientations of the particles are described by the center-of-mass positions $\vec{r}_i = (x_{1,i}, x_{2,i}, x_{3,i})$ and the Eulerian angles $\vec{\omega}_i = (\phi_i, \theta_i, \chi_i)$ or equivalently by the position-orientation vectors $\vec{\mathbf{x}}_i = (\vec{r}_i, \vec{\omega}_i)$ with $i = 1, \dots, N$. Their instantaneous velocities are given by the translational velocities $\dot{\vec{r}}_i = d\vec{r}_i/dt$ and angular velocities $\dot{\vec{\omega}}_i$. To simplify the notation, they are collected in the generalized velocity vectors $\vec{\mathbf{v}}_i = (\dot{\vec{r}}_i, \dot{\vec{\omega}}_i)$. The whole set of particles is then characterized by the “multivectors” $\vec{r}^N = (\vec{r}_1, \dots, \vec{r}_N)$, $\vec{\omega}^N = (\vec{\omega}_1, \dots, \vec{\omega}_N)$, and $\vec{\omega}^N = (\vec{\omega}_1, \dots, \vec{\omega}_N)$ or equivalently by $\vec{\mathbf{x}}^N = (\vec{r}^N, \vec{\omega}^N)$ and $\vec{\mathbf{v}}^N = (\dot{\vec{r}}^N, \dot{\vec{\omega}}^N)$ with $\dot{\vec{r}}^N = d\vec{r}^N/dt$. The particles are exposed to the (time-dependent) total potential

$$U(\vec{\mathbf{x}}^N, t) = U_{\text{ext}}(\vec{\mathbf{x}}^N, t) + U_{\text{int}}(\vec{\mathbf{x}}^N), \quad (4.1)$$

which consists of the total external potential

$$U_{\text{ext}}(\vec{\mathbf{x}}^N, t) = \sum_{i=1}^N U_1(\vec{\mathbf{x}}_i, t) \quad (4.2)$$

and the total particle interaction potential

$$U_{\text{int}}(\vec{\mathbf{r}}^N) = \sum_{\substack{i,j=1 \\ i < j}}^N U_2(\vec{\mathbf{r}}_i, \vec{\mathbf{r}}_j) . \quad (4.3)$$

For both the one-particle potentials $U_1(\vec{\mathbf{r}}_i, t)$ and the two-particle interaction potentials $U_2(\vec{\mathbf{r}}_i, \vec{\mathbf{r}}_j)$, pairwise additivity is assumed². Moreover, many-particle interaction potentials of higher order than pair-interaction potentials are neglected. Furthermore, the N -particle probability distribution function $P(\vec{\mathbf{r}}^N, t)$ for the probability density to find the N particles at time t at $\vec{\mathbf{r}}^N$ is introduced. Successive integration of this function with respect to its positional and orientational degrees of freedom leads to the n -particle density [AE04]

$$\rho^{(n)}(\vec{\mathbf{r}}^n, t) = \frac{N!}{(N-n)!} \int_{\mathfrak{G}} d\mathfrak{Y}_{n+1} \cdots \int_{\mathfrak{G}} d\mathfrak{Y}_N P(\vec{\mathbf{r}}^N, t) , \quad (4.4)$$

where the integration operator

$$\int_{\mathfrak{G}} d\mathfrak{Y} = \int_{\mathcal{V}} dV \int_{\mathcal{S}} d\Omega \quad (4.5)$$

with the total integration domain $\mathfrak{G} = \mathcal{V} \times \mathcal{S}$ and with the corresponding differential $d\mathfrak{Y} = dV d\Omega$ is introduced in order to combine spatial and orientational integration. The integration operators for spatial and orientational integration are in turn given by

$$\begin{aligned} \int_{\mathcal{V}} dV &= \int_0^\infty dx_1 \int_0^\infty dx_2 \int_0^\infty dx_3 , \\ \int_{\mathcal{S}} d\Omega &= \int_0^{2\pi} d\phi \int_0^\pi d\theta \sin(\theta) \int_0^{2\pi} d\chi \end{aligned} \quad (4.6)$$

with the domains $\mathcal{V} = \mathbb{R}^3$ and $\mathcal{S} = [0, 2\pi) \times [0, \pi] \times [0, 2\pi)$ and with the differentials $dV = dx_1 dx_2 dx_3$ and $d\Omega = d\phi d\theta \sin(\theta) d\chi$.

4.2.1 Smoluchowski equation

To proceed, the Smoluchowski equation for the overdamped Brownian dynamics of the N active biaxial particles has to be derived. In this context, it is useful to define the operators $\vec{\nabla}_{\vec{\mathbf{r}}^N} = (\vec{\nabla}_{\vec{\mathbf{r}}_1}, \dots, \vec{\nabla}_{\vec{\mathbf{r}}_N})$, $\vec{\nabla}_{\vec{\mathbf{a}}^N} = (\vec{\nabla}_{\vec{\mathbf{a}}_1}, \dots, \vec{\nabla}_{\vec{\mathbf{a}}_N})$, and $\vec{\nabla}_{\vec{\mathbf{r}}^N, \vec{\mathbf{a}}^N} = (\vec{\nabla}_{\vec{\mathbf{r}}^N}, \vec{\nabla}_{\vec{\mathbf{a}}^N})$. With these operators, the *continuity equation* for the probability distribution can be written as

$$\dot{P}(\vec{\mathbf{r}}^N, t) = -\vec{\nabla}_{\vec{\mathbf{r}}^N, \vec{\mathbf{a}}^N} \cdot (\vec{\mathbf{v}}^N P(\vec{\mathbf{r}}^N, t)) . \quad (4.7)$$

²A statement on pairwise additivity of potentials is given by Gray and Gubbins [GG84].

This is a trivial generalization of the continuity equation for passive rods that is described by Dhont in reference [Dho96]. On the Brownian time scale, the total force and torque acting on an arbitrary particle $i \in \{1, \dots, N\}$ are zero. The total force and torque on particle i consist of the force $\vec{F}_i^{(A)}(\vec{\mathbf{x}}^N, t)$ and torque $\vec{T}_i^{(A)}(\vec{\mathbf{x}}^N, t)$ due to the activity of the self-propelled particle i , the hydrodynamic force $\vec{F}_i^{(H)}(\vec{\mathbf{x}}^N)$ and torque $\vec{T}_i^{(H)}(\vec{\mathbf{x}}^N)$, the interaction force $\vec{F}_i^{(I)}(\vec{\mathbf{x}}^N, t)$ and torque $\vec{T}_i^{(I)}(\vec{\mathbf{x}}^N, t)$ due to the potential $U(\vec{\mathbf{x}}^N, t)$, and the Brownian force $\vec{F}_i^{(\text{Br})}(\vec{\mathbf{x}}^N, t)$ and torque $\vec{T}_i^{(\text{Br})}(\vec{\mathbf{x}}^N, t)$. With the abbreviating notation $\vec{X} = (\vec{X}_1, \dots, \vec{X}_N)$ for $\vec{X} \in \{\vec{F}^{(\cdot)}, \vec{T}^{(\cdot)}, \vec{K}^{(\cdot)}\}$ and the definitions

$$\begin{aligned}\vec{K}^{(A)}(\vec{\mathbf{x}}^N, t) &= (\vec{F}^{(A)}(\vec{\mathbf{x}}^N, t), \vec{T}^{(A)}(\vec{\mathbf{x}}^N, t)) , \\ \vec{K}^{(H)}(\vec{\mathbf{x}}^N) &= (\vec{F}^{(H)}(\vec{\mathbf{x}}^N), \vec{T}^{(H)}(\vec{\mathbf{x}}^N)) , \\ \vec{K}^{(I)}(\vec{\mathbf{x}}^N, t) &= (\vec{F}^{(I)}(\vec{\mathbf{x}}^N, t), \vec{T}^{(I)}(\vec{\mathbf{x}}^N, t)) , \\ \vec{K}^{(\text{Br})}(\vec{\mathbf{x}}^N, t) &= (\vec{F}^{(\text{Br})}(\vec{\mathbf{x}}^N, t), \vec{T}^{(\text{Br})}(\vec{\mathbf{x}}^N, t)) ,\end{aligned}\tag{4.8}$$

the force and torque balance for the N colloidal particles can be expressed by

$$\vec{0} = \vec{K}^{(A)}(\vec{\mathbf{x}}^N, t) + \vec{K}^{(H)}(\vec{\mathbf{x}}^N) + \vec{K}^{(I)}(\vec{\mathbf{x}}^N, t) + \vec{K}^{(\text{Br})}(\vec{\mathbf{x}}^N, t) .\tag{4.9}$$

The forces and torques resulting from the self-propulsion mechanism of the particles are supposed to be constant with respect to their orientations in the respective body-fixed coordinate systems, but their strengths may vary slowly with time. These forces and torques for a certain particle $i \in \{1, \dots, N\}$ in body-fixed Cartesian coordinates are denoted by the vector $\vec{K}_{0,i}^{(A)}(\vec{r}_i, t)$ and the corresponding vector in space-fixed coordinates is denoted by

$$\vec{K}_i^{(A)}(\vec{\mathbf{x}}_i, t) = \mathcal{R}^{-1}(\vec{\omega}_i) \vec{K}_{0,i}^{(A)}(\vec{r}_i, t)\tag{4.10}$$

with the block diagonal rotation matrix (3.4). The vector $\vec{K}_{0,i}^{(A)}$ depends most often only on time t , but one could also think of swimming microorganisms in a poisoned environment, where $\vec{K}_{0,i}^{(A)}$ also depends on \vec{r}_i . To simplify the notation in the following, all the N vectors $\vec{K}_i^{(A)}(\vec{\mathbf{x}}_i, t)$ are collected in the vector

$$\vec{K}^{(A)}(\vec{\mathbf{x}}^N, t) = \mathcal{R}_N^{-1}(\vec{\omega}^N) \vec{K}_0^{(A)}(\vec{r}^N, t)\tag{4.11}$$

with the $6N \times 6N$ -dimensional block diagonal rotation matrix

$$\mathcal{R}_N(\vec{\omega}^N) = \text{diag}(\mathcal{R}(\vec{\omega}_1), \dots, \mathcal{R}(\vec{\omega}_N))\tag{4.12}$$

and the $6N$ -dimensional vector

$$\vec{K}_0^{(A)}(\vec{r}^N, t) = (\vec{K}_{0,1}^{(A)}(\vec{r}_1, t), \dots, \vec{K}_{0,N}^{(A)}(\vec{r}_N, t)) .\tag{4.13}$$

Next, the hydrodynamic force and torque are considered. They are given by

$$\vec{K}^{(H)}(\vec{\mathbf{r}}^N) = -\Upsilon_N(\vec{\mathbf{r}}^N)\vec{\mathbf{v}}^N \quad (4.14)$$

with the microscopic friction tensor [Dho96]

$$\Upsilon_N(\vec{\mathbf{r}}^N) = \begin{pmatrix} \Upsilon_N^{\text{TT}}(\vec{\mathbf{r}}^N) & \Upsilon_N^{\text{TR}}(\vec{\mathbf{r}}^N) \\ \Upsilon_N^{\text{RT}}(\vec{\mathbf{r}}^N) & \Upsilon_N^{\text{RR}}(\vec{\mathbf{r}}^N) \end{pmatrix}, \quad (4.15)$$

where $\Upsilon_N^{\text{TT}}(\vec{\mathbf{r}}^N)$, $\Upsilon_N^{\text{TR}}(\vec{\mathbf{r}}^N) = (\Upsilon_N^{\text{RT}}(\vec{\mathbf{r}}^N))^{\text{T}}$, and $\Upsilon_N^{\text{RR}}(\vec{\mathbf{r}}^N)$ are $3N \times 3N$ -dimensional submatrices. The submatrices $\Upsilon_N^{\text{TT}}(\vec{\mathbf{r}}^N)$ and $\Upsilon_N^{\text{RR}}(\vec{\mathbf{r}}^N)$ correspond to pure translational and rotational motion, respectively, while $\Upsilon_N^{\text{TR}}(\vec{\mathbf{r}}^N)$ and $\Upsilon_N^{\text{RT}}(\vec{\mathbf{r}}^N)$ have to be taken into account for particles with a translational-rotational coupling as, for example, screw-like particles. For many symmetric (e. g., orthotropic) particles, however, $\Upsilon_N^{\text{TR}}(\vec{\mathbf{r}}^N)$ and $\Upsilon_N^{\text{RT}}(\vec{\mathbf{r}}^N)$ vanish.

In the following, hydrodynamic interactions between different colloidal particles are neglected.³ With this assumption, the microscopic friction submatrices simplify to the block diagonal matrices

$$\Upsilon_N^{\text{TT}}(\vec{\omega}^N) = \text{diag}(\Upsilon_{11}^{\text{TT}}(\vec{\omega}_1), \dots, \Upsilon_{NN}^{\text{TT}}(\vec{\omega}_N)), \quad (4.16)$$

$$\Upsilon_N^{\text{TR}}(\vec{\omega}^N) = \text{diag}(\Upsilon_{11}^{\text{TR}}(\vec{\omega}_1), \dots, \Upsilon_{NN}^{\text{TR}}(\vec{\omega}_N)), \quad (4.17)$$

$$\Upsilon_N^{\text{RT}}(\vec{\omega}^N) = \text{diag}(\Upsilon_{11}^{\text{RT}}(\vec{\omega}_1), \dots, \Upsilon_{NN}^{\text{RT}}(\vec{\omega}_N)), \quad (4.18)$$

$$\Upsilon_N^{\text{RR}}(\vec{\omega}^N) = \text{diag}(\Upsilon_{11}^{\text{RR}}(\vec{\omega}_1), \dots, \Upsilon_{NN}^{\text{RR}}(\vec{\omega}_N)) \quad (4.19)$$

with the 3×3 -dimensional submatrices

$$\Upsilon_{ii}^{\text{TT}}(\vec{\omega}_i) = \eta \mathbf{R}^{-1}(\vec{\omega}_i) \mathbf{K} \mathbf{R}(\vec{\omega}_i), \quad (4.20)$$

$$\Upsilon_{ii}^{\text{TR}}(\vec{\omega}_i) = \eta \mathbf{R}^{-1}(\vec{\omega}_i) \mathbf{C}_S^{\text{T}} \mathbf{R}(\vec{\omega}_i), \quad (4.21)$$

$$\Upsilon_{ii}^{\text{RT}}(\vec{\omega}_i) = \eta \mathbf{R}^{-1}(\vec{\omega}_i) \mathbf{C}_S \mathbf{R}(\vec{\omega}_i), \quad (4.22)$$

$$\Upsilon_{ii}^{\text{RR}}(\vec{\omega}_i) = \eta \mathbf{R}^{-1}(\vec{\omega}_i) \Omega_S \mathbf{R}(\vec{\omega}_i) \quad (4.23)$$

for $i = 1, \dots, N$ that are related to the translation tensor \mathbf{K} , the coupling tensor \mathbf{C}_S , its transpose \mathbf{C}_S^{T} , and the rotation tensor Ω_S [HB91] by similarity transformations with the rotation matrix $\mathbf{R}(\vec{\omega})$. In the special case of no hydrodynamic interactions, the inverse of the microscopic friction tensor

$$\Upsilon_N^{-1}(\vec{\mathbf{r}}^N) = \beta \mathcal{D}_N(\vec{\mathbf{r}}^N) \quad (4.24)$$

with the microscopic short-time diffusion tensor

$$\mathcal{D}_N(\vec{\mathbf{r}}^N) = \begin{pmatrix} \mathcal{D}_N^{\text{TT}}(\vec{\mathbf{r}}^N) & \mathcal{D}_N^{\text{TR}}(\vec{\mathbf{r}}^N) \\ \mathcal{D}_N^{\text{RT}}(\vec{\mathbf{r}}^N) & \mathcal{D}_N^{\text{RR}}(\vec{\mathbf{r}}^N) \end{pmatrix}, \quad (4.25)$$

³Hydrodynamic interactions between the colloidal particles are not regarded directly. They are usual taken into account by means of an effective shape and size of the colloidal particles.

which is needed in the following, has the same band structure as the microscopic friction tensor $\Upsilon_N(\vec{\mathbf{r}}^N)$. This can be proved with the help of the block matrix inverse

$$\begin{pmatrix} \mathbf{A} & \mathbf{B} \\ \mathbf{C} & \mathbf{D} \end{pmatrix}^{-1} = \begin{pmatrix} \mathbf{S}_D^{-1} & -\mathbf{A}^{-1} \mathbf{B} \mathbf{S}_A^{-1} \\ -\mathbf{D}^{-1} \mathbf{C} \mathbf{S}_D^{-1} & \mathbf{S}_A^{-1} \end{pmatrix} \quad (4.26)$$

with matrices \mathbf{A} , \mathbf{B} , \mathbf{C} , and \mathbf{D} and with the *Schur complements*

$$\mathbf{S}_A = \mathbf{D} - \mathbf{C} \mathbf{A}^{-1} \mathbf{B}, \quad \mathbf{S}_D = \mathbf{A} - \mathbf{B} \mathbf{D}^{-1} \mathbf{C}. \quad (4.27)$$

One further has the equation

$$\vec{K}^{(I)}(\vec{\mathbf{r}}^N, t) = -\vec{\nabla}_{\vec{\mathbf{r}}^N} U(\vec{\mathbf{r}}^N, t) \quad (4.28)$$

for the interaction force and torque. Moreover, the Brownian force $\vec{F}^{(\text{Br})}(\vec{\mathbf{r}}^N, t)$ and torque $\vec{T}^{(\text{Br})}(\vec{\mathbf{r}}^N, t)$ can be derived from the equilibrium condition

$$\lim_{t \rightarrow \infty} P(\vec{\mathbf{r}}^N, t) \propto e^{-\beta U(\vec{\mathbf{r}}^N, t)}, \quad (4.29)$$

when $\vec{K}^{(A)}(\vec{\mathbf{r}}^N, t)$ is neglected and the vector $\vec{\mathbf{v}}^N$ in equation (4.7) is expressed in terms of the vectors $\vec{\mathbf{r}}^N$, $\vec{K}^{(I)}(\vec{\mathbf{r}}^N, t)$, $\vec{K}^{(\text{Br})}(\vec{\mathbf{r}}^N, t)$ using equations (4.9) and (4.14). This yields

$$\vec{K}^{(\text{Br})}(\vec{\mathbf{r}}^N, t) = -\frac{1}{\beta} \vec{\nabla}_{\vec{\mathbf{r}}^N} \ln(P(\vec{\mathbf{r}}^N, t)). \quad (4.30)$$

With the help of equations (4.9), (4.14), (4.28), and (4.30), the Smoluchowski equation

$$\dot{P}(\vec{\mathbf{r}}^N, t) = \hat{\mathcal{L}} P(\vec{\mathbf{r}}^N, t) \quad (4.31)$$

with the Smoluchowski operator

$$\hat{\mathcal{L}} = \vec{\nabla}_{\vec{\mathbf{r}}^N} \cdot \left(\mathcal{D}_N(\vec{\mathbf{r}}^N) (\beta \vec{\nabla}_{\vec{\mathbf{r}}^N} U(\vec{\mathbf{r}}^N, t) - \beta \vec{K}^{(A)}(\vec{\mathbf{r}}^N, t) + \vec{\nabla}_{\vec{\mathbf{r}}^N}) \right) \quad (4.32)$$

follows now directly from the continuity equation (4.7).

4.2.2 DDFT equation

The derivation is continued by applying the integration operator

$$N \int_{\mathfrak{E}} d\mathfrak{Y}_2 \cdots \int_{\mathfrak{E}} d\mathfrak{Y}_N \quad (4.33)$$

from the left on the Smoluchowski equation (4.31). This results in the expression

$$\dot{\rho}(\vec{\mathbf{r}}, t) = \vec{\nabla}_{\vec{\mathbf{r}}} \cdot \left(\mathcal{D}(\vec{\mathbf{r}}) (\vec{\nabla}_{\vec{\mathbf{r}}} \rho(\vec{\mathbf{r}}, t) - \beta \vec{K}(\vec{\mathbf{r}}, t) + \beta \rho(\vec{\mathbf{r}}, t) \vec{\nabla}_{\vec{\mathbf{r}}} U_1(\vec{\mathbf{r}}, t) - \beta \vec{K}_A(\vec{\mathbf{r}}, t) \rho(\vec{\mathbf{r}}, t)) \right) \quad (4.34)$$

with the symmetric short-time diffusion tensor⁴

$$\mathcal{D}(\vec{\omega}) = \begin{pmatrix} (\mathcal{D}_N^{\text{TT}}(\vec{\omega}))_{11} & (\mathcal{D}_N^{\text{TR}}(\vec{\omega}))_{11} \\ (\mathcal{D}_N^{\text{RT}}(\vec{\omega}))_{11} & (\mathcal{D}_N^{\text{RR}}(\vec{\omega}))_{11} \end{pmatrix} \quad (4.35)$$

for the one-particle density $\rho(\vec{\mathbf{r}}, t) \equiv \rho^{(1)}(\vec{\mathbf{r}}, t)$, where the index 1 is omitted in \vec{r}_1 and $\vec{\omega}_1$ and the abbreviations $\vec{K}_A(\vec{\mathbf{r}}, t) \equiv \vec{K}_1^{(A)}(\vec{\mathbf{r}}, t)$ and $\vec{K}(\vec{\mathbf{r}}, t) = (\bar{F}(\vec{\mathbf{r}}, t), \bar{T}(\vec{\mathbf{r}}, t))$ are used. With equation (4.26) it can be shown that the diffusion tensor (4.35) is in fact identical with the diffusion tensor (3.9) in the Langevin equation (3.1) in the previous chapter. The average force $\bar{F}(\vec{\mathbf{r}}, t)$ and torque $\bar{T}(\vec{\mathbf{r}}, t)$ due to the interactions with other particles in equation (4.34) are given by

$$\vec{K}(\vec{\mathbf{r}}, t) = - \int_{\mathfrak{G}} d\mathfrak{R}' \rho^{(2)}(\vec{\mathbf{r}}, \vec{\mathbf{r}}', t) \vec{\nabla}_{\vec{\mathbf{r}}} U_2(\vec{\mathbf{r}}, \vec{\mathbf{r}}'). \quad (4.36)$$

In thermodynamic equilibrium with $\vec{K}_A(\vec{\mathbf{r}}, t) = \vec{0}$ and $U_1 \rightarrow \bar{U}_1(\vec{\mathbf{r}})$, the dynamic equation (4.34) reduces to the first equation of the Yvon-Born-Green (YBG) hierarchy⁵ for molecular fluids [GG84]:

$$\beta \vec{K}(\vec{\mathbf{r}}) = \vec{\nabla}_{\vec{\mathbf{r}}} \rho(\vec{\mathbf{r}}) + \beta \rho(\vec{\mathbf{r}}) \vec{\nabla}_{\vec{\mathbf{r}}} \bar{U}_1(\vec{\mathbf{r}}). \quad (4.37)$$

Here, the function $\rho(\vec{\mathbf{r}})$ denotes the equilibrium one-particle density field that corresponds to the time-independent “substitute” external potential $\bar{U}_1(\vec{\mathbf{r}})$. On the other hand, in thermodynamic equilibrium, the relation

$$\vec{\nabla}_{\vec{\mathbf{r}}} \rho(\vec{\mathbf{r}}) + \beta \rho(\vec{\mathbf{r}}) \vec{\nabla}_{\vec{\mathbf{r}}} \bar{U}_1(\vec{\mathbf{r}}) = -\beta \rho(\vec{\mathbf{r}}) \vec{\nabla}_{\vec{\mathbf{r}}} \frac{\delta \mathcal{F}_{\text{exc}}[\rho(\vec{\mathbf{r}})]}{\delta \rho(\vec{\mathbf{r}})} \quad (4.38)$$

with the equilibrium Helmholtz excess free-energy functional $\mathcal{F}_{\text{exc}}[\rho(\vec{\mathbf{r}})]$ holds (compare section 5.1.1.1). This relation follows with

$$\vec{\nabla}_{\vec{\mathbf{r}}} c^{(1)}(\vec{\mathbf{r}}) = \int_{\mathfrak{G}} d\mathfrak{R}' c^{(2)}(\vec{\mathbf{r}}, \vec{\mathbf{r}}') \vec{\nabla}_{\vec{\mathbf{r}}} \rho(\vec{\mathbf{r}}'), \quad (4.39)$$

where $c^{(n)}(\vec{\mathbf{r}}_1, \dots, \vec{\mathbf{r}}_n)$ is the n -particle direct correlation function in equilibrium (see section 5.1.1.1 or reference [HM06]), and

$$c^{(1)}(\vec{\mathbf{r}}) = -\beta \frac{\delta \mathcal{F}_{\text{exc}}[\rho(\vec{\mathbf{r}})]}{\delta \rho(\vec{\mathbf{r}})} \quad (4.40)$$

⁴The reason to write $\mathcal{D}(\vec{\mathbf{r}})$ instead of $\mathcal{D}(\vec{\omega})$ in equation (4.34) is that one could in principle also describe systems with a space-dependent short-time diffusion tensor. This is especially relevant for liquids with a space-dependent viscosity.

⁵The *Yvon-Born-Green hierarchy* is the equilibrium form of the *Bogoliubov-Born-Green-Kirkwood-Yvon* (BBGKY) *hierarchy* [HM06].

from the more general form

$$\vec{\nabla}_{\vec{x}}\rho(\vec{x}) + \beta\rho(\vec{x})\vec{\nabla}_{\vec{x}}\bar{U}_1(\vec{x}) = \rho(\vec{x}) \int_{\mathfrak{G}} d\mathfrak{Y}' c^{(2)}(\vec{x}, \vec{x}') \vec{\nabla}_{\vec{x}'}\rho(\vec{x}') \quad (4.41)$$

of equations (14) and (16) in reference [Gub80]. Equations (4.37) and (4.38) lead to the equilibrium relation

$$\bar{K}(\vec{x}) = -\rho(\vec{x})\vec{\nabla}_{\vec{x}} \frac{\delta\mathcal{F}_{\text{exc}}[\rho(\vec{x})]}{\delta\rho(\vec{x})} \quad (4.42)$$

that is used instead of equation (4.36) as closure relation for equation (4.34) in the time-dependent non-equilibrium situation. A similar *adiabatic approximation* was used in the derivations of the DDFT equations for isotropic [MT99, AE04] and uniaxial [RWL07] colloidal particles (see section 5.1.1.2). The approximation results in the *generalized DDFT equation for three spatial dimensions*

$$\boxed{\frac{\partial\rho(\vec{x}, t)}{\partial t} = \beta\vec{\nabla}_{\vec{x}} \cdot \left(\mathcal{D}(\vec{x})\rho(\vec{x}, t) \left(\vec{\nabla}_{\vec{x}} \frac{\delta\mathcal{F}[\rho(\vec{x}, t)]}{\delta\rho(\vec{x}, t)} - \bar{K}_A(\vec{x}, t) \right) \right)} \quad (4.43)$$

with the total equilibrium Helmholtz free-energy functional $\mathcal{F}[\rho(\vec{x}, t)]$. For possible approximations of this functional, see section 5.1.1.1.

4.2.3 Special cases

In analogy to the procedure in the previous chapter, where the Langevin equation (3.1) was reduced to two spatial dimensions, also the DDFT equation (4.43) can be reduced to the case of two spatial dimensions. For this purpose, the values $x_3 = 0$, $\theta = \pi/2$, and $\chi = 0$ are chosen. The *generalized DDFT equation for two spatial dimensions* is then given by

$$\begin{aligned} \frac{\partial\rho(\vec{r}, \phi, t)}{\partial t} = & \beta\vec{\nabla}_{\vec{r}} \cdot \left(D_T(\phi)\rho(\vec{r}, \phi, t) \left(\vec{\nabla}_{\vec{r}} \frac{\delta\mathcal{F}[\rho(\vec{r}, \phi, t)]}{\delta\rho(\vec{r}, \phi, t)} - \vec{F}_A(\phi, t) \right) \right) \\ & - \beta\vec{\nabla}_{\vec{r}} \cdot \left(\vec{D}_C(\phi)\rho(\vec{r}, \phi, t) \left(\partial_\phi \frac{\delta\mathcal{F}[\rho(\vec{r}, \phi, t)]}{\delta\rho(\vec{r}, \phi, t)} - M(t) \right) \right) \\ & - \beta\partial_\phi \left(\vec{D}_C(\phi) \cdot \rho(\vec{r}, \phi, t) \left(\vec{\nabla}_{\vec{r}} \frac{\delta\mathcal{F}[\rho(\vec{r}, \phi, t)]}{\delta\rho(\vec{r}, \phi, t)} - \vec{F}_A(\phi, t) \right) \right) \\ & + \beta\partial_\phi \left(D_R\rho(\vec{r}, \phi, t) \left(\partial_\phi \frac{\delta\mathcal{F}[\rho(\vec{r}, \phi, t)]}{\delta\rho(\vec{r}, \phi, t)} - M(t) \right) \right) \end{aligned} \quad (4.44)$$

with the same notation as in the Langevin equations (3.17) in section 3.2.1.2. This DDFT equation describes the motion of arbitrarily shaped active colloidal particles in two spatial dimensions. When the translational-rotational coupling coefficients, i. e., the elements of the coupling tensor C_S , are set to zero, one obtains a DDFT

equation that describes only rod-like active particles in two spatial dimensions. Such a DDFT equation was published by Wensink and Löwen in 2008 [WL08]. Also the general DDFT equation (4.43) for three spatial dimensions can be simplified by the omission of the elements of the coupling tensor so that $\mathcal{D}_N^{\text{TR}}(\vec{\mathbf{r}}^N)$ and $\mathcal{D}_N^{\text{RT}}(\vec{\mathbf{r}}^N)$ and therefore also $(\mathcal{D}_N^{\text{TR}}(\vec{\varpi}))_{11}$ and $(\mathcal{D}_N^{\text{RT}}(\vec{\varpi}))_{11}$ vanish. The resulting DDFT equation is only applicable to orthotropic particles that have no translational-rotational coupling. This DDFT equation can further be simplified to uniaxial rod-like particles with one axis of symmetry. Due to the rotational symmetry, the one-particle density and the free-energy functional for uniaxial particles do not depend on the angle χ and the translational diffusion tensor can then be written as the matrix

$$\mathbf{D}^{\text{TT}}(\hat{u}) = D_{\parallel} \hat{u} \otimes \hat{u} + D_{\perp} (\mathbb{1} - \hat{u} \otimes \hat{u}), \quad (4.45)$$

which obviously only depends on the two independent short-time diffusion coefficients D_{\parallel} and D_{\perp} for diffusion parallel and perpendicular to the orientation of the axis of symmetry

$$\hat{u} = (\sin(\theta) \cos(\phi), \sin(\theta) \sin(\phi), \cos(\theta)) \quad (4.46)$$

of the uniaxial particle, respectively, where $\mathbb{1}$ denotes the 3×3 -dimensional unit matrix. The rotational diffusion tensor, too, becomes quite simple for uniaxial particles. When one defines $\mathbf{D}^{\text{RR}} = D_{\text{R}} \mathbb{1}$ with the rotational short-time diffusion coefficient D_{R} and neglects the self-propulsion, the DDFT equation of Rex, Wensink, and Löwen [RWL07] for uniaxial particles is obtained. From the uniaxial DDFT equation, one can in turn derive the DDFT equation for colloidal particles with spherical symmetry [MT99, AE04] as a special case.

4.3 Reformulation of DDFT using a dissipation functional

In linear irreversible thermodynamics [MPP72, GM84, Rei98], dissipation functionals \mathfrak{R} are used to derive the dissipative dynamics of thermodynamic variables.⁶ Such a *dissipation functional*

$$\mathfrak{R} = \int_{\mathcal{V}} dV \mathfrak{r}(\vec{r}, t) \quad (4.47)$$

with the integrand $\mathfrak{r}(\vec{r}, t)$ that is often called a *dissipation function* and that is quadratic in the thermodynamic forces⁷ corresponding to the thermodynamic variables, is closely related to the *entropy production* $\mathfrak{r}(\vec{r}, t)/T$ of the thermodynamic system [MPP72,

⁶For an introduction to symmetry-based theories of linear irreversible thermodynamics that use dissipation functionals, see section 5.1.

⁷The term *thermodynamic force* is defined by equation (5.69) in section 5.1.4.2.

PB96]. This entropy production appears naturally in the balance equation

$$\dot{\sigma} + \partial_i J_i^\sigma = \frac{\mathfrak{r}}{T} \quad (4.48)$$

for the entropy density $\sigma(\vec{r}, t)$, where $J_i^\sigma(\vec{r}, t)$ are the elements of the entropy current $\vec{J}^\sigma(\vec{r}, t)$. The most important feature of a dissipation functional and the basis for the derivation of the dissipative dynamics of thermodynamic variables from this dissipation functional is its optimization at local thermodynamic equilibrium.

A dissipation functional can be constructed for thermodynamic systems close to thermodynamic equilibrium and the dissipative dynamics of the thermodynamic variables of such systems follows then from the functional derivatives of the dissipation functional with respect to the thermodynamic forces [MPP72, GM84, For89, PB96, Rei98]. If a thermodynamic system is not close to thermodynamic equilibrium, as it is the case for strongly driven systems, a dissipation functional cannot be derived [For89, Rei98], but for special situations, where certain potential conditions are satisfied [GH71a, GH71b, Ris72, Gra74, Ris96], it is at least possible to construct a *Ljapunov functional*, which is a generalized dissipation functional for systems that can also be far from thermodynamic equilibrium and that are therefore not any more subject to linear irreversible thermodynamics. In the context of path integral methods in thermodynamics, dissipation functionals are closely related to the generalized Onsager-Machlup function of Graham [Gra77b, Gra78].

The DDFT equation (4.43) for active and passive colloidal particles with arbitrary shape, whose dynamics is solely dissipative, can be derived from a dissipation functional, too. For this purpose, the DDFT equation is written here as the conservation equation⁸

$$\dot{\rho} + \mathfrak{d}_i J_i^\rho = 0 \quad (4.49)$$

for the one-particle density field $\rho(\vec{\mathfrak{x}}, t)$ with the elements \mathfrak{d}_i of the generalized gradient operator $\vec{\nabla}_{\vec{\mathfrak{x}}} = (\mathfrak{d}_1, \dots, \mathfrak{d}_6)$ and with the dissipative one-particle density current

$$J_i^\rho = -\beta \mathcal{D}_{ij} \rho (\mathfrak{d}_j \rho^\natural - K_{A,j}) . \quad (4.50)$$

Here, the components of the diffusion tensor $\mathcal{D}(\vec{\mathfrak{x}})$ are denoted as $\mathcal{D}_{ij}(\vec{\mathfrak{x}})$, the thermodynamic conjugate $\rho^\natural(\vec{\mathfrak{x}}, t)$ (compare equation 5.64 in section 5.1.4.2) of the one-particle density $\rho(\vec{\mathfrak{x}}, t)$ is given by

$$\rho^\natural(\vec{\mathfrak{x}}, t) = \frac{\delta \mathcal{F}[\rho(\vec{\mathfrak{x}}, t)]}{\delta \rho(\vec{\mathfrak{x}}, t)} , \quad (4.51)$$

and $K_{A,i}$ are the components of the vector \vec{K}_A . The consideration of possible internal forces and torques through the vector \vec{K}_A is, however, only reasonable in the limit of a sufficiently small internal drive so that the system is not driven too far from local thermodynamic equilibrium. Since the one-particle density field $\rho(\vec{\mathfrak{x}}, t)$ is conserved, the

⁸Einstein's sum convention is used throughout this work.

thermodynamic force $\rho_i^\ddagger(\vec{\mathbf{x}}, t)$, that corresponds to the conjugated one-particle density field $\rho^\ddagger(\vec{\mathbf{x}}, t)$, is defined as $\rho_i^\ddagger(\vec{\mathbf{x}}, t) = -\mathfrak{d}_i \rho^\ddagger(\vec{\mathbf{x}}, t)$ (see section 5.1.4.2). The dissipative current $J_i^\rho(\vec{\mathbf{x}}, t)$ can therefore be derived from an appropriate dissipation functional \mathfrak{R} by the functional derivative

$$J_i^\rho = -\frac{\delta \mathfrak{R}}{\delta(\mathfrak{d}_i \rho^\ddagger)}. \quad (4.52)$$

This dissipation functional for the dissipative dynamics of the one-particle density field $\rho(\vec{\mathbf{x}}, t)$, that is described by the DDFT equation (4.43), is given by the expression

$$\mathfrak{R} = \frac{\beta}{2} \int_{\mathfrak{G}} d\mathfrak{V} \mathcal{D}_{ij} \rho (\mathfrak{d}_i \rho^\ddagger - K_{A,i}) (\mathfrak{d}_j \rho^\ddagger - K_{A,j}). \quad (4.53)$$

Also this expression can be reduced to the case of only two spatial dimensions by choosing $x_3 = 0$, $\theta = \pi/2$, and $\chi = 0$.

4.4 Applications and further development of DDFT

The generalized DDFT equation (4.43) for active and passive colloidal particles with arbitrary shape has many applications. While with previous versions of DDFT, biaxial colloidal particles could not be treated, the new version makes an investigation of the dynamics of arbitrary colloidal liquid crystals possible. In experiments, biaxial particles exhibit a great number of interesting additional liquid crystalline phases that cannot be observed with uniaxial particles. By numerical explorations, one could investigate, for example, the relaxation dynamics of colloidal systems toward equilibrium [RWL07], the response of these systems to time-dependent external potentials [HBL10], the nucleation kinetics of liquid crystalline phases [SF04, ZD06, MC09], and the growth of a thermodynamically stable phase into a metastable phase [TBVL09].

The generalized DDFT equation could further be used to model the collective Brownian motion of active particles like swarms of swimming microorganisms (see figure 4.1 on the next page). Interesting observable effects in the non-equilibrium dynamics of interacting active colloidal particles include self-organization, clustering [WL08], flocking, swarming [WL08, EG09], laning, turbulence, and jamming [PDB06, LGG⁺09]. In such numerical investigations, the external potential can also be time-dependent. Furthermore, the dissipation functional (4.53) that constitutes an alternative representation for the DDFT equation (4.43) can be used to derive the dynamics of PFC models (see next chapter). Especially for PFC models with various order-parameter fields, the corresponding dynamic equations can be derived much faster and much more easily with this dissipation functional than with the DDFT equation itself.

The results of numerical evaluations of the DDFT equation (4.43) should be compared with experiments and computer simulations [Sat10] like molecular dynamics simulations [L w94a, WCH01]. Additionally, the new DDFT equation could be further generalized. A very important success would be the generalization of DDFT toward

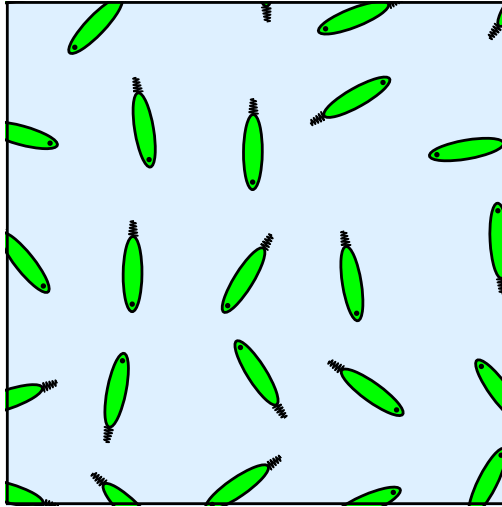


Figure 4.1: A swarm of swimming microorganisms, that are subjected to gravity and interact with each other, are a possible application of the DDFT equation for active colloidal particles [ES11].

the not overdamped molecular dynamics, where the inertia of the colloidal particles has to be taken into account in terms of a momentum density field. Such a generalization would be applicable to molecular liquid crystals and the dynamics would no longer be exclusively dissipative so that reversible currents [BCP09] could arise. Up to now, there are only several unsatisfying attempts by Marconi, Melchionna, Tarazona, and Cecconi [MTCM08, MM09, MM10] and by Archer [Arc06, Arc09] in this respect. Also a generalization of DDFT for mixtures of different species of colloidal particles would allow many new applications. The attempt of Archer in reference [Arc05] is a first step in this direction, but it has to be improved.

One of the most important possible generalizations of DDFT would be the incorporation of hydrodynamic interactions between the colloidal particles. This was indeed already done for spherical particles by Rex and Löwen [RL08, RL09] a few years ago, but remains to be done for anisotropic colloidal particles. Further goals for the future are the consideration of a flowing liquid, as it was regarded for spherical particles by Rauscher et al. [RDKP07], the back-reaction of the colloidal suspension on the flow field of the liquid, and colloidal suspensions in confinement. For confined colloidal systems, as they often appear in nanofluidics, the hydrodynamic interactions of the colloidal particles with the system boundaries have to be taken into account, too. This was recently done for spherical particles by Almenar and Rauscher [AR11], but is still an unsolved problem for anisotropic particles.

More special possible generalizations of DDFT could describe interacting colloidal particles in curved geometry as well as relativistic systems [Gra77a]. Finally, a systematic microscopic derivation of the dissipation functional (4.53) would be desirable as well. Such a derivation could provide a starting point for further generalizations of DDFT.

5 Statics and dynamics of colloidal liquid crystals

This chapter deals with the statics and dynamics of interacting colloidal particles in the form of apolar and polar colloidal liquid crystals. At the beginning, microscopic, mesoscopic, and macroscopic classical mean-field theories that can be used to derive models for colloidal liquid crystals are introduced. These mean-field theories are in particular DFT, PFC models, Ginzburg-Landau theory, and generalized hydrodynamics both in their static and dynamic versions. Afterwards, microscopic static DFT and DDFT are used to derive mesoscopic static and dynamic PFC models for apolar and polar colloidal liquid crystals in two and three spatial dimensions. Together with the dynamic equations, as well the corresponding dissipation functionals are given. Special cases of the derived PFC models, that are already known from the literature, are identified and the PFC model for apolar liquid crystals in two spatial dimensions is evaluated numerically. In doing so, phase diagrams are calculated and the arising liquid crystalline phases are discussed. Furthermore, all PFC models are compared with static and dynamic symmetry-based approaches on the basis of Ginzburg-Landau theory and generalized hydrodynamics. Finally, applications and possible extensions of the derived PFC models are addressed.

5.1 Classical mean-field theories for the modeling of liquid crystals

To describe the static and dynamic properties of colloidal liquid crystals, a great number of models and theories is available. Most of them are rather special and only applicable to very particular systems. Among them are *Onsager's hard-rod model* [Ons49, VL92] for the isotropic-nematic phase transition of lyotropic¹ liquid crystals, the *Maier-Saupe mean-field theory* [MS58, MS59, MS60] for the isotropic-nematic phase transition of thermotropic liquid crystals, the related *McMillan model* [McM71] for the nematic-smectic A phase transition, the *Ericksen-Leslie theory* [Eri59, Eri61, Les66] for the hydrodynamics of liquid crystals, and the *Landau-de Gennes theory* [Gen71, GP95] for liquid crystalline phase transitions. Because of their limited applicability, such special models and theories are not considered here. This section presents instead four

¹A liquid crystalline system is called *lyotropic*, if phase transitions are induced by a change of the concentration, and *thermotropic*, if a variation of the temperature leads to a phase transition.

very general theories that can be used to derive special models for arbitrary liquid crystalline systems and other complex fluids. These fundamental theories are classical *mean-field theories*, which implies that they describe a system using space- and time-dependent continuous density fields and that fluctuations are neglected. Table 5.1 gives an overview about these mean-field theories, their nomenclature, and their classification. Two of these theories, namely density functional theory and Ginzburg-Landau

Table 5.1: Classical mean-field theories for the modeling of complex fluids.

Type of the theory:	microscopic	mesoscopic	macroscopic	macroscopic
Type of the derivation:	microscopic	microscopic or symmetry-based	symmetry-based	symmetry-based
Name of the theory:	density functional theory (DFT)	phase field crystal (PFC) models	Ginzburg-Landau (GL) theory	generalized hydrodynamics
⇒ static version:	static DFT	static PFC models	static GL theory	generalized hydrostatics
⇒ dynamic version:	dynamical DFT (DDFT)	dynamic PFC models	dynamic GL theory	generalized hydrodynamics

theory, have well-known quantum mechanical complements, but these quantum mechanical theories are only relevant for problems of solid state physics and not considered in this work, which deals with the classical physics of colloidal dispersions. Except for dynamical density functional theory, the theories in table 5.1 are furthermore not only applicable to colloidal systems, but also to molecular and atomic fluids.

Classical *density functional theory* (DFT) can be used to describe a colloidal system on microscopic length and time scales. Such a microscopic description regards the microscopic correlations between the particles and the underlying thermodynamic conditions like temperature and chemical potential. Due to the involvement of microscopic correlation functions, the application of DFT is often very difficult and tedious. A simpler and more coarse-grained description is possible with *phase field crystal* (PFC) *models*. They describe a system on microscopic length and diffusive time scales and involve microscopic correlations at most through parameters that are generalized moments of microscopic correlation functions. These parameters do not necessarily need to be calculated from the microscopic correlation functions, but can also be used as fit parameters that may be determined by a comparison with experimental results or microscopic simulations. Although PFC models have already been applied successfully to various problems of hard and soft condensed matter physics, there are also systems like colloidal dispersions in a flowing liquid, where PFC models cannot be derived or where their derivation would be too complicated. In such situations, macroscopic theories, that describe the system on macroscopic length and time scales and do not consider microscopic correlations explicitly, can be applied. Two macroscopic mean-field theories are included in table 5.1. The first of them is classical *Ginzburg-Landau theory*

that can be used to describe thermodynamic systems in the vicinity of a phase transition. Systems in the bulk of a phase far away from phase transitions are in contrast described by the second theory, which is called *generalized hydrodynamics*.

All these theories include a static and a dynamic version. Static systems are addressed within each of these theories by the construction of a thermodynamic functional that corresponds to a suitable thermodynamic potential and that is approximatively expressed in terms of the thermodynamic variables of the system under consideration. This functional can be written as a spatial integral over a generalized energy density and in the context of DFT it can also be nonlocal. For the remaining theories, this functional is always local. A further difference between static DFT and the three other static mean-field theories is the fact that in the context of DFT also non-perturbative approximations for the thermodynamic functional exist, while PFC models, Ginzburg-Landau theory, and generalized hydrodynamics are perturbative. The thermodynamic variables that are used to parametrize the thermodynamic functional are assumed to be space- and time-dependent density fields. This is in contrast to the spatially homogeneous scalar variables like magnetization in the Landau theory of phase transitions of second order [CL95, LL08]. Aside from the space-dependent density fields, their gradients and higher-order derivatives also contribute to the generalized energy density. The local energy densities of PFC models and of the macroscopic theories are thus approximated by a *gradient expansion* in the thermodynamic variables. By partial integration in the thermodynamic functional, it is always possible to rearrange the terms of the gradient expansion. When unbounded systems are considered, as it is the case throughout this work, partial integration can especially be used in order to remove surface terms in the gradient expansion.

On the basis of a static model, the corresponding dynamics for the particular system can be derived also, if the system is close to thermodynamic equilibrium, where linear irreversible thermodynamics applies and Onsager's principle [LL08] holds. For each of the four fundamental mean-field theories, the dynamics is given by dynamic equations for the thermodynamic variables. The restriction on systems, that are close to thermodynamic equilibrium, is necessary, since the dynamic versions of the mean-field theories are also perturbative. They involve dynamic equations that are linear perturbative expansions about the equilibrium state of the thermodynamic system.

The fundamental mean-field theories mentioned use different types of thermodynamic potentials and thermodynamic variables. Static DFT is based on the grand canonical free-energy functional, while dynamical DFT is grounded on the Helmholtz free-energy functional. In the context of DFT, the functionals depend only on the one-particle density field. When mixtures of different species of colloidal particles are considered, the one-particle densities of all these types of colloidal particles contribute to the functional, but additional fields like an entropy density or equivalently a temperature density are not taken into account. Contrarily, static and dynamic PFC models use the Helmholtz free-energy functional and express the corresponding energy density by a gradient expansion in terms of one or several order-parameter fields. Simple PFC models deal usually only with the particle number density as order-parameter

field, but for the description of mixtures or systems with orientational degrees of freedom, further order-parameter fields have to be taken into account. However, it is not possible to consider arbitrary order-parameter fields in the context of DFT and PFC models. Velocity and momentum fields, for example, have up to now not been successfully incorporated in these theories. The situation is completely different for the macroscopic theories. Both Ginzburg-Landau theory and generalized hydrodynamics use an arbitrary thermodynamic functional, that is most appropriate for the considered system, and various thermodynamic variables. Regarding these theories, the most common choice for the functional is the internal energy functional, but equivalently other functionals like the Helmholtz free-energy functional can be used. A main difference between Ginzburg-Landau theory and generalized hydrodynamics consists in the choice of the thermodynamic variables. In the context of Ginzburg-Landau theory, the order-parameter fields, that define the considered phase transition, are chosen, while for the application of generalized hydrodynamics the hydrodynamic variables of the system must be determined. In addition to the hydrodynamic variables, it is sometimes necessary to include additional non-hydrodynamic macroscopic variables leading to a *generalized macroscopic model*.

On a very general level, the mean-field theories can be distinguished with respect to their type. The only truly *microscopic* theory among them is DFT. Against this, the more coarse-grained description by means of a PFC model is called *mesoscopic*. Ginzburg-Landau theory and generalized hydrodynamics are even more coarse-grained and therefore termed *macroscopic* theories. While all theories can be used to derive special models for particular thermodynamic systems on certain length and time scales, macroscopic models can be derived both from macroscopic and microscopic theories. The mesoscopic PFC models can be derived from microscopic DFT and further compared with macroscopic models on the basis of Ginzburg-Landau theory or generalized hydrodynamics. Such a derivation of mesoscopic and macroscopic models from microscopic theories helps to clarify the relations between the different theories and constitutes a bridge from microscopic to macroscopic modeling (see the next sections of this chapter). Although there are always microscopic theories, where a certain model can be derived from, one should not make it a rule, since macroscopic derivations are usually much simpler and can be performed faster. The derivation of a particular PFC model from DFT is, for example, very complicated and time consuming. Sometimes it is not possible at all within an acceptable effort.

Macroscopic theories use general conservation laws, symmetry considerations, and basic thermodynamic principles instead of microscopic calculations involving various correlation functions in order to derive a macroscopic model. PFC models can also be derived with the help of such general considerations. Symmetry-based macroscopic theories are in general very powerful and elegant, since they allow faster and more general derivations than microscopic theories. The symmetries that are considered in a symmetry-based macroscopic derivation are the basic symmetries of the system that has to be described. In the case of Ginzburg-Landau theory, one considers the joint symmetries of the adjacent phases at the phase transition regarded, and for deriva-

tions by means of generalized hydrodynamics, one chooses the symmetry properties of the described bulk phase. Symmetries that have to be considered regularly are, for example, time reversal symmetry, parity inversion symmetry, invariance against global translations and rotations, and behavior under Galilean transformations.

Symmetry-based macroscopic derivations unfortunately have two big disadvantages. The first of them is the obvious inability to describe systems on a microscopic length and time scale and the second drawback is the appearance of a number of unknown parameters that cannot be determined within the macroscopic theories², in the symmetry-based models. The same parameters also appear in microscopically derived models, but there, they are given explicitly in the form of analytic expressions that involve microscopic correlation functions and the underlying thermodynamic conditions like temperature and mean particle density. Unknown parameters do not exist in microscopic derivations and are a special feature of symmetry-based macroscopic models. The unknown parameters of macroscopic theories can always depend on all scalar quantities of the described system like temperature, mean particle number density, and modulus of polarization. When certain values have to be assigned to these parameters and they shall not be derived from microscopic theories, the parameters can be fitted to results from experiments and microscopic simulations. A famous example in this context is the macroscopic *quantum mechanical Ginzburg-Landau theory* [GL50] that was proposed in 1950 by Ginzburg and Landau in order to model superconductivity. This theory contains an unknown charge parameter q that was determined not until the derivation of the microscopic *Bardeen-Cooper-Schrieffer (BCS) theory* [BCS57a, BCS57b] in 1957. By comparison with the BCS theory, the identification $q = -2e$ with the elementary charge e was concluded and could be related to the charge of a Cooper pair.

In the following paragraphs of this section, the fundamental mean-field theories, that are summarized in table 5.1 on page 54, are described in detail. To simplify the presentation, many exemplary expressions given are rather special and only formulated for systems with three spatial dimensions in the domain $\mathcal{V} = \mathbb{R}^3$. Nevertheless, analogous expressions can be formulated for two spatial dimensions as well as for more complicated situations.

5.1.1 Density functional theory

Originally, classical DFT comprised only a static theory for equilibrium systems. This static classical DFT is a microscopic theory for inhomogeneous complex fluids [Eva79, Sin91, Löw94d, Rot10] that needs only the particle interactions and the underlying thermodynamic conditions as input. It is an adaptation of the quantum mechanical DFT of Kohn, Hohenberg, and Sham [HK64, KS65] that was first proposed in the 1960s. The classical adaptation goes back to the work of Ebner, Saam, Yang, et al. [ESS76, YFG76, SE77] in the 1970s and in the meantime proved to be a very useful

²Unknown parameters of macroscopic theories can only be determined in combination with an appropriate microscopic model. With such a model, it is, for example, possible to relate transport coefficients of generalized hydrodynamics to correlation functions [For89].

tool in soft condensed matter physics. Static DFT describes inhomogeneous fluids and crystallization of an ensemble of colloidal particles in an external potential on microscopic length and time scales. It is typically used for isotropic particles [Eva79, Sin91, RELK02], but it can also be applied to anisotropic particles [PH88, GL99, HM09, Löw10b]. The applications of static DFT include crystallization and melting in equilibrium [RY79, Sin91, Löw94d, RSLT97], anisotropic liquids in confinement and in external potentials [Eva79, GL99], as well as fluid-fluid interfaces [Eva79]. Further information about this theory and a detailed historic overview can be found in several articles and books like [CA86, Eva92, Löw02, HM06, Kal10].

In contrast to static DFT, its dynamic extension for non-equilibrium problems, dynamical DFT (DDFT), is a rather new theory. It was first derived for isotropic particles by Marconi and Tarazona [MT99, MT00] from a Langevin equation in 1999. Then the same DDFT was rederived by Archer and Evans [AE04] from a Smoluchowski equation in 2004 and finally Español and Löwen [EL09] rederived it again now using a projection operator technique in 2009. The first generalization of DDFT to special non-spherical particles was achieved by Rex, Wensink, and Löwen [RWL07] in 2007. In the meantime, DDFT has been generalized for many particular applications. The most important generalizations and especially the derivation of a generalized DDFT for arbitrarily shaped particles are described in chapter 4.

5.1.1.1 Static density functional theory

Static DFT describes a system of N colloidal particles, whose center-of-mass positions and orientations are defined through the vectors $\vec{\mathbf{x}}_i$ with $i \in \{1, \dots, N\}$, by a one-particle density field $\rho(\vec{\mathbf{r}})$. This one-particle density field is proportional to the probability density to find a colloidal particle at a certain position with a certain orientation. Due to its dependence on the Eulerian angles that are incorporated by the vector $\vec{\mathbf{r}}$, the one-particle density field $\rho(\vec{\mathbf{r}})$ characterizes an ensemble of colloidal particles with arbitrary shape. When only uniaxial particles are considered, it is sufficient to denote the orientation of a colloidal particle by a unit vector \hat{u} instead of the Eulerian angles $\vec{\omega}$, where the orientational unit vector \hat{u} should be chosen parallel to the axis of symmetry of the respective uniaxial colloidal particle. For spherical particles it is not necessary to denote their orientation at all. In this case, the equilibrium one-particle density field depends only on the position \vec{r} . Nevertheless, the most general notation is used in the following to take arbitrarily shaped particles into account as well. The field $\rho(\vec{\mathbf{r}})$ that is used in the general case for static DFT is the ensemble-averaged *one-particle density*

$$\rho(\vec{\mathbf{r}}) = \left\langle \sum_{i=1}^N \delta(\vec{\mathbf{r}} - \vec{\mathbf{x}}_i) \right\rangle \quad (5.1)$$

with the normalized classical canonical ensemble-average $\langle \cdot \rangle$. Static DFT is based on a theorem and on a variational principle.

The **basic theorem** of static DFT can be formulated as follows:

The grand canonical functional³ $\Omega(T, \mu, [\rho(\vec{\mathbf{r}})])$ exists and is a unique functional of the one-particle density $\rho(\vec{\mathbf{r}})$ for a given temperature T and chemical potential μ .

This theorem is complemented by the **variational principle** of static DFT:

At fixed temperature T and chemical potential μ , the equilibrium one-particle density $\rho(\vec{\mathbf{r}})$ minimizes the grand canonical functional:

$$\frac{\delta\Omega(T, \mu, [\rho(\vec{\mathbf{r}})])}{\delta\rho(\vec{\mathbf{r}})} = 0 . \quad (5.2)$$

The value of the grand canonical functional $\Omega(T, \mu, [\rho(\vec{\mathbf{r}})])$ at the equilibrium one-particle density $\rho(\vec{\mathbf{r}})$ is the equilibrium grand canonical free energy of the system.

Static DFT thus establishes a basis for the determination of the equilibrium one-particle density field $\rho(\vec{\mathbf{r}})$ of an arbitrary colloidal system. The difficulty in the application of static DFT consists in the necessity of a good approximation for the grand canonical functional $\Omega(T, \mu, [\rho(\vec{\mathbf{r}})])$. In general, the grand canonical functional can be related to the equivalent Helmholtz free-energy functional $\mathcal{F}(T, [\rho(\vec{\mathbf{r}})])$ with the help of the *Legendre transformation*⁴

$$\Omega(T, \mu, [\rho(\vec{\mathbf{r}})]) = \mathcal{F}(T, [\rho(\vec{\mathbf{r}})]) - \mu \int_{\mathfrak{G}} d\mathfrak{V} \rho(\vec{\mathbf{r}}) . \quad (5.3)$$

The Helmholtz free-energy functional $\mathcal{F}(T, [\rho(\vec{\mathbf{r}})])$ in turn can be decomposed into three separate contributions:

$$\mathcal{F}(T, [\rho(\vec{\mathbf{r}})]) = \mathcal{F}_{\text{id}}(T, [\rho(\vec{\mathbf{r}})]) + \mathcal{F}_{\text{exc}}(T, [\rho(\vec{\mathbf{r}})]) + \mathcal{F}_{\text{ext}}(T, [\rho(\vec{\mathbf{r}})]) . \quad (5.4)$$

Its first contribution is the *ideal rotator-gas free-energy functional*⁵ [Eva79]

$$\beta\mathcal{F}_{\text{id}}(T, [\rho(\vec{\mathbf{r}})]) = \int_{\mathfrak{G}} d\mathfrak{V} \rho(\vec{\mathbf{r}}) (\ln(\Lambda^3 \rho(\vec{\mathbf{r}})) - 1) \quad (5.5)$$

with the thermal de Broglie wavelength Λ . It describes the free energy of an ideal rotator gas, i. e., of non-interacting anisotropic particles in the absence of external forces and torques. The second term on the right-hand-side of equation (5.4) is the *excess free-energy functional* $\mathcal{F}_{\text{exc}}(T, [\rho(\vec{\mathbf{r}})])$. For this term, a general analytic expression is not

³The grand canonical functional $\Omega(T, \mu, [\rho(\vec{\mathbf{r}})])$ is also called *density functional* in the context of DFT.

⁴The spatially homogeneous parameters T and μ are often omitted in the arguments of the functionals $\Omega(T, \mu, [\rho(\vec{\mathbf{r}})])$ and $\mathcal{F}(T, [\rho(\vec{\mathbf{r}})])$.

⁵This is different from the quantum mechanical DFT, where it is much more difficult to represent the kinetic energy as a functional of the electron density.

available. This contribution incorporates all correlations due to interactions between the particles and needs to be approximated appropriately [Eva79, Sin91]. The last contribution is the *external free-energy functional* [Eva79]

$$\mathcal{F}_{\text{ext}}(T, [\rho(\vec{\mathbf{r}})]) = \int_{\mathfrak{G}} d\mathfrak{Y} \rho(\vec{\mathbf{r}}) U_1(\vec{\mathbf{r}}), \quad (5.6)$$

which regards the influence of an external potential $U_1(\vec{\mathbf{r}})$ on the free energy of the system. Such a potential includes the effects of system boundaries, gravitational fields, and laser fields on the considered colloidal dispersion. Since analytic expressions are available for the ideal rotator-gas free-energy functional $\mathcal{F}_{\text{id}}(T, [\rho(\vec{\mathbf{r}})])$ and for the external free-energy functional $\mathcal{F}_{\text{ext}}(T, [\rho(\vec{\mathbf{r}})])$, the main problem in the context of DFT is the approximation of the excess free-energy functional $\mathcal{F}_{\text{exc}}(T, [\rho(\vec{\mathbf{r}})])$. An exact analytic expression for this functional exists only for an ideal gas, where this contribution to the total free-energy functional vanishes, and for hard rods in one spatial dimension, but several possible approximations with different advantages and disadvantages including perturbative as well as non-perturbative approximations are currently available. A natural perturbative approximation for the excess free-energy functional is a functional Taylor expansion in the density variation $\Delta\rho(\vec{\mathbf{r}}) = \rho(\vec{\mathbf{r}}) - \bar{\rho}$ around a homogeneous reference density $\bar{\rho}$ [Eva79, RY79]:

$$\beta\mathcal{F}_{\text{exc}}(T, [\rho(\vec{\mathbf{r}})]) = \beta\mathcal{F}_{\text{exc}}^{(0)}(\bar{\rho}) - \sum_{n=1}^{\infty} \frac{1}{n!} \mathcal{F}_{\text{exc}}^{(n)}(T, [\rho(\vec{\mathbf{r}})]). \quad (5.7)$$

The n th-order contribution $\mathcal{F}_{\text{exc}}^{(n)}(T, [\rho(\vec{\mathbf{r}})])$ in this functional Taylor expansion considers the n -particle correlations of the colloidal particles. Its explicit dependence on the n th-order direct correlation function $c^{(n)}(\vec{\mathbf{r}}_1, \dots, \vec{\mathbf{r}}_n)$ of the homogeneous bulk reference fluid follows directly from the elementary relation [HM06]

$$c^{(n)}(\vec{\mathbf{r}}_1, \dots, \vec{\mathbf{r}}_n) = -\beta \frac{\delta^n \mathcal{F}_{\text{exc}}(T, [\rho(\vec{\mathbf{r}})])}{\delta\rho(\vec{\mathbf{r}}_1) \cdots \delta\rho(\vec{\mathbf{r}}_n)}. \quad (5.8)$$

With this relation, the n th-order contribution of the functional Taylor expansion obtains the form

$$\mathcal{F}_{\text{exc}}^{(n)}(T, [\rho(\vec{\mathbf{r}})]) = \int_{\mathfrak{G}} d\mathfrak{Y}_1 \cdots \int_{\mathfrak{G}} d\mathfrak{Y}_n c^{(n)}(\vec{\mathbf{r}}_1, \dots, \vec{\mathbf{r}}_n) \prod_{i=1}^n \Delta\rho(\vec{\mathbf{r}}_i) \quad (5.9)$$

with the differentials $d\mathfrak{Y}_i = d^6\mathbf{r}_i$. In the functional Taylor expansion (5.7), the zeroth-order contribution $\mathcal{F}_{\text{exc}}^{(0)}(\bar{\rho})$ is constant and can therefore be neglected. The first-order contribution corresponding to $n = 1$ can be neglected, too, since it is zero. This follows from the representation (5.9) under consideration of the translational and rotational symmetries of the isotropic bulk fluid that also apply to the direct correlation function $c^{(1)}(\vec{\mathbf{r}}_1) = \text{const.}$ The other terms in the functional Taylor expansion with $n > 1$ are

due to the translational and rotational symmetries of the direct correlation functions⁶ nonlocal and in general not zero. For many situations it is sufficient to take pair-correlations between the particles into account and to truncate the functional Taylor expansion at second order. The resulting approximation is known as the *Ramakrishnan-Yussouff approximation* [RY79]

$$\beta\mathcal{F}_{\text{exc}}(T, [\rho(\vec{\mathfrak{r}})]) = -\frac{1}{2} \int_{\mathfrak{G}} d\mathfrak{W}_1 \int_{\mathfrak{G}} d\mathfrak{W}_2 c^{(2)}(\vec{\mathfrak{r}}_1, \vec{\mathfrak{r}}_2) \Delta\rho(\vec{\mathfrak{r}}_1) \Delta\rho(\vec{\mathfrak{r}}_2) \quad (5.10)$$

and has been proved to predict the freezing transition of hard spheres both in three [RY79] and two spatial dimensions [TLHL06] accurately. More refined approaches include also the third-order term [Bar87] with an approximate triplet direct correlation function [BHP87, BHP88] or even the fourth-order term [WLB11b]. The main problem of the Ramakrishnan-Yussouff approximation is its dependence on the in general unknown direct pair-correlation function $c^{(2)}(\vec{\mathfrak{r}}_1, \vec{\mathfrak{r}}_2)$. Approximations for this direct pair-correlation function can, for example, be obtained from microscopic simulations. There are also some more or less appropriate analytic approximations for the direct pair-correlation function in terms of the pair-interaction potential $U_2(\vec{\mathfrak{r}}_1, \vec{\mathfrak{r}}_2)$ that defines the interactions between two particles, whose positions and orientations are given by the vectors $\vec{\mathfrak{r}}_1$ and $\vec{\mathfrak{r}}_2$. Well-known analytic approximations for the direct pair-correlation function include the second-order *virial expression* [RBMF95]

$$c^{(2)}(\vec{\mathfrak{r}}_1, \vec{\mathfrak{r}}_2) = e^{-\beta U_2(\vec{\mathfrak{r}}_1, \vec{\mathfrak{r}}_2)} - 1, \quad (5.11)$$

which leads in combination with the Ramakrishnan-Yussouff approximation (5.10) to the *Onsager functional* for the excess free energy that becomes asymptotically exact in the low density limit [Fre91]. An alternative is the *random-phase approximation*⁷ [RWL07]

$$c^{(2)}(\vec{\mathfrak{r}}_1, \vec{\mathfrak{r}}_2) = -\beta U_2(\vec{\mathfrak{r}}_1, \vec{\mathfrak{r}}_2). \quad (5.12)$$

For bounded potentials, this mean-field approximation becomes asymptotically exact at high densities [RWL07]. A further possibility to construct an excess free-energy functional for colloidal particles is a mean-field approximation for repulsive segment potentials [RWL07]. More accurate expressions for the excess free-energy functional for colloidal particles are given by *weighted-density approximations* [PH88, GL99] or follow from *fundamental measure theory* [HM09, HM10]. In contrast to the functional Taylor expansion (5.7), fundamental measure theory is a non-perturbative theory that includes correlation functions of arbitrarily high order. It was originally introduced in 1989 by Rosenfeld for isotropic particles [Ros89, Eva92], later improved by Rosenfeld

⁶Since the functional Taylor expansion (5.7) was performed about the isotropic phase of a homogeneous reference fluid with short-range order, also the direct correlation functions (5.8) are isotropic and short-ranged [PE10].

⁷This expression makes obvious that the symmetries of the pair-interaction potential $U_2(\vec{\mathfrak{r}}_1, \vec{\mathfrak{r}}_2)$ apply also to the direct pair-correlation function $c^{(2)}(\vec{\mathfrak{r}}_1, \vec{\mathfrak{r}}_2)$, if no additional symmetry-breaking objects are present.

et al. [RSLT96, RSLT97, RELK02], then generalized to arbitrarily shaped particles by Rosenfeld [Ros94], and finally optimized by Hansen-Goos and Mecke [HM09, HM10]. Especially for convex particles, fundamental measure theory provides in general very good approximations for the excess free-energy functional.

5.1.1.2 Dynamical density functional theory

The nomenclature of dynamical DFT (DDFT) is not yet unified. DDFT was originally called “dynamic density functional theory” by Marconi and Tarazona [MT99]. Later, the term “dynamical density functional theory”, that is used throughout this work, was introduced by Archer and Evans [AE04]. Their naming is presently widely used, but sometimes DDFT is also called “time-dependent density functional theory”. DDFT is the time-dependent analog of static DFT and can be classified as *linear-response theory*. It describes the slow dissipative non-equilibrium relaxation dynamics of a system of N colloidal particles near thermodynamic equilibrium. The basis of DDFT consists in a deterministic dynamic equation, the *DDFT equation*, that describes the time-evolution of the time-dependent noise-averaged non-equilibrium one-particle density field

$$\rho(\vec{\mathbf{r}}, t) = \left\langle \sum_{i=1}^N \delta(\vec{\mathbf{r}} - \vec{\mathbf{r}}_i(t)) \right\rangle, \quad (5.13)$$

where $\langle \cdot \rangle$ denotes the normalized classical canonical noise-average. This one-particle density is conserved and its dynamics is assumed to be dissipative. The simplest reasonable DDFT equation describes N equal spherical colloidal particles that are immersed in a quiescent and homogeneous viscous liquid with constant temperature T . When the colloidal dispersion is sufficiently dilute so that hydrodynamic interactions between the colloidal particles can be neglected, the overdamped Brownian motion [Dho96] of these colloidal particles can be described by the *simple DDFT equation*

$$\frac{\partial \rho(\vec{\mathbf{r}}, t)}{\partial t} = \beta D_{\text{T}} \vec{\nabla}_{\vec{\mathbf{r}}} \cdot \left(\rho(\vec{\mathbf{r}}, t) \vec{\nabla}_{\vec{\mathbf{r}}} \frac{\delta \mathcal{F}(T, [\rho(\vec{\mathbf{r}}, t)])}{\delta \rho(\vec{\mathbf{r}}, t)} \right) \quad (5.14)$$

with the translational diffusion coefficient D_{T} . The structure of this DDFT equation reveals directly the linear-response character of DDFT. Referring to equations (5.2) and (5.3), the functional derivative in the DDFT equation can be interpreted as the *chemical potential*

$$\mu(\vec{\mathbf{r}}, t) = \frac{\delta \mathcal{F}(T, [\rho(\vec{\mathbf{r}}, t)])}{\delta \rho(\vec{\mathbf{r}}, t)}, \quad (5.15)$$

which is – in contrast to static DFT – now space- and time-dependent and drives the dynamics toward thermodynamic equilibrium. In practice, the time-dependent free-energy functional $\mathcal{F}(T, [\rho(\vec{\mathbf{r}}, t)])$ is not known and approximated by the equilibrium free-energy functional of static DFT. The instantaneous dynamic correlations of the colloidal particles are thus replaced by the equilibrium correlations of a sim-

ilar colloidal system with a modified external potential $\bar{U}_1(\vec{r})$ that is in thermodynamic equilibrium and has the same spatial one-particle density distribution. It can be shown generally that such a modified external potential exists for any physical instantaneous one-particle density distribution and that it is a unique functional of the equilibrium one-particle density field [Eva79]. This approximation of the instantaneous time-dependent correlation functions of a non-equilibrium system by the static correlations of a comparable equilibrium system is called *adiabatic approximation*⁸ and constitutes the main approximation in the derivation of current DDFT. It implies that all other fields besides the one-particle density field like, for example, all many-particle density fields and the momentum density field of the colloidal dispersion relax much faster than the one-particle density field itself [EL09]. The adiabatic approximation is the reason, why DDFT applies only for dissipative systems close to thermodynamic equilibrium and fails for systems that are driven far out of thermodynamic equilibrium. Actually, DDFT can be interpreted as a linear time-dependent perturbation of static DFT about the equilibrium state. This illustrates its linear-response character and its affiliation to the theories of linear irreversible thermodynamics.

The simple DDFT equation (5.14) can be derived⁹ from the Langevin equations that describe the stochastic motion of the N isotropic colloidal particles in a liquid with dynamic viscosity η (compare chapter 3). These coupled Langevin equations for the positions $\vec{r}_i(t)$ of the colloidal spheres with radius R_s are given by [Dho96, Ris96]

$$\dot{\vec{r}}_i = \xi^{-1}(\vec{F}_i + \vec{f}_i), \quad i = 1, \dots, N \quad (5.16)$$

with the Stokesian friction coefficient $\xi = 6\pi\eta R_s$ and with the forces

$$\vec{F}_i(t) = -\vec{\nabla}_{\vec{r}_i} U(\vec{r}_1, \dots, \vec{r}_N, t), \quad (5.17)$$

that are caused by the total potential

$$U(\vec{r}_1, \dots, \vec{r}_N, t) = U_{\text{ext}}(\vec{r}_1, \dots, \vec{r}_N, t) + U_{\text{int}}(\vec{r}_1, \dots, \vec{r}_N). \quad (5.18)$$

This potential has two different contributions. The first one is the total external potential

$$U_{\text{ext}}(\vec{r}_1, \dots, \vec{r}_N, t) = \sum_{i=1}^N U_1(\vec{r}_i, t), \quad (5.19)$$

that describes the influence of an external potential $U_1(\vec{r}, t)$ on the colloidal particles, and the second contribution is the total particle interaction potential

$$U_{\text{int}}(\vec{r}_1, \dots, \vec{r}_N) = \sum_{\substack{i,j=1 \\ i < j}}^N U_2(\vec{r}_i, \vec{r}_j). \quad (5.20)$$

⁸The term *adiabatic approximation* refers to the *adiabatic theorem* of quantum mechanics and has nothing to do with adiabatic processes in thermodynamics.

⁹The following derivation can be found in several references like [TBVL09, Löw10b].

It incorporates the pair-interaction potentials $U_2(\vec{r}_i, \vec{r}_j)$ for the interactions between the particles i and j . In general, also three-body and higher-order interaction potentials could be taken into account, but they are irrelevant for colloidal systems and therefore neglected here. Furthermore, both the one-particle potentials $U_1(\vec{r}_i, t)$ and the two-particle interaction potentials $U_2(\vec{r}_i, \vec{r}_j)$ are assumed to be pairwise additive [GG84]. Aside from the deterministic forces $\vec{F}_i(t)$, also stochastic forces $\vec{f}_i(t)$ due to thermal fluctuations act on the Brownian particles. These random forces are modeled by Gaussian white noises with vanishing mean values

$$\langle \vec{f}_i(t) \rangle = \vec{0} \quad (5.21)$$

and with the singular correlations

$$\langle \vec{f}_i(t_1) \otimes \vec{f}_j(t_2) \rangle = \mathbb{1} \frac{2\xi}{\beta} \delta_{ij} \delta(t_1 - t_2), \quad (5.22)$$

where $\langle \cdot \rangle$ is a normalized noise average and $\mathbb{1}$ denotes the 3×3 -dimensional unit matrix. This modeling of the stochastic forces is in accordance with the fluctuation-dissipation theorem. In the special case of spherical particles, the fluctuation-dissipation theorem involves Einstein's fluctuation-dissipation relation $D_T = 1/(\beta\xi)$ [Ein05] that relates the translational short-time diffusion coefficient D_T of the colloidal particles to the friction coefficient ξ . This route with a set of coupled Langevin equations was chosen by Marconi and Tarazona [MT99, MT00] for their derivation of the DDFT equation. For the further derivation, it is, however, more convenient to replace the Langevin equations (5.16) by an equivalent Smoluchowski equation (compare chapter 4), as it was done by Archer and Evans [AE04] in their alternative derivation of the DDFT equation. In contrast to Langevin equations, a Smoluchowski equation describes not the particular stochastic trajectories of the colloidal particles, but the time-evolution of the N -particle probability density $P(\vec{r}_1, \dots, \vec{r}_N, t)$. The particular Smoluchowski equation, that corresponds to the Langevin equations (5.16), is given by [Smo16, Ris96]

$$\dot{P}(\vec{r}_1, \dots, \vec{r}_N, t) = \hat{\mathcal{L}} P(\vec{r}_1, \dots, \vec{r}_N, t) \quad (5.23)$$

with the Smoluchowski operator

$$\hat{\mathcal{L}} = D_T \sum_{i=1}^N \vec{\nabla}_{\vec{r}_i} \cdot (\beta \vec{\nabla}_{\vec{r}_i} U(\vec{r}_1, \dots, \vec{r}_N, t) + \vec{\nabla}_{\vec{r}_i}). \quad (5.24)$$

The N -particle probability density $P(\vec{r}_1, \dots, \vec{r}_N, t)$ in this Smoluchowski equation is a very complicated function and for usual purposes not required. It is often sufficient to consider the one-particle probability density $P(\vec{r}, t)$ that is proportional to the one-particle number density $\rho(\vec{r}, t)$. In general, all n -particle densities with $1 \leq n \leq N$ can be obtained from the N -particle probability density $P(\vec{r}_1, \dots, \vec{r}_N, t)$ by integration

over the negligible degrees of freedom:

$$\rho^{(n)}(\vec{r}_1, \dots, \vec{r}_n, t) = \frac{N!}{(N-n)!} \int_{\mathcal{V}} dV_{n+1} \cdots \int_{\mathcal{V}} dV_N P(\vec{r}_1, \dots, \vec{r}_N, t). \quad (5.25)$$

It is thus possible to derive a dynamic equation for the one-particle density field $\rho(\vec{r}, t) \equiv \rho^{(1)}(\vec{r}_1, t)$ from the Smoluchowski equation (5.23) by integration over the positions of $N-1$ particles. This integration results in the equation

$$\dot{\rho}(\vec{r}, t) = D_T \vec{\nabla}_{\vec{r}} \cdot (\vec{\nabla}_{\vec{r}} \rho(\vec{r}, t) - \beta \bar{F}(\vec{r}, t) + \beta \rho(\vec{r}, t) \vec{\nabla}_{\vec{r}} U_1(\vec{r}, t)) \quad (5.26)$$

for the one-particle density $\rho(\vec{r}, t)$ with the average force density

$$\bar{F}(\vec{r}, t) = - \int_{\mathcal{V}} dV' \rho^{(2)}(\vec{r}, \vec{r}', t) \vec{\nabla}_{\vec{r}} U_2(\vec{r}, \vec{r}'), \quad (5.27)$$

that in turn depends on the two-particle density $\rho^{(2)}(\vec{r}_1, \vec{r}_2, t)$. By integration over $N-2$ position variables, also a dynamic equation for the two-particle density could be derived from the Smoluchowski equation, but this equation would again depend on the three-particle density and so on resulting in a BBGKY hierarchy of dependent dynamic equations for many-particle densities of increasing order. This hierarchy of equations must be truncated at a certain order. In the context of DDFT, it is directly truncated after the first order so that a suitable approximation for the average force $\bar{F}(\vec{r}, t)$, that depends on the unknown two-particle density, is required. The average force $\bar{F}(\vec{r}, t)$ and the other terms in the outer round brackets on the right-hand-side of equation (5.26) can be expressed by the functional derivative of the *equilibrium*¹⁰ Helmholtz free-energy functional $\mathcal{F}(T, [\rho(\vec{r}, t)])$ with respect to the one-particle density $\rho(\vec{r}, t)$. The first term in the round brackets on the right-hand-side of equation (5.26) can be related to the ideal gas free-energy functional, which is the special case of the ideal rotator-gas free-energy functional (5.5) for spherical particles without orientational degrees of freedom. A functional derivation of equation (5.5) with respect to the one-particle density and the successive application of a spatial gradient leads to the relation

$$\vec{\nabla}_{\vec{r}} \rho(\vec{r}, t) = \beta \rho(\vec{r}, t) \vec{\nabla}_{\vec{r}} \frac{\delta \mathcal{F}_{\text{id}}(T, [\rho(\vec{r}, t)])}{\delta \rho(\vec{r}, t)}. \quad (5.28)$$

The second term in the round brackets of equation (5.26) is the problematic term and has to be approximated appropriately. For this purpose, the variational principle (5.2) is applied to the *equilibrium* grand canonical functional (5.3) under consideration of the decomposition (5.4). With equations (5.5), (5.6), and (5.8), this results in the

¹⁰The equilibrium Helmholtz free-energy functional $\mathcal{F}(T, [\rho(\vec{r})])$ becomes time-dependent, when the equilibrium one-particle density $\rho(\vec{r})$ is replaced by the time-dependent one-particle density $\rho(\vec{r}, t)$, but the resulting functional is *not* the non-equilibrium Helmholtz free-energy functional, but only an approximation for it.

expression

$$c^{(1)}(\vec{r}) = \ln(\Lambda^3 \rho(\vec{r})) + \beta(\bar{U}_1(\vec{r}) - \mu) \quad (5.29)$$

for the equilibrium direct correlation function $c^{(1)}(\vec{r})$, where the “substitute” external potential $\bar{U}_1(\vec{r})$ is assumed to be time-independent. From this equation, the equilibrium expression [LMB76]

$$\rho(\vec{r}) \vec{\nabla}_{\vec{r}} c^{(1)}(\vec{r}) = \vec{\nabla}_{\vec{r}} \rho(\vec{r}) + \beta \rho(\vec{r}) \vec{\nabla}_{\vec{r}} \bar{U}_1(\vec{r}) \quad (5.30)$$

follows directly. This expression can be compared with another equilibrium relation that follows from equation (5.26) in the equilibrium limit and is known as the first equation of the YBG hierarchy [HM06]:

$$\vec{\nabla}_{\vec{r}} \rho(\vec{r}) + \beta \rho(\vec{r}) \vec{\nabla}_{\vec{r}} \bar{U}_1(\vec{r}) = \beta \bar{F}(\vec{r}) . \quad (5.31)$$

Under consideration of equation (5.8) for $n = 1$, a comparison of equations (5.30) and (5.31) leads to the equilibrium relation

$$\bar{F}(\vec{r}) = -\rho(\vec{r}) \vec{\nabla}_{\vec{r}} \frac{\delta \mathcal{F}_{\text{exc}}(T, [\rho(\vec{r})])}{\delta \rho(\vec{r})} \quad (5.32)$$

for the average force density $\bar{F}(\vec{r})$ in thermodynamic equilibrium. The adiabatic approximation consists now in the application of this relation to non-equilibrium situations:

$$-\beta \bar{F}(\vec{r}, t) \approx \beta \rho(\vec{r}, t) \vec{\nabla}_{\vec{r}} \frac{\delta \mathcal{F}_{\text{exc}}(T, [\rho(\vec{r}, t)])}{\delta \rho(\vec{r}, t)} . \quad (5.33)$$

It still remains to relate the last term in the round brackets on the right-hand-side of equation (5.26) to the Helmholtz free-energy functional. This can easily be done by a functional and spatial derivation of equation (5.6) yielding to the expression

$$\beta \rho(\vec{r}, t) \vec{\nabla}_{\vec{r}} U_1(\vec{r}, t) = \beta \rho(\vec{r}, t) \vec{\nabla}_{\vec{r}} \frac{\delta \mathcal{F}_{\text{ext}}(T, [\rho(\vec{r}, t)])}{\delta \rho(\vec{r}, t)} . \quad (5.34)$$

The relations (5.28), (5.33), and (5.34) can now be inserted into equation (5.26). When finally the decomposition (5.4) is reversed in the resulting expression, the simple DDFT equation (5.14) for isotropic particles is obtained.

As a further equivalent alternative to the usage of Langevin equations, one can also utilize a projection operator technique in order to derive the DDFT equation. This possibility was pursued by Español and Löwen [EL09] in their derivation of the DDFT equation, but it is more complicated and less intuitive than the derivation that is presented in this section. Aside from the three alternative derivations for the simple DDFT equation (5.14), a few further extensions of DDFT have been proposed in recent years. For a short historic overview over the establishment and further development of DDFT including the newest generalizations, see chapter 4.

5.1.2 Phase field crystal models

The first *phase field crystal* (PFC) *model* has been developed by Elder et al. [EKHG02] in 2002 as an improvement of the older *phase field* (PF) *models*. Static PFC models are useful for the description of colloidal systems in thermodynamic equilibrium, while dynamic PFC models provide the corresponding non-equilibrium dynamics. Similar to static DFT, static PFC models are based on an equilibrium Helmholtz free-energy functional in terms of an order-parameter field that describes the thermodynamic state of the regarded system and can often be interpreted as the particle number density. Dynamic PFC models, on the other hand, consist in a dynamic equation for the time-evolution of the order-parameter field and need the static free-energy functional as input. The derivation of static and dynamic PFC models is in principle possible in two different ways. As a first possibility, general symmetry considerations can be used in order to derive a PFC model. This was done by Elder et al. in connection with the derivation of the first PFC model [EKHG02]. Alternatively, it is also possible to derive PFC models directly from microscopic DFT.

PFC models themselves are mesoscopic and describe inhomogeneous fluids and crystals on microscopic length and diffusive time scales. Their spatial resolution is therefore comparable with the spatial resolution of molecular dynamics (MD) simulations and sufficient to resolve a crystal lattice. To the contrary, the diffusive time scale of PFC models is much larger than the characteristic time scale for MD simulations. This facilitates fast numerical simulations on the basis of dynamic PFC models with much larger time steps than they are possible for MD simulations and makes dynamic PFC models to an important tool for the investigation of dynamic processes that are associated with a microscopic spatial resolution and that take place on diffusive or larger time scales. A further interesting feature of PFC models is that their equilibrium free-energy functional is minimized by periodic equilibrium order-parameter fields for suitable parameter combinations. These periodic patterns are usually interpreted as crystalline density fields and do not arise in PF models. PFC models thus incorporate effects like elastic deformations, that are associated with the periodic pattern of a crystalline phase and that are therefore not properly described by PF models, in a natural manner.

Although PFC models are a relatively new tool of soft condensed matter physics, they have already been used successfully for the modeling and investigation of various non-trivial materials phenomena. Important applications include the consideration of elastic and plastic deformations [EG04, SHP06, SHP09], the modeling of crystal growth [EKHG02, TBVL09, TGT⁺09] and melting [MKP08], the description of fluid-crystal interfaces [JAEAN09, YLV09], the structure [EG04, MKP08] and dynamics [MGV09, TGT⁺09] of grain boundaries, and the dynamics of crack propagation [EG04] in solid materials. Further special applications concern the Asaro-Tiller-Grinfeld instability [AT72, Gri86, HE08, WV09] and the description of glass formation over multiple time scales [BG11]. However, due to some strong approximations in the derivation of PFC models, there are also limitations for their applicability. Especially when the parameters of PFC models are chosen arbitrarily and not fitted to experimental data,

the PFC models are usually not appropriate for the calculation of precise numerical values that are related to certain materials properties. Instead, PFC models are rather appropriate for the investigation of qualitative relations and scaling laws. PFC models can, for example, be used to investigate the structure of crystalline phases and phase diagrams, while the predictions for actual values of elastic constants or for the amplitude of density variations in crystalline phases are often rather imprecise, but this disadvantage of PFC models is not characteristic for them and shared by other approximate theories.

In the following paragraphs, static and dynamic PFC models are addressed in detail and by basic examples. For clarity, the examples and derivations shown are kept intentionally simple and always involve only a single order-parameter field and a system of spherical particles [EPB⁺07, JA10]. Nevertheless, also much more complicated PF and PFC models involving multiple phase fields [EPB⁺07] as well as orientational degrees of freedom [L ow10a], as they become important for systems consisting of anisotropic particles, exist. For further details on PF and PFC models, the new book [PE10] of Provatas and Elder is recommended for reading.

5.1.2.1 Static phase field crystal models

The introduction of PF models is usually ascribed to the work of Fix and Langer [Fix83, Lan86] in the 1980s. Static PF models describe the equilibrium state of a physically relevant or auxiliary scalar phase field $\psi(\vec{r})$ that is spatially averaged and has the role of an order parameter. The local value of the phase field defines the present phase of the described thermodynamic system. Since each of the possible phases is associated with a certain value of the phase field, the value of the phase field changes rapidly between two different phases, while the phase field is spatially uniform in the bulk equilibrium phases. A static PF model usually consists in a free-energy functional $\mathcal{F}[\psi(\vec{r})]$ that is minimized by the equilibrium phase field, but there are also non-variational formulations. The integrand of the free-energy functional is a Ginzburg-Landau-type gradient expansion in the phase field that is assumed to be sufficiently small and smooth. PF models are therefore perturbative. A simple example for a free-energy functional of a PF model is given by [EG04]

$$\mathcal{F}_{\text{PF}}[\psi(\vec{r})] = \int_{\mathcal{V}} dV (f_0(\psi) + K_0(\vec{\nabla}_{\vec{r}}\psi)^2) \quad (5.35)$$

with the polynomial $f_0(x)$, that is supposed to possess two wells, and the parameter K_0 . To possess two wells, the polynomial $f_0(x)$ must have an even order that is at least four. Since the minimizing phase field of a free-energy functional, that corresponds to a PF model, is spatially uniform in the bulk phases, such a model is especially appropriate for the description of gas-liquid phase transitions. For crystalline phases, a spatially uniform phase field is not a good representation instead and properties like elastic and plastic deformability that are associated with the symmetries of a crystal lattice are neglected by PF models.

To solve this problem, PFC models have been developed by Elder et al. in 2002 [EKHG02]. They constitute an improvement of PF models and retain most of their features. As static PF models, static PFC models are also based on a free-energy functional that is minimized by an equilibrium phase field. This phase field is usually interpreted as the particle density field of the described system, but it can also be, for example, a local concentration or magnetization. The derivation of a PFC model can happen on the basis of symmetry considerations [EKHG02, PE10] or with the help of DFT. After the first PFC model had been proposed as a result of symmetry considerations in 2002, the same model was rederived from static DFT in 2007 [EPB⁺07]. This was the first derivation of a PFC model from DFT at all. PFC models are different from PF models for two main reasons. Firstly, the phase field $\psi(\vec{r})$ of a PFC model is not averaged locally in space [EG04] and changes on molecular length scales. It can therefore also represent a crystalline lattice. Secondly, the equilibrium phase field, that minimizes the free-energy functional of a PFC model, has a periodic pattern, if the parameters of the PFC model are chosen accordingly. The periodic phases of a PFC model are usually interpreted as the particle density field of a crystal. Thus, physical properties, that result from the periodicity of the density field, are naturally included in PFC models [EPB⁺07]. This is in contrast not the case for PF models. Such symmetry-related properties include especially the behavior of a certain material under elastic and plastic deformations and make PFC models applicable to situations, where PF models can hardly be used.

The main problem in the context of PFC models is the construction of a free-energy functional that is minimized by a periodic phase field. Similar to PF models, the free-energy density of a PFC model is also given by a gradient expansion of the phase field. This gradient expansion is truncated at a certain order in the phase field and at a certain order in the gradient operators. To give rise to periodic equilibrium structures of the phase field, it is necessary to include fourth-order derivatives [PE10]. A positive term proportional to $(\Delta_{\vec{r}}\psi(\vec{r}))^2$ in the gradient expansion disadvantages phase fields with a big curvature like phase fields that are highly oscillatory and that have a large amplitude through an increase of the free energy. Furthermore, a negative term proportional to $(\vec{\nabla}_{\vec{r}}\psi(\vec{r}))^2$ is needed in order to favor non-uniform phase fields. For the terms that include no derivatives, i. e., for terms of the form $\psi^n(\vec{r})$ with $n \in \mathbb{N}$, it is required that the highest-order contribution is of even order and that it has a positive coefficient. This term guarantees that the values of the phase field do not become too big and that the free-energy functional is bounded below. Finally, the free-energy functional must also be convex about the equilibrium state in the gradient expansion. The simplest and most prevalent possibility for the highest-order monomial term is the fourth-order term $\psi^4(\vec{r})$. This term is also present in the *Swift-Hohenberg* (SH) model for Rayleigh-Bénard convection [SH77]

$$\mathcal{F}_{\text{SH}}[\psi(\vec{r})] = \int_{\mathcal{V}} dV \left(\frac{\psi}{2} ((q_0^2 + \Delta_{\vec{r}})^2 - \varepsilon_0) \psi + \frac{\psi^4}{4} \right) \quad (5.36)$$

with the control parameters q_0 and ε_0 , which is the simplest model that provides

periodic phases. The SH model describes periodic stripe patterns, but no crystalline phases with, for example, a triangular (hexagonal) pattern. To include such phases, Elder et al. modified the SH model leading to their first PFC model, which is also called the *traditional PFC model* [EKHG02]. This model contains a cubic term in addition to the SH terms and provides also triangular patterns that can be interpreted as triangular crystal lattices. It is given by

$$\mathcal{F}_{\text{EM}}[\psi(\vec{r})] = \int_{\mathcal{V}} dV \left(\frac{\psi}{2} ((q_0^2 + \Delta_{\vec{r}})^2 - \varepsilon_0) \psi + \alpha_0 \frac{\psi^3}{3} + \frac{\psi^4}{4} \right) \quad (5.37)$$

with the additional parameter α_0 . Due to the symmetry-based derivation of the traditional PFC model, the values of its three parameters q_0 , ε_0 , and α_0 are not known and can be used as fit parameters. Alternatively, they can be derived from a microscopic theory. This derivation, that follows mainly the procedure in reference [EKHG02], is presented in the following.

As for the derivation of the simple DDFT equation (5.14) in section 5.1.1.2, again a colloidal dispersion of N isotropic particles at the center-of-mass positions $\vec{r}_i \in \mathcal{V}$ with $i \in \{1, \dots, N\}$ in the domain $\mathcal{V} \subseteq \mathbb{R}^3$ are considered. This domain has the measure

$$V = \int_{\mathcal{V}} dV \quad (5.38)$$

and the particles, that are located in this domain, are exposed to the external potential $U_1(\vec{r})$. Their spatial distribution is described by the one-particle density $\rho(\vec{r})$, as it is usual in the context of DFT. Reminiscent of Ginzburg-Landau theory (see section 5.1.3), a small order-parameter field is introduced by the parametrization

$$\rho(\vec{r}) = \bar{\rho}(1 + \psi(\vec{r})) \quad (5.39)$$

of the one-particle density $\rho(\vec{r})$ with the fluid reference density $\bar{\rho}$. This small order-parameter field $\psi(\vec{r}) = (\rho(\vec{r}) - \bar{\rho})/\bar{\rho}$ is the dimensionless reduced translational density variation. In terms of the order-parameter field $\psi(\vec{r})$, the Helmholtz free-energy functional (5.4) has to be approximated, where the orientational dependence in equation (5.4) and in its components has to be neglected. At first, the ideal gas free-energy functional (5.5) is approximated. Insertion of the parametrization (5.39) for the one-particle density into equation (5.5) and a Taylor expansion of the logarithm¹¹ in the integrand of the ideal gas free-energy functional result in the approximation¹²

$$\frac{\beta}{\bar{\rho}} \mathcal{F}_{\text{id}}[\psi(\vec{r})] = F_{\text{id}} + \int_{\mathcal{V}} dV \left(\psi + \frac{\psi^2}{2} - \frac{\psi^3}{6} + \frac{\psi^4}{12} \right) \quad (5.40)$$

¹¹This Taylor approximation of the logarithm has the serious consequence that the non-negative-density constraint $\rho(\vec{r}) \geq 0$ gets lost in the PFC model.

¹²Symbols like \mathcal{F}_{id} and F_{id} are also used in the derivation of other PFC models in subsequent sections and not distinguished by additional subscripts. The particular expression, that is associated with these symbols, depends on the currently considered model.

with the irrelevant constant

$$F_{\text{id}} = V (\ln(\Lambda^3 \bar{\rho}) - 1). \quad (5.41)$$

The polynomial in the integrand of equation (5.40) was truncated at fourth order, since this is the lowest order in $\psi(\vec{r})$ that enables the formation of stable crystalline phases. The approximation of the excess free-energy functional $\mathcal{F}_{\text{exc}}[\psi(\vec{r})]$ is less simple. For this purpose, the Ramakrishnan-Yussouff approximation (5.10) is used. In the homogeneous bulk phase, to which the direct pair-correlation function $c^{(2)}(\vec{r}_1, \vec{r}_2)$ in the Ramakrishnan-Yussouff approximation corresponds, two symmetries are present. These are the *translational invariance* and the *rotational invariance* of the system. The same symmetries also apply to the direct pair-correlation function. This means¹³

$$c^{(2)}(\vec{r}_1, \vec{r}_2) \equiv c^{(2)}(\vec{r}_1 - \vec{r}_2) \equiv c^{(2)}(R) \quad (5.42)$$

with the relative distance $R = \|\vec{r}_1 - \vec{r}_2\|$. As a consequence of equation (5.42), the Ramakrishnan-Yussouff approximation can be written as the integral of a convolution integral. A local approximation of this convolution integral can then be obtained from a gradient expansion (see appendix A) of the direct pair-correlation function. The gradient expansion of the translationally invariant direct pair-correlation function $c^{(2)}(\vec{r})$ with $\vec{r} = \vec{r}_1 - \vec{r}_2$ is based on a Taylor expansion of the Fourier transformed direct pair-correlation function $\tilde{c}^{(2)}(\vec{k})$ around the wave vector $\vec{k} = \vec{0}$. In Fourier space, this Taylor expansion can be written as

$$\tilde{c}^{(2)}(\vec{k}) = \tilde{c}_0^{(2)} + \tilde{c}_2^{(2)} \vec{k}^2 + \tilde{c}_4^{(2)} \vec{k}^4 + \dots \quad (5.43)$$

with the Fourier expansion coefficients $\tilde{c}_i^{(2)}$. From this Taylor expansion, the desired gradient expansion of $c^{(2)}(\vec{r})$ follows by an inverse Fourier transformation. Back in position space, the Taylor expansion (5.43) becomes the gradient expansion

$$c^{(2)}(\vec{r}) = c_0^{(2)} - c_2^{(2)} \Delta_{\vec{r}} + c_4^{(2)} \Delta_{\vec{r}}^2 \mp \dots \quad (5.44)$$

with the gradient expansion coefficients $c_i^{(2)}$. In equations (5.43) and (5.44), gradients of odd order have been neglected, since they would violate the parity inversion symmetry of the direct pair-correlation function. For the derivation of the traditional PFC model (5.37), it is sufficient to perform the gradient expansion up to fourth order, since this order in the gradient $\vec{\nabla}_{\vec{r}}$ is the lowest one that makes stable periodic crystalline phases possible. It constitutes furthermore an important difference between the PFC model of Elder et al. and the older PF models that do not include fourth-order derivatives of the

¹³In the case of anisotropic particles with orientational degrees of freedom and especially for higher-order direct correlation functions, it is much more difficult to identify the existing symmetries of the direct correlation functions and to take advantage of them (compare section 5.3).

phase field. The gradient expansion up to fourth order results in the approximation

$$\frac{\beta}{\bar{\rho}} \mathcal{F}_{\text{exc}}[\psi(\vec{r})] = F_{\text{exc}} - \frac{1}{2} \int_{\mathcal{V}} dV \left(A_1 \psi^2 + A_2 \psi \Delta_{\vec{r}} \psi + A_3 \psi \Delta_{\vec{r}}^2 \psi \right) \quad (5.45)$$

with the irrelevant constant

$$F_{\text{exc}} = \frac{\beta}{\bar{\rho}} \mathcal{F}_{\text{exc}}^{(0)}(\bar{\rho}) \quad (5.46)$$

and the coefficients

$$A_1 = 4 M(0) , \quad A_2 = \frac{2}{3} M(2) , \quad A_3 = \frac{1}{30} M(4) . \quad (5.47)$$

These coefficients depend on the moments

$$M(n) = \pi \bar{\rho} \int_0^\infty dR R^{n+2} c^{(2)}(R) \quad (5.48)$$

of the direct pair-correlation function $c^{(2)}(R)$. The last contribution to the total Helmholtz free-energy functional (5.4) is the external free-energy functional (5.6) that can be written as

$$\frac{\beta}{\bar{\rho}} \mathcal{F}_{\text{ext}}[\psi(\vec{r})] = F_{\text{ext}} + \int_{\mathcal{V}} dV \psi(\vec{r}) \beta U_1(\vec{r}) \quad (5.49)$$

with the constant

$$F_{\text{ext}} = \int_{\mathcal{V}} dV \beta U_1(\vec{r}) , \quad (5.50)$$

which is not a functional of $\psi(\vec{r})$ and can therefore be neglected like F_{id} and F_{exc} before. Altogether, the expressions (5.40), (5.45), and (5.49) lead to the approximation

$$\frac{\beta}{\bar{\rho}} \mathcal{F}[\psi(\vec{r})] = \int_{\mathcal{V}} dV \left(\psi U' + A'_1 \psi^2 + A'_2 \psi \Delta_{\vec{r}} \psi + A'_3 \psi \Delta_{\vec{r}}^2 \psi - \frac{\psi^3}{6} + \frac{\psi^4}{12} \right) \quad (5.51)$$

for the total Helmholtz free-energy functional. Here, the dimensionless potential

$$U'(\vec{r}) = 1 + \beta U_1(\vec{r}) \quad (5.52)$$

and the scaled coefficients

$$A'_1 = \frac{1}{2} (1 - A_1) , \quad A'_2 = -\frac{1}{2} A_2 , \quad A'_3 = -\frac{1}{2} A_3 \quad (5.53)$$

are used for abbreviation, where the coefficient A'_2 should be positive in order to favor non-uniform phases and the last coefficient A'_3 is assumed to be positive for stability reasons. Through the moments (5.48), the three coefficients (5.53) in the microscopically derived PFC model (5.51) are related to the microscopic direct pair-correlation function. By comparison of equations (5.37) and (5.51), that are equivalent except for the external potential and the scaling, analytic expressions can be assigned to the three initially unknown coefficients ε_0 , q_0 , and α_0 in the traditional PFC model (5.37).

The free-energy functional (5.51) constitutes a simple local approximation for the actual Helmholtz free-energy functional of static DFT. Due to the truncation of the gradient expansion in the derivation of the approximation (5.51), the spatial patterns of the equilibrium order-parameter field, that minimizes this functional, can usually be described by first-order Fourier modes. This observation suggests simple analytic approaches like the *one-mode approximation* [JA10] and the *amplitude expansion* [PE10] for the order-parameter field. With such approaches, the free-energy functionals of simple PFC models can be minimized analytically, but usually, the PFC models are more complicated and the functionals have to be minimized numerically.

5.1.2.2 Dynamic phase field crystal models

Dynamic PFC models are based on the equilibrium Helmholtz free-energy functional of static PFC models and provide them with a dynamic equation for the time-evolution of the non-equilibrium order-parameter field $\psi(\vec{r}, t)$. Both in dynamic PF models and dynamic PFC models, the time-dependent order-parameter field $\psi(\vec{r}, t)$ is averaged locally in time, but only for PF models, the order-parameter field is in addition averaged locally in space. In accordance with DDFT, the dynamics of the order-parameter field is assumed to be dissipative and it is driven by the functional derivative of the equilibrium Helmholtz free-energy functional with respect to the order-parameter field so that it intends to minimize the free-energy functional. In the traditional PFC model of Elder et al. [EKHG02] and in most other PFC models, the order-parameter field is conserved [EG04], but it can in principle also be non-conserved. Depending on the conservation-type of the order-parameter field $\psi(\vec{r}, t)$, an appropriate dynamic equation is needed. For PFC models with only one order-parameter field, this appropriate dynamic equation can be obtained by a simple ansatz. When a dynamic equation for a conserved order-parameter field $\psi_c(\vec{r}, t)$ has to be written down, the most simple choice is the conservation equation

$$\frac{\partial \psi_c(\vec{r}, t)}{\partial t} = \Gamma_c \Delta_{\vec{r}} \frac{\delta \mathcal{F}[\psi_c(\vec{r}, t)]}{\delta \psi_c(\vec{r}, t)} \quad (5.54)$$

with the positive mobility parameter Γ_c . If in contrast the order-parameter field $\psi_n(\vec{r}, t)$ is non-conserved, the balance equation

$$\frac{\partial \psi_n(\vec{r}, t)}{\partial t} = -\Gamma_n \frac{\delta \mathcal{F}[\psi_n(\vec{r}, t)]}{\delta \psi_n(\vec{r}, t)} \quad (5.55)$$

with the positive constant Γ_n should be used. For a conserved order-parameter field, that is related to the one-particle density field $\rho(\vec{r}, t)$, also a DDFT equation can be used to describe its time-evolution. The application of a DDFT equation has the advantage that it describes the dynamics of the order-parameter field usually more accurate than the simple conservation law (5.54) and that DDFT equations are also available for more complicated situations including suspensions of anisotropic colloidal particles. In

the case of spherical particles, the simple DDFT equation (5.14) is appropriate and can be used as an alternative to equation (5.54). To obtain a dynamic PFC model, it is sufficient to insert the representation (5.39) for the one-particle density field and the approximation (5.51) for the free-energy functional into equation (5.14). The resulting dynamic equation for the order-parameter field $\psi(\vec{r}, t)$ is given by

$$\frac{\partial\psi(\vec{r}, t)}{\partial t} = D_{\text{T}}\vec{\nabla}_{\vec{r}'} \cdot \left((1 + \psi)\vec{\nabla}_{\vec{r}'} \left(U' + 2A_1'\psi + 2A_2'\Delta_{\vec{r}}\psi + 2A_3'\Delta_{\vec{r}}^2\psi - \frac{\psi^2}{2} + \frac{\psi^3}{3} \right) \right) \quad (5.56)$$

and constitutes a simple local approximation for the DDFT equation (5.14) with its general free-energy functional. The DDFT equation can also be simplified before it is applied. A common simplification is the *constant-mobility approximation* (CMA), where the space- and time-dependent mobility $D_{\text{T}}\rho(\vec{r}, t)$ between the two gradients in the DDFT equation is replaced by the constant mobility $D_{\text{T}}\bar{\rho}$. An analogous approximation is possible for more complicated versions of the DDFT equation involving, for example, also an orientational dependence of the mobility. In the above example for the traditional PFC model, the CMA reduces the simple DDFT equation (5.14) to the trivial diffusion equation (5.54) and leads to the dynamic equation

$$\frac{\partial\psi(\vec{r}, t)}{\partial t} = D_{\text{T}}\Delta_{\vec{r}} \left(U' + 2A_1'\psi + 2A_2'\Delta_{\vec{r}}\psi + 2A_3'\Delta_{\vec{r}}^2\psi - \frac{\psi^2}{2} + \frac{\psi^3}{3} \right) \quad (5.57)$$

for the translational density $\psi(\vec{r}, t)$. The dynamics of equations like (5.56) and (5.57) have usually to be investigated numerically. Since PFC models are associated with molecular length and diffusive time scales, the time step size of numerical methods for the solution of dynamic PFC equations can be chosen relatively large. This is in contrast to MD simulations that can also be used to simulate colloidal systems on microscopic length scales, but require much smaller time steps. The reason for the difference in the size of the time steps consists in the fact that MD simulations have to resolve the lattice vibrations of crystalline phases that takes place on the phonon time scale, while computer simulations on the basis of PFC models are only limited by the characteristic diffusion time that can be 10^6 - 10^8 times larger than the characteristic phonon time [PE10]. Therefore, a PFC-based simulation can be much faster than a corresponding MD simulation. However, a MD simulation can provide better results, since the derivation of PFC models involves a few serious approximations.

5.1.3 Ginzburg-Landau theory

Similar to classical DFT, also classical Ginzburg-Landau theory is an adaptation of a quantum mechanical theory. The quantum mechanical Ginzburg-Landau theory was originally proposed by Ginzburg and Landau in 1950 in order to describe superconductivity [GL50]. Its classical adaptation is a macroscopic theory for the description of thermodynamic systems in the vicinity of a certain phase transition. To describe this phase transition, Ginzburg-Landau theory relies on the order-parameter fields that define the phase transition considered. These order-parameter fields must be sufficiently small and smooth close to the phase transition described and can be scalars, vectors, and tensors of higher order. They are the same for static and dynamic Ginzburg-Landau theory and regarded as time-dependent in the dynamic case.

Static Ginzburg-Landau theory consists of a symmetry-based gradient expansion of the density of a generalized thermodynamic functional in terms of the space-dependent order-parameter fields. In particular, one starts with the lowest-order structure of the adjacent phases of the phase transition under consideration and makes a gradient expansion ansatz, that must respect the basic common symmetries of the adjacent phases, in the order-parameter fields that characterize the structure of the phase with higher order. Static Ginzburg-Landau theory is thus an extension of the Landau theory of phase transitions of second order [CL95, LL08], which predicts the order and the scaling behavior of phase transitions [LL08] in mean-field approximation and consists in a Taylor expansion of a thermodynamic potential in convenient order parameters instead of a more general gradient expansion of the density of a generalized thermodynamic functional in space-dependent order-parameter fields. Dynamic Ginzburg-Landau theory, on the other hand, is based on linear irreversible thermodynamics [MPP72, GM84, Rei98] and provides dynamic equations for the time-evolution of the order-parameter fields. The Ginzburg-Landau dynamics is usually dissipative and can then be derived from a dissipation functional. In several aspects, Ginzburg-Landau theory is similar to PFC models that are derived from DFT. Their common features include the perturbative expansion of a thermodynamic functional in terms of order-parameter fields and their gradients as well as the existence of a dissipation functional, where the dissipative dynamics can be derived from (see below).

Ginzburg-Landau theory can be applied to various thermodynamic problems including the liquid-gas phase transition [Eva79], the paraelectric-ferroelectric phase transition [AL78, FMH86, Kit95], and equilibrium interfaces between two coexisting phases [Eva79]. It was also applied to freezing and melting [LBW90, Lut06] and to liquid crystals. The application to phase transitions in liquid crystals is due to de Gennes [Gen71, Gen73, GP95] and proved to be very successful. Examples for liquid crystalline phase transitions, that have been described in the framework of Ginzburg-Landau theory, are the isotropic-nematic phase transition [Gen71, PB89], the isotropic-smectic A phase transition [MPB01], the isotropic-smectic C phase transition [MPB02], the isotropic-smectic C* phase transition [MPB05], as well as the nematic-smectic A and the nematic-smectic C phase transitions [Gen73, GP95]. However, Ginzburg-Landau theory has also some disadvantages. It is, for example, not valid in bulk phases far

from phase transitions and not applicable to critical regimes, since it is a mean-field theory and therefore neglects fluctuations, although fluctuations are very important in the context of critical systems.

Further information about Landau theory and Ginzburg-Landau theory can be found in the literature. A detailed explanation of the Landau theory of phase transitions is given in the book [TT87] by Toledano and Toledano. The classical textbook [LL08] by Landau and Lifschitz contains the basic ideas of the Landau theory and of the more general static Ginzburg-Landau theory, although the term *Ginzburg-Landau theory* is not used there explicitly. Especially with regard to the application of static Ginzburg-Landau theory on liquid crystals, the books [CL95, GP95] are readable.

About dynamic Ginzburg-Landau theory, there is less literature. A special reference, that addresses the dynamics of phase transitions and uses dynamic Ginzburg-Landau theory, is the book [Onu02] by Onuki, but there is not yet a recommendable standard reference on this topic.

5.1.3.1 Static Ginzburg-Landau theory

The traditional Landau theory was originally introduced by Landau as a general theory for second-order phase transitions [TT87, LL08] like the paramagnetic-ferromagnetic phase transition in magnetic materials. This phase transition takes place at a critical temperature T_c and the deviation of the absolute temperature T from the critical temperature T_c decides over the modulus of magnetization in the considered material. In a magnetic material, the magnetization is related to the amount of collective alignment of magnetic dipole moments. The magnetization is therefore used as an order parameter ψ to describe the ordering state of the magnetic material. Below the critical temperature T_c , the magnetization is non-zero, but it approaches zero, when the temperature T tends to T_c , and above the critical temperature, the magnetization vanishes completely. The change of the order parameter ψ from zero to non-zero thus defines the paramagnetic-ferromagnetic phase transition. Together with the magnetization, also the total free energy of the magnetic material varies. The free energy or an equivalent thermodynamic potential of the system can therefore be written as a function $E(T, \psi)$ that depends on the order parameter ψ and on the underlying thermodynamic conditions, which are here given in form of the temperature T . Furthermore, the function $E(T, \psi)$ is assumed to be analytic in the order parameter ψ . Since this order parameter is small in the vicinity of the phase transition, the extensive thermodynamic potential $E(T, \psi)$ can be expanded into a Taylor series with respect to ψ around the phase transition at $\psi = 0$. The *Landau theory* consists in fact in this Taylor expansion

$$E = E_0 + \sum_{n=1}^N \alpha_n \psi^n, \quad (5.58)$$

which is truncated at a certain order N , and is thus only valid in the vicinity of the phase transition. In this Taylor expansion, the unimportant offset term E_0 and the

expansion coefficients α_n with $n \in \{1, \dots, N\}$ are unknown functions of the scalar quantities like the temperature T of the system, but they are independent of the order parameter ψ . Their values cannot be determined within the Landau theory, but thermodynamic arguments and symmetry considerations can be used to clarify the dependence of the expansion coefficients on the scalar thermodynamic quantities of the system. The thermodynamic potential is assumed to possess the same symmetries as the Hamiltonian of the described system and these symmetries lead to information about the coefficients E_0 and α_n . For example, a $\psi \rightarrow -\psi$ symmetry of the thermodynamic potential leads to the vanishing of all coefficients α_n with an odd index n . Furthermore, the coefficients α_n and the maximal exponent N in the Taylor expansion have to ensure that the thermodynamic potential is bounded below so that it provides a stable equilibrium state. The Taylor expansion is therefore usually truncated at fourth order. In the example of a magnetic material, the equilibrium magnetization follows by minimization of the thermodynamic potential $E(T, \psi)$ with respect to the order parameter ψ . For the equilibrium order parameter, the scaling

$$\psi \propto |T - T_c|^{-\alpha_c} \quad (5.59)$$

with the critical exponent α_c is found. The calculation of critical exponents is therefore an important application of the Landau theory. In principle, also multiple order parameters ψ_ν with $\nu = 1, \dots, \nu_{\max}$ can be introduced in the Landau theory.

Ginzburg-Landau theory is in contrast a generalization of the Landau theory for spatially inhomogeneous systems. This generalization is due to Ginzburg and uses an analytic space-dependent order-parameter field¹⁴ $\psi(\vec{r})$ for the definition of the considered phase transition instead of a convenient spatially homogeneous order parameter ψ . The thermodynamic potential $E(T, \psi)$ being a function of the order parameter ψ is further extended to a *generalized thermodynamic functional*

$$\mathcal{E} = \int_{\mathcal{V}} dV \varepsilon(\vec{r}) \quad (5.60)$$

of the space-dependent order-parameter field $\psi(\vec{r})$. Often, this functional corresponds to the internal energy of the described thermodynamic system, but it can also be the Helmholtz free-energy functional or another equivalent thermodynamic functional, where the underlying thermodynamic potential should always be chosen as most appropriate for the described thermodynamic system. The generalized energy density $\varepsilon(\vec{r})$ in the generalized thermodynamic functional (5.60) depends on the order-parameter field $\psi(\vec{r})$. It is not expanded into a Taylor series, but more generally into a gradient expansion in the order-parameter field $\psi(\vec{r})$. This gradient expansion of the generalized energy density $\varepsilon(\vec{r})$ is the basis of static *Ginzburg-Landau theory*. It must be intensive,

¹⁴Examples for order-parameter fields in Ginzburg-Landau theory are given in section 5.5.

since the *generalized energy density* $\varepsilon(\vec{r})$ is intensive, and has the general form

$$\varepsilon(\vec{r}) = \varepsilon_0 + \sum_{n=1}^N \alpha_n(i_1^{(n)}, \dots, i_n^{(n)}, j_1^{(n)}, \dots, j_n^{(n)}) \prod_{\nu=1}^n \left(\partial_{i_\nu^{(n)}}^{j_\nu^{(n)}} \psi \right) \quad (5.61)$$

with the irrelevant offset term ε_0 and the unknown expansion coefficients $\alpha_n(\dots)$, where Einstein's sum convention is used for the indices $i_\nu^{(n)}$ and $j_\nu^{(n)}$. The expansion (5.61) contains not only the order-parameter field $\psi(\vec{r})$ but also its gradients. This gradient expansion is truncated at certain orders in $\psi(\vec{r})$ and in the derivatives providing a non-trivial and stable functional. Therefore, most gradient expansions are truncated at second or fourth order. Higher-order contributions can often be neglected, since they are usually not physically meaningful. This argument is especially relevant for the maximal order of derivatives. While a gradient considers an inhomogeneity of the order-parameter field and the Laplace operator regards the curvature of this field, higher-order derivatives can usually not be related to an obvious physical meaning. Static Ginzburg-Landau theory is thus very similar to PFC models, where the functional $\mathcal{E}[\psi(\vec{r})]$ is the free-energy functional $\mathcal{F}[\psi(\vec{r})]$. The coefficients ε_0 and $\alpha_n(\dots)$ can in general depend on all scalar quantities of the system such as, for example, temperature and pressure. Since the gradient expansion must not be an arbitrary sum of products of any derivatives of the order-parameter field without physical relevance, the expansion coefficients cannot be independent. There are in fact certain relations between the expansion coefficients. These relations ensure that the gradient expansion is a sum of products of the order-parameter field and the gradient operator.

Between the order-parameter fields, which are scalars, vectors, or tensors of higher order, and the gradient operator, which can be represented by a vector, there are only two independent types of multiplications possible in three spatial dimensions. These are the matrix multiplication that includes the scalar product as a special case and the cross product. In a gradient expansion of a scalar function like the generalized energy density $\varepsilon(\vec{r})$, these two products have to be combined in an appropriate way to guarantee that all terms in the gradient expansion are scalars. For phase transitions from or to the isotropic phase, the various expansion coefficients $\alpha_n(\dots)$ can therefore be represented by a polynomial in Kronecker delta symbols δ_{ij} and Levy-Civita symbols ϵ_{ijk} with the indices of the expansion coefficients. In two spatial dimensions, the cross product does not exist and the expansion coefficients can entirely be represented by Kronecker delta symbols. The situation is different for other phase transitions without the involvement of the isotropic phase. For such phase transitions, preferred directions like the nematic director in the case of the nematic-smectic A phase transition have to be taken into account as well. These preferred directions can appear in addition to the Kronecker delta symbols and Levy-Civita symbols in the representation of the expansion coefficients $\alpha_n(\dots)$. With the reduction of the various expansion coefficients to a much smaller number of independent parameters, the set of possible terms in the general gradient expansion is usually manageable, if the previously chosen truncation orders for the order-parameter field and for the gradient are not too high.

The still rather general form of the gradient expansion must further be simplified by the application of additional relations between the coefficients. These relations follow from basic symmetry and stability considerations and help to avoid unphysical additional degrees of freedom in the gradient expansion. The basic symmetries, which the generalized thermodynamic functional (5.60) has to incorporate, are those of the phase transition considered. Usually, the adjacent phases of the phase transition have certain symmetry-properties and the joint symmetries of both phases must therefore also apply to the generalized thermodynamic functional. Common symmetries are time reversal symmetry, parity inversion symmetry, invariance against global translations and rotations, and the behavior under Galilean transformations. These symmetry requirements restrict the set of possible terms in the gradient expansion considerably.

A further simplification can be obtained by partial integration of the terms in the gradient expansion. Partial integration is necessary in order to provide only those terms that are really independent with independent prefactors. When the described system is unbounded, it is possible to neglect surface terms that arise by partial integration. Such unbounded systems are often considered and true divergence terms in their gradient expansions can always be removed. To ensure stability, the generalized thermodynamic functional (5.60) must be positive semidefinite or convex about the equilibrium state in the order-parameter field. Since the equilibrium order-parameter field $\psi(\vec{r})$ is determined by functional minimization of the generalized thermodynamic functional, it must be bounded below so that the equilibrium generalized energy is finite. This is the reason, why the gradient expansion (5.61) is usually truncated at second or fourth order in the order-parameter field. Furthermore, such stability considerations lead to requirements for the signs of the unknown expansion coefficients in the gradient expansion.

As in the other theories, it is also possible and in fact usual in Ginzburg-Landau theory to introduce several different order-parameter fields $\psi_\nu(\vec{r})$. The generalized energy density $\varepsilon(\vec{r})$ must then be expanded in all these order-parameter fields and the corresponding gradients [GP95].

5.1.3.2 Dynamic Ginzburg-Landau theory

On the basis of the generalized energy functional of static Ginzburg-Landau theory and its symmetries, dynamic equations for the time-evolution of the time-dependent order-parameter fields $\psi_\nu(\vec{r}, t)$ can be derived using dynamic Ginzburg-Landau theory. The dynamics of these order-parameter fields near a phase transition is usually relaxational and purely dissipative so that reversible currents do not arise. Often, the dynamics of the order-parameter fields that correspond to a static Ginzburg-Landau model is not considered at all. For the case that the dynamics of such a Ginzburg-Landau model has in fact to be derived, it can be done in direct analogy to the procedure of generalized hydrodynamics that is described further below in section 5.1.4.2. Except for the different variables, which are order-parameter fields in the context of dynamic Ginzburg-Landau theory and hydrodynamic variables in the context of generalized hy-

drodynamics, and the considered symmetries that are related to a phase transition in dynamic Ginzburg-Landau theory and to a bulk phase in generalized hydrodynamics, there are no appreciable differences between both theories. Since the basic procedure is exactly the same for dynamic Ginzburg-Landau theory and generalized hydrodynamics, it is described in detail only for generalized hydrodynamics in section 5.1.4.2 and omitted here.

5.1.4 Generalized hydrodynamics

As a generalization of the traditional hydrodynamics for simple liquids [For74, Ach90, HB91, LL91b, Lam93, Bat00], generalized hydrodynamics has been developed to also describe the statics and dynamics of complex liquids like liquid crystals and polymer melts in bulk phases. The hypernym “generalized hydrodynamics” comprises generalized hydrostatics and generalized hydrodynamics for the description of the statics and of the dynamics, respectively. This naming is not consistent, since the hypernym and the dynamic version are named identically, but the alternative term “generalized hydromechanics”, that would be in direct analogy to the term “hydromechanics”, which is sometimes used in the context of simple liquids as a hypernym for traditional hydrostatics and traditional hydrodynamics, is unusual. In contrast to Ginzburg-Landau theory, generalized hydrodynamics requires that the described liquid is sufficiently far away from phase transitions. It is further assumed that the considered system is in or at least close to thermodynamic equilibrium.

The description of a thermodynamic system in the framework of generalized hydrodynamics is macroscopic and mainly based on a separation of length and time scales. While in a microscopic view, a liquid consists of a huge number of small interacting particles with fast relaxing microscopic degrees of freedom, the same liquid appears as a continuum and can entirely be characterized by only a few slow relaxing macroscopic variables, when it is described on sufficiently large length and time scales. A *hydrodynamic description* takes place on these large length and time scales, on which the microscopic degrees of freedom are relaxed to local thermodynamic equilibrium (this is the *local equilibrium approximation*) and only a few macroscopic variables have to be taken into account in order to describe the system completely. The macroscopic frame for the hydrodynamic description is referred to as the *hydrodynamic range*, which is characterized by small wave numbers k and small frequencies ω . It goes along with the *continuum hypothesis*

$$k\lambda_c \ll 1, \quad \omega\tau_c \ll 1 \quad (5.62)$$

with the characteristic mean free path length λ_c and the characteristic collision time τ_c . These two inequalities state that the microscopic particles collide very often and move only over small distances between two collisions compared to the macroscopic length and time scales that are defined by k and ω , respectively. Within a hydrodynamic description therefore, only hydrodynamic modes that are slow and widely extended in space are considered. A mode or variable is in general called *hydrodynamic*, if its

relaxation becomes infinitely slow in the limit of an infinitely large wavelength:

$$\lim_{k \rightarrow 0} \omega(k) = 0 . \quad (5.63)$$

This condition is necessary in order to assure that generalized hydrodynamics becomes exact in the *hydrodynamic limit* $k \rightarrow 0$, $\omega \rightarrow 0$. It also helps to identify the *hydrodynamic variables* of a particular system that are needed to describe this system.

In general, there are two different types of hydrodynamic variables. The first one contains the *densities of conserved quantities* [Bal97] like the energy density, the translational momentum density¹⁵, and a local concentration. These conserved quantities are associated with global *continuous symmetries* of the system described. Since conserved quantities can only be transported and not created or destroyed, their dynamics is slower than the relaxation of the microscopic degrees of freedom. The currents of conserved quantities are driven by gradients of the densities of the conserved quantities and become zero for spatially uniform distributions so that the relaxation times for the densities of conserved quantities diverge, when the characteristic lengths for spatial inhomogeneities of the densities of the conserved quantities tend to infinity. Densities of conserved quantities are therefore hydrodynamic variables.

The second type of hydrodynamic variables contains *non-conserved symmetry variables* that are associated with *spontaneously broken continuous symmetries* of the regarded system [PB96]. “Spontaneously broken” means here that these symmetries are broken although they are present in the Hamiltonian of the considered system. An example for a *symmetry-breaking quantity* is the nematic director \hat{n} in liquid crystals. This unit vector defines the mean local orientation of the liquid crystalline particles in a nematic phase and breaks the global rotational symmetry of the isotropic phase. When there are no boundary conditions or external fields that could give rise to a preferred direction in the nematic phase, the rotational symmetry is broken spontaneously. The whole nematic phase is thus oriented according to the nematic director \hat{n} , although there is no energetic reason for its particular direction. Its direction can therefore be changed globally¹⁶ without energy loss. Since such a global rotation is not accompanied by a restoring force, its relaxation time is infinite. The variation $\delta\hat{n}$ with $\delta\hat{n} \cdot \hat{n} = 0$ and $\hat{n} \cdot \hat{n} = 1$ of the nematic director \hat{n} is therefore a hydrodynamic variable and called a *symmetry variable*. In general, there is a symmetry variable that describes the indifferent variation of a symmetry-breaking quantity for each spontaneously broken continuous symmetry, if long-range interactions are not present [For89, PB96]. Further examples for spontaneously broken symmetries are the broken translational symmetry in smectic phases and the broken translational and rotational symmetries in crystal lattices. The symmetry-breaking quantities in these examples are the smectic layer normal and the crystal lattice vectors, respectively, and the corresponding symmetry variables are the variations of the smectic layer normal and of the crystal lattice vectors.

¹⁵The conservation of the total angular momentum is not associated with a conserved density. It is instead respected by the symmetry of the hydrodynamic stress tensor [Ple94].

¹⁶Local distortions of the director field instead cost energy and cause an elastic restoring force.

Aside from the hydrodynamic variables, it can be necessary to also consider a few slowly relaxing *non-hydrodynamic macroscopic variables* like order-parameter fields that arise close to a phase transition [PB96]. These macroscopic variables relax for any reasons so slowly that they cannot be neglected on the hydrodynamic time scale and have to be taken into account – although they are not hydrodynamic – in order to describe the system completely. Otherwise, one would have to switch to an even larger time scale for the description, where all non-hydrodynamic variables are also relaxed to local thermodynamic equilibrium. In the above example, the relaxation time of an order-parameter field becomes too large in the vicinity of a phase transition so that this non-hydrodynamic macroscopic variable has to be taken into account, if the macroscopic description shall also be applicable close to a phase transition. An example for such an order-parameter field is the amount of local nematic order in liquid crystals that is defined below in this chapter. Also, the elastic strain in polymers is a slowly relaxing non-hydrodynamic macroscopic variable. Whenever non-hydrodynamic variables are considered, the resulting description is not any longer hydrodynamic and is therefore called a non-hydrodynamic *generalized macroscopic description*.

The formalism of generalized hydrodynamics has a few similarities with Ginzburg-Landau theory and PFC models, but it is much more general and can beyond the description of a bulk phase be also extended toward phase transitions and fluctuations [PB96]. Generalized hydrostatics describes only the equilibrium properties of a simple or complex liquid and consists basically in the construction of a symmetry-based gradient expansion of a generalized energy density. In this respect, it is analogous to Ginzburg-Landau theory, but the chosen variables are different from Ginzburg-Landau theory. In both theories, the gradient expansion is required to respect the basic symmetries of the system, which are the symmetries of the phase transition considered in static Ginzburg-Landau theory and the symmetries of the bulk phase described in generalized hydrostatics. A further similarity between generalized hydrostatics and static Ginzburg-Landau theory is the fact that both theories are perturbative, but they are perturbative with respect to different expansion parameters. While in static Ginzburg-Landau theory the generalized energy density is expanded in the order-parameter fields and their gradients that are assumed to be small in the vicinity of the phase transition the generalized energy density of generalized hydrostatics is gradient-expanded in the hydrodynamic and macroscopic variables, where the variables can be big and the wave vector \vec{k} related to a gradient by Fourier transformation is the small expansion parameter. Generalized hydrodynamics, on the other hand, can be used to derive the dynamics of the hydrodynamic and macroscopic variables. The derivation of their dynamic equations is based on the same symmetry considerations as the statics.

Generalized hydrostatics and generalized hydrodynamics have been applied to various thermodynamic systems including liquid crystalline phases like the nematic phase [BP87, BPZ06, BCP09] and the smectic phases [BP80, BP87, CL95, BCP98]. It is also applicable to solids and contains *elasticity theory* [LL91a] as a special case. Due to the local equilibrium approximation it is, however, not applicable to steady states and glasses. An overview about generalized hydrodynamics itself and about impor-

tant applications of this theory is given in references [Ple94, PB96, Ple97]. These book chapters by Pleiner and Brand were the basis for this section. They also contain detailed instructions for the utilization of generalized hydrodynamics and are highly recommendable as supplementary literature.

5.1.4.1 Generalized hydrostatics

Generalized hydrostatics is very similar to static Ginzburg-Landau theory. Both theories consist in the construction of a symmetry-based gradient expansion for a generalized thermodynamic functional \mathcal{E} that has to respect the basic symmetries of the system. In particular, the symmetries of the Hamiltonian of the system that lead to conserved quantities or symmetry variables in the hydrodynamic description are shared by the generalized thermodynamic functional \mathcal{E} . Generalized hydrostatics and static Ginzburg-Landau theory are only different with respect to the chosen variables and the considered symmetries. While in static Ginzburg-Landau theory order-parameter fields are used to expand the generalized energy density $\varepsilon(\vec{r})$, the deviations $\delta X(\vec{r}) = X(\vec{r}) - X_0$ of hydrodynamic and macroscopic variables from their equilibrium values X_0 are used for the gradient expansion in the context of generalized hydrostatics. The symmetries, that the gradient expansion in generalized hydrostatics has to respect, are identical with the symmetries of the considered bulk phase and not with symmetries that are related to a certain phase transition as it is the case for Ginzburg-Landau theory. Nevertheless, the symmetries are of the same type in both theories, i. e., one considers time reversal symmetries, parity inversion symmetries, invariances against global translations and rotations, and behavior under Galilean transformations. Due to this analogy, the procedure for the derivation of a macroscopic model from generalized hydrostatics is basically the same as for the derivation of a static Ginzburg-Landau model that has been described in detail in section 5.1.3.1 and does not have to be explained here again.

5.1.4.2 Generalized hydrodynamics

On the basis of a model from generalized hydrostatics comprising a gradient-expanded generalized energy density and a set of hydrodynamic and macroscopic variables dynamic equations for the time evolution of these hydrodynamic and macroscopic variables can be derived within the framework of generalized hydrodynamics. To distinguish hydrodynamic and macroscopic variables from the order-parameter fields of Ginzburg-Landau theory, the symbol $X(\vec{r}, t)$ is used here for a general time-dependent hydrodynamic or macroscopic variable. Examples for $X(\vec{r}, t)$ are the entropy density $\sigma(\vec{r})$, particle number density $\rho(\vec{r})$, local concentration $c(\vec{r})$, and momentum density $g_i(\vec{r})$. On this occasion, also the *thermodynamic conjugate* [LL08]

$$X^\natural = \frac{\delta \mathcal{E}}{\delta X} \quad (5.64)$$

of the variable $X(\vec{r}, t)$ is defined. Corresponding examples for the thermodynamic conjugate $X^{\natural}(\vec{r}, t)$ of the hydrodynamic or macroscopic variable $X(\vec{r}, t)$ are the absolute temperature field $T(\vec{r}, t)$, the local chemical potential $\mu(\vec{r}, t)$, the local relative chemical potential $\mu_c(\vec{r}, t)$, and the velocity field $v_i(\vec{r}, t)$, respectively. In general, there is always a unique thermodynamic conjugate for each hydrodynamic or macroscopic variable. They appear in pairs in the *total differential of the generalized energy density* [GM84, PB96, Rei98]

$$d\varepsilon = Td\sigma + \mu d\rho + \mu_c dc + v_i dg_i + \dots, \quad (5.65)$$

that is equivalent to the local form of the first law of thermodynamics and sometimes also called *Gibbs relation* [BPZ06]. In this fundamental thermodynamic relation, each term combines a thermodynamic conjugate variable $X^{\natural}(\vec{r}, t)$ with the total differential $dX(\vec{r}, t)$ of the corresponding variable $X(\vec{r}, t)$. Which of both is the variable and which is the thermodynamic conjugate variable depends on the choice of the underlying thermodynamic potential due to the definition (5.64). Through a Legendre transformation, the thermodynamic potential can always be transformed into an equivalent thermodynamic potential, where a certain variable and its thermodynamic conjugate are interchanged. It is thus possible to adapt the generalized thermodynamic functional \mathcal{E} in order to obtain a different combination of the hydrodynamic or macroscopic variables and their thermodynamic conjugates. This is important, since the dynamic equations are only formulated for the hydrodynamic and macroscopic variables and not for their equivalent thermodynamic conjugates. In the formulation of the dynamic equations, one has at first to distinguish the conserved variables $X_c(\vec{r}, t)$ from the non-conserved variables $X_n(\vec{r}, t)$, since both types of variables exhibit a fundamentally different dynamics [Gen71, MPP72, For89, Kha89, PB96, PLB02]. While conserved variables obey a local *conservation equation*

$$\dot{X}_c + \partial_i J_i^{X_c} = 0 \quad (5.66)$$

with the *current* $J_i^{X_c}(\vec{r}, t)$, the dynamics of non-conserved variables is described by a *balance equation*

$$\dot{X}_n + \Phi^{X_n} = 0 \quad (5.67)$$

with the *quasi-current* $\Phi^{X_n}(\vec{r}, t)$. These dynamic equations relate the symmetry properties of the hydrodynamic and macroscopic variables to the symmetry properties of the corresponding and yet unknown currents and quasi-currents. In order to define the dynamics of the hydrodynamic and macroscopic variables, it is necessary to determine their currents and quasi-currents. To begin with, these currents $J_i^{X_c}(\vec{r}, t)$ and quasi-currents $\Phi^{X_n}(\vec{r}, t)$ are decomposed into reversible (non-dissipative) contributions $J_{R,i}^{X_c}(\vec{r}, t)$ and $\Phi_R^{X_n}(\vec{r}, t)$ and irreversible (dissipative) contributions $J_{D,i}^{X_c}(\vec{r}, t)$ and $\Phi_D^{X_n}(\vec{r}, t)$, respectively:

$$\begin{aligned} J_i^{X_c} &= J_{R,i}^{X_c} + J_{D,i}^{X_c}, \\ \Phi^{X_n} &= \Phi_R^{X_n} + \Phi_D^{X_n}. \end{aligned} \quad (5.68)$$

While reversible currents and quasi-currents do not change the total entropy of the described thermodynamic system, the dissipative currents and quasi-currents are associated with entropy production. Reversible currents are invariant against time reversal and can only arise, when quantities are present that are odd under time reversal like, for example, a velocity field or equivalently a density of translational momentum. Also a symmetry-breaking preferred direction in the considered system can make reversible currents possible. In contrast, dissipative currents are not invariant against time reversal and are nearly always present.

The currents and quasi-currents (5.68) including their reversible and irreversible contributions are driven by the thermodynamic forces of the system. Such a thermodynamic force $X^\sharp(\vec{r}, t)$ exists for each thermodynamic conjugate variable $X^\natural(\vec{r}, t)$, but there are different definitions for thermodynamic forces in the literature. While they are sometimes regarded as identical with the thermodynamic conjugate variables, other authors define them as the gradients of the thermodynamic conjugates. Here, the *thermodynamic forces*

$$X_{c,i}^\sharp = -\partial_i X_c^\natural, \quad X_n^\sharp = X_n^\natural \quad (5.69)$$

are defined differently for conserved and for non-conserved variables. This definition is chosen for convenience, since it simplifies the notation in some of the following expressions considerably.

The reversible and irreversible contributions of the currents and quasi-currents (5.68) are determined in rather different ways. For the reversible contributions, linear expansions in terms of the thermodynamic forces are performed. These expansions usually contain only a few terms consisting of a thermodynamic force and unknown expansion coefficients, since only thermodynamic forces with appropriate dimensions can appear in the expansion of a certain reversible current or quasi-current. Moreover, terms with other symmetry properties than the respective reversible current or quasi-current have to be omitted also. The linear expansion in terms of thermodynamic forces is in accordance with linear thermodynamics that states the validity of *Onsager's principle*. This principle reveals general *Onsager reciprocity relations* between the expansion coefficients. With these relations, the number of independent expansion coefficients is reduced considerably. Although the reversible currents and quasi-currents are only expanded linearly in the thermodynamic forces, the currents and quasi-currents are in fact not linear and the described dynamics is not trivial, since the expansion coefficients can as always depend on all scalar quantities of the considered thermodynamic system. To ensure that the constructed reversible currents and quasi-currents do not change the entropy of the system, they are inserted into the dynamic equations (5.66) and (5.67) under negligence of the dissipative currents and quasi-currents and these dynamic equations are in turn inserted into the time-derivative

$$\frac{d\varepsilon}{dt} = T \frac{\partial \sigma}{\partial t} + \mu \frac{\partial \rho}{\partial t} + \mu_c \frac{\partial c}{\partial t} + v_i \frac{\partial g_i}{\partial t} + \dots = -\partial_i J_i^\varepsilon \quad (5.70)$$

of the generalized energy density $\varepsilon(\vec{r}, t)$ in equation (5.65). This time derivative relates

the time derivative of the energy density to the time derivatives of the hydrodynamic and macroscopic variables including the entropy density. It can also be used to determine the reversible current $J_{\mathbf{R},i}^\varepsilon(\vec{r}, t)$ of the conserved generalized energy density.

The dissipative contributions of the currents and quasi-currents (5.68) are derived very differently. Within linear irreversible thermodynamics, dissipative currents and quasi-currents can be derived from a dissipation functional \mathfrak{R} (see equation (4.47) in section 4.3). Due to the second law of thermodynamics and the connection of dissipation functionals with entropy production [compare equation (4.48)], a dissipation functional is in general positive semi-definite: $\mathfrak{R} \geq 0$. In the special case of a purely reversible process, the dissipation functional vanishes, $\mathfrak{R} = 0$, and for purely dissipative processes, it is positive: $\mathfrak{R} > 0$. When the dissipation functional \mathfrak{R} is known, the dissipative contributions of the currents and quasi-currents follow directly by functional differentiation of \mathfrak{R} with respect to the thermodynamic forces $X^\sharp(\vec{r}, t)$:

$$\begin{aligned} J_{\mathbf{D},i}^{X_c} &= \frac{\delta \mathfrak{R}}{\delta X_{c,i}^\sharp}, \\ \Phi_{\mathbf{D}}^{X_n} &= \frac{\delta \mathfrak{R}}{\delta X_n^\sharp}. \end{aligned} \tag{5.71}$$

Since the dissipative currents and quasi-currents shall also be linear in the thermodynamic forces within the context of linear irreversible thermodynamics, the dissipation functional must be expanded quadratically in the thermodynamic forces with expansion coefficients that can again depend on all scalar quantities of the described thermodynamic system [MPP72, GM84, PB96, Rei98]. The construction of the dissipation function $\mathfrak{r}(\vec{r}, t)$, which is the density corresponding to the dissipation functional \mathfrak{R} , in terms of the thermodynamic forces $X^\sharp(\vec{r}, t)$ proceeds similarly to the construction of the generalized energy density $\varepsilon(\vec{r}, t)$ in terms of the hydrodynamic and macroscopic variables $X(\vec{r}, t)$ and their gradients. All terms that are quadratic in the thermodynamic forces (5.69) and that are scalar are initially taken into account. Then, all terms that do not have the same symmetry-properties as the considered phase are discarded, i. e., the same symmetry considerations are applied to the dissipation function as to the generalized energy density in generalized hydrostatics. It is further possible to simplify the dissipation functional by partial integration. When the dissipation functional is formulated in its most simple form, which is the physically consistent form without unjustified additional terms or coefficients, the dissipative currents and quasi-currents follow by simple functional differentiation according to equations (5.71). With the determination of the dissipative contributions of the currents and quasi-currents (5.68), the derivation of the dynamics of the considered simple or complex liquid is finished.

5.2 Derivation of phase field crystal models from DFT

In recent years, several static and dynamic PFC models have been derived from static and dynamical DFT, respectively. After the traditional PFC model for isotropic particles had been derived from DFT by Elder et al. in 2007 (see section 5.1.2.1), there were some efforts to generalize this PFC model toward systems consisting of anisotropic particles. An attempt to generalize the traditional PFC model toward anisotropic systems with oriented particles was recently undertaken by Choudhary et al. [CLEL11], whereas the first PFC model for freely orientable anisotropic particles was derived from DFT by Löwen [Löw10a] in 2010. This model describes apolar particles with an orientational degree of freedom in two spatial dimensions. It also includes the dynamics of the anisotropic particles obtained from DDFT and is of special interest, since it describes various liquid crystalline phases.

In the following, this PFC model is generalized in basically two respects using a compact and consistent notation. At first, a PFC model for polar anisotropic particles in two spatial dimensions is derived. This model contains the previous PFC model for apolar particles as special case with vanishing polarization. Afterwards, the derivation of a PFC model for apolar anisotropic particles in three spatial dimensions is presented. Both PFC models consider uniaxial particles without a hydrodynamic translational-rotational coupling. The N uniaxial particles are described by their center-of-mass positions \vec{r}_i and orientations \hat{u}_i for $i \in \{1, \dots, N\}$, where \vec{r}_i is given in Cartesian coordinates and \hat{u}_i is an orientational unit vector parallel to the axis of symmetry of the i th particle. They are assumed to occupy the d -dimensional domain $\mathcal{G} \in \{\mathcal{A}, \mathcal{V}\}$ with measure $G \in \{A, V\}$ at the constant absolute temperature T . Here, the domain $\mathcal{G} \in \mathbb{R}^d$ is denoted as \mathcal{A} for $d = 2$ and as \mathcal{V} for $d = 3$. Analogously, the measure G is the total area A for $d = 2$ and the total volume V for $d = 3$. Since the basic procedures in the derivation of static PFC models on the one hand and dynamic PFC models on the other hand are very different, they are explained separately in the two following sections.

5.3 Static phase field crystal models for liquid crystals

The basic procedure in the derivation of static PFC models makes use of static DFT to find an approximating expression for the equilibrium Helmholtz free-energy functional $\mathcal{F}[\rho(\vec{r}, \hat{u})]$ of the considered system in terms of suitable order-parameter fields that parametrize the static ensemble-averaged one-particle number density

$$\rho(\vec{r}, \hat{u}) = \left\langle \sum_{i=1}^N \delta(\vec{r} - \vec{r}_i) \delta(\hat{u} - \hat{u}_i) \right\rangle. \quad (5.72)$$

This one-particle density is proportional to the probability to find a particle with center-of-mass position $\vec{r} = (x_1, \dots, x_d)$ and orientation $\hat{u} = (u_1, \dots, u_d)$. Its mean is

given by the mean particle number density

$$\frac{1}{G} \frac{1}{2^{d-1}\pi} \int_{\mathcal{G}} dG \int_{\mathcal{S}_{d-1}} d\Omega \rho(\vec{r}, \hat{u}) = \frac{N}{G} \quad (5.73)$$

with the differential $dG = d^d r$ with $dA = d^2 r$ and $dV = d^3 r$ for spatial integration, the differential $d\Omega = d^{d-1} u$ for angular integration, and the d -dimensional unit sphere $\mathcal{S}_{d-1} \in \{\mathcal{S}_1, \mathcal{S}_2\}$. The derivation of a static PFC model always begins with the choice of suitable order-parameter fields and with the parametrization of the one-particle density in terms of these order-parameter fields. In the next step, the free-energy functional

$$\mathcal{F}[\rho(\vec{r}, \hat{u})] = \mathcal{F}_{\text{id}}[\rho(\vec{r}, \hat{u})] + \mathcal{F}_{\text{exc}}[\rho(\vec{r}, \hat{u})] + \mathcal{F}_{\text{ext}}[\rho(\vec{r}, \hat{u})] \quad (5.74)$$

is decomposed into the ideal rotator-gas free-energy contribution $\mathcal{F}_{\text{id}}[\rho(\vec{r}, \hat{u})]$, the correlational excess free-energy contribution $\mathcal{F}_{\text{exc}}[\rho(\vec{r}, \hat{u})]$, and the external free-energy contribution $\mathcal{F}_{\text{ext}}[\rho(\vec{r}, \hat{u})]$ (see section 5.1.1.1).

For the ideal rotator-gas free-energy contribution, it is obvious to start with the general expression [Eva79]

$$\beta \mathcal{F}_{\text{id}}[\rho(\vec{r}, \hat{u})] = \int_{\mathcal{G}} dG \int_{\mathcal{S}_{d-1}} d\Omega \rho(\vec{r}, \hat{u}) (\ln(\Lambda^d \rho(\vec{r}, \hat{u})) - 1). \quad (5.75)$$

To approximate this expression, it is sufficient to insert the parametrization for $\rho(\vec{r}, \hat{u})$, to perform a Taylor expansion of the logarithm, and to carry out the angular integration. The Taylor expansion is usually truncated at fourth order, since this is the first nontrivial and stabilizing order (see section 5.1.2.1).

The approximation of the excess free-energy contribution is much more complicated, since it regards all correlations between the particles. To separate the correlations with respect to their order, it is appropriate to perform a functional Taylor expansion of the excess free-energy contribution in the density variation $\Delta\rho(\vec{r}, \hat{u}) = \rho(\vec{r}, \hat{u}) - \bar{\rho}$ around a homogeneous reference density $\bar{\rho}$ [see equation (5.7)]:

$$\beta \mathcal{F}_{\text{exc}}[\rho(\vec{r}, \hat{u})] = \beta \mathcal{F}_{\text{exc}}^{(0)}(\bar{\rho}) - \sum_{n=1}^{\infty} \frac{1}{n!} \mathcal{F}_{\text{exc}}^{(n)}[\rho(\vec{r}, \hat{u})]. \quad (5.76)$$

Here, the n th-order contributions are given by

$$\mathcal{F}_{\text{exc}}^{(n)}[\rho(\vec{r}, \hat{u})] = \int_{\mathcal{G}^n} d^n G \int_{\mathcal{S}_{d-1}^n} d^n \Omega c^{(n)}(\vec{r}^n, \hat{u}^n) \prod_{i=1}^n \Delta\rho(\vec{r}_i, \hat{u}_i) \quad (5.77)$$

and $c^{(n)}(\vec{r}^n, \hat{u}^n)$ denotes the n -particle direct correlation function¹⁷. To keep the repre-

¹⁷An expression for the n th-order direct correlation function of the isotropic phase can, for example, be obtained from the superposition of the n th functional derivative of a hard-core fundamental measure functional for anisotropic hard particles [HM09] and – in the case of a polar model – a

sensation of equation (5.77) compact, the notation

$$\mathcal{G}^n = \bigotimes_{i=1}^n \mathcal{G}, \quad \mathcal{S}_{d-1}^n = \bigotimes_{i=1}^n \mathcal{S}_{d-1}, \quad d^n G = \prod_{i=1}^n d^d r_i, \quad d^n \Omega = \prod_{i=1}^n d^{d-1} u_i \quad (5.78)$$

and the abbreviations

$$\vec{r}^n = (\vec{r}_1, \dots, \vec{r}_n), \quad \hat{u}^n = (\hat{u}_1, \dots, \hat{u}_n) \quad (5.79)$$

are used. The constant zeroth-order contribution of the functional Taylor expansion (5.76) and the vanishing first-order contribution can be neglected. For many situations, it is sufficient to take pair-correlations between the particles into account and to truncate the functional Taylor expansion at second order (Ramakrishnan-Yussouff approximation). However, it is sometimes necessary to take also correlations of higher order into account. All the correlation functions in the functional Taylor expansion (5.76) are not known explicitly and are approximated by the bulk correlation functions of the isotropic reference state¹⁸. This approximation involves several symmetries of the direct correlation functions. For a general polar system, three symmetries are present: *translational invariance*, *rotational invariance*, and the *invariance against renumbering of particles*. When the system is apolar, also the head-tail symmetry of the particles leading to an $\hat{u}_i \rightarrow -\hat{u}_i$ *invariance* of the direct correlation functions has to be considered. All these symmetries of the direct correlation functions $c^{(n)}(\vec{r}^n, \hat{u}^n)$ hold equally for the n th-order interaction potentials $U_n(\vec{r}^n, \hat{u}^n)$ of the particles. In order to obtain a PFC model that is as simple as possible, all symmetries have to be considered during the following steps of the derivation. For example, the first-order direct correlation function $c^{(1)}(\vec{r}_1, \hat{u}_1)$ is constant and the first-order contribution of the functional Taylor expansion (5.76) vanishes therefore as a consequence of translational and rotational invariance. The next step in the derivation is the expansion of the direct correlation functions with respect to their orientational degrees of freedom. This can be achieved by an expansion into a Fourier series in the case of two spatial dimensions and by an expansion into a series of spherical harmonics in the case of three spatial dimensions. After this expansion, the angular integration can be carried out. The result is still nonlocal and a gradient expansion [Eva79, LBW89, LBW90, OLV91, Lut06, EPB⁺07] (see appendix A) up to a nontrivial and stable order in the order-parameter fields, that are assumed to be sufficiently smooth, is performed to obtain a local functional. To ensure that surface terms can always be removed from the gradient expansion by partial integration, the domain \mathcal{G} is assumed to be unconstrained: $\mathcal{G} = \mathbb{R}^d$.

mean-field-type expression for the polar pair interaction. A related calculation for Stockmayer fluids is presented in references [GD94, GD96]. Another possibility is a simulation in combination with liquid-integral equations for anisotropic systems [WDCK90].

¹⁸This leads to a fluid perturbation theory of the free-energy functional. Alternatively, one could also expand around a different phase with less symmetries than the isotropic phase, but the resulting model would be much more complicated.

Finally, it is necessary to also express the external free-energy contribution in terms of the chosen order-parameter fields. This can be achieved by inserting the parametrization of the one-particle density into the exact expression [Eva79, EPB⁺07]

$$\mathcal{F}_{\text{ext}}[\rho(\vec{r}, \hat{u})] = \int_{\mathcal{G}} dG \int_{\mathcal{S}_{d-1}} d\Omega \rho(\vec{r}, \hat{u}) U_1(\vec{r}, \hat{u}) \quad (5.80)$$

for the external free-energy contribution, where the external potential $U_1(\vec{r}, \hat{u})$ is usually independent of the orientation \hat{u} , and by performing the angular integration.

All these approximations lead to a stable and local functional for the Helmholtz free energy in terms of the order-parameter fields and their spatial derivatives with prefactors that are given as generalized moments of the direct correlation functions. This functional constitutes a PFC model. Its parameters, the generalized moments, are moments of the expansion coefficients of the direct correlation functions in the isotropic state and depend on the particular thermodynamic conditions and therefore on mean particle number density and temperature. For stability reasons, one has to assume that the coefficients of the highest-order terms in the gradients and order-parameter fields in the PFC model are positive in the full free-energy functional. If this is not the case for a certain system, it is necessary to take into account further terms of the respective order-parameter field up to the first stabilizing order.

Although the given instructions for the derivation of a PFC model are the same for every particular PFC model that was derived from DFT up to now, it is necessary to describe the particular derivations in more detail (see below), since some of the main steps in the derivations are rather different and involve special difficulties. For example, the symmetry considerations, that are related to the direct correlation functions, are nontrivial and very different for two and three spatial dimensions as well as for apolar and polar particles and are especially complicated for correlation functions of higher order. Therefore, the rest of this section describes the different derivations in detail.

5.3.1 Two spatial dimensions

In two spatial dimensions, one has to choose $d = 2$, $\mathcal{G} = \mathcal{A}$, and $G = A$ in the general expressions of sections 5.2 and 5.3. The orientational unit vector is entirely defined as $\hat{u}(\varphi) = (\cos(\varphi), \sin(\varphi))$ and can be parametrized by a polar angle $\varphi \in [0, 2\pi)$. Moreover, a possible external potential and therefore the whole external contribution (5.80) to the free-energy functional are neglected in the following, since the additional consideration of an external potential is trivial and since the special form of the potential depends on the particular system that has to be described. The PFC model for liquid crystalline particles in two spatial dimensions, that is derived in the following, considers polar particles and contains the apolar model of Löwen [Löw10a] as a special case with vanishing polarization. Typical examples for polar particles include particles with an embedded dipole moment [LLW00, FBLL03, AMW08], colloidal pear-like particles [KBEP06, HJL⁺09], Janus particles [HCLG06, HCS⁺08], and asymmetric brush polymers modeled by Gaussian segment potentials [RWL07].

5.3.1.1 Static free-energy functional

To start with the derivation, the *reduced translational density*

$$\psi(\vec{r}) = \frac{1}{2\pi\bar{\rho}} \int_{S_1} d\Omega (\rho(\vec{r}, \hat{u}) - \bar{\rho}), \quad (5.81)$$

which measures deviations of the one-particle density $\rho(\vec{r}, \hat{u})$ from the reference density $\bar{\rho}$, the *polarization* $\vec{P}(\vec{r})$ with the components

$$P_i(\vec{r}) = \frac{1}{\pi\bar{\rho}} \int_{S_1} d\Omega \rho(\vec{r}, \hat{u}) u_i, \quad (5.82)$$

which describes the local averaged dipolar orientation of the particles, and the symmetric and traceless *nematic tensor* with the components

$$Q_{ij}(\vec{r}) = \frac{2}{\pi\bar{\rho}} \int_{S_1} d\Omega \rho(\vec{r}, \hat{u}) \left(u_i u_j - \frac{1}{2} \delta_{ij} \right), \quad (5.83)$$

which describes quadrupolar ordering of the particles, are chosen as order-parameter fields. Equivalently, one could decompose the polarization $\vec{P}(\vec{r}) = P(\vec{r})\hat{p}(\vec{r})$ into its modulus $P(\vec{r})$ and the local normalized dipolar orientation $\hat{p}(\vec{r})$ and use the two order parameters $P(\vec{r})$ and $\hat{p}(\vec{r})$ instead of $\vec{P}(\vec{r})$, but this would lead to more complicated expressions for the free-energy functional. Similarly, the nematic tensor can be expressed by [Gen71, GP95]

$$Q_{ij}(\vec{r}) = S(\vec{r}) \left(n_i(\vec{r}) n_j(\vec{r}) - \frac{1}{2} \delta_{ij} \right) \quad (5.84)$$

through the *nematic order parameter* $S(\vec{r})$, which measures the local degree of quadrupolar orientational order and is important near topological defects [BK86], and the *nematic director* $\hat{n}(\vec{r}) = (n_1(\vec{r}), n_2(\vec{r}))$, which is normalized and denotes the local direction of nematic order. While the vector $\hat{p}(\vec{r})$ describes the local direction of dipolar order, which results from a collective orientational ordering of a set of particles leading to a macroscopic polarization, the vector $\hat{n}(\vec{r})$ describes the local direction of quadrupolar order. In general, these two types of order may have two different preferred directions [BCP00]. Under the assumption of small anisotropies in the orientation, the chosen dimensionless and real-valued order-parameter fields $\psi(\vec{r})$, $P_i(\vec{r})$, and $Q_{ij}(\vec{r})$ are now used to approximate the one-particle density as follows:

$$\rho(\vec{r}, \hat{u}) = \bar{\rho} \left(1 + \psi(\vec{r}) + P_i(\vec{r}) u_i + u_i Q_{ij}(\vec{r}) u_j \right). \quad (5.85)$$

This parametrization is equivalent to an expansion of the one-particle density $\rho(\vec{r}, \hat{u})$ into a Fourier series up to second order with respect to the angle between the vectors \hat{u} and $\hat{p}(\vec{r})$, on the one hand, and the angle between the vectors \hat{u} and $\hat{n}(\vec{r})$, on the other hand. Inserting the parametrization (5.85) into equation (5.75), performing a Taylor expansion of the integrand up to fourth order in the order-parameter fields,

which guarantees stability of the solutions, and carrying out the angular integration yields to the approximation

$$\beta\mathcal{F}_{\text{id}}[\psi, P_i, Q_{ij}] = F_{\text{id}} + \pi\bar{\rho} \int_{\mathcal{A}} dA f_{\text{id}}(\vec{r}) \quad (5.86)$$

with the local scaled ideal rotator-gas free-energy density

$$f_{\text{id}} = \frac{\psi}{4}(8 - 2P_i^2 + 2P_i Q_{ij} P_j - Q_{ij}^2) + \frac{\psi^2}{4}(4 + 2P_i^2 + Q_{ij}^2) - \frac{\psi^3}{3} + \frac{\psi^4}{6} \quad (5.87)$$

$$+ \frac{P_i^2}{8}(4 + Q_{kl}^2) - \frac{P_i Q_{ij} P_j}{4} + \frac{P_i^2 P_j^2}{16} + \frac{Q_{ij}^2}{4} + \frac{Q_{ij}^2 Q_{kl}^2}{64},$$

where

$$F_{\text{id}} = 2\pi\bar{\rho} A (\ln(\Lambda^2\bar{\rho}) - 1) \quad (5.88)$$

is an irrelevant constant. For the excess free-energy functional, the functional Taylor expansion (5.76) is truncated at fourth order and the approximation (5.85) for the one-particle density is inserted. The direct correlation functions $c^{(n)}(\vec{r}^n, \hat{u}^n)$ for $n \in \{2, 3, 4\}$ have now to be expanded with respect to their orientational degrees of freedom. By considering the global translational and rotational invariance of the direct correlation functions, one can use the parametrization $c^{(n+1)}(R^n, \phi_{\text{R}}^n, \phi^n)$ with $R^n = (R_1, \dots, R_n)$, $\phi_{\text{R}}^n = (\phi_{\text{R}_1}, \dots, \phi_{\text{R}_n})$, and $\phi^n = (\phi_1, \dots, \phi_n)$ for the direct correlation function $c^{(n+1)}(\vec{r}^{n+1}, \hat{u}^{n+1})$ to reduce its orientational degrees of freedom¹⁹ from $2n + 2$ to $2n$. Here, the new variables are related to the previous ones by $\vec{r}_1 - \vec{r}_{i+1} = R_i \hat{u}(\varphi_{\text{R}_i})$, $\hat{u}_i = \hat{u}(\varphi_i)$, $\phi_{\text{R}_i} = \varphi_1 - \varphi_{\text{R}_i}$, and $\phi_i = \varphi_1 - \varphi_{i+1}$. With this parametrization and the multi-index notation $X^n = (X_1, \dots, X_n)$ for $X \in \{l, m, 1, \alpha\}$, the Fourier expansion of the direct correlation function reads

$$c^{(n+1)}(R^n, \phi_{\text{R}}^n, \phi^n) = \sum_{\substack{l_j, m_j = -\infty \\ 1 \leq j \leq n}}^{\infty} \tilde{c}_{l^n, m^n}^{(n+1)}(R^n) e^{i(l^n \cdot \phi_{\text{R}}^n + m^n \cdot \phi^n)} \quad (5.89)$$

with the expansion coefficients

$$\tilde{c}_{l^n, m^n}^{(n+1)}(R^n) = \frac{1}{(2\pi)^{2n}} \int_0^{2\pi} d\phi_{\text{R}}^n \int_0^{2\pi} d\phi^n c^{(n+1)}(R^n, \phi_{\text{R}}^n, \phi^n) e^{-i(l^n \cdot \phi_{\text{R}}^n + m^n \cdot \phi^n)}. \quad (5.90)$$

Next, a gradient expansion in the order-parameter fields is performed for $\mathcal{A} = \mathbb{R}^2$. For the term (5.77) corresponding to $n = 2$, this gradient expansion is performed up to fourth-order gradients in $\psi^2(\vec{r})$ to allow stable crystalline phases and up to second-order gradients in all other order-parameter products, where always is assumed that the highest-order gradient terms ensure stability. However, for $n = 3$ and $n = 4$ the

¹⁹Aside from the orientation \hat{u} , also the position vector \vec{r} is associated with an orientational degree of freedom.

gradient expansion is truncated at first and zeroth order, respectively. This results in the contributions

$$\mathcal{F}_{\text{exc}}^{(n)}[\psi, P_i, Q_{ij}] = \int_{\mathbb{R}^2} dA f_{\text{exc}}^{(n)}(\vec{r}) \quad (5.91)$$

of the static excess free-energy functional. In this equation, the scaled excess free-energy densities $f_{\text{exc}}^{(n)}(\vec{r})$ are local and approximatively given by

$$f_{\text{exc}}^{(2)} = A_1 \psi^2 + A_2 (\partial_i \psi)^2 + A_3 (\partial_k^2 \psi)^2 + B_1 (\partial_i \psi) P_i + B_2 P_i (\partial_j Q_{ij}) + B_3 (\partial_i \psi) (\partial_j Q_{ij}) \\ + C_1 P_i^2 + C_2 P_i (\partial_k^2 P_i) + C_3 (\partial_i P_i)^2 + D_1 Q_{ij}^2 + D_2 (\partial_j Q_{ij})^2, \quad (5.92)$$

$$f_{\text{exc}}^{(3)} = E_1 \psi^3 + E_2 \psi P_i^2 + E_3 \psi Q_{ij}^2 + E_4 P_i Q_{ij} P_j + F_1 \psi^2 (\partial_i P_i) + F_2 \psi P_i (\partial_j Q_{ij}) \\ + F_3 (\partial_i \psi) Q_{ij} P_j + F_4 P_i^2 (\partial_j P_j) + F_5 (\partial_i P_i) Q_{kl}^2 + F_6 P_i Q_{ki} (\partial_j Q_{kj}), \quad (5.93)$$

$$f_{\text{exc}}^{(4)} = G_1 \psi^4 + G_2 \psi^2 P_i^2 + G_3 \psi^2 Q_{ij}^2 + G_4 \psi P_i Q_{ij} P_j + G_5 P_i^2 Q_{kl}^2 + G_6 P_i^2 P_j^2 \\ + G_7 Q_{ij}^2 Q_{kl}^2 \quad (5.94)$$

with the coefficients

$$A_1 = 8 M_0^0(1), \quad A_2 = -2 M_0^0(3), \quad A_3 = \frac{1}{8} M_0^0(5) \quad (5.95)$$

in the gradient expansion of $\psi^2(\vec{r})$. These coefficients also appear – in a different form – in the traditional PFC model of Elder and co-workers [EPB⁺07]. The coefficients

$$B_1 = 4 \left(M_{-1}^1(2) - M_1^0(2) \right), \quad (5.96)$$

$$B_2 = 2 \left(M_1^1(2) - M_{-1}^2(2) \right), \quad (5.97)$$

$$B_3 = -M_{-2}^2(3) - M_2^0(3) \quad (5.98)$$

in contrast belong to the terms that describe the coupling of the polarization $\vec{P}(\vec{r})$ with the gradient of the translational density $\psi(\vec{r})$ and with the gradient of the nematic tensor $Q_{ij}(\vec{r})$ as well as the coupling of the gradient of the translational density with the gradient of the nematic tensor. The three coefficients

$$C_1 = 4 M_0^1(1), \quad C_2 = M_0^1(3) - \frac{1}{2} M_{-2}^1(3), \quad C_3 = -M_{-2}^1(3) \quad (5.99)$$

appear in the gradient expansion regarding the polarization $\vec{P}(\vec{r})$ and

$$D_1 = 2 M_0^2(1), \quad D_2 = -M_0^2(3) \quad (5.100)$$

are the coefficients of the gradient expansion in the nematic tensor $Q_{ij}(\vec{r})$. So far, all these coefficients can also be obtained by using the second-order Ramakrishnan-Yusouff functional for the excess free energy. The remaining coefficients, however, result

from higher-order contributions in the functional Taylor expansion. In third order, one obtains for the homogeneous terms the coefficients

$$E_1 = 32 \widehat{M}_{00}^{00}, \quad (5.101)$$

$$E_2 = 16 \left(\widehat{M}_{00}^{-11} + 2 \widehat{M}_{00}^{01} \right), \quad (5.102)$$

$$E_3 = 8 \left(\widehat{M}_{00}^{-22} + 2 \widehat{M}_{00}^{02} \right), \quad (5.103)$$

$$E_4 = 8 \left(2 \widehat{M}_{00}^{-21} + \widehat{M}_{00}^{11} \right) \quad (5.104)$$

and for the terms containing a gradient the coefficients

$$F_1 = 16 \left(\widetilde{M}_{01}^{-10} - 2 \widetilde{M}_{01}^{0-1} + \widetilde{M}_{01}^{00} \right), \quad (5.105)$$

$$F_2 = 16 \left(\widetilde{M}_{01}^{-21} - \widetilde{M}_{01}^{0-2} + \widetilde{M}_{01}^{01} - \widetilde{M}_{01}^{1-2} \right), \quad (5.106)$$

$$F_3 = -16 \left(\widetilde{M}_{01}^{-20} - \widetilde{M}_{01}^{-21} - \widetilde{M}_{01}^{01} + \widetilde{M}_{01}^{10} \right), \quad (5.107)$$

$$F_4 = -8 \left(\widetilde{M}_{01}^{-1-1} - 2 \widetilde{M}_{01}^{-11} + \widetilde{M}_{01}^{1-1} \right), \quad (5.108)$$

$$F_5 = -4 \left(\widetilde{M}_{01}^{-2-1} - \widetilde{M}_{01}^{-22} - \widetilde{M}_{01}^{-12} + \widetilde{M}_{01}^{2-1} \right), \quad (5.109)$$

$$F_6 = 8 \left(\widetilde{M}_{01}^{-22} - \widetilde{M}_{01}^{-1-2} + \widetilde{M}_{01}^{-12} - \widetilde{M}_{01}^{2-2} \right). \quad (5.110)$$

In fourth order, only homogeneous terms are kept. The corresponding coefficients are

$$G_1 = 128 \widehat{M}_{000}^{000}, \quad (5.111)$$

$$G_2 = 192 \left(\widehat{M}_{000}^{-101} + \widehat{M}_{000}^{001} \right), \quad (5.112)$$

$$G_3 = 96 \left(\widehat{M}_{000}^{-202} + \widehat{M}_{000}^{002} \right), \quad (5.113)$$

$$G_4 = 96 \left(2 \widehat{M}_{000}^{-201} + \widehat{M}_{000}^{-211} + \widehat{M}_{000}^{011} \right), \quad (5.114)$$

$$G_5 = 48 \left(\widehat{M}_{000}^{-212} + \widehat{M}_{000}^{-112} \right), \quad (5.115)$$

$$G_6 = 48 \widehat{M}_{000}^{-111}, \quad (5.116)$$

$$G_7 = 12 \widehat{M}_{000}^{-222}. \quad (5.117)$$

All the coefficients from above are linear combinations of moments of the Fourier expansion coefficients of the direct correlation functions. These moments are defined through

$$M_{l^n}^{m^n}(\alpha^n) = \pi^{2n+1} \bar{\rho}^{n+1} \left(\prod_{i=1}^n \int_0^\infty dR_i R_i^{\alpha_i} \right) \tilde{c}_{l^n, m^n}^{(n+1)}(R^n) \quad (5.118)$$

with the abbreviations $\widehat{M}_{l^n}^{m^n} = M_{l^n}^{m^n}(1^n)$ and $\widetilde{M}_{l_1 l_2}^{m_1 m_2} = M_{l_1 l_2}^{m_1 m_2}(1, 2)$. To reduce the total number of coefficients in the PFC model, the symmetry properties of the direct correlation functions and of their expansion coefficients (5.90) have been used. The translational and rotational invariance of the direct correlation functions were already considered in the context of the expansion with respect to the orientational degrees of freedom. The invariance against renumbering of particles,

$$\begin{aligned} & c^{(n)}(\dots, \vec{r}_i, \dots, \vec{r}_j, \dots, \dots, \hat{u}_i, \dots, \hat{u}_j, \dots) \\ &= c^{(n)}(\dots, \vec{r}_j, \dots, \vec{r}_i, \dots, \dots, \hat{u}_j, \dots, \hat{u}_i, \dots), \end{aligned} \quad (5.119)$$

on the other hand implies that generalized moments, arising from each other by simultaneous permutations of the elements of the multi-indices l^n , m^n , and α^n , are equal:

$$M_{\dots, l_i, \dots, l_j, \dots}^{\dots, m_i, \dots, m_j, \dots}(\dots, \alpha_i, \dots, \alpha_j, \dots) = M_{\dots, l_j, \dots, l_i, \dots}^{\dots, m_j, \dots, m_i, \dots}(\dots, \alpha_j, \dots, \alpha_i, \dots). \quad (5.120)$$

Furthermore, there is the invariance of the expansion coefficients (5.90) against complex conjugation:

$$\overline{\tilde{c}_{l^n, m^n}^{(n)}(R^n)} = \tilde{c}_{l^n, m^n}^{(n)}(R^n). \quad (5.121)$$

This symmetry involves the invariance of the expansion coefficients $\tilde{c}_{l^n, m^n}^{(n)}(R^n)$ against simultaneous reversal of the signs of the elements in l^n and m^n :

$$\tilde{c}_{-l_1, \dots, -l_n, -m_1, \dots, -m_n}^{(n)}(R_1, \dots, R_n) = \tilde{c}_{l_1, \dots, l_n, m_1, \dots, m_n}^{(n)}(R_1, \dots, R_n). \quad (5.122)$$

It is equivalent to the invariance of the direct correlation functions against reflection of the system at the first axis of coordinates. For the generalized moments this means:

$$M_{-l_1, \dots, -l_n}^{-m_1, \dots, -m_n}(\alpha_1, \dots, \alpha_n) = M_{l_1, \dots, l_n}^{m_1, \dots, m_n}(\alpha_1, \dots, \alpha_n). \quad (5.123)$$

When the system is apolar, the modulus $P(\vec{r})$ of the polarization $\vec{P}(\vec{r})$ is zero and its orientation $\hat{p}(\vec{r})$ is not defined, while the direction $\hat{n}(\vec{r})$ associated with quadrupolar order still exists. Then, further symmetry considerations lead to the equalities

$$\tilde{c}_{-1,1}^{(2)}(R) = \tilde{c}_{1,0}^{(2)}(R), \quad \tilde{c}_{-1,2}^{(2)}(R) = \tilde{c}_{1,1}^{(2)}(R), \quad \tilde{c}_{-2,2}^{(2)}(R) = \tilde{c}_{2,0}^{(2)}(R) \quad (5.124)$$

between expansion coefficients of the direct pair-correlation function and to the equations

$$M_{-1}^1(2) = M_1^0(2), \quad M_{-1}^2(2) = M_1^1(2), \quad M_{-2}^2(2) = M_2^0(2) \quad (5.125)$$

for the generalized moments. A consequence of these equations is that the coefficients B_1 and B_2 vanish and B_3 becomes more simple.

5.3.1.2 Special cases of the PFC model

The polar PFC model for two spatial dimensions contains several special cases known from the literature. These special cases follow from the full free-energy functional by choosing some of the order-parameter fields as zero or as a constant different from zero and by taking into account the contributions of the functional Taylor expansion (5.76) only up to a certain order $n_{\max} \in \{2, 3, 4\}$. Table 5.2 gives an overview about the most relevant special cases. For an arbitrary n_{\max} , the three most simple special cases are

Table 5.2: Relevant special cases that are contained in the polar PFC model for two spatial dimensions. If n_{\max} is not specified, it can be arbitrary (arb.).

ψ	P_i	Q_{ij}	n_{\max}	Associated model
0	0	<i>const.</i>	<i>arb.</i>	Landau expansion in Q_{ij}
0	0	$Q_{ij}(\vec{r})$	2	Landau-de Gennes free energy for uniaxial nematics [GP95]
0	0	$Q_{ij}(\vec{r})$	<i>arb.</i>	Gradient expansion in $Q_{ij}(\vec{r})$
0	<i>const.</i>	0	<i>arb.</i>	Landau expansion in P_i
0	$P_i(\vec{r})$	0	<i>arb.</i>	Gradient expansion in $P_i(\vec{r})$
<i>const.</i>	0	0	<i>arb.</i>	Landau expansion in ψ
$\psi(\vec{r})$	0	0	2	PFC model of Elder et al. [EPB ⁺ 07]
$\psi(\vec{r})$	0	0	<i>arb.</i>	Gradient expansion in $\psi(\vec{r})$
<i>const.</i>	$P_i(\vec{r})$	$Q_{ij}(\vec{r})$	4	Constant-density approximation
$\psi(\vec{r})$	0	$Q_{ij}(\vec{r})$	2	PFC model of Löwen [L ^ö w10a]
$\psi(\vec{r})$	$P_i(\vec{r})$	$Q_{ij}(\vec{r})$	4	Full free-energy functional

obtained for either a constant translational density ψ , a constant polarization P_i , or a constant nematic tensor Q_{ij} , when all remaining order-parameter fields are assumed to be zero. These special cases are Landau expansions in ψ , P_i , and Q_{ij} , respectively. If $\psi(\vec{r})$, $P_i(\vec{r})$, or $Q_{ij}(\vec{r})$ are space-dependent and the other order-parameter fields vanish, the free-energy functional contains also gradients of the respective space-dependent order-parameter field and can be called a gradient expansion in $\psi(\vec{r})$, $P_i(\vec{r})$, or $Q_{ij}(\vec{r})$, respectively. When additionally $n_{\max} = 2$ is chosen, the gradient expansion in $\psi(\vec{r})$ becomes the traditional PFC model of Elder et al. [EPB⁺07] and from the gradient expansion in $Q_{ij}(\vec{r})$ the Landau-de Gennes free energy for inhomogeneous uniaxial nematics [GP95] is recovered. In the case that only $\psi(\vec{r})$ is constant and the other order-parameter fields are space-dependent, a constant-density approximation of the full free-energy functional $\mathcal{F}[\psi, P_i, Q_{ij}]$ is established. The PFC model of Löwen [L^öw10a] is obtained for $n_{\max} = 2$, if the translational density is space-dependent, the polarization is zero, and the nematic tensor is space-dependent and parametrized according to equation (5.84). In the polar PFC model for two spatial dimensions, one can also consider the case of a space-dependent translational density $\psi(\vec{r})$, a space-dependent

polarization $P_i(\vec{r})$, and a vanishing nematic tensor, which corresponds to a ferroelectric phase without orientational order, but such a phase was never observed in experiments. Therefore, this case is not included in table 5.2 on the preceding page.

5.3.1.3 Equilibrium bulk phase diagram

The PFC model for two spatial dimensions can be solved numerically in order to determine the stable liquid crystalline phases. In the following paragraphs, this PFC model is at first reduced to an apolar PFC model by choosing $\vec{P}(\vec{r}) = \vec{0}$ and then rescaled by a suitable choice of the length and energy scales to reduce its complexity. The resulting model is investigated using semi-analytical and completely numerical methods and the predictions of these rather different methods are afterwards compared and discussed.

a) Rescaled dimensionless free-energy functional

The PFC model for two spatial dimensions has originally six remaining parameters for $\vec{P}(\vec{r}) = \vec{0}$ of which one can be scaled out by introducing the dimensionless area A' , the dimensionless free energy \mathcal{F}' , the dimensionless position $\vec{r}' = (x'_1, x'_2)$, and the dimensionless operator ∂'_i for the quantities $A = l_c^2 A'$, $\mathcal{F} = E_c \mathcal{F}'$, the position $\vec{r} = l_c \vec{r}'$, and the operator $\partial_i = \partial'_i / l_c$ with the characteristic length l_c and the characteristic energy E_c . When these characteristic quantities are chosen as $l_c = \sqrt{-A_3/A_2}$ and $E_c = -\pi \bar{\rho} A_3 / (\beta A_2)$, the apolar PFC model obtains the dimensionless form

$$\begin{aligned} \mathcal{F}'[\psi', Q'_{ij}] = \int_{\mathbb{R}^2} dA' & \left(-\frac{\psi'^3}{3} + \frac{\psi'^4}{6} + (\psi' - 1) \frac{\psi' Q'_{ij}{}^2}{4} + \frac{Q'_{ij}{}^2 Q'_{kl}{}^2}{64} \right. \\ & + A'_1 \psi'^2 + A'_2 \psi' (\partial_k'^2 + \partial_l'^2) \psi' \\ & \left. + B'_3 (\partial'_i \psi') (\partial'_j Q'_{ij}) + D'_1 Q'_{ij}{}^2 + D'_2 (\partial'_j Q'_{ij})^2 \right) \end{aligned} \quad (5.126)$$

with the new order-parameter fields $\psi'(\vec{r}') \equiv \psi(\vec{r})$ and $Q'_{ij}(\vec{r}') \equiv Q_{ij}(\vec{r})$. The new dimensionless parameters can be expressed by the original parameters through

$$A'_1 = 1 - \frac{A_1}{2\pi \bar{\rho}}, \quad A'_2 = -\frac{A_2^2}{2\pi \bar{\rho} A_3}, \quad B'_3 = \frac{A_2 B_3}{2\pi \bar{\rho} A_3}, \quad (5.127)$$

and

$$D'_1 = \frac{1}{4} - \frac{D_1}{2\pi \bar{\rho}}, \quad D'_2 = \frac{A_2 D_2}{2\pi \bar{\rho} A_3}. \quad (5.128)$$

With the parametrization (5.84), the rescaled PFC model (5.126) is equivalent to the model of Löwen in reference [Löw10a] and to its dimensionless version in reference [AWL11]. By comparison of equation (5.126) with the latter dimensionless model, one obtains the relations

$$A'_1 = B_l, \quad A'_2 = 4B_x, \quad B'_3 = -4F, \quad D'_1 = 2D, \quad D'_2 = 8E \quad (5.129)$$

between the dimensionless parameters and the two further relations

$$l_c = \frac{1}{\sqrt{2}} \tilde{l}_c, \quad E_c = \frac{1}{2} \tilde{E}_c \quad (5.130)$$

between the characteristic quantities of these two dimensionless models, where \tilde{l}_c and \tilde{E}_c denote the characteristic length and the characteristic energy in the model of reference [AWL11], respectively. The relation between the characteristic lengths in equation (5.130) is necessary, especially when the length scales of these two models have to be converted into each other.

In the integrand of functional (5.126), the first four terms approximate the free-energy density of an ideal rotator gas. Also the terms $\psi'^2(\vec{r}')$ and $Q'_{ij}{}^2(\vec{r}')$ appear in the ideal rotator entropy, but since there are corresponding terms in the excess free energy for anisotropic particles, the different contributions to these terms were combined to $A'_1 \psi'^2(\vec{r}')$ and $D'_1 Q'_{ij}{}^2(\vec{r}')$ in equation (5.126). Aside from the already mentioned polynomial terms in the order-parameter fields, their gradients also contribute to the free energy. The amount of their contribution is controlled by the parameters A'_2 , B'_3 , and D'_2 in the free-energy functional. Contributions of the gradient and curvature of the translational density field $\psi'(\vec{r}')$ appear in the term proportional to A'_2 . The couplings between the gradients of $\psi'(\vec{r}')$ and $Q'_{ij}(\vec{r}')$ are taken into account in the term proportional to the parameter B'_3 and the last term in the free-energy functional is scaled by the parameter D'_2 . It contains the divergence of the nematic tensor quadratically.

b) Minimization of the free-energy functional

The equilibrium phases corresponding to the free-energy functional (5.126) can be determined by minimization of this functional. Basic properties of the phase diagram can directly be read off equation (5.126). Since the parameter D'_1 controls the contribution of the nematic tensor $Q'_{ij}(\vec{r}')$ and therefore also of the nematic order parameter $S'(\vec{r}') \equiv S(\vec{r}')$, the nematic phase can be expected to be stable for large negative values of D'_1 . In the opposite case, if D'_1 is large enough and positive, the term $D'_1 Q'_{ij}{}^2(\vec{r}') + Q'_{ij}{}^2(\vec{r}') Q'_{kl}{}^2(\vec{r}')/64$ dominates the free energy and only phases with $Q'_{ij}(\vec{r}') \propto S'(\vec{r}') = 0$ can be stable. Crystalline phases with a non-vanishing nematic order can therefore only appear in a region around $D'_1 = 0$. From previous work, it is known that the difference $A'_1 - A'_2/4$ has a big influence on the translational density field [EPB⁺07, AWL11]. If the parameter A'_1 is large and positive, variations of the translational density field enlarge the free energy. Similarly, gradients of the translational density field enlarge the free energy for large and negative values of A'_2 . Therefore, it is obvious that phases without any density modulations, i. e., the isotropic and the nematic phase, are preferred for positive values of the difference $A'_1 - A'_2/4$, while all other phases with a periodic translational density field are preferred for negative values of this difference. Furthermore, there is a symmetry concerning the reversal of the sign of the parameter B'_3 in the free-energy functional. From equation (5.126) follows directly that the free-energy functional is invariant under a simultaneous change of the

signs of the parameter B'_3 and the nematic order-parameter field $S'(\vec{r}')$. Due to this symmetry, $B'_3 \geq 0$ is assumed in the phase diagrams that are presented further below.

In order to find the stable phases in the PFC model, the free-energy functional (5.126) can be minimized numerically using the *steepest descent method* for fixed parameters A'_1, A'_2, B'_3, D'_1 , and D'_2 . This method is based on pseudo-dynamic equations that become stationary for the equilibrium phase that minimizes the functional. The pseudo-dynamic equations were discretized using a finite-difference scheme and solved on a grid with 32×32 grid points per unit cell. In order to find the global minimum of the functional, a set of different phases was used as initial conditions and the functional was also minimized with respect to the lattice constant of the periodic phases by a variation of the length of the grid cells.

In addition, the *one-mode approximation* [PE10] was used to determine the phase diagram of the PFC model. The one-mode approximation is a semi-analytical approach consisting of periodic approximations for the order-parameter fields $\psi'(\vec{r}')$, $S'(\vec{r}')$, and $\hat{n}'(\vec{r}') \equiv \hat{n}(\vec{r})$. It reduces the PFC model to the lowest Fourier modes and is much faster than the free numerical minimization with the steepest descent method, since the minimization of the functional is reduced to the much easier minimization of a nonlinear equation with respect to a few parameters. However, the one-mode approximation can only be used to calculate the phase diagram for phases whose order-parameter fields can be well approximated by simple analytic expressions. For the liquid crystalline phases that appear as equilibrium solutions of the functional (5.126), the following parametrizations with the minimization parameters a_1, b_0, b_1 , and k were used:

- isotropic phase:

$$\begin{aligned}\psi'(\vec{r}') &= 0, \\ S'(\vec{r}') &= 0,\end{aligned}\tag{5.131}$$

- nematic phase:

$$\begin{aligned}\psi'(\vec{r}') &= 0, \\ S'(\vec{r}') &= b_0,\end{aligned}\tag{5.132}$$

- stripe phase:

$$\begin{aligned}\psi'(\vec{r}') &= a_1 \cos(kx'_2), \\ S'(\vec{r}') &= 0,\end{aligned}\tag{5.133}$$

- columnar phase:

$$\begin{aligned}\psi'(\vec{r}') &= a_1 \cos(kx'_2), \\ S'(\vec{r}') &= b_0 + b_1 \cos(kx'_2), \\ \hat{n}'(\vec{r}') &= (1, 0),\end{aligned}\tag{5.134}$$

- smectic A phase:

$$\begin{aligned}\psi'(\vec{r}') &= a_1 \cos(kx'_2) , \\ S'(\vec{r}') &= b_0 + b_1 \cos(kx'_2) , \\ \hat{n}'(\vec{r}') &= (0, 1) ,\end{aligned}\tag{5.135}$$

- triangular crystalline phase:

$$\begin{aligned}\psi'(\vec{r}') &= a_1 \left(\cos\left(\frac{\sqrt{3}}{2}kx'_1\right) \cos\left(\frac{k}{2}x'_2\right) - \frac{\cos(kx'_2)}{2} \right) , \\ S'(\vec{r}') &= b_0 + b_1 \left(\cos\left(\frac{\sqrt{3}}{2}kx'_1\right) \cos\left(\frac{k}{2}x'_2\right) - \frac{\cos(kx'_2)}{2} \right) , \\ \hat{n}'(\vec{r}') &= (\cos(\phi_0), \sin(\phi_0)) ,\end{aligned}\tag{5.136}$$

- square crystalline phase:

$$\begin{aligned}\psi'(\vec{r}') &= a_1 (\cos(kx'_1) + \cos(kx'_2)) , \\ S'(\vec{r}') &= b_0 + b_1 \cos(kx'_1) \cos(kx'_2) , \\ \hat{n}'(\vec{r}') &= (\cos(\phi_0), \sin(\phi_0)) .\end{aligned}\tag{5.137}$$

The constant angle ϕ_0 can be set to zero, because the free energy does not depend on it. Furthermore, due to equivalent free energies it is not necessary to distinguish between the columnar phase and the smectic A phase. They are therefore called “columnar/smectic A phase” in the following. Notice that there is no additive offset term a_0 for the density variation $\psi'(\vec{r}')$, since its spatial average is assumed to be zero, i. e., the considered phase transitions are assumed to be isochoric in this section. The minimization of the free energy in the context of the one-mode approximation was performed for fixed parameters A'_1 , A'_2 , B'_3 , D'_1 , and D'_2 . It is possible to minimize the free energy for the nematic phase and for all phases with a vanishing nematic order $S'(\vec{r}')$ analytically. The more complicated free energies of the remaining phases were minimized numerically with respect to the parameters a_1 , b_0 , b_1 , and k . For the global minimization of the free energy, a random search routine in the four-dimensional parameter space in combination with a local minimization by the Newton method was used.

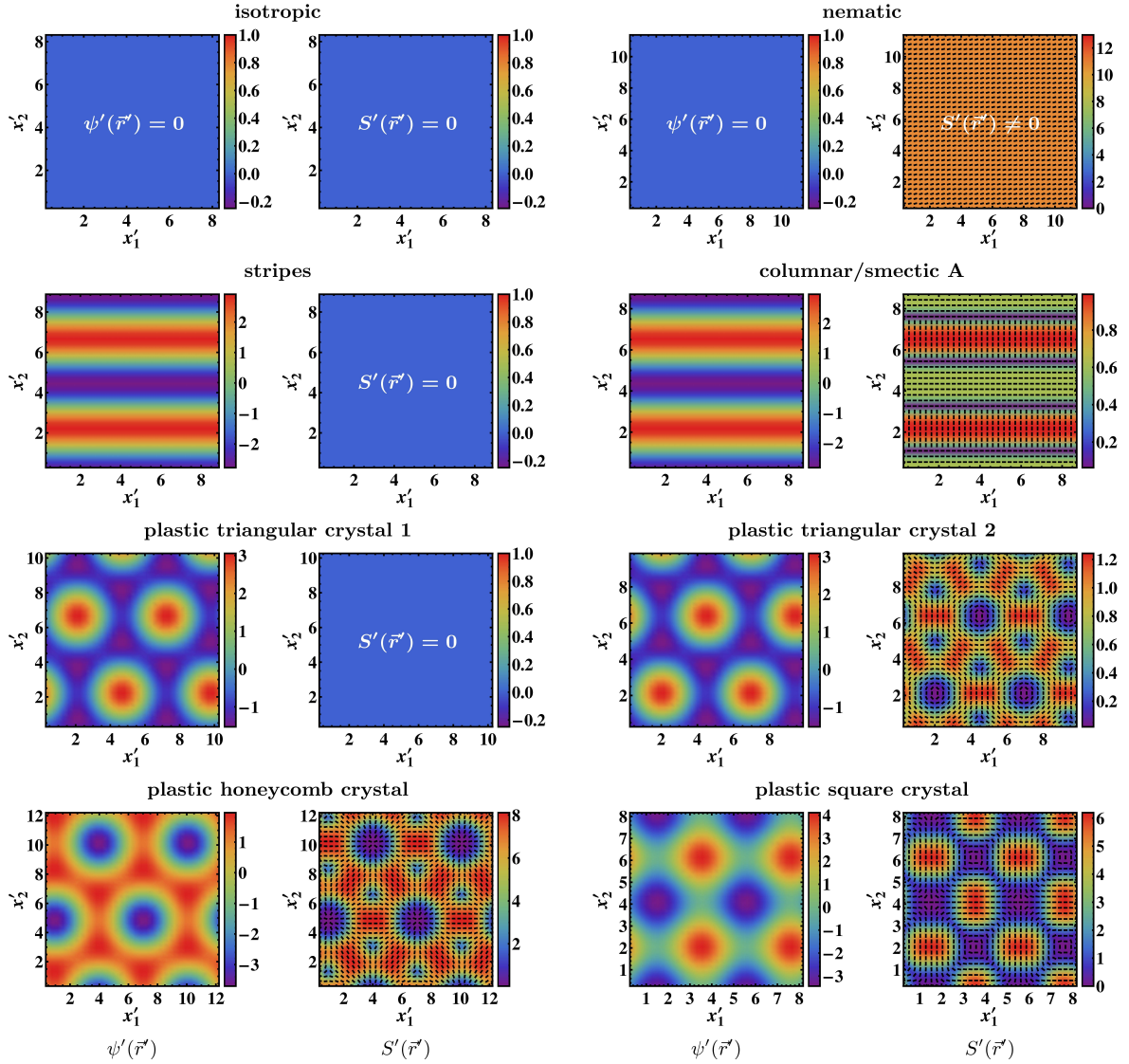


Figure 5.1: Stable liquid crystalline phases. The density plots show the order-parameter fields $\psi'(\vec{r}')$ and $S'(\vec{r}')$ in the (x'_1, x'_2) -plane for the isotropic and nematic phases, the stripe phase and columnar/smectic A phase, two plastic triangular crystals with different orientational ordering, and a plastic honeycomb crystal as well as a plastic square crystal. The black lines in the plots of the second and fourth column represent the director field $\hat{n}'(\vec{r}')$. In the plots with $S'(\vec{r}') = 0$, the director field is not shown because it is not defined. The parameters are $A'_2 = 14$, $D'_2 = 8$, and $B'_3 = 0$ for the stripe phase and the plastic triangular crystal 1 and $A'_2 = 14$, $D'_2 = 0.8$, and $B'_3 = -4$ for all other phases. Appropriate values for A'_1 and D'_1 follow from the phase diagrams in figure 5.3 on page 104. In the one-mode approximation, only the first five of these phases with a constant director field for the columnar/smectic A phase can be observed.

c) Numerical results

Apart from the fully isotropic phase with $\psi'(\vec{r}') = 0$ and $S'(\vec{r}') = 0$, which appears for $A'_1 > A'_2/4$ and $D'_1 > 0$, several other phases were found to minimize the free energy (see figure 5.1 on the preceding page). As expected, for negative and large D'_1 a nematic phase was found. In the columnar/smectic A phase, the system has positional ordering in one direction, while it is isotropic perpendicular to this direction. The nematic order-parameter field $S'(\vec{r}')$ for this phase has a similar profile to the reduced translational density field $\psi'(\vec{r}')$ with maxima of these two fields at the same positions. Near the maxima of the translational density $\psi'(\vec{r}')$, the director field $\hat{n}'(\vec{r}')$ is preferentially parallel to the gradient $\partial'_i \psi'(\vec{r}')$, while it is perpendicular to $\partial'_i \psi'(\vec{r}')$ around the minima of $\psi'(\vec{r}')$. This behavior of the director field follows from the term proportional to B'_3 in the free-energy functional (5.126). This term is proportional to

$$(\partial'_i \psi')(\partial'_i S') + 2S' n'_i n'_j (\partial'_i \partial'_j \psi') . \quad (5.138)$$

Its second contribution describes the coupling between the curvature $\partial'_i \partial'_j \psi'(\vec{r}')$ of the translational density and the orientation field $\hat{n}'(\vec{r}')$. For the columnar/smectic A phase, the term $S' n'_i n'_j (\partial'_i \partial'_j \psi')$ simplifies to

$$S' n'^2_2 (\partial'^2_2 \psi') . \quad (5.139)$$

Since the nematic order parameter $S'(\vec{r}')$ is positive in the columnar/smectic A phase, the curvature $\partial'^2_2 \psi'(\vec{r}')$ decides over the sign of this term. Two cases can be distinguished: in the first case, the curvature $\partial'^2_2 \psi'(\vec{r}')$ is negative, which is true close to the maxima of $\psi'(\vec{r}')$. In the other case, $\partial'^2_2 \psi'(\vec{r}')$ is positive. This happens near the minima of $\psi'(\vec{r}')$. The director field behaves differently in these two cases. When the free-energy functional is minimized, the term (5.139), too, tends to become minimal. Therefore, one observes $\hat{n}'(\vec{r}') = (0, 1) \parallel \partial'_i \psi'(\vec{r}')$ in the case where $\partial'^2_2 \psi'(\vec{r}')$ is negative, while $\hat{n}'(\vec{r}') = (1, 0) \perp \partial'_i \psi'(\vec{r}')$ holds in the second case. This explains the observed behavior of the director field (see figure 5.1 on the previous page for the columnar/smectic A phase). A similar flipping of the orientational field from perpendicular to parallel to the stripe direction was identified as transverse intralayer order in the three-dimensional smectic A phase of hard spherocylinders [RBMF95]. For a plastic crystal, everything is more complicated, since there are two spatial coordinates that are coupled. The resulting structure of the orientation field is a result of these different couplings.

Four plastic crystals with different symmetries were found by free numerical minimization of the functional (5.126). The first two phases are plastic triangular crystals with a vanishing and a non-vanishing nematic order parameter, respectively, where the first crystal with $S'(\vec{r}') = 0$ is a special degenerate case of the second one. The third plastic crystalline structure involves instead a honeycomb lattice. As a fourth case, there is also a plastic crystal with square symmetry. Such a plastic crystal with square symmetry does not appear in the traditional PFC model, but is known from other free-energy functionals [SB97]. For all plastic crystals, $S'(\vec{r}')$ vanishes both at the maxima and minima of $\psi'(\vec{r}')$. The director fields $\hat{n}'(\vec{r}')$ of the different plastic

crystalline phases exhibit quite different topologies. While the director field is not defined for the plastic triangular crystal 1 with a vanishing field $S'(\vec{r}')$, it possesses in general topological defects at positions, where the field $S'(\vec{r}')$ vanishes. This guarantees that there is a finite core energy of the topological defects [TSPT02]. The topological defects form another lattice with more lattice points than given by the maxima of the field $\psi'(\vec{r}')$, since there are additional *interstitial* topological defects at the minima of $\psi'(\vec{r}')$. The lattices of topological defects are schematically shown in figure 5.2. For the

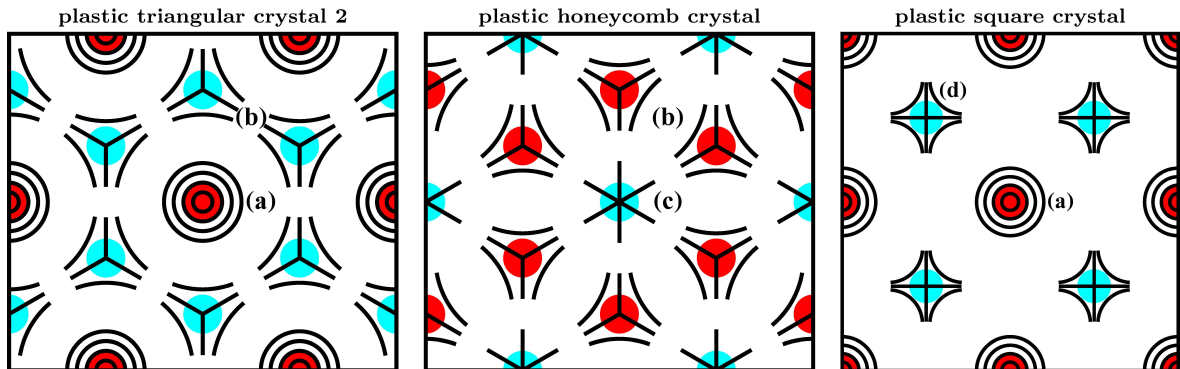


Figure 5.2: Topological defects in three different plastic liquid crystals in the (x'_1, x'_2) -plane (schematic). The defects coincide with the maxima (red disks) and minima (cyan disks) of the translational density field $\psi'(\vec{r}')$. The symbols in the plots represent the following defects: (a) vortices with the *topological winding number* $m = 1$, (b) disclinations with $m = -1/2$, (c) sources/sinks with $m = 1$, and (d) hyperbolic points with $m = -1$.

plastic triangular crystal 2 and for the plastic honeycomb crystal, the associated defect crystal is triangular albeit with a lattice constant that is the factor $1/\sqrt{3}$ smaller than the original one. Likewise, for the plastic square crystal, the defect lattice is a square lattice with a lattice constant reduced by the factor $1/\sqrt{2}$. The topological defects in the liquid crystalline phases can be classified according to the *winding number* of their director field [Mer79, GP95]. In the investigated PFC model (5.126), three types of point defects occur. These are vortices with the topological winding number $m = 1$, sources/sinks with $m = 1$, and hyperbolic points with $m = -1$. Furthermore, disclination line defects with $m = -1/2$ are found. Vortices and disclination lines occur in the plastic triangular crystal 2, which is schematically drawn in the first plot in figure 5.2. In the plastic honeycomb crystal, disclination lines arise together with sources/sinks (see second plot in figure 5.2), while vortices and hyperbolic points are found in the plastic square crystal (see last plot in figure 5.2). The sum of the topological winding numbers of all topological defects in a unit cell vanishes for all plastic crystals.

The director fields of all observed crystalline phases are periodic and vanish, when they are averaged in space. Therefore, these crystals are identified as being *plastic*. Plastic crystals appear both in special molecular [SIGK99, TP10] and colloidal [MD08, DJK⁺10, GAO⁺10] systems. While the lattice constant for molecular plastic crystals is

about a few nanometers, it is between 10 nm and 1000 nm for colloidal plastic crystals. Orientationally ordered crystalline phases were instead not found in the PFC model in the explored parameter range. Parameters for which the mentioned phases are stable follow from the phase diagrams in figure 5.3. For these phase diagrams, the parameters

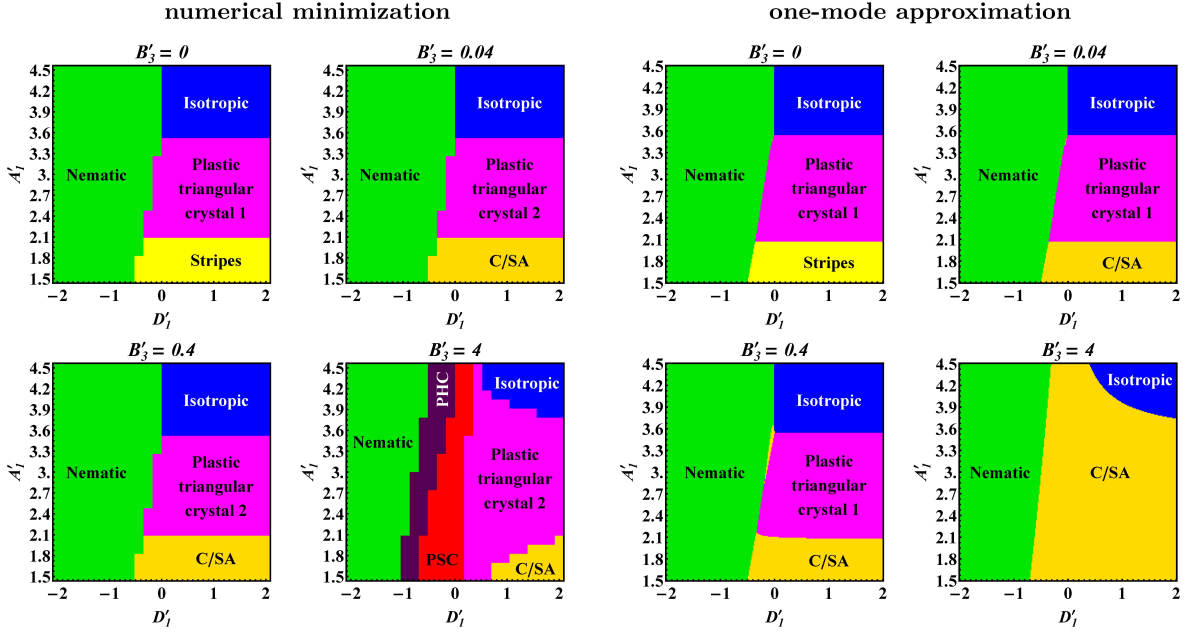


Figure 5.3: Phase diagrams calculated by free numerical minimization and with the one-mode approximation for the parameters $A'_2 = 14$ and $D'_2 = 0.8$. The relevant liquid crystalline phases are isotropic (blue), nematic (green), stripes (yellow), columnar/smectic A (C/SA, light orange), plastic triangular crystals (magenta), plastic honeycomb crystal (PHC, dark purple), and plastic square crystal (PSC, red). Due to the finite numerical resolution of the parameter space that is especially low for the free numerical minimization the separation lines between different phases are cornered.

$1.5 \leq A'_1 \leq 4.5$, $A'_2 = 14$, $B'_3 \in \{0, 0.04, 0.4, 4\}$, $-2 \leq D'_1 \leq 2$, and $D'_2 = 0.8$ were chosen. The parameter A'_2 was kept constant and the parameter A'_1 was varied in order to obtain all the phases of the traditional PFC model, when the orientational degrees of freedom are neglected. Moreover, the parameters B'_3 and D'_2 were selected from the regions, where the richest phase diagrams were found, and the parameter D'_1 was varied from -2 to higher values, because the free energy of the nematic phase is significantly smaller than the free energy of any other phase of the traditional PFC model at the value $D'_1 = -2$. For $B'_3 = 0$, there is a degenerate case with $S'(\vec{r}') = 0$ for $D'_1 > 0$ and $D'_2 > 0$. In this case, a stripe phase and the plastic triangular crystal 1 were observed. These phases are replaced by the columnar/smectic A phase and by the plastic triangular crystal 2, respectively, when B'_3 becomes positive. The richest phase diagram with six different phases was obtained for $B'_3 = 4$. Independent of the particular value of the parameter B'_3 , the phase transition between the isotropic and

the nematic phase turned out to be continuous, while all other phase transitions are discontinuous. This result agrees with the fact that the PFC model reduces to the Landau-de Gennes model for the isotropic-nematic phase transition, which describes this phase transition as continuous. On the other hand, symmetries are broken for the remaining phase transitions so that they must be discontinuous.

In comparison with the free numerical minimization of the free-energy functional, the one-mode approximation appears to provide an approximative but much faster alternative to determine the phase diagram of the PFC model (see figure 5.3 on the preceding page). A speed-up factor of 100 can easily be achieved. This allows the fast calculation of phase diagrams for various parameter combinations as well as single phase diagrams with a rather high resolution (compare the left and the right column in figure 5.3 on the facing page). The one-mode approximation leads to the same phase diagram as the free numerical minimization for $B'_3 = 0$ (see figure 5.3 on the preceding page), but for higher values of B'_3 , the phase diagrams deviate increasingly from the actual phase diagrams that were obtained by free numerical minimization. This is due to the complicated director field of some crystalline phases that is not represented in the one-mode approximation. While the isotropic phase, the nematic phase, the stripe phase, and the plastic triangular crystal 1 are described precisely by the one-mode approximation, there are small deviations for the columnar/smectic A phase and a complete negligence of the topology of the director field for the plastic triangular crystal 2, for the plastic honeycomb crystal, and for the plastic square crystal. The latter three phases do not appear in the phase diagrams for the one-mode approximation, since their director fields are approximated by director fields with a constant orientation in the one-mode approximation, but the actual plastic crystals have a vanishing global orientation. When the free-energy functional is minimized for the plastic triangular crystal 2 using the one-mode approximation, the improper ansatz for the director field makes that the minimum of the free energy is always found for a vanishing nematic order parameter $S'(\vec{r}')$. This is the reason for the appearance of the plastic triangular crystal 1 instead of the plastic triangular crystals 2 in the phase diagrams of the one-mode approximation for $B'_3 \neq 0$. A further difference between the phase diagrams of the one-mode approximation and those for the free numerical minimization is an island of the columnar/smectic A phase near the lower end of the phase transition line between the isotropic and the nematic phase for $B'_3 = 0.4$. Also this island results from an inaccurate consideration of the director field for some liquid crystalline phases and is not physically justified.

To check that the above mentioned disadvantages of the phase diagrams for the one-mode approximation really arise from the improper approximation of the director field $\hat{n}'(\vec{r}')$, a Fourier analysis of the numerical results, that are shown in figure 5.1 on page 101, was performed. This Fourier analysis exhibited that the first Fourier mode is always dominant. Only for the plastic honeycomb crystal and for the plastic square crystal there appears a small contribution of the second mode that might be relevant. A look at the behavior of the order parameters near phase transitions confirmed the results of the free numerical minimization regarding the order of the phase transitions.

Despite the already discussed disadvantages of the one-mode approximation, it proved to be a useful method to calculate phase diagrams for a given PFC model with low computational effort. The one-mode approximation is also useful for exploring the phase diagram for suitable parameters or for a large number of different parameter combinations and for finding interesting regions in a high-dimensional parameter space that are worth to be investigated more precisely by a much more expensive direct minimization of the free-energy functional.

5.3.2 Three spatial dimensions

In the case of three spatial dimensions, one has to choose $d = 3$, $\mathcal{G} = \mathcal{V}$, and $G = V$ in the general equations of sections 5.2 and 5.3. Since only uniaxial particles with an axis of symmetry are considered in this chapter, the orientational unit vector \hat{u} , that is parallel to this axis of symmetry, is entirely defined using spherical coordinates by

$$\hat{u}(\theta, \phi) = (\sin(\theta) \cos(\phi), \sin(\theta) \sin(\phi), \cos(\theta)) \quad (5.140)$$

with the polar angle $\theta \in [0, \pi]$ and the azimuthal angle $\phi \in [0, 2\pi)$. In addition to their rotational symmetry, the particles are assumed to have head-tail symmetry so that a macroscopic polarization through collective self-organization of the particles cannot arise. As in the previously derived PFC model for two spatial dimensions, a possible external potential is again neglected. Relevant uniaxial particles are, for example, hard spherocylinders [L6w94a, BF97] and hard ellipsoids [FMM84], whose interactions can be modeled by Yukawa-segment models [L6w94b, L6w94c, KKK96] and Gay-Berne potentials [CCAN96, FTD04, MZ06].

5.3.2.1 Static free-energy functional

The derivation of a static PFC model for three spatial dimensions as presented in this section proceeds analogously to the previously shown derivation for two spatial dimensions. For the dimensionless and real-valued order-parameter fields $\psi(\vec{r})$ and $Q_{ij}(\vec{r})$ that were chosen in section 5.3.1 for the polar PFC model for two spatial dimensions, also three-dimensional analogs exist. These are used for the derivation in the present section. The reduced translational density for three spatial dimensions is given by

$$\psi(\vec{r}) = \frac{1}{4\pi\bar{\rho}} \int_{\mathcal{S}_2} d\Omega (\rho(\vec{r}, \hat{u}) - \bar{\rho}) \quad (5.141)$$

and the 3×3 -dimensional symmetric and traceless nematic tensor is defined through

$$Q_{ij}(\vec{r}) = \frac{15}{8\pi\bar{\rho}} \int_{\mathcal{S}_2} d\Omega \rho(\vec{r}, \hat{u}) \left(u_i u_j - \frac{1}{3} \delta_{ij} \right). \quad (5.142)$$

Again, the nematic tensor can be expressed by the nematic order-parameter field $S(\vec{r})$ and the nematic director $\hat{n}(\vec{r}) = (n_1(\vec{r}), n_2(\vec{r}), n_3(\vec{r}))$ that is here the only unit vec-

tor that denotes a preferred direction in the liquid crystalline system. In the three-dimensional case, the decomposition of the nematic tensor is given by [Gen71, GP95]

$$Q_{ij}(\vec{r}) = S(\vec{r}) \left(\frac{3}{2} n_i(\vec{r}) n_j(\vec{r}) - \frac{1}{2} \delta_{ij} \right). \quad (5.143)$$

Notice that the nematic order-parameter field $S(\vec{r})$ is the biggest eigenvalue of the nematic tensor $Q_{ij}(\vec{r})$ and the nematic director $\hat{n}(\vec{r})$ is the corresponding eigenvector. With the order-parameter fields $\psi(\vec{r})$ and $Q_{ij}(\vec{r})$, the one-particle density is approximated by

$$\rho(\vec{r}, \hat{u}) = \bar{\rho} \left(1 + \psi(\vec{r}) + u_i Q_{ij}(\vec{r}) u_j \right). \quad (5.144)$$

As before, the Helmholtz free-energy functional has to be approximated in the next step. An approximative equation for the ideal rotator-gas free-energy functional is again obtained from equation (5.75), when the approximation (5.144) is used and the integrand is expanded up to fourth order in the order-parameter fields. This results in

$$\beta \mathcal{F}_{\text{id}}[\psi, Q_{ij}] = F_{\text{id}} + \pi \bar{\rho} \int_{\mathcal{V}} dV f_{\text{id}}(\vec{r}) \quad (5.145)$$

with the local scaled ideal rotator-gas free-energy density

$$\begin{aligned} f_{\text{id}} = & 4\psi \left(1 - \frac{\text{tr}(Q^2)}{15} + \frac{8 \text{tr}(Q^3)}{315} \right) + 2\psi^2 \left(1 + \frac{2 \text{tr}(Q^2)}{15} \right) - \frac{2\psi^3}{3} + \frac{\psi^4}{3} \\ & + \frac{4 \text{tr}(Q^2)}{15} - \frac{16 \text{tr}(Q^3)}{315} + \frac{8 \text{tr}(Q^4)}{315}, \end{aligned} \quad (5.146)$$

where $\text{tr}(\cdot)$ denotes the trace operator, and the irrelevant constant

$$F_{\text{id}} = 4\pi \bar{\rho} V \left(\ln(\Lambda^3 \bar{\rho}) - 1 \right). \quad (5.147)$$

For the excess free-energy functional, the Ramakrishnan-Yussouff approximation (5.10) is used together with equation (5.144) involving the direct pair-correlation function $c^{(2)}(\vec{r}_1, \vec{r}_2, \hat{u}_1, \hat{u}_2)$. Respecting translational symmetry and decomposing the difference vector $\vec{r}_1 - \vec{r}_2 = R\hat{u}_R$ into its modulus R and orientational unit vector \hat{u}_R , the direct pair-correlation function can also be written as $c^{(2)}(R\hat{u}_R, \hat{u}_1, \hat{u}_2)$. It can therefore be expanded with respect to the three orientations \hat{u}_R , \hat{u}_1 , and \hat{u}_2 into rotational invariants [GG84, GL98]. This expansion is by construction invariant against global rotations and defined by

$$\begin{aligned} c^{(2)}(R\hat{u}_R, \hat{u}_1, \hat{u}_2) = & \sum_{l_1, l_2, l=0}^{\infty} \omega_{l_1 l_2 l}(R) \sum_{\substack{m_j = -l_j \\ 1 \leq j \leq 2}}^{l_j} \sum_{m=-l}^l C(l_1, l_2, l, m_1, m_2, m) \\ & \times Y_{l_1 m_1}(\hat{u}_1) Y_{l_2 m_2}(\hat{u}_2) \bar{Y}_{lm}(\hat{u}_R) \end{aligned} \quad (5.148)$$

with the expansion coefficients

$$\begin{aligned} \omega_{l_1 l_2 l}(R) &= \sqrt{\frac{4\pi}{2l+1}} \sum_{m=-\min\{l_1, l_2\}}^{\min\{l_1, l_2\}} C(l_1, l_2, l, m, -m, 0) \\ &\times \int_{\mathcal{S}_2^2} d^2\Omega c^{(2)}(R\hat{e}_3, \hat{u}_1, \hat{u}_2) \bar{Y}_{l_1 m}(\hat{u}_1) \bar{Y}_{l_2 - m}(\hat{u}_2). \end{aligned} \quad (5.149)$$

Here, the symbol $C(l_1, l_2, l, m_1, m_2, m)$ denotes a Clebsch-Gordan coefficient, $Y_{lm}(\hat{u})$ is a spherical harmonic, \hat{e}_3 stands for the Cartesian unit vector co-directional with the x_3 -axis, and $\bar{\cdot}$ denotes complex conjugation. Contributions with an odd index l_1 , l_2 , or l vanish as a consequence of apolarity. A gradient expansion with $\mathcal{V} = \mathbb{R}^3$ leads now to the final result. This gradient expansion is performed up to fourth-order gradients in terms that are quadratic in the translational density $\psi(\vec{r})$ and up to second-order derivatives in all other order-parameter products. The result is given by

$$\mathcal{F}_{\text{exc}}^{(2)}[\psi, Q_{ij}] = \int_{\mathbb{R}^3} dV f_{\text{exc}}^{(2)}(\vec{r}) \quad (5.150)$$

with the local scaled excess free-energy density

$$\begin{aligned} f_{\text{exc}}^{(2)} &= A_1 \psi^2 + A_2 (\partial_i \psi)^2 + A_3 (\partial_k^2 \psi)^2 + B_1 Q_{ij}^2 + B_2 (\partial_i \psi)(\partial_j Q_{ij}) \\ &+ \tilde{K}_1 (\partial_j Q_{ij})^2 + \tilde{K}_2 Q_{ij} (\partial_k^2 Q_{ij}). \end{aligned} \quad (5.151)$$

The coefficients in $f_{\text{exc}}^{(2)}(\vec{r})$ appear in three different groups. The first group consists of the three coefficients

$$A_1 = 8 \Omega_{000}(0), \quad A_2 = -\frac{4}{3} \Omega_{000}(2), \quad A_3 = \frac{1}{15} \Omega_{000}(4), \quad (5.152)$$

that are already known from the traditional PFC model [EPB⁺07] and belong to the gradient expansion of the translational density. In the next group, the two coefficients

$$B_1 = \frac{16}{15\sqrt{5}} \Omega_{220}(0), \quad B_2 = -\frac{16}{15} \Omega_{022}(2), \quad (5.153)$$

that go along with the nematic tensor and the coupling of its gradient with the gradient of the translational density, are collected. The last group contains the Frank constants

$$\tilde{K}_1 = \frac{16}{15} \sqrt{\frac{2}{35}} \Omega_{222}(2), \quad \tilde{K}_2 = \frac{8}{45\sqrt{5}} \Omega_{220}(2) + \frac{1}{3} \tilde{K}_1, \quad (5.154)$$

which appear in the Frank free-energy density [Cha92, GP95]. All these coefficients are expressed in terms of the generalized moments

$$\Omega_{l_1 l_2 l}(n) = \pi^{3/2} \bar{\rho}^2 \int_0^\infty dR R^{n+2} \omega_{l_1 l_2 l}(R). \quad (5.155)$$

As before, equalities between generalized moments with different index-combinations, which can be derived using symmetry considerations, have been taken into account in order to reduce the set of generalized moments in equation (5.151) to its seven independent members.

5.3.2.2 Special cases of the PFC model

For the apolar PFC model for three spatial dimensions, some relevant special cases are summarized in table 5.3. As for the PFC model for two spatial dimensions, one

Table 5.3: Relevant special cases that are contained in the apolar PFC model for three spatial dimensions.

ψ	Q_{ij}	Associated model
0	<i>const.</i>	Landau expansion in Q_{ij}
0	$Q_{ij}(\vec{r})$	Landau-de Gennes free energy for uniaxial nematics [GP95]
<i>const.</i>	0	Landau expansion in ψ
$\psi(\vec{r})$	0	PFC model of Elder et al. [EPB ⁺ 07]
<i>const.</i>	$Q_{ij}(\vec{r})$	Constant-density approximation
$\psi(\vec{r})$	$Q_{ij}(\vec{r})$	Full free-energy functional

obtains a Landau expansion in the translational density ψ or in the nematic tensor Q_{ij} , if this order-parameter field is constant and the respective other order-parameter field is zero. When $\psi(\vec{r})$ is space-dependent and $Q_{ij}(\vec{r})$ vanishes, the traditional PFC model of Elder et al. [EPB⁺07] for isotropic particles in three spatial dimensions is obtained from the full free-energy functional. In the opposite case, where $\psi(\vec{r})$ vanishes and $Q_{ij}(\vec{r})$ is space-dependent, the Landau-de Gennes free energy for inhomogeneous uniaxial nematics [GP95] is recovered. Also the constant-density approximation can again be established. This is the case, if ψ is constant and $Q_{ij}(\vec{r})$ is space-dependent. In the full free-energy functional $\mathcal{F}[\psi, Q_{ij}]$, all these special cases are properly comprised. This functional clarifies the relations between already existing simpler PFC models, contains the appropriate couplings of the order-parameter fields $\psi(\vec{r})$ and $Q_{ij}(\vec{r})$, and relates the constant prefactors of the terms in the functional to the direct pair-correlation function. After the publication of this functional in reference [WLB10], where the parametrization (5.143) was used for the nematic tensor, it was rederived by Yabunaka and Araki in reference [YA11] using the random-phase approximation (5.12) for the direct pair-correlation function. Their model is thus included in the PFC model for three spatial dimensions that is derived in this work. Nevertheless, reference [YA11] also contains some numerical evaluations of the PFC model that are new.

5.4 Dynamic phase field crystal models for liquid crystals

The dynamic equations corresponding to the static PFC models can be derived from DDFT. Boundary effects are thereby neglected through the consideration of an infinite domain $\mathcal{G} = \mathbb{R}^d$. Depending on the particular situation, one can choose the most appropriate special version of the DDFT equation, whose most general form for biaxial particles was derived in chapter 4. If, for example, only uniaxial particles or particles in two spatial dimensions are considered, one should use a more special and at once simpler form of the DDFT equation. The basic derivation is then performed in three steps. At first, the order-parameter fields, that have been chosen for the statics, are assumed to be time-dependent and the time-dependent one-particle density $\rho(\vec{r}, \hat{u}, t)$ is approximated in terms of these time-dependent order-parameter fields in analogy to the static parametrization. Secondly, the chain rule for functional differentiation is used to express the functional derivative $\delta\mathcal{F}/\delta\rho$ of the Helmholtz free-energy functional \mathcal{F} , that is also assumed to be time-dependent, in terms of the functional derivatives of the free-energy functional with respect to the chosen order-parameter fields. Finally, the time-dependent parametrization for the one-particle density and the time-dependent expression for the functional derivative $\delta\mathcal{F}/\delta\rho$ are inserted into the DDFT equation and a set of in general coupled dynamic equations for the single order-parameter fields is obtained by an orthogonal projection of the DDFT equation with respect to the orientation \hat{u} .

5.4.1 Two spatial dimensions

On the basis of the static PFC model, that is described in section 5.3.1, and a suitable DDFT equation, the dynamic equations for the time-dependent order-parameter fields $\psi(\vec{r}, t)$, $P_i(\vec{r}, t)$, and $Q_{ij}(\vec{r}, t)$, that parametrize the time-dependent noise-averaged one-particle number density

$$\rho(\vec{r}, \hat{u}, t) = \left\langle \sum_{i=1}^N \delta(\vec{r} - \vec{r}_i(t)) \delta(\hat{u} - \hat{u}_i(t)) \right\rangle, \quad (5.156)$$

are derived in this section. The parametrization of the time-dependent one-particle density is analogous to the parametrization (5.85) in the static case:

$$\rho(\vec{r}, \hat{u}, t) = \bar{\rho} \left(1 + \psi(\vec{r}, t) + P_i(\vec{r}, t) u_i + u_i Q_{ij}(\vec{r}, t) u_j \right). \quad (5.157)$$

For the derivation of the dynamic equations, the DDFT equation (4.44) for two spatial dimensions is used. In the case of passive symmetric particles without a translational-

rotational coupling, this DDFT equation simplifies to

$$\begin{aligned} \dot{\rho}(\vec{r}, \hat{u}, t) = & \beta \vec{\nabla}_{\vec{r}} \cdot (\mathbf{D}_T(\hat{u}) \rho(\vec{r}, \hat{u}, t) \vec{\nabla}_{\vec{r}} \rho^{\natural}(\vec{r}, \hat{u}, t)) \\ & + \beta D_R \partial_{\varphi} (\rho(\vec{r}, \hat{u}, t) \partial_{\varphi} \rho^{\natural}(\vec{r}, \hat{u}, t)) \end{aligned} \quad (5.158)$$

with the translational short-time diffusion tensor

$$\mathbf{D}_T(\hat{u}) = D_{\parallel} \hat{u} \otimes \hat{u} + D_{\perp} (\mathbb{1} - \hat{u} \otimes \hat{u}) . \quad (5.159)$$

Here, $D_{\parallel} \equiv D_1$ and $D_{\perp} \equiv D_2$ (see equations (3.24) and (3.25) in section 3.2.1.2) are the translational diffusion coefficients for translation parallel and perpendicular to the orientation \hat{u} , respectively, and the symbol $\mathbb{1}$ denotes the 2×2 -dimensional unit matrix. The two terms on the right-hand-side of this DDFT equation for uniaxial particles correspond to pure translation and pure rotation, respectively. Translational-rotational coupling terms, which are present in the general DDFT equation (4.44), are neglected in this section. Since the DDFT equation (5.158) is still rather complicated, the CMA

$$\dot{\rho}(\vec{r}, \hat{u}, t) = \beta \bar{\rho} \vec{\nabla}_{\vec{r}} \cdot (\mathbf{D}_T(\hat{u}) \vec{\nabla}_{\vec{r}} \rho^{\natural}(\vec{r}, \hat{u}, t)) + \beta \bar{\rho} D_R \partial_{\varphi}^2 \rho^{\natural}(\vec{r}, \hat{u}, t) \quad (5.160)$$

might be desirable for numerical calculations (see section 5.1.2.2). Using the short notation for thermodynamic conjugates introduced by equation (5.64) in section 5.1.4.2, the expression

$$\rho^{\natural} = \frac{1}{2\pi\bar{\rho}} \psi^{\natural} + \frac{u_i}{\pi\bar{\rho}} P_i^{\natural} + \frac{u_i u_j}{\pi\bar{\rho}} Q_{ij}^{\natural} \quad (5.161)$$

follows from the chain rule of functional differentiation [Gro88]. When performing functional derivatives with respect to Q_{ij} or Q_{ij}^{\natural} , one has to notice that Q_{ij} as well as Q_{ij}^{\natural} are symmetric and traceless. The interdependence of the elements of these tensors leads to more complicated derivatives that respect the symmetry properties of these tensors. A very useful equation in this context is

$$\frac{\delta Q_{kl}}{\delta Q_{ij}^{\natural}} = \frac{\delta Q_{kl}^{\natural}}{\delta Q_{ij}^{\natural}} = \delta_{ik} \delta_{jl} + \delta_{jk} \delta_{il} - \delta_{ij} \delta_{kl} . \quad (5.162)$$

For the time-dependent Helmholtz free-energy functional in the DDFT equation, the equilibrium Helmholtz free-energy functional (5.74) with $\rho(\vec{r}, \hat{u}, t)$ instead of $\rho(\vec{r}, \hat{u})$ is used. The explicit forms of the conjugated order-parameter fields $\psi^{\natural}(\vec{r}, t)$, $P_i^{\natural}(\vec{r}, t)$, and $Q_{ij}^{\natural}(\vec{r}, t)$ result therefore directly from the functional derivatives of equations (5.76), (5.80), and (5.86) with respect to the order-parameter fields:

$$\Xi^{\natural} = \frac{\delta \mathcal{F}}{\delta \Xi} = \frac{\delta \mathcal{F}_{\text{id}}}{\delta \Xi} + \frac{\delta \mathcal{F}_{\text{exc}}}{\delta \Xi} + \frac{\delta \mathcal{F}_{\text{ext}}}{\delta \Xi} \quad \text{with} \quad \Xi \in \{\rho, \psi, P_i, Q_{ij}\} . \quad (5.163)$$

With the abbreviation $\lambda = \pi\bar{\rho}/\beta$, these functional derivatives are given for $n \leq 2$ by

$$\frac{1}{\lambda} \frac{\delta \mathcal{F}_{\text{id}}}{\delta \psi} = 2 - \frac{P_i^2}{2} + \frac{P_i Q_{ij} P_j}{2} - \frac{Q_{ij}^2}{4} + \frac{\psi}{2} (4 + 2P_i^2 + Q_{ij}^2) - \psi^2 + \frac{2}{3} \psi^3, \quad (5.164)$$

$$\frac{1}{\lambda} \frac{\delta \mathcal{F}_{\text{id}}}{\delta P_i} = -\psi (P_i - Q_{ij} P_j) + \psi^2 P_i + \frac{P_i}{4} (4 + Q_{kl}^2) - \frac{Q_{ij} P_j}{2} + \frac{P_i P_j^2}{4}, \quad (5.165)$$

$$\begin{aligned} \frac{1}{\lambda} \frac{\delta \mathcal{F}_{\text{id}}}{\delta Q_{ij}} &= \frac{\psi}{2} (2P_i P_j - \delta_{ij} P_l^2 - 2Q_{ij}) + \psi^2 Q_{ij} + \frac{P_k^2}{2} Q_{ij} - \frac{1}{4} (2P_i P_j - \delta_{ij} P_l^2) \\ &\quad + Q_{ij} + \frac{Q_{ij} Q_{kl}^2}{8} \end{aligned} \quad (5.166)$$

and

$$-2\beta \frac{\delta \mathcal{F}_{\text{exc}}}{\delta \psi} = 2A_1 \psi - 2A_2 (\partial_k^2 \psi) + 2A_3 (\partial_k^2 \partial_l^2 \psi) - B_1 (\partial_i P_i) - B_3 (\partial_i \partial_j Q_{ij}), \quad (5.167)$$

$$-2\beta \frac{\delta \mathcal{F}_{\text{exc}}}{\delta P_i} = B_1 (\partial_i \psi) + B_2 (\partial_j Q_{ij}) + 2C_1 P_i + 2C_2 (\partial_k^2 P_i) - 2C_3 (\partial_i \partial_j P_j), \quad (5.168)$$

$$\begin{aligned} -2\beta \frac{\delta \mathcal{F}_{\text{exc}}}{\delta Q_{ij}} &= -B_2 (\partial_i P_j + \partial_j P_i - \delta_{ij} (\partial_l P_l)) - B_3 (2(\partial_i \partial_j \psi) - \delta_{ij} (\partial_l^2 \psi)) \\ &\quad + 4D_1 Q_{ij} - 2D_2 \partial_k (\partial_i Q_{kj} + \partial_j Q_{ki} - \delta_{ij} (\partial_l Q_{kl})), \end{aligned} \quad (5.169)$$

where the functional derivatives of $\mathcal{F}_{\text{ext}}[\psi, P_i, Q_{ij}]$ vanish, since $U_1(\vec{r}, \hat{u}, t) = 0$ is assumed here.

5.4.1.1 Dynamic equations

The parametrization (5.157) and the relation (5.161) can now be inserted into the DDFT equation (5.158). The dynamic equations for the order-parameter fields are then obtained by an orthogonal projection that separates the evolution equations for the particular order-parameter fields from each other. This projection is achieved by a multiplication of equation (5.158) with 1, u_i , and $u_i u_j - \delta_{ij}/2$, respectively, with a subsequent integration over the orientation \hat{u} . In doing so, the translational density $\psi(\vec{r}, t)$ turns out to be conserved, while $P_i(\vec{r}, t)$ and $Q_{ij}(\vec{r}, t)$ are not conserved due to their association with orientational degrees of freedom. The dynamic equations can thus be written in the form

$$\dot{\psi} + \partial_i J_i^\psi = 0, \quad (5.170)$$

$$\dot{P}_i + \Phi_i^P = 0, \quad (5.171)$$

$$\dot{Q}_{ij} + \Phi_{ij}^Q = 0 \quad (5.172)$$

with the current J_i^ψ and the quasi-currents Φ_i^P and Φ_{ij}^Q . These dissipative currents and quasi-currents are given by the expressions

$$J_i^\psi = -\alpha_1(2(1+\psi)(\partial_i\psi^\natural) + Q_{kl}(\partial_i Q_{kl}^\natural)) - \alpha_2 P_j(\partial_i P_j^\natural) - \alpha_3(2(1+\psi)(\partial_j Q_{ij}^\natural) + P_i(\partial_j P_j^\natural) + P_j(\partial_j P_i^\natural) + Q_{ij}(\partial_j\psi^\natural)) , \quad (5.173)$$

$$\Phi_i^P = -2\alpha_1\partial_k(Q_{ij}(\partial_k P_j^\natural) + P_j(\partial_k Q_{ij}^\natural)) - \alpha_2\partial_k(2(1+\psi)(\partial_k P_i^\natural) + P_i(\partial_k\psi^\natural)) - \alpha_3\left(2\partial_i((1+\psi)(\partial_j P_j^\natural)) + 2\partial_j((1+\psi)(\partial_i P_j^\natural)) + \partial_i(P_j(\partial_j\psi^\natural)) + \partial_j(P_j(\partial_i\psi^\natural)) + 2\partial_j(P_i(\partial_k Q_{jk}^\natural) + Q_{jk}(\partial_k P_i^\natural))\right) + \alpha_4(2(1+\psi)P_i^\natural + 2P_j Q_{ij}^\natural - Q_{ij} P_j^\natural) , \quad (5.174)$$

$$\Phi_{ij}^Q = -2\alpha_1\partial_k(2(1+\psi)(\partial_k Q_{ij}^\natural) + P_i(\partial_k P_j^\natural) + P_j(\partial_k P_i^\natural) - \delta_{ij}P_l(\partial_k P_l^\natural) + Q_{ij}(\partial_k\psi^\natural)) - \frac{\alpha_3}{2}\left(4\partial_i((1+\psi)(\partial_j\psi^\natural)) + 4\partial_j((1+\psi)(\partial_i\psi^\natural)) - 4\delta_{ij}\partial_l((1+\psi)(\partial_l\psi^\natural)) + 4\partial_i(P_k(\partial_j P_k^\natural)) + 4\partial_j(P_k(\partial_i P_k^\natural)) - 4\delta_{ij}\partial_l(P_k(\partial_l P_k^\natural)) + \partial_i(Q_{kl}(\partial_j Q_{kl}^\natural)) + \partial_j(Q_{kl}(\partial_i Q_{kl}^\natural)) - \delta_{ij}\partial_l(Q_{km}(\partial_l Q_{km}^\natural)) + 2\partial_k(Q_{ij}(\partial_l Q_{kl}^\natural)) + 2\partial_k(Q_{kl}(\partial_l Q_{ij}^\natural))\right) + 2\alpha_4(4(1+\psi)Q_{ij}^\natural + P_i P_j^\natural + P_j P_i^\natural - \delta_{ij}P_l P_l^\natural) . \quad (5.175)$$

Four positive coefficients of which three are independent appear in these equations. They are defined as

$$\alpha_1 = \frac{D_{\parallel} + D_{\perp}}{8\lambda} , \quad \alpha_2 = \frac{D_{\parallel} + 3D_{\perp}}{8\lambda} , \quad \alpha_3 = \frac{D_{\parallel} - D_{\perp}}{8\lambda} , \quad \alpha_4 = \frac{D_R}{2\lambda} . \quad (5.176)$$

Notice that $D_{\parallel} \geq D_{\perp}$ holds for all types of uniaxial particles as long as the vector \hat{u} for the orientation of the axis of symmetry is chosen properly.²⁰ With the CMA (5.160) instead of the DDFT equation (5.158), the following dissipative currents and quasi-currents are obtained:

$$J_i^\psi = -2\alpha_1(\partial_i\psi^\natural) - 2\alpha_3(\partial_j Q_{ij}^\natural) , \quad (5.177)$$

$$\Phi_i^P = -2\alpha_2(\partial_k^2 P_i^\natural) - 4\alpha_3(\partial_i\partial_j P_j^\natural) + 2\alpha_4 P_i^\natural , \quad (5.178)$$

$$\Phi_{ij}^Q = -4\alpha_1(\partial_k^2 Q_{ij}^\natural) - 2\alpha_3(2(\partial_i\partial_j\psi^\natural) - \delta_{ij}(\partial_k^2\psi^\natural)) + 8\alpha_4 Q_{ij}^\natural . \quad (5.179)$$

It has to be emphasized that the DDFT approach (5.158) a priori contains only three independent mobility coefficients, namely the two translational diffusion coefficients D_{\parallel} and D_{\perp} and the rotational diffusion coefficient D_R . Therefore, all other mobility coefficients for the order-parameter fields can be expressed in terms of these three basic coefficients. In general, the diffusion coefficients in DDFT are always related to translational or orientational degrees of freedom and not to certain order-parameter

²⁰The situation described and analyzed here for two spatial dimensions has to be contrasted to the case of three spatial dimensions, where one has for all rod-like particles, flexible as well as rigid ones, the inequality $D_{\parallel} \geq D_{\perp}$, while for disk-like particles typically $D_{\parallel} \leq D_{\perp}$ applies.

fields, since order-parameter fields enter DDFT only with the parametrization of the one-particle density. The parametrization of the one-particle density (5.85), however, does not involve further dissipation coefficients. This is in sharp contrast to Ginzburg-Landau theory, where every additional order parameter involves at least one new dissipative coefficient, as is discussed in section 5.5 in more detail.

5.4.1.2 Dissipation functional

The currents and quasi-currents J_i^ψ , Φ_i^P , and Φ_{ij}^Q are merely dissipative and can therefore be derived from a dissipation functional \mathfrak{R} . According to equation (5.71), the dissipative currents and quasi-currents J_i^ψ , Φ_i^P , and Φ_{ij}^Q can be expressed by the functional derivatives

$$J_i^\psi = -\frac{\delta\mathfrak{R}}{\delta(\partial_i\psi^\natural)}, \quad (5.180)$$

$$\Phi_i^P = \frac{\delta\mathfrak{R}}{\delta P_i^\natural}, \quad (5.181)$$

$$\Phi_{ij}^Q = \frac{\delta\mathfrak{R}}{\delta Q_{ij}^\natural} \quad (5.182)$$

of this dissipation functional \mathfrak{R} . Moreover, the dissipation functional, that corresponds to the dissipative currents and quasi-currents (5.173)-(5.175) of the general PFC model, is given by

$$\mathfrak{R}^{(\text{PFC})} = \int_{\mathbb{R}^2} dA \mathfrak{r}^{(\text{PFC})}(\vec{r}) \quad (5.183)$$

with the local dissipation function

$$\begin{aligned} \mathfrak{r}^{(\text{PFC})} = & \alpha_1 \left((1 + \psi) \left((\partial_i \psi^\natural)^2 + (\partial_k Q_{ij}^\natural)^2 \right) + Q_{ij} (\partial_k \psi^\natural) (\partial_k Q_{ij}^\natural) + Q_{ij} (\partial_k P_i^\natural) (\partial_k P_j^\natural) \right. \\ & \left. + 2P_i (\partial_k P_j^\natural) (\partial_k Q_{ij}^\natural) \right) + \alpha_2 \left(P_i (\partial_j \psi^\natural) (\partial_j P_i^\natural) + (1 + \psi) (\partial_j P_i^\natural)^2 \right) \\ & + \alpha_3 \left((\partial_i \psi^\natural) \left(\frac{1}{2} Q_{ij} (\partial_j \psi^\natural) + P_i (\partial_j P_j^\natural) + P_j (\partial_j P_i^\natural) + 2(1 + \psi) (\partial_j Q_{ij}^\natural) \right) \right. \\ & \left. + (1 + \psi) (\partial_i P_i^\natural)^2 + (\partial_j P_i^\natural) \left((1 + \psi) (\partial_i P_j^\natural) + Q_{jk} (\partial_k P_i^\natural) + 2P_i (\partial_k Q_{jk}^\natural) \right) \right. \\ & \left. + \frac{1}{4} Q_{ij} (\partial_i Q_{kl}^\natural) (\partial_j Q_{kl}^\natural) + \frac{1}{2} Q_{ij} (\partial_k Q_{ij}^\natural) (\partial_l Q_{kl}^\natural) \right) \quad (5.184) \\ & + \alpha_4 \left((1 + \psi) \left((P_i^\natural)^2 + 2(Q_{ij}^\natural)^2 \right) - \frac{1}{2} Q_{ij} P_i^\natural P_j^\natural + 2P_i P_j^\natural Q_{ij}^\natural \right). \end{aligned}$$

The dissipation functional, that corresponds to the currents and quasi-currents (5.177)-(5.179) of the CMA, is on the other hand much simpler and given by

$$\mathfrak{R}^{(\text{CMA})} = \int_{\mathbb{R}^2} dA \mathfrak{r}^{(\text{CMA})}(\vec{r}) \quad (5.185)$$

with the local dissipation function

$$\begin{aligned} \mathfrak{r}^{(\text{CMA})} = & \alpha_1((\partial_i \psi^\natural)^2 + (\partial_k Q_{ij}^\natural)^2) + \alpha_2(\partial_k P_i^\natural)^2 + 2\alpha_3((\partial_i \psi^\natural)(\partial_j Q_{ij}^\natural) + (\partial_i P_i^\natural)^2) \\ & + \alpha_4((P_i^\natural)^2 + 2(Q_{ij}^\natural)^2). \end{aligned} \quad (5.186)$$

By construction, both dissipation functions (5.184) and (5.186) are positive. This is obvious for equation (5.186), but not manifest for equation (5.184).

5.4.2 Three spatial dimensions

The dynamic equations corresponding to the PFC model for three spatial dimensions, which is discussed in section 5.3.2, can be derived in direct analogy to the dynamics for two spatial dimensions in the previous section. Since the dynamics is much more complicated in three spatial dimensions than only in two spatial dimensions, it would be interesting to also consider the general dynamic equations for three spatial dimensions, but their derivation requires a huge analytic effort and has not been carried out up to now. However, a special case of the dynamic PFC model in three spatial dimensions that follows from the DDFT equation in reference [RWL07] together with the CMA has recently been considered in reference [YA11] and evaluated numerically.

5.5 Comparison with macroscopic models

The static and dynamic PFC models for colloidal liquid crystals, that have been derived in the previous sections from static DFT and DDFT, are compared in this section with symmetry-based macroscopic approaches that can be derived from Ginzburg-Landau theory and generalized hydrodynamics following the procedure described in sections 5.1.3 and 5.1.4. For a comparison with the static and dynamic PFC models, expressions for the free-energy density and dynamic equations for the order-parameter fields are derived from the macroscopic theories. Contributions to the statics and dynamics are thereby only taken into account up to the same order in the order-parameter fields and gradients as for the PFC models.

It turns out that every PFC model is included as a special case in the corresponding symmetry-based macroscopic models and therefore in accordance with basic symmetry considerations and thermodynamic laws [BP87, PB96]. To the contrary, the macroscopic approaches are more general and usually involve more terms and more independent coefficients than the microscopically derived PFC models, since the macroscopic theories lead to the most general models that are just allowed by general symmetry considerations and thermodynamic laws. Microscopic derivations instead lead to analytic expressions for the coefficients in the models and these expressions can depend on each other leading to relations between the coefficients and a reduction of the actual number of independent coefficients. It is even possible that approximative derivations from microscopic theories reveal that certain coefficients of the macroscopic models are zero.

In the case of PFC models derived from static DFT or DDFT, the coefficients are given explicitly as microscopic expressions and provide therefore a bridge between microscopic and macroscopic approaches. By comparison, a strong analogy between PFC models derived from static DFT or DDFT and macroscopic models on the basis of Ginzburg-Landau theory becomes apparent. Under the same conditions, they contain the same terms and the same number of independent coefficients. This is very different for macroscopic models on the basis of generalized hydrodynamics. Such models are commonly much more general and include more terms and also more independent coefficients than the corresponding PFC models. The following paragraphs summarize the comparison of the previously derived PFC models for colloidal liquid crystals with macroscopic models. For a more detailed comparison, see references [WLB10, WLB11a, WLB11b].

5.5.1 Static macroscopic models

At first, the polar PFC model for two spatial dimensions consisting of equations (5.87) and (5.92)-(5.94) and the apolar PFC model for three spatial dimensions with the scaled free-energy densities (5.146) and (5.151) are compared with static Ginzburg-Landau theory and generalized hydrostatics. As a general feature, the Ginzburg-Landau models turn out to be equivalent to the PFC models, while generalized hydrostatics leads to models with considerably more terms and a larger number of independent coefficients. Further details are described below and in references [WLB10, WLB11b].

5.5.1.1 Static Ginzburg-Landau theory

For the comparison with the PFC models that are available, static Ginzburg-Landau theory can be applied to the isotropic-uniaxial nematic phase transition [Gen71], the isotropic-polar nematic phase transition [PB89], and a number of further phase transitions with the involvement of several apolar or polar smectic phases. The latter phase transitions are the isotropic-smectic A phase transition [MPB01], the isotropic-smectic C phase transition [MPB02], the isotropic-smectic C* phase transition [MPB05], as well as the nematic-smectic A and the nematic-smectic C phase transitions [Gen73, GP95]. Furthermore, the paraelectric-ferroelectric phase transition [AL78, FMH86, Kit95] can be also considered.

In order to describe these phase transitions within the framework of static Ginzburg-Landau theory, a few order-parameter fields have to be chosen. The first of them is the complex *smectic order-parameter field* [Gen73, CL95, GP95]

$$\psi(\vec{r}) = \psi_0 e^{-i\phi(\vec{r})} \quad (5.187)$$

with magnitude ψ_0 and phase $\phi(\vec{r})$. It is scalar and related to variations of the particle number density [CL95]. One can also choose the real *number density* [CL95]

$$\rho_\psi(\vec{r}) = \bar{\rho} + \psi_0 (e^{i\phi(\vec{r})} + e^{-i\phi(\vec{r})}) \quad (5.188)$$

as an order-parameter field. In addition, the macroscopic polarization $\vec{P}(\vec{r}) = P(\vec{r})\hat{p}(\vec{r})$ with modulus $P(\vec{r})$ and direction $\hat{p}(\vec{r})$, which is odd under parity inversion, has to be taken into account in order to regard polar phases appropriately. Nematic phases, on the other hand, require the traceless and symmetric nematic tensor with the elements $Q_{ij}(\vec{r})$ [Gen71] as tensorial order-parameter field. It vanishes in the isotropic phase and has the form²¹ [GP95]

$$Q_{ij}(\vec{r}) = S(\vec{r})(n_i(\vec{r})n_j(\vec{r}) - d^{-1}\delta_{ij}) \quad (5.189)$$

in a d -dimensional uniaxial nematic phase. The usage of only the nematic tensor $Q_{ij}(\vec{r})$ instead of the nematic order parameter $S(\vec{r})$ and the nematic director $\hat{n}(\vec{r})$ separately has the advantage that $Q_{ij}(\vec{r})$ already incorporates the appropriate properties like the $\hat{n}(\vec{r}) \rightarrow -\hat{n}(\vec{r})$ invariance.

Using these order-parameter fields, a free-energy density for colloidal liquid crystals can be constructed from static Ginzburg-Landau theory and compared with the derived PFC models. As a special contribution, this free-energy density contains the Frank free-energy density $f_{\text{F}}(\vec{r})$, which describes the energy associated with elastic deformations of the director field $\hat{n}(\vec{r})$. In three spatial dimensions, three different types of elastic deformations of a nematic phase are possible. These elementary deformations are splay, twist, and bend [GP95]. Splay and bend also exist in two spatial dimensions, but twist appears only in three spatial dimensions. Each type of deformation goes along with a certain term in the Frank free-energy density. The prefactors of these terms are called *Frank constants*. In the isotropic phase²², gradients of the nematic tensor in second order lead to the contribution [Gen71]

$$f_{\text{F}}(\vec{r}) = L_1(\partial_i Q_{jk})^2 + L_2(\partial_i Q_{ij})^2 \quad (5.190)$$

with the two independent coefficients L_1 and L_2 . The two terms in this free-energy density become proportional in two spatial dimensions so that only one coefficient remains. This is in accordance with the PFC models for two and three spatial dimensions. Also all other terms that can be constructed from the chosen order-parameter fields and their gradients for the isotropic phase and the accompanying independent coefficients have distinct equivalents in the PFC models.

5.5.1.2 Generalized hydrostatics

Macroscopic models for liquid crystalline bulk phases can be derived with the help of generalized hydrostatics. For a comparison with the PFC models, especially the isotropic phase, the uniaxial nematic phase [BP87], the polar nematic phase [BPZ06, BCP09], smectic phases [BP80, CL95], and polar smectic phases [BP87, BCP98] are

²¹In three spatial dimensions, the alternative representation (5.143) that deviates from the form (5.189) by the factor 3/2 is often used as well.

²²In the uniaxial nematic phase, six independent terms including three independent Frank constants can be constructed from two gradients and two nematic tensors.

relevant. To describe these phases, a few appropriate hydrodynamic and macroscopic variables have to be chosen. The most obvious hydrodynamic variable is the conserved particle number density $\rho(\vec{r})$. For polar phases, also the local polarization of the liquid crystalline system has to be taken into account, but unlike in the preceding derivation of macroscopic models using Ginzburg-Landau theory, it is normal to choose the modulus $P(\vec{r})$ of the local polarization, which is a slowly relaxing non-hydrodynamic and non-conserved macroscopic variable, and the variation $\delta\hat{p}(\vec{r})$ of the direction $\hat{p}(\vec{r})$ of the local polarization instead of the whole polarization vector $\vec{P}(\vec{r}) = P(\vec{r})\hat{p}(\vec{r})$ as separate variables. The variation $\delta\hat{p}(\vec{r})$ of the polar direction $\hat{p}(\vec{r})$ is a non-conserved hydrodynamic variable with the property $\hat{p}(\vec{r}) \cdot \delta\hat{p}(\vec{r}) = 0$. It is further odd under parity inversion and under time reversal. For the uniaxial nematic phase²³, the nematic order parameter $S(\vec{r})$ and the variation $\delta\hat{n}(\vec{r})$ of the nematic director $\hat{n}(\vec{r})$ are taken into account. Similar to the modulus and direction of the polarization, the nematic order parameter $S(\vec{r})$ is also a slowly relaxing non-hydrodynamic and non-conserved macroscopic variable, while the variation $\delta\hat{n}(\vec{r})$ of the nematic director constitutes a non-conserved hydrodynamic variable with the property $\hat{n}(\vec{r}) \cdot \delta\hat{n}(\vec{r}) = 0$. In connection with smectic phases, the scalar *layer displacement* $u(\vec{r})$ in the direction of the layer normal is an additional hydrodynamic variable [Gen69, GP95].

The actual macroscopic modeling consists in the construction of a free-energy density for colloidal liquid crystals in terms of the deviations $\delta\rho(\vec{r}) = \rho(\vec{r}) - \rho_0$, $\delta P(\vec{r}) = P(\vec{r}) - P_0$, $\delta\hat{p}(\vec{r})$, $\delta S(\vec{r}) = S(\vec{r}) - S_0$, $\delta\hat{n}(\vec{r})$, and $\delta u(\vec{r}) = u(\vec{r}) - u_0$ of the hydrodynamic and macroscopic variables from their equilibrium values²⁴ ρ_0 , P_0 , S_0 , and u_0 , respectively, and in terms of gradients of these deviations. In doing so, it is necessary to respect that the free-energy density must be invariant against inversion $\hat{n}(\vec{r}) \rightarrow -\hat{n}(\vec{r})$ of the nematic director. An important contribution to the free-energy density, that also appeared in the Ginzburg-Landau model in the previous paragraph, is the *Frank free-energy density* for elastic deformations of the director field $\hat{n}(\vec{r})$ of uniaxial nematics. In the generalized hydrostatic model, it appears in its traditional formulation [Fra58, GP95]

$$f_F(\vec{r}) = K_1(\vec{\nabla}_{\vec{r}} \cdot \hat{n})^2 + K_2(\hat{n} \cdot (\vec{\nabla}_{\vec{r}} \times \hat{n}))^2 + K_3(\hat{n} \times (\vec{\nabla}_{\vec{r}} \times \hat{n}))^2 \quad (5.191)$$

with the Frank constants K_1 , K_2 , and K_3 that are associated with splay, twist, and bend, respectively. As all coefficients in macroscopic models, the Frank constants can also depend on all scalar quantities of the system. This includes especially the nematic order parameter $S(\vec{r})$. There are therefore two independent Frank constants in two spatial dimensions and three different Frank constants in three spatial dimensions, while in the PFC models and the Ginzburg-Landau models in the isotropic phase one has only one Frank constant in two spatial dimensions and two Frank constants in three spatial dimensions, since the Frank constants for splay and bend are equal in

²³Biaxial nematic phases in three spatial dimensions require a second director $\hat{m}(\vec{r})$ in addition to the convenient nematic director $\hat{n}(\vec{r})$ [GP95].

²⁴Notice that $\delta\hat{p}(\vec{r})$ and $\delta\hat{n}(\vec{r})$ are associated with spontaneously broken continuous symmetries and have therefore no certain equilibrium state.

these models. Also in other respects, the hydrostatic models are more general than the Ginzburg-Landau models and the PFC models. They comprise more independent coefficients and additional terms that do not exist in the PFC models.

5.5.2 Dynamic macroscopic models

After the static PFC models, now the dynamic equations (5.170)-(5.172) are compared with macroscopic approaches on the basis of symmetry considerations. These macroscopic approaches are based on dynamic Ginzburg-Landau theory and generalized hydrodynamics. Since the dynamics of the DDFT equation (5.158), that was used for the derivation of the dynamic equations (5.170)-(5.172), is purely dissipative, there are no reversible currents or quasi-currents in these dynamic equations. The dynamics can therefore be completely derived from a dissipation functional so that the comparison of the dynamic PFC model with dynamic Ginzburg-Landau theory and generalized hydrodynamics is more convenient, when it is based on the dissipation function (5.184) instead of the dynamic equations (5.170)-(5.172) that involve the complicated currents and quasi-currents (5.173)-(5.175).

As the static PFC models, also the dynamic PFC model is in accordance with symmetry-based macroscopic approaches and thus also with basic symmetry considerations and thermodynamic laws. These symmetry-based approaches are as usual more general than the dynamic PFC model and involve more independent coefficients and also a few additional terms. The reasons for missing these terms in the dynamic PFC equations are identified and explained below. A further similarity to the comparison of the static PFC models with macroscopic approaches consists in a strong analogy of the dynamic PFC model and the corresponding dynamic Ginzburg-Landau approach, while the application of generalized hydrodynamics leads here also to much more general equations. Details beyond the presented comparison can be found in reference [WLB11a].

5.5.2.1 Dynamic Ginzburg-Landau theory

The dynamic PFC model in section 5.4.1.1 has to be compared with the Ginzburg-Landau dynamics in the vicinity of the isotropic-polar nematic phase transition and of the isotropic-polar smectic phase transition. This description involves a few order-parameter fields. These are the particle number density $\rho(\vec{r}, t)$, the smectic density $\rho_\psi(\vec{r}, t)$ [Gen73, CL95], the macroscopic polarization $P_i(\vec{r}, t)$ [PB89, BPZ06, BCP09], and the nematic tensor $Q_{ij}(\vec{r}, t)$ [Gen71, GP95]. The order-parameter fields are accompanied by their thermodynamic conjugates, namely by the chemical potential $\mu(\vec{r}, t)$, the chemical potential $\mu_\psi(\vec{r}, t)$ associated with the smectic layering, the thermodynamic force $h_i^P(\vec{r}, t)$ associated with the macroscopic polarization, and the thermodynamic conjugate $S_{ij}(\vec{r}, t)$ of the nematic tensor. In terms of these order-parameter fields and thermodynamic conjugates, the total differential of the generalized energy

density $\varepsilon(\vec{r}, t)$ can be written in the form [WLB11a]

$$d\varepsilon = Td\sigma + \mu d\rho + \mu_\psi d\rho_\psi + h_i^P dP_i + S_{ij} dQ_{ij} \quad (5.192)$$

with the absolute temperature field $T(\vec{r}, t)$ and the entropy density $\sigma(\vec{r}, t)$. Based on this expression and following the procedure, that has been described in section 5.1.3.2, a dissipation function for the Ginzburg-Landau dynamics in terms of the thermodynamic forces associated with the chosen order-parameter fields can be derived [WLB11a].

It turns out that all terms in the PFC dissipation function (5.184) are also included in the Ginzburg-Landau dissipation function, but there are in addition three cross-coupling terms that do not exist in the dynamic PFC model. The reason for the absence of these terms lies in the fact that all missing terms contain only one gradient, while in the DDFT equation (5.158), from which the dynamic PFC model is derived, the gradients appear quadratically. To also derive the terms with only one gradient from DFT, one would have to use the more general DDFT equation (4.44) for colloidal particles with a translational-rotational coupling instead of equation (5.158).

Moreover, the PFC dissipation function (5.184) contains much less independent coefficients than the corresponding Ginzburg-Landau dissipation function, since in a dynamic Ginzburg-Landau approach, there is at least one independent dissipative coefficient for every order-parameter field. Dissipative cross-coupling terms can bring along further independent coefficients. This is widely different in the dynamic PFC models, where all dissipative coefficients result from the elements of the diffusion tensor in the DDFT equation. To generalize the dynamic PFC models in this respect, one would have to use a more complicated expression for the mobility in the DDFT equation [EL09]. Such a generalized mobility depends on the order-parameter fields and includes a number of additional dissipative constants. It is a necessary generalization, if the hydrodynamic interactions between the colloidal particles that are entirely neglected by the DDFT equation (5.158) shall be taken into account.

5.5.2.2 Generalized hydrodynamics

A further comparison of the PFC dissipation function (5.184) with a dissipation function on the basis of generalized hydrodynamics would be possible as well, but it is not reasonable, since the generalized hydrodynamics approach would be even more general than the dynamic Ginzburg-Landau approach as addressed in the previous section and all the additional terms would not have a corresponding term in the PFC dissipation function. Furthermore, the typical hydrodynamic variable $\vec{v}(\vec{r}, t)$ for the velocity field of the colloidal particles or equivalently the momentum density $\vec{g}(\vec{r}, t)$ cannot be considered in this context, since they are neglected in the completely overdamped Brownian dynamics described by the DDFT equation (5.158). Reversible currents and quasi-currents [BCP09] can therefore not arise in such a model.

5.6 Applications and enhanced models

The apolar and polar PFC models for two and three spatial dimensions, respectively, as derived in this chapter can be applied to colloidal liquid crystals in order to explore their equilibrium phase diagrams containing many different stable liquid crystalline phases. When these stable phases are known, the structure of interfaces between two coexisting phases [BHD05] can be addressed. While the isotropic-nematic interface has already been studied by theory, computer simulation, and experiment, it would be interesting to get structural information about interfaces between other liquid crystalline phases. In this context, one could also calculate interfacial tensions [MAS01]. Besides that, the polar PFC model is in particular useful for the modeling of certain biological systems that exhibit polar order [VSB99, CDGK06]. The dynamic PFC models can furthermore be used to describe various dynamic processes including the phase transition dynamics of colloidal liquid crystals. Special possible applications affect the relaxation dynamics of an orientational glass [RLB95] and the formation of metastable phases at a growing interface [BLT91]. As became apparent in the determination of the director field of plastic crystalline phases in section 5.3.1.3, several types of topological defects appear naturally in certain liquid crystalline phases. The investigation of the structure [TDY02] and dissipative dynamics [LM97, TDY02] of topological defects in liquid crystalline phases [Ru09] is another possibility to use the PFC models that were derived. In the context of topological defects in liquid crystals, fundamental phenomena can be investigated also [CYDT91]. An impressive example for that is the cosmological Kibble mechanism that can also be observed in liquid crystals [BCSS94]. Moreover, the comparison of the PFC models with macroscopic approaches gives important insights into the relationship between DFT, PFC models, and symmetry-based macroscopic approaches.

For the future, a further numerical evaluation of the PFC models and a comparison of the results with experiments and computer simulations would be desirable. These comparable results include phase diagrams and especially the defect lattice of the orientation field in plastic crystals (see section 5.3.1.3) [MD08, DJK⁺10, GAO⁺10] as well as dynamic processes of polar liquid crystals [TYN⁺03, FST⁺09, FS10]. Experiments could be performed with concentrated suspensions of anisotropic colloidal particles in a liquid [VL92, BDW⁺08] or with anisotropic mesoscopic dust particles in a plasma [AKI⁺01, IKK⁺03]. For such colloidal systems, the phase diagrams could be determined and compared with the phase diagrams of the PFC models for a given particle interaction potential.²⁵ Some phase diagrams, which are appropriate for a comparison with the PFC models, have already been calculated by computer simulations [Sat10] for different colloidal systems. Among these systems are hard spherocylinders [BF97], hard ellipsoids [FM85], the Gay-Berne model [MRBA96, KBH10], and Yukawa-segment models [GL99]. Especially simulations of liquid crystalline phases of rod-like particles

²⁵In order to do this, the phase diagrams of the PFC models that depend initially on generalized expansion coefficients of the direct correlation functions must be written as a function of the thermodynamic variables particle number density and temperature.

in two spatial dimensions [Vin07, WT07, THT09, LLRC10] could be used to verify special liquid crystalline phases like plastic honeycomb crystals and plastic square crystals that are predicted by the PFC models presented.

Nevertheless, there are also some possibilities for further generalizations of the work presented here. At first, the derived PFC models could be improved by taking higher-order contributions in the order-parameter fields and gradients into account. Secondly, an extension of the PFC models to static and dynamic polar systems in three spatial dimensions would also be possible following the procedure that is described in this chapter. However, these kinds of generalizations involve expressions that are even larger than those for the PFC models above. Since the PFC models in this chapter were derived for uniaxial colloidal particles, one could further derive the statics and dynamics of PFC models for biaxial particles in three spatial dimensions. With the help of the new DDFT equation in chapter 4, which is applicable to biaxial particles, the derivation of dynamic biaxial PFC models has now become possible for the first time. Such biaxial PFC models would involve considerably more terms than the presented PFC models for particles with an axis of symmetry. The new DDFT equation (4.44) could additionally be used instead of equation (5.158) in order to derive dynamic PFC models for active colloidal particles on the basis of the static polar²⁶ PFC model. A dynamic PFC model for active particles could, for example, be used to investigate the dynamic properties of bacterial growth patterns of *Proteus mirabilis* [WWI⁺02]. Both for active and passive colloidal particles, external forces, that drive the system like a periodic driving field [HBL10], can always be regarded in addition. Colloidal systems can further be considered in confinement, where PFC models could be used in order to calculate wall tensions, or on an arbitrary Riemannian manifold. Even a generalization to relativistic systems with cosmological applications is possible [Gra77a].

²⁶Active particles are polar by definition.

6 Summary

In the previous chapters, the Brownian dynamics of interacting active and passive colloidal particles with an anisotropic shape was investigated. The colloidal particles under consideration were assumed to be solid and non-deformable. At first, the dynamics of an individual active colloidal particle with arbitrary shape in a viscous liquid at rest at infinity with a low Reynolds number was considered. Its stochastic motion under the influence of thermal fluctuations as well as internal, external, and hydrodynamic forces and torques was described by a Langevin equation, that is also valid for particles with a hydrodynamic translational-rotational coupling. This Langevin equation is too complicated to be solved analytically. Therefore, special Langevin equations for particles that move only in two spatial dimensions and for orthotropic particles were derived from it. These special Langevin equations were solved analytically for certain situations. For more general situations like the motion of an arbitrarily shaped particle in three spatial dimensions, analytical solutions were not available and numerical results have been presented. It turned out that the three-dimensional trajectories of an active colloidal particle with arbitrary shape involve transient regimes and are very complicated. They are so diverse that a complete classification appeared to be not possible even for vanishing temperature. Among these trajectories are *superhelical* trajectories that were observed for a vanishing external force and no thermal fluctuations. Orthotropic particles in contrast do not possess a hydrodynamic translational-rotational coupling and their trajectories have no transient regimes. In the absence of thermal fluctuations and external forces and torques, an analytical solution for the trajectory of an orthotropic particle was found. This trajectory is a circular helix. When thermal fluctuations are taken into account, the noise average of this circular helix becomes a generalized *conchospiral*. This was shown by computer simulation.

Also the restricted motion of an arbitrarily shaped colloidal particle in two spatial dimensions is much simpler than the general three-dimensional trajectories. For zero temperature, a vanishing external torque, and a non-vanishing constant external force, these trajectories were classified with respect to the properties of the drive and the symmetry of the shape of the colloidal particle. Thereby, a vanishing drive, a drive that generates only either a force or a torque, and a drive that generates both an internal force and an internal torque were distinguished. The shape of the particle was distinguished between being asymmetric, having inflection symmetry with respect to one axis of symmetry, having two perpendicular axes of symmetry, and having rotational symmetry. The observed trajectories for asymmetric particles in two spatial dimensions were always straight lines after a transient regime or periodic curves. These trajectories were also observed for particles with inflection symmetry, but those ran

parallel to an external force, if the drive had certain properties. Similar to orthotropic particles in three spatial dimensions, a transient regime was not observed for particles with two perpendicular axes of symmetry that move in two spatial dimensions. Such particles move either along a straight line with a certain orientation or along a periodic curve that is oriented parallel to the external force. The trajectory of a particle with rotational symmetry is a cycloid parallel to the external force or a straight line. In this classification, the external torque was assumed to be zero without loss of generality, since the internal and the external torque can be combined to an effective torque in two spatial dimensions. The external force was assumed to be non-vanishing in the classification, since all trajectories are a circle or there is no motion at all, if the external force is zero. For these circular trajectories, an analytic expression was given.

Furthermore, the effect of an imposed shear flow on the motion of an active particle was discussed for the example of a spherical active colloidal particle in two-dimensional Couette flow. The corresponding Langevin equations for this example were formulated and analytical solutions for the deterministic trajectories in the absence of thermal fluctuations as well as for the mean trajectories in the case of a positive temperature were given. Additionally, the scaling of the mean square displacement with time was considered. For its time-dependence $\propto t^\nu$, the five exponents $\nu \in \{0, 1, 2, 3, 4\}$ were identified and the associated regimes were discussed. The dynamics of the colloidal particle turned out to be in general greatly amplified by shear flow and the fast t^4 -regime emerged to arise from a combination of self-propulsion and shear flow, when the external torque due to the shear flow is exactly compensated by the internal torque that results from the drive of the particle. By computer simulation, the spatial probability distribution of the active Brownian particle in shear flow was also determined. This probability distribution has a transient double-peak structure due to the self-propulsion and becomes asymmetric under the influence of shear flow.

Secondly, the collective dynamics of a large set of interacting active colloidal particles with arbitrary shape was addressed by DDFT. Since previous formulations of DDFT were only applicable to spherical and uniaxial particles with no hydrodynamic translational-rotational coupling, a generalized DDFT, that describes active and passive colloidal particles with arbitrary shape, was derived from a many-body Smoluchowski equation. This generalization of DDFT also describes particles with a hydrodynamic translational-rotational coupling as screw-like particles and includes previous versions of DDFT as special cases. It was proved that the new and generalized DDFT can be reformulated as a variational optimization problem for a certain dissipation functional. This alternative representation of DDFT in terms of a dissipation functional establishes a basis for the interpretation of DDFT out of linear irreversible thermodynamics. The reformulated DDFT furthermore allows an easier and much faster derivation of the dynamic equations of complicated PFC models that involve various order-parameter fields, than the traditional formulation of DDFT.

At last, the statics and dynamics of colloidal liquid crystals composed of uniaxial colloidal particles that are apolar or polar were examined in two and three spatial dimensions. For this purpose, microscopic, mesoscopic, and macroscopic classical mean-

field theories were used. Starting from microscopic static DFT and DDFT, the statics and dynamics of mesoscopic PFC models were derived. The dynamic equations of the PFC models were supplemented by the corresponding dissipation functionals. Some special cases of these PFC models were already known from the literature. One of them is the PFC model for apolar colloidal liquid crystals in two spatial dimensions. Since this PFC model had never been evaluated numerically before, its stable liquid crystalline phases were determined by numerical minimization of the associated free-energy functional. Moreover, a few phase diagrams for different choices of the parameters of the PFC model have been calculated for this work. Among the stable liquid crystalline phases in the phase diagrams are isotropic, nematic, columnar, smectic A, and plastic crystalline phases. The observed plastic crystals had triangular, honeycomb, and square lattices, respectively, and involved orientational patterns with a complex topology. An interesting feature of these orientational patterns was a sublattice with topological defects that could be classified as vortices, disclinations, sources, sinks, and hyperbolic points. In all plastic crystals, the topological defects were arranged in such a way that the total topological winding number vanished.

Besides this numerical evaluation, all PFC models were compared with static and dynamic symmetry-based approaches on the basis of classical Ginzburg-Landau theory and generalized hydrodynamics. The comparison confirmed that all terms in the PFC models also appear in the macroscopic models and that they therefore are in accordance with basic symmetry considerations and thermodynamic laws. On the contrary, there are additional terms in the macroscopic models that are not present in the PFC models, but the reasons for missing these terms were identified and explained. It became apparent that there is a strong analogy between PFC models derived from DFT and Ginzburg-Landau models, while models on the basis of generalized hydrodynamics contain usually much more terms than the corresponding PFC models. Furthermore, the terms of the macroscopic models go along with a large number of independent unknown coefficients, while the analogous coefficients in the PFC models are known explicitly and often depend on each other. But this is a general feature of macroscopic models in contrast to models derived from microscopic theories.

The results of this work are relevant for soft condensed matter physics and biophysics and have various applications. For example, the Langevin equation for an active colloidal particle with arbitrary shape could be used to describe the Brownian motion of artificial microswimmers and swimming microorganisms theoretically. It should also be possible to describe the motion of microorganisms in flowing water, when the Langevin equation is modified properly. The generalized DDFT for active colloidal particles with arbitrary shape makes an investigation of the dynamics of colloidal liquid crystals possible. In contrast to the previous versions of DDFT, the new generalization allows for the first time to also treat biaxial particles. From experiments, biaxial particles are known to evolve a great number of interesting additional liquid crystalline phases, which cannot be observed for uniaxial particles. Since active particles can also be considered within the generalized DDFT, it could be used further to model the collective Brownian motion of active particles. In the non-equilibrium dynamics of self-propelled

microswimmers and swimming microorganisms, collective effects like flocking, swarming, laning, turbulence, and jamming could be addressed. The dissipation functional that was shown to be equivalent to the new DDFT is of great value for the derivation of the dynamics of PFC models. Especially if a PFC model involves various order-parameter fields, its dynamics can be derived much faster and much more easily with the help of the dissipation functional than with the differential DDFT equation. The PFC models as derived in this work can be applied to apolar and polar colloidal liquid crystals in order to explore their equilibrium phase diagram and their phase transition dynamics. Also the structure of interfaces between two coexisting phases and dynamic processes of two-dimensional polar liquid crystals can be investigated with these PFC models. With respect to microorganisms, the PFC models could be used to model biological systems that exhibit polar order or to reproduce the dynamics of bacterial growth patterns. The investigation of the dissipative dynamics of topological defects in liquid crystalline phases should be very interesting as well. Finally, the results of this work give insights into the relationship between classical density functional theory, phase field crystal models, and symmetry-based macroscopic approaches.

For the future, a comparison of the results in this work with experiments and computer simulations would be desirable. Additionally, the further generalization of some basic results should be intended. The Langevin equation for active colloidal particles with arbitrary shape could, for example, be extended to incorporate an arbitrary prescribed flow field of the surrounding liquid. This flow field could also depend on time. Another possible generalization would be the consideration of system boundaries, which allows to address the stochastic motion of an arbitrarily shaped colloidal particle in confinement. In this case, the hydrodynamic interaction of the particle with the system boundaries would have to be taken into account. The derived DDFT for active colloidal particles with arbitrary shape can be improved, too. With a generalization toward confinement, it would have multifarious applications in nanofluidics. Even more important would be the appropriate incorporation of hydrodynamic interactions between the colloidal particles. This is one of the most important goals for the future. Of similar importance are efforts to generalize DDFT toward molecular dynamics, where the dynamics of the particles is not overdamped anymore and the inertia of the particles has to be taken into account in terms of a momentum density field. Such a generalization would be applicable to molecular liquid crystals and thanks to the presence of a non-vanishing momentum density field, the dynamics would no longer be solely dissipative and reversible currents could also arise. Further tasks for the future concerning DDFT are a generalization toward mixtures and a microscopic derivation of the dissipation functional that was shown to be equivalent to DDFT. Furthermore, there are many possibilities for improvement for the PFC models presented here. In principle, the statics and dynamics of a polar PFC model in three spatial dimensions could be derived following the procedure that is described in this work. However, this model was not derived here deliberately, since it involves expressions that are even larger than those for the PFC models derived. With the help of static DFT and the new DDFT, it is now also possible to derive the statics and dynamics of a PFC model

for biaxial particles in three spatial dimensions. The new DDFT could additionally be used to derive a dynamic PFC model for active particles. In any case, one could regard external forces that drive the system. Finally, it should also be possible to construct PFC models for colloidal systems under confinement and for liquid crystalline systems on a Riemannian manifold.

Appendix

This appendix is intended to provide further information about two special topics that are not sufficiently discussed in the standard textbooks about physics. The first of these topics is considered in part A of the appendix. There, instructions for the gradient expansion of a multiple convolution integral are given. Gradient expansions have to be carried out, whenever a phase field crystal model is derived from density functional theory. For the phase field crystal models that are presented in this work, such gradient expansions had to be performed a couple of times. Therefore, this appendix might be useful for everyone who wants to derive a new phase field crystal model from density functional theory. For this purpose, part A of the appendix can serve as formulary.

The second topic treats numerical methods for the solution of stochastic differential equations. It is discussed in part B of this appendix. This part is based on the book [KP06], which gives a very detailed and entire overview about appropriate numerical methods, and summarizes the most important background information. The discussion of the various numerical methods is reduced to the advantages and disadvantages of the different types of numerical methods and includes the presentation of a stochastic Runge-Kutta scheme of weak order 2.0 that appears to be most appropriate for the problems in the context of this work and that was used for the numerical solution of Langevin equations in chapter 3.

A Gradient expansion of a multiple convolution integral

Nonlocal functionals of multi-convolution type appear, for example, in the functional Taylor expansion of the Helmholtz free-energy functional. In a d -dimensional space with $d \in \{2, 3\}$, these functionals have the general form

$$\begin{aligned}
\mathfrak{J}[c^{(n)}, f_1, \dots, f_n] &= \int_{\mathbb{R}^d} d^d r_1 \cdots \int_{\mathbb{R}^d} d^d r_n c^{(n)}(\vec{r}_1 - \vec{r}_2, \dots, \vec{r}_1 - \vec{r}_n) f_1(\vec{r}_1) \cdots f_n(\vec{r}_n) \\
&= \int_{\mathbb{R}^d} d^d r_1 f_1(\vec{r}_1) \int_{\mathbb{R}^d} d^d r_2 f_2(\vec{r}_1 - \vec{r}_2) \cdots \int_{\mathbb{R}^d} d^d r_n f_n(\vec{r}_1 - \vec{r}_n) c^{(n)}(\vec{r}_2, \dots, \vec{r}_n) \\
&= \int_{\mathbb{R}^d} d^d r_1 f_1(\vec{r}_1) (c^{(n)}(\vec{r}_2, \dots, \vec{r}_n) * f_2(\vec{r}_2) * \cdots * f_n(\vec{r}_n))(\vec{r}_1, \dots, \vec{r}_1) \\
&= \int_{\mathbb{R}^d} d^d r_1 f_1(\vec{r}_1) \mathfrak{F}^{-1}[\tilde{c}^{(n)}(\vec{k}_2, \dots, \vec{k}_n) \tilde{f}_2(\vec{k}_2) \cdots \tilde{f}_n(\vec{k}_n)](\vec{r}_1, \dots, \vec{r}_1)
\end{aligned} \tag{A.1}$$

with the n th-order correlation function $c^{(n)}(\vec{r}_2, \dots, \vec{r}_n)$, the densities $f_i(\vec{r}_i)$ with $i = 1, \dots, n$, and their Fourier transforms $\tilde{c}^{(n)}(\vec{k}_2, \dots, \vec{k}_n) = \mathfrak{F}[c^{(n)}(\vec{r}_2, \dots, \vec{r}_n)](\vec{k}_2, \dots, \vec{k}_n)$ and $\tilde{f}_i(\vec{k}_i) = \mathfrak{F}[f_i(\vec{r}_i)](\vec{k}_i)$, respectively. Functionals of this type can be approximated by a gradient expansion [Eva79] in the densities $f_i(\vec{r}_i)$, which leads to a local functional, if the densities vary sufficiently slow in space. The basic idea behind the gradient expansion is to take advantage of the convolution theorem [We03] and to expand the correlation function in the functional (A.1) in Fourier space by a Taylor expansion. This Taylor expansion of $\tilde{c}^{(n)}(\underline{k})$ is performed here around $\underline{k} = \underline{0}$,

$$\tilde{c}^{(n)}(\underline{k}) = \sum_{l=0}^{\infty} \frac{1}{l!} \sum_{\substack{\alpha_j=1 \\ 1 \leq j \leq l}}^N \left[\frac{\partial^l \tilde{c}^{(n)}(\underline{k})}{\partial k_{\alpha_1} \cdots \partial k_{\alpha_l}} \right]_{\underline{k}=\underline{0}} \prod_{j=1}^l k_{\alpha_j} = \sum_{l=0}^{\infty} \frac{i^l}{l!} \sum_{\substack{\alpha_j=1 \\ 1 \leq j \leq l}}^N \Gamma_{\alpha_1, \dots, \alpha_l} \prod_{j=1}^l k_{\alpha_j}, \tag{A.2}$$

where the abbreviation $\underline{X} = (X_{2,1}, \dots, X_{2,d}, \dots, X_{n,1}, \dots, X_{n,d})$ for $X \in \{k, x, 0\}$ and the length $N = d(n-1)$ of \underline{X} are introduced, but can in principle be performed around another value for \underline{k} as well. The coefficients in this Taylor expansion are defined as

$$\Gamma_{\alpha_1, \dots, \alpha_l} = \int_{\mathbb{R}^N} d^N x c^{(n)}(\underline{x}) \prod_{j=1}^l x_{\alpha_j}. \tag{A.3}$$

Since the prefactor of these coefficients depends on the particular definition of the Fourier transformation, it is remarked that for the Fourier transformation [Wei02] the convention

$$\tilde{f}(\vec{k}) = \mathfrak{F}[f(\vec{x})](\vec{k}) = \int_{\mathbb{R}^d} d^d x f(\vec{x}) e^{i\vec{k} \cdot \vec{x}}, \tag{A.4}$$

$$f(\vec{x}) = \mathfrak{F}^{-1}[\tilde{f}(\vec{k})](\vec{x}) = \frac{1}{(2\pi)^d} \int_{\mathbb{R}^d} d^d k \tilde{f}(\vec{k}) e^{-i\vec{k} \cdot \vec{x}} \tag{A.5}$$

is used in this work. Inserting the expanded and Fourier transformed direct correlation function (A.2) into the functional in the last line of equation (A.1) leads to the *gradient expansion*

$$\mathfrak{J}[c^{(n)}, f_1, \dots, f_n] = \sum_{l=0}^{\infty} \frac{(-1)^l}{l!} \sum_{\substack{\alpha_j=1 \\ 1 \leq j \leq l}}^N \Gamma_{\alpha_1, \dots, \alpha_l} \int_{\mathbb{R}^d} d^d x f_1(\vec{x}) \left[\frac{\partial^l \prod_{j=2}^n f_j(\vec{x}_j)}{\partial x_{\alpha_1} \cdots \partial x_{\alpha_l}} \right]_{\substack{\vec{x}_j = \vec{x} \\ 2 \leq j \leq n}} \quad (\text{A.6})$$

in its most general form.

B Numerical solution of stochastic differential equations

Although the first application of *stochastic differential equations* (SDEs) goes back to the theoretical description of Brownian motion by Einstein [Ein05, Ein06a, Ein06b], Langevin [Lan08], and Smoluchowski [Smo06, Smo16] at the beginning of the 20th century, it took up to the 1940s until a rigorous mathematical theory of SDEs was formulated by Itô and Stratonovich [Has07, Pro10]. Since stochastic calculus is much more complicated and less far developed than the mathematical theory of deterministic differential equations (DDEs), analytical solutions are very few [Ado01, Øks03, Has07, Gar09, HØUZ09] and the need of numerical schemes for the solution of SDEs is very high. Unfortunately, it is not possible to rely on the enormous variety of numerical schemes that have been developed for DDEs [PTVF92, GDN95, Krö97, HLW06], since these methods converge very poorly for SDEs and cannot be improved by simple modifications. Instead, numerical schemes for SDEs had to be developed independently from already existing methods for DDEs. The first numerical scheme for simple SDEs was developed in 1955 by Maruyama [Mar55]. This first and not very efficient scheme is a generalization of the simple Euler method for DDEs and is therefore called the *Euler-Maruyama method*. Later, the more efficient *Milstein method* [Mil75] was developed by Milstein. Today, there is a large number of numerical schemes for different types of SDEs including the rather efficient *stochastic Runge-Kutta methods* [KP06].

Further numerical schemes with better convergence properties are still being derived for SDEs these days. The derivation always uses stochastic calculus, but in this context different versions of stochastic calculus have to be distinguished. These are especially the formulations of Itô and Stratonovich [Ris96, LL07] leading to different classes of numerical schemes for the solution of SDEs. The different versions of stochastic calculus¹ are equivalent, but have different advantages and disadvantages so that one always has to choose the most appropriate version for a certain application [Øks03]. In the most general case, the non-autonomous *Itô SDE* is given in differential form by

$$dX_t = a(t, X_t)dt + b(t, X_t)dW_t \quad (\text{A.7})$$

or equivalently as an integral equation by

$$X_t = X_{t_0} + \int_{t_0}^t a(s, X_s)ds + \int_{t_0}^t b(s, X_s)dW_s \quad (\text{A.8})$$

with the time variable $t \geq t_0$, the Itô process $X = \{X_t \mid t \in \mathbb{R}, t \geq t_0\}$, the (random) initial value X_{t_0} , the drift coefficient $a(t, X_t)$, the diffusion coefficient $b(t, X_t)$, and the

¹Besides the formulations of Itô and Stratonovich, there are also further conventions like the Klimontovich stochastic calculus or *isothermal convention* of Lancon et al. [LBLO01, LBLO02]. A general treatment of the different conventions including the correct adaptation of Langevin equations with multiplicative noise is described in reference [LL07].

Wiener process $\{W_t | t \in \mathbb{R}, t \geq t_0\}$. Notice that equations (A.7) and (A.8) may also be d -dimensional vector SDEs with $X_t \in \mathbb{R}^d$, $a \in \mathbb{R}^d$, $b \in \mathbb{R}^{d \times m}$, and $W_t \in \mathbb{R}^m$, where the elements of W_t are scalar and independent Wiener processes [KP06]. The first term on the right-hand-side of equation (A.7) is a deterministic contribution, while the second term is a stochastic noise term. This noise is called *additive*, if $b(t, X_t)$ does not depend on X_t , and *multiplicative* otherwise. Additive noise is usually predominant in simple physical systems. Multiplicative noise can in contrast be observed in more complicated systems like electric circuits [FFFG85]. In the integral equation (A.8), the first integral is a usual deterministic Lebesgue integral, but the second integral is a stochastic integral. The latter is defined as an Itô integral in the case of an Itô SDE. However, stochastic integrals can also be defined as Stratonovich integrals and in the case of multiplicative noise one has to distinguish strictly between the definitions of Itô and Stratonovich. Therefore, it is convenient to denote Stratonovich integrals in a different way. Here, the symbol \circ is used in the context of the Stratonovich stochastic calculus. In contrast to equations (A.7) and (A.8), the general non-autonomous *Stratonovich SDE* is denoted by

$$dX_t = \tilde{a}(t, X_t)dt + b(t, X_t) \circ dW_t \quad (\text{A.9})$$

respectively

$$X_t = X_{t_0} + \int_{t_0}^t \tilde{a}(s, X_s)ds + \int_{t_0}^t b(s, X_s) \circ dW_s \quad (\text{A.10})$$

with the drift coefficient $\tilde{a}(t, X_t)$ in this work. The equivalence of the Itô stochastic calculus and the Stratonovich stochastic calculus implies that there is a bijective transformation between equations (A.7) and (A.9) respectively (A.8) and (A.10) and that every solution, which satisfies the Itô SDE, is also a solution of the Stratonovich SDE with a modified drift coefficient $\tilde{a}(t, X_t)$ [KP06]. Between the drift coefficients $a(t, X_t)$ and $\tilde{a}(t, X_t)$, the simple relation [KP06, LL07]

$$a(t, X_t) = \tilde{a}(t, X_t) + \frac{1}{2} b(t, X_t) \frac{\partial b}{\partial X_t}(t, X_t) \quad (\text{A.11})$$

holds. Besides numerical schemes for Itô and Stratonovich SDEs, one has to distinguish further numerical schemes that approximate weak or strong solutions of the particular SDE. A *strong solution* of an SDE corresponds to a prescribed Wiener process and strong numerical schemes provide good pathwise approximations of a stochastic process. They are especially appropriate to approximate individual sample trajectories. In contrast, a *weak solution* is obtained from an SDE for a general Wiener process. Weak numerical schemes are usually computationally faster than their strong converging analogs, but they reproduce only the statistics of the solution well and not particular trajectories. Such weak schemes are therefore appropriate, if one is only interested in functionals of the probability distribution of the random variable X_t . This is usually the case in statistical physics, where moments like mean value and mean square displacement of the probability density are often the only quantities that need to be determined. Corresponding to the two classes of strong and weak solutions of

SDEs, there are also two different convergence terms that can be used to characterize the order of convergence of a stochastic numerical scheme. When $Y^\delta(t_n)$ denotes the Markov chain of time discrete approximations at times t_n for a given numerical scheme with an arbitrary time discretization $t_0 < \dots < t_n < \dots < t_N$ with maximum time step size $\delta > 0$, X_{t_n} is the exact solution of a given SDE at time t_n , and $E(\cdot)$ denotes the expectation value, then this scheme is *strongly convergent* with order $\gamma_s > 0$, if there exist a constant $0 < C < \infty$, that is independent of δ , and an upper limit $\delta_{\max} > 0$ for the step size so that the condition [KP06]

$$E(\|X_{t_n} - Y^\delta(t_n)\|) \leq C\delta^{\gamma_s} \quad \forall \delta \in (0, \delta_{\max}) \quad (\text{A.12})$$

holds. On the other hand, a numerical scheme is *weakly convergent* with order $\gamma_w > 0$, if there exist two constants $0 < C < \infty$ and $\delta_{\max} > 0$ so that [KP06]

$$\|E(g(X_{t_n})) - E(g(Y^\delta(t_n)))\| \leq C\delta^{\gamma_w} \quad \forall \delta \in (0, \delta_{\max}) \quad (\text{A.13})$$

holds for any polynomial $g(x)$. On a third stage, the numerical schemes are distinguished with respect to their type of discretization. As for DDEs, also for SDEs exist explicit and implicit discretizations. An *explicit* scheme is usually fast, but it becomes unstable for stiff SDEs and for step sizes that are too large. This does not happen with *implicit* schemes, but they involve the iterative solution of nonlinear simultaneous equations for each time step and are therefore computationally much more expensive. With these distinctions of Itô or Stratonovich, strong or weak, and explicit or implicit schemes, there are already eight different classes of numerical schemes for the approximate solution of SDEs.

As numerical schemes for the approximate solution of DDEs are usually constructed and analyzed on the basis of the deterministic Taylor expansion², its stochastic generalization for smooth functions of stochastic processes – the stochastic Taylor expansion [KP06] – is usually used as a starting point to derive new numerical schemes for SDEs. The application of either the *Itô-Taylor expansion*, that is a generalization of the famous Itô formula, or the *Stratonovich-Taylor expansion*, that is similar to the Itô-Taylor expansion but has a simpler structure, decides whether the derivation results in an Itô scheme or in a Stratonovich scheme. Under all numerical schemes for SDEs that have been developed up to now and of whom a large number is discussed in the book [KP06], are Taylor approximations like the Euler-Maruyama scheme and the Milstein scheme, multistep schemes, and predictor-corrector methods. It is in principle possible to extend these schemes to new methods with an arbitrary high order of convergence, but with increasing order of convergence these schemes become increasingly complicated and computationally expensive.

Nevertheless, numerical mathematics of SDEs is a currently very active field and the publication of further schemes with higher efficiency can be expected in the near future. Most of the available schemes have the big disadvantage that they involve

²Exponential integrators for the solution of highly oscillatory differential equations, for example, constitute an exception and cannot be analyzed using a Taylor expansion [HLW06].

derivatives of the diffusion coefficient that have to be approximated in turn. Stochastic Runge-Kutta schemes avoid these derivatives and are therefore preferable, if SDEs with multiplicative noise have to be solved numerically.

In chapter 3 of this work, numerical solutions of d -dimensional systems of coupled nonlinear SDEs with multiplicative noise are presented. These systems of SDEs are autonomous and defined in the Itô sense. They can be written in the form

$$\dot{X}_t = a(X_t) + b(X_t)\xi_t \quad (\text{A.14})$$

with the vector $a \in \mathbb{R}^d$, the matrix $b \in \mathbb{R}^{d \times d}$, and the stochastic noise $\xi_t \in \mathbb{R}^d$. This noise can be formally interpreted as the time derivative $\xi_t = dW_t/dt$ of the d -dimensional Wiener process W_t , but this derivative is mathematically not defined, since a Wiener process is nowhere differentiable. Pathwise numerical solutions of the vector SDE (A.14) were not needed for this work. Therefore, the following multi-dimensional explicit *stochastic Runge-Kutta scheme* of weak order 2.0 for Itô SDEs to be found on page 486 of reference [KP06] appeared to be most appropriate and was used:

$$\begin{aligned} Y_i^{n+1} = & Y_i^n + \frac{\Delta t}{2} (a_i(\bar{Y}^n) + a_i(Y^n)) \\ & + \frac{\sqrt{\Delta t}}{4} \sum_{j,k=1}^m \left(b_{ij}(\bar{Y}_{jk}^{n+}) (\Delta Z_j^n (1 + \Delta Z_k^n) - \hat{Z}_{jk}^n) \right. \\ & \quad \left. + b_{ij}(\bar{Y}_{jk}^{n-}) (\Delta Z_j^n (1 - \Delta Z_k^n) + \hat{Z}_{jk}^n) \right. \\ & \quad \left. + 2(2\delta_{jk} - 1)b_{ij}(Y^n)\Delta Z_j^n \right). \end{aligned} \quad (\text{A.15})$$

Here, the symbol Y_i^n denotes the i th element of the d -dimensional numerical solution $Y^n \equiv Y^\delta(t_n)$ at time $t_n = n\Delta t$, Δt is the step size of the equidistant time discretization $t_0 < \dots < t_n < \dots < t_N$, a_i is the i th element of the d -dimensional vector a , b_{ij} is the (i, j) th element of the $d \times m$ -dimensional matrix b , and $\bar{Y}^n = (\bar{Y}_i^n)_{i=1, \dots, d}$ is the vector with the elements

$$\bar{Y}_i^n = Y_i^n + a_i(Y^n)\Delta t + \sqrt{\Delta t} \sum_{j=1}^m b_{ij}(Y^n)\Delta Z_j^n \quad (\text{A.16})$$

and with the standard normal distributed Gaussian random numbers³

$$\Delta Z_j^n \sim \mathcal{N}(0, 1) . \quad (\text{A.17})$$

The vectors $\bar{Y}_{jk}^{n+} = (\bar{Y}_{ijk}^{n+})_{i=1, \dots, d}$ and $\bar{Y}_{jk}^{n-} = (\bar{Y}_{ijk}^{n-})_{i=1, \dots, d}$ are further defined by

$$\bar{Y}_{ijk}^{n\pm} = Y_i^n + a_i(Y^n)\Delta t \delta_{jk} \pm b_{ij}(Y^n)\sqrt{\Delta t} \quad (\text{A.18})$$

³The notation $X \sim \mathcal{N}(\mu, \sigma^2)$ means that the random variable X is Gaussian distributed with mean μ and variance σ^2 . Such a random variable can always be replaced by a standard normal distributed random variable $X' = (X - \mu)/\sigma \sim \mathcal{N}(0, 1)$.

and \hat{Z}_{jk}^n are two-point distributed random numbers with the probability distribution

$$P(\hat{Z}_{jk}^n = \pm 1) = \frac{1}{2} \quad \text{for } k = 1, \dots, j-1, \quad \hat{Z}_{jj}^n = 1, \quad \text{and} \quad \hat{Z}_{jk}^n = -\hat{Z}_{kj}^n. \quad (\text{A.19})$$

Two-point distributed random numbers can easily be calculated from $\sim \mathcal{U}(0, 1)$ random numbers that are uniformly distributed on the interval $(0, 1)$. Notice that the random numbers⁴ ΔZ_j^n and \hat{Z}_{jk}^n are uncorrelated with respect to time, i. e., with respect to the index n . For stochastic integrations in the context of this work, the stochastic Runge-Kutta scheme (A.15) is sufficient. In other situations, one might have to solve stiff vector SDEs, for which the scheme (A.15) is not applicable. In this case, the corresponding multi-dimensional implicit stochastic Runge-Kutta scheme of weak order 2.0 can be found on page 501 of reference [KP06].

If weak convergence of order 2.0 appears to be not sufficient for a certain application, an *extrapolation method* can be used to enlarge the order of a numerical approximation from 2.0 to 4.0. In general, extrapolation methods can be used to construct a weak approximation of order $2\gamma_w$ from weak approximations of order γ_w that are obtained by a numerical scheme for equidistant time discretizations with different step sizes δ . For example, if one wants to calculate numerical approximations $E(g(Y^\delta(t)))$ for the functional $E(g(X_t))$ with the second-order scheme (A.15), then an improved approximation of order 4.0 is given by [KP06]

$$V_{g,4}^\delta(t) = \frac{1}{21} \left(32E(g(Y^\delta(t))) - 12E(g(Y^{2\delta}(t))) + E(g(Y^{4\delta}(t))) \right). \quad (\text{A.20})$$

Similar extrapolation methods exist for different orders γ_w of the scheme that is used initially. Often it is easier to use an extrapolation method than an improved scheme of the double order, because the numerical schemes usually become very complicated for higher orders of convergence and for many numerical schemes higher-order versions do not yet exist.

⁴A good pseudo-random number generator is the *Mersenne Twister MT 19937* of Matsumoto and Nishimura [MN98], which is fast and has the extremely large period $2^{19937} - 1$. It can be used for the simulation of ΔZ_j^n and \hat{Z}_{jk}^n .

Bibliography

- [Ach90] ACHESON, J. D.: *Oxford Applied Mathematics and Computing Science Series*. Vol. 22: *Elementary Fluid Dynamics*. 1. Ed. Oxford: Oxford University Press, 1990. – 397 p. – ISBN 978–0–198–59679–0
- [Ado01] ADOMIAN, G.: *Mathematics and its Applications*. Vol. 46: *Nonlinear Stochastic Systems Theory and Application to Physics*. 1. Ed. Dordrecht: Kluwer Academic Publishers, 2001. – 248 p. – ISBN 978–1–402–00338–7
- [AE04] ARCHER, A. J.; EVANS, R.: Dynamical density functional theory and its application to spinodal decomposition. In: *Journal of Chemical Physics* 121 (2004), September, No. 9, p. 4246–4254
- [AKI+01] ANNARATONE, B. M.; KHRAPAK, A. G.; IVLEV, A. V.; SÖLLNER, G.; BRYANT, P.; SÜTTERLIN, R.; KONOPKA, U.; YOSHINO, K.; ZUZIC, M.; THOMAS, H. M.; MORFILL, G. E.: Levitation of cylindrical particles in the sheath of an rf plasma. In: *Physical Review E* 63 (2001), March, No. 3, p. 036406
- [AL78] ASLANYAN, T. A.; LEVANYUK, A. P.: Lifshits critical points. In: *Soviet Physics - Solid State* 20 (1978), March, No. 3, p. 466–469
- [AMW08] ALVAREZ, C.; MAZARS, M.; WEIS, J. J.: Structure and thermodynamics of a ferrofluid bilayer. In: *Physical Review E* 77 (2008), May, No. 5, p. 051501
- [AR11] ALMENAR, L.; RAUSCHER, M.: Dynamics of colloids in confined geometries. In: *Journal of Physics: Condensed Matter* 23 (2011), April, No. 18, p. 184115
- [Arc05] ARCHER, A. J.: Dynamical density functional theory: binary phase-separating colloidal fluid in a cavity. In: *Journal of Physics: Condensed Matter* 17 (2005), March, No. 10, p. 1405–1427
- [Arc06] ARCHER, A. J.: Dynamical density functional theory for dense atomic liquids. In: *Journal of Physics: Condensed Matter* 18 (2006), June, No. 24, p. 5617–5628
- [Arc09] ARCHER, A. J.: Dynamical density functional theory for molecular and colloidal fluids: a microscopic approach to fluid mechanics. In: *Journal of Chemical Physics* 130 (2009), January, No. 1, p. 014509

- [AS72] ABRAMOWITZ, M.; STEGUN, I. A.: *Handbook of Mathematical Functions: with Formulas, Graphs, and Mathematical Tables*. 9. Ed. New York: Dover Publications, 1972. – 1046 p. – ISBN 0-486-61272-4
- [AT72] ASARO, R. J.; TILLER, W. A.: Interface morphology development during stress corrosion cracking: Part I. Via surface diffusion. In: *Metallurgical Transactions* 3 (1972), July, No. 7, p. 1789–1796
- [AW05] ARFKEN, G. B.; WEBER, H. J.: *Mathematical Methods for Physicists*. 6. Ed. Oxford: Elsevier, 2005. – 1182 p. – ISBN 0-120-59876-0
- [AWL11] ACHIM, C. V.; WITTKOWSKI, R.; LÖWEN, H.: Stability of liquid crystalline phases in the phase-field-crystal model. In: *Physical Review E* 83 (2011), June, No. 6, p. 061712
- [Bal97] BALESCU, R.: *Statistical Dynamics: Matter out of Equilibrium*. 1. Ed. London: Imperial College Press, 1997. – 330 p. – ISBN 1-860-94045-5
- [Bar87] BARRAT, J.-L.: Role of triple correlations in the freezing of the one-component plasma. In: *Europhysics Letters* 3 (1987), March, No. 5, p. 523–526
- [Bat00] BATCHELOR, G. K.: *Cambridge Mathematical Library*. Vol. 5: *An Introduction to Fluid Dynamics*. 1. Ed. New York: Cambridge University Press, 2000. – 615 p. – ISBN 978-0-521-66396-0
- [BC09] BELOVS, M.; ČEBERS, A.: Ferromagnetic microswimmer. In: *Physical Review E* 79 (2009), May, No. 5, p. 051503
- [BCP92] BRAND, H. R.; CLADIS, P. E.; PLEINER, H.: Symmetry and defects in the CM phase of polymeric liquid crystals. In: *Macromolecules* 25 (1992), December, No. 26, p. 7223–7226
- [BCP98] BRAND, H. R.; CLADIS, P. E.; PLEINER, H.: Macroscopic properties of smectic liquid crystals. In: *European Physical Journal B* 6 (1998), November, No. 3, p. 347–353
- [BCP00] BRAND, H. R.; CLADIS, P. E.; PLEINER, H.: Polar biaxial liquid crystalline phases with fluidity in two and three spatial dimensions. In: *International Journal of Engineering Science* 38 (2000), June, No. 9-10, p. 1099–1112
- [BCP09] BRAND, H. R.; CLADIS, P. E.; PLEINER, H.: Reversible macroscopic dynamics of polar nematic liquid crystals: reversible currents and their experimental consequences. In: *Physical Review E* 79 (2009), March, No. 3, p. 032701

- [BCS57a] BARDEEN, J.; COOPER, L. N.; SCHRIEFFER, J. R.: Microscopic theory of superconductivity. In: *Physical Review* 106 (1957), April, No. 1, p. 162–164
- [BCS57b] BARDEEN, J.; COOPER, L. N.; SCHRIEFFER, J. R.: Theory of superconductivity. In: *Physical Review* 108 (1957), December, No. 5, p. 1175–1204
- [BCSS94] BOWICK, M. J.; CHANDAR, L.; SCHIFF, E. A.; SRIVASTAVA, A. M.: The cosmological Kibble mechanism in the laboratory: string formation in liquid crystals. In: *Science* 263 (1994), February, No. 5149, p. 943–945
- [BDW⁺08] BEEK, D. van d.; DAVIDSON, P.; WENSINK, H. H.; VROEGE, G. J.; LEKKERKERKER, H. N. W.: Influence of a magnetic field on the nematic phase of hard colloidal platelets. In: *Physical Review E* 77 (2008), March, No. 3, p. 031708
- [BF97] BOLHUIS, P.; FRENKEL, D.: Tracing the phase boundaries of hard spherocylinders. In: *Journal of Chemical Physics* 106 (1997), January, No. 2, p. 666–687
- [BG11] BERRY, J.; GRANT, M.: Modeling multiple time scales during glass formation with phase-field crystals. In: *Physical Review Letters* 106 (2011), April, No. 17, p. 175702
- [BH03] BARRAT, J.-L.; HANSEN, J.-P.: *Basic Concepts for Simple and Complex Liquids*. 1. Ed. Cambridge: Cambridge University Press, 2003. – 308 p. – ISBN 0–521–78344–5
- [BHD05] BIER, M.; HARNAU, L.; DIETRICH, S.: Free isotropic-nematic interfaces in fluids of charged platelike colloids. In: *Journal of Chemical Physics* 123 (2005), September, No. 11, p. 114906
- [BHP87] BARRAT, J.-L.; HANSEN, J.-P.; PASTORE, G.: Factorization of the triplet direct correlation function in dense fluids. In: *Physical Review Letters* 58 (1987), May, No. 20, p. 2075–2078
- [BHP88] BARRAT, J.-L.; HANSEN, J.-P.; PASTORE, G.: On the equilibrium structure of dense fluids. In: *Molecular Physics* 63 (1988), April, No. 5, p. 747–767
- [BK86] BRAND, H. R.; KAWASAKI, K.: Gradient free energy of nematic liquid crystals with topological defects. In: *Journal of Physics C* 19 (1986), March, No. 7, p. 937–942
- [BK11] BRADER, J. M.; KRÜGER, M.: Density profiles of a colloidal liquid at a wall under shear flow. In: *Molecular Physics* 7 (2011), April, No. 7, p. 1029–1041

- [BLT91] BECHHOEFER, J.; LÖWEN, H.; TUCKERMAN, L. S.: Dynamical mechanism for the formation of metastable phases. In: *Physical Review Letters* 67 (1991), September, No. 10, p. 1266–1269
- [BLT⁺06] BIANCHI, E.; LARGO, J.; TARTAGLIA, P.; ZACCARELLI, E.; SCIORTINO, F.: Phase diagram of patchy colloids: towards empty liquids. In: *Physical Review Letters* 97 (2006), October, No. 16, p. 168301
- [Bou99] BOUCHOULE, A.: *Dusty Plasmas: Physics, Chemistry, and Technological Impact in Plasma Processing*. 1. Ed. Chichester: John Wiley & Sons, 1999. – 408 p. – ISBN 0-471-97386-6
- [Boy99] BOYADZHIEV, K. N.: Spirals and conchospirals in the flight of insects. In: *The College Mathematics Journal* 30 (1999), January, No. 1, p. 23–31
- [Boy08] *Chapter 5.6: Nonlinear Optics of Liquid Crystals*. In: BOYD, R. W.: *Nonlinear Optics*. Vol. 1. 3. Ed. Amsterdam: Academic Press, 2008. – ISBN 978-0-123-69470-6, p. 271–276
- [BP80] BRAND, H. R.; PLEINER, H.: Nonlinear reversible hydrodynamics of liquid crystals and crystals. In: *Journal de Physique* 41 (1980), No. 6, p. 553–564
- [BP87] BRAND, H. R.; PLEINER, H.: Nonlinear effects in the electrohydrodynamics of uniaxial nematic liquid crystals. In: *Physical Review A* 35 (1987), April, No. 7, p. 3122–3127
- [BPBF36] BAWDEN, F. C.; PIRIE, N. W.; BERNAL, J. D.; FANKUCHEN, I.: Liquid crystalline substances from virus-infected plants. In: *Nature* 138 (1936), December, No. 3503, p. 1051–1052
- [BPZ06] BRAND, H. R.; PLEINER, H.; ZIEBERT, F.: Macroscopic dynamics of polar nematic liquid crystals. In: *Physical Review E* 74 (2006), August, No. 2, p. 021713
- [Bre65] BRENNER, H.: Coupling between the translational and rotational Brownian motions of rigid particles of arbitrary shape I: helicoidally isotropic particles. In: *Journal of Colloid Science* 20 (1965), February, No. 2, p. 104–122
- [Bre67] BRENNER, H.: Coupling between the translational and rotational Brownian motions of rigid particles of arbitrary shape II: general theory. In: *Journal of Colloid and Interface Science* 23 (1967), March, No. 3, p. 407–436

- [BRS⁺06] BEEK, D. van d.; REICH, H.; SCHOOT, P. van d.; DIJKSTRA, M.; SCHILLING, T.; VINK, R.; SCHMIDT, M.; ROIJ, R. van; LEKKERKERKER, H.: Isotropic-nematic interface and wetting in suspensions of colloidal platelets. In: *Physical Review Letters* 97 (2006), August, No. 8, p. 087801
- [But08] BUTCHER, J. C.: *Numerical Methods for Ordinary Differential Equations*. 2. Ed. Chichester: John Wiley & Sons, 2008. – 482 p. – ISBN 0-470-72335-1
- [CA86] CURTIN, W. A.; ASHCROFT, N. W.: Density-functional theory and freezing of simple liquids. In: *Physical Review Letters* 56 (1986), June, No. 26, p. 2775-2778
- [CCAN96] CLEAVER, D. J.; CARE, C. M.; ALLEN, M. P.; NEAL, M. P.: Extension and generalization of the Gay-Berne potential. In: *Physical Review E* 54 (1996), July, No. 1, p. 559-567
- [CDGK06] CISNEROS, L.; DOMBROWSKI, C.; GOLDSTEIN, R. E.; KESSLER, J. O.: Reversal of bacterial locomotion at an obstacle. In: *Physical Review E* 73 (2006), March, No. 3, p. 030901
- [CFM⁺08] CATES, M. E.; FIELDING, S. M.; MARENDUZZO, D.; ORLANDINI, E.; YEOMANS, J. M.: Shearing active gels close to the isotropic-nematic transition. In: *Physical Review Letters* 101 (2008), August, No. 6, p. 068102
- [CFW04] CALDERER, M. C.; FOREST, M. G.; WANG, Q.: Kinetic theories and mesoscopic models for solutions of nonhomogeneous liquid crystal polymers. In: *Journal of Non-Newtonian Fluid Mechanics* 120 (2004), July, No. 1-3, p. 69-78
- [Cha92] CHANDRASEKHAR, S.: *Liquid crystals*. 2. Ed. Cambridge: Cambridge University Press, 1992. – 480 p. – ISBN 0-521-41747-3
- [CKW04] COFFEY, W. T.; KALMYKOV, Y. P.; WALDRON, J. T.: *World Scientific Series in Contemporary Chemical Physics*. Vol. 14: *The Langevin Equation: With Applications to Stochastic Problems in Physics, Chemistry and Electrical Engineering*. 2. Ed. Singapore: World Scientific Publishing, 2004. – 678 p. – ISBN 978-9-812-38462-1
- [CL95] CHAIKIN, P. M.; LUBENSKY, T. C.: *Principles of Condensed Matter Physics*. 1. Ed. Cambridge: Cambridge University Press, 1995. – 699 p. – ISBN 0-521-79450-1
- [CLEL11] CHOUDHARY, M. A.; LI, D.; EMMERICH, H.; LÖWEN, H.: DDFT calibration and investigation of an anisotropic phase-field crystal model. In: *Journal of Physics: Condensed Matter* 23 (2011), July, No. 26, p. 265005

- [CM97] CUESTA, J. A.; MARTÍNEZ-RATÓN, Y.: Fundamental measure theory for mixtures of parallel hard cubes: I. General formalism. In: *Journal of Chemical Physics* 107 (1997), October, No. 16, p. 6379–6389
- [CV83] CERDA, C. M.; VEN, T. G. M. v. d.: Translational diffusion of axisymmetrical particles in shear flow. In: *Journal of Colloid and Interface Science* 93 (1983), May, No. 1, p. 54–62
- [CWG10] CHELAKKOT, R.; WINKLER, R. G.; GOMPPER, G.: Migration of semiflexible polymers in microcapillary flow. In: *Europhysics Letters* 91 (2010), July, No. 1, p. 14001
- [CYDT91] CHUANG, I.; YURKE, B.; DURRER, R.; TUROK, N.: Cosmology in the laboratory – defect dynamics in liquid crystals. In: *Science* 251 (1991), March, No. 4999, p. 1336–1342
- [CYK⁺07] CHO, Y.; YI, G.; KIM, S.; JEON, S.; ELSESSER, M. T.; YU, H. K.; YANG, S.; PINE, D. J.: Particles with coordinated patches or windows from oil-in-water emulsions. In: *Chemistry of Materials* 19 (2007), May, No. 13, p. 3183–3193
- [DBR⁺05] DREYFUS, R.; BAUDRY, J.; ROPER, M. L.; FERMIGIER, M.; STONE, H. A.; BIBETTE, J.: Microscopic artificial swimmers. In: *Nature* 437 (2005), October, No. 7060, p. 862–865
- [DE07] DOI, M.; EDWARDS, S. F.: *International Series of Monographs on Physics*. Vol. 73: *The Theory of Polymer Dynamics*. 1. Ed. Oxford: Oxford University Press, 2007. – 391 p. – ISBN 978-0-198-52033-7
- [Dea96] DEAN, D. S.: Langevin equation for the density of a system of interacting Langevin processes. In: *Journal of Physics A: Mathematical and General* 29 (1996), December, No. 24, p. L613–L617
- [DFM90] DIETERICH, W.; FRISCH, H. L.; MAJHOFFER, A.: Nonlinear diffusion and density functional theory. In: *Zeitschrift für Physik B: Condensed Matter* 78 (1990), June, No. 2, p. 317–323
- [DFW⁺06] DHAR, P.; FISCHER, T. M.; WANG, Y.; MALLOUK, T. E.; PAXTON, W. F.; SEN, A.: Autonomously moving nanorods at a viscous interface. In: *Nano Letters* 6 (2006), January, No. 1, p. 66–72
- [DHM95] DIJKSTRA, M.; HANSEN, J.-P.; MADDEN, P. A.: Gelation of a clay colloid suspension. In: *Physical Review Letters* 75 (1995), September, No. 11, p. 2236–2239

- [DHM97] DIJKSTRA, M.; HANSEN, J.-P.; MADDEN, P. A.: Statistical model for the structure and gelation of smectite clay suspensions. In: *Physical Review E* 55 (1997), March, No. 3, p. 3044–3053
- [Dho96] DHONT, J. K. G.: *Studies in Interface Science*. Vol. 2: *An Introduction to Dynamics of Colloids*. 1. Ed. Amsterdam: Elsevier Science, 1996. – 642 p. – ISBN 0–444–82009–4
- [DJK⁺10] DEMIRÖRS, A. F.; JOHNSON, P. M.; KATS, C. M. v.; BLAADEREN, A. van; IMHOF, A.: Directed self-assembly of colloidal dumbbells with an electric field. In: *Langmuir* 26 (2010), September, No. 18, p. 14466–14471
- [DMD⁺10] DEKA, S.; MISZTA, K.; DORFS, D.; GENOVESE, A.; BERTONI, G.; MANNA, L.: Octapod-shaped colloidal nanocrystals of cadmium chalcogenides via “one-pot” cation exchange and seeded growth. In: *Nano Letters* 10 (2010), September, No. 9, p. 3770–3776
- [DPZY10] DUNKEL, J.; PUTZ, V. B.; ZAID, I. M.; YEOMANS, J. M.: Swimmer-tracer scattering at low Reynolds number. In: *Soft Matter* 6 (2010), July, No. 17, p. 4268–4276
- [DS09] DOWNTON, M. T.; STARK, H.: Beating kinematics of magnetically actuated cilia. In: *Europhysics Letters* 85 (2009), February, No. 4, p. 44002
- [DZ09] DUNKEL, J.; ZAID, I. M.: Noisy swimming at low Reynolds numbers. In: *Physical Review E* 80 (2009), August, No. 2, p. 021903
- [EG04] ELDER, K. R.; GRANT, M.: Modeling elastic and plastic deformations in nonequilibrium processing using phase field crystals. In: *Physical Review E* 70 (2004), November, No. 5, p. 051605
- [EG09] ELGETI, J.; GOMPPER, G.: Self-propelled rods near surfaces. In: *Europhysics Letters* 85 (2009), February, No. 3, p. 38002
- [EH10] EBBENS, S. J.; HOWSE, J. R.: In pursuit of propulsion at the nanoscale. In: *Soft Matter* 6 (2010), February, No. 4, p. 726–738
- [Ein05] EINSTEIN, A.: Über die von der molekularkinetischen Theorie der Wärme geforderte Bewegung von in ruhenden Flüssigkeiten suspendierten Teilchen. In: *Annalen der Physik* 322 (1905), June, No. 8, p. 549–560
- [Ein06a] EINSTEIN, A.: Eine neue Bestimmung der Moleküldimensionen. In: *Annalen der Physik* 324 (1906), February, No. 2, p. 289–306
- [Ein06b] EINSTEIN, A.: Zur Theorie der Brownschen Bewegung. In: *Annalen der Physik* 324 (1906), February, No. 2, p. 371–381

- [EKHG02] ELDER, K. R.; KATAKOWSKI, M.; HAATAJA, M.; GRANT, M.: Modeling elasticity in crystal growth. In: *Physical Review Letters* 88 (2002), June, No. 24, p. 245701
- [EL09] ESPAÑOL, P.; LÖWEN, H.: Derivation of dynamical density functional theory using the projection operator technique. In: *Journal of Chemical Physics* 131 (2009), December, No. 24, p. 244101
- [EPB⁺07] ELDER, K. R.; PROVATAS, N.; BERRY, J.; STEFANOVIC, P.; GRANT, M.: Phase-field crystal modeling and classical density functional theory of freezing. In: *Physical Review B* 75 (2007), February, No. 6, p. 064107
- [Eri59] ERICKSEN, J. L.: Anisotropic fluids. In: *Archive for Rational Mechanics and Analysis* 4 (1959), January, No. 1, p. 231–237
- [Eri61] ERICKSEN, J. L.: Conservation laws for liquid crystals. In: *Journal of Rheology* 5 (1961), March, No. 1, p. 23–34
- [ES11] ENCULESCU, M.; STARK, H.: Active colloidal suspensions exhibit polar order under gravity. In: *Physical Review Letters* 107 (2011), July, No. 5, p. 058301
- [ESS76] EBNER, C.; SAAM, W. F.; STROUD, D.: Density-functional theory of simple classical fluids: I. Surfaces. In: *Physical Review A* 14 (1976), December, No. 6, p. 2264–2273
- [Eva79] EVANS, R.: The nature of the liquid-vapour interface and other topics in the statistical mechanics of non-uniform, classical fluids. In: *Advances in Physics* 28 (1979), March, p. 143–200
- [Eva92] *Chapter 3: Density Functionals in the Theory of Nonuniform Fluids.* In: EVANS, R.: *Fundamentals of Inhomogeneous Fluids*. 1. Ed. New York: Marcel Dekker, 1992. – ISBN 0–824–78711–0, p. 85–176
- [EZB⁺08] ERBE, A.; ZIENTARA, M.; BARABAN, L.; KREIDLER, C.; LEIDERER, P.: Various driving mechanisms for generating motion of colloidal particles. In: *Journal of Physics: Condensed Matter* 20 (2008), October, No. 40, p. 4215
- [FBLL03] FROLTSOV, V. A.; BLAAK, R.; LIKOS, C. N.; LÖWEN, H.: Crystal structures of two-dimensional magnetic colloids in tilted external magnetic fields. In: *Physical Review E* 68 (2003), December, No. 6, p. 061406
- [FFFG85] *Chapter 10: Experimental Investigation on the Effect of Multiplicative Noise by Means of Electric Circuits.* In: FAETTI, S.; FESTA, C.; FRONZONI, L.; GRIGOLINI, P.: *Advances in Chemical Physics*. Vol. 62: *Memory Function Approaches to Stochastic Problems in Condensed Matter*. 1. Ed.

- New York: John Wiley & Sons, 1985. – ISBN 978-0-470-14331-5, p. 445–475
- [Fix83] FIX, G. J.: Phase Field Models for Free Boundary Problems. In: FASANO, A. (ed.); PRIMICERIO, M. (ed.): *Free Boundary Problems: Theory and Applications*. Vol. 2. Boston: Pitman, 1983, p. 580–589
- [FM85] FRENKEL, D.; MULDER, B. M.: The hard ellipsoid-of-revolution fluid. In: *Molecular Physics* 55 (1985), January, No. 5, p. 1171–1192
- [FMH86] FELIX, J. W.; MUKAMEL, D.; HORNREICH, R. M.: Novel class of continuous phase transitions to incommensurate structures. In: *Physical Review Letters* 57 (1986), October, No. 17, p. 2180–2183
- [FMM84] FRENKEL, D.; MULDER, B. M.; MCTAGUE, J. P.: Phase diagram of a system of hard ellipsoids. In: *Physical Review Letters* 52 (1984), January, No. 4, p. 287–290
- [For74] FORSTER, D.: Hydrodynamics and correlation functions in ordered systems: nematic liquid crystals. In: *Annals of Physics* 84 (1974), May, No. 1-2, p. 505–534
- [For89] FORSTER, D.: *Frontiers in Physics*. Vol. 47: *Hydrodynamic Fluctuations, Broken Symmetry, and Correlation Functions*. 1. Ed. Redwood City: Addison Wesley, 1989. – 326 p. – ISBN 978-0-201-50882-6
- [Fra58] FRANK, F. C.: On the theory of liquid crystals. In: *Discussions of the Faraday Society* 25 (1958), February, No. 1, p. 19–28
- [Fre91] FRENKEL, D.: Course 9: Statistical Mechanics of Liquid Crystals. In: HANSEN, J.-P. (ed.); LEVESQUE, D. (ed.); ZINN-JUSTIN, J. (ed.); USMG, NATO Advanced Study Institute (org.): *Liquids, Freezing and Glass Transition*. Vol. 2. Amsterdam: North Holland, Elsevier Science Publishers B. V., July 1991 (Proceedings of the Les Houches Summer School, Course LI, 3-28 July 1989), p. 689–762
- [FS10] FRANCESCANGELI, O.; SAMULSKI, E. T.: Insights into the cybotactic nematic phase of bent-core molecules. In: *Soft Matter* 6 (2010), March, No. 11, p. 2413–2420
- [FST⁺09] FRANCESCANGELI, O.; STANIC, V.; TORGOVA, S.; STRIGAZZI, A.; SCARAMUZZA, N.; FERRERO, C.; DOLBANYA, I. P.; WEISS, T. M.; BERRARDI, R.; MUCCIOLI, L.; ORLANDI, S.; ZANNONI, C.: Ferroelectric response and induced biaxiality in the nematic phase of bent-core mesogens. In: *Advanced Functional Materials* 19 (2009), August, No. 16, p. 2592–2600

- [FT02] FERNANDES, M. X.; TORRE, J. G. d. l.: Brownian dynamics simulation of rigid particles of arbitrary shape in external fields. In: *Biophysical Journal* 83 (2002), December, No. 6, p. 3039–3048
- [FTD04] FUKUNAGA, H.; TAKIMOTO, J.-I.; DOI, M.: Molecular dynamics simulation study on the phase behavior of the Gay-Berne model with a terminal dipole and a flexible tail. In: *Journal of Chemical Physics* 120 (2004), April, p. 7792–7800
- [FTO08] FAN, D.; THOMAS, P. J.; O'BRIEN, P.: Pyramidal lead sulfide crystallites with high energy {113} facets. In: *Journal of the American Chemical Society* 130 (2008), July, No. 33, p. 10892–10894
- [GAO⁺10] GERBODE, S. J.; AGARWAL, U.; ONG, D. C.; LIDDELL, C. M.; ESCOBEDO, F.; COHEN, I.: Glassy dislocation dynamics in 2D colloidal dimer crystals. In: *Physical Review Letters* 105 (2010), August, No. 7, p. 078301
- [Gar09] GARDINER, C. W.: *Springer Series in Synergetics*. Vol. 13: *Handbook of Stochastic Methods: for Physics, Chemistry and the Natural Sciences*. 4. Ed. Berlin: Springer, 2009. – 447 p. – ISBN 978–3–540–70712–7
- [GD94] GROH, B.; DIETRICH, S.: Ferroelectric phase in Stockmayer fluids. In: *Physical Review E* 50 (1994), November, No. 5, p. 3814–3833
- [GD96] GROH, B.; DIETRICH, S.: Density-functional theory for the freezing of Stockmayer fluids. In: *Physical Review E* 54 (1996), August, No. 2, p. 1687–1697
- [GDN95] GRIEBEL, M.; DORNSEIFER, T.; NEUNHOEFFER, T.: *Numerische Simulation in der Strömungsmechanik: Eine praxisorientierte Einführung*. Braunschweig, Wiesbaden: Vieweg Verlag, 1995 (Lehrbuch Scientific Computing). – 219 p. – ISBN 3–528–06761–6
- [GDS09] GAUGER, E. M.; DOWNTON, M. T.; STARK, H.: Fluid transport at low Reynolds number with magnetically actuated artificial cilia. In: *European Physical Journal E* 28 (2009), February, No. 2, p. 231–242
- [Gen69] GENNES, P.-G. de: Conjectures sur l'état smectique. In: *Journal de Physique Colloques* 30 (1969), November, No. C4, p. 65–71
- [Gen71] GENNES, P.-G. de: Short range order effects in the isotropic phase of nematics and cholesterics. In: *Molecular Crystals and Liquid Crystals* 12 (1971), February, No. 3, p. 193–214

- [Gen73] GENNES, P.-G. de: Some remarks on polymorphism of smectics. In: *Molecular Crystals and Liquid Crystals* 21 (1973), January, No. 1-2, p. 49–76
- [GG84] GRAY, C. G.; GUBBINS, K. E.: *International Series of Monographs on Chemistry* 9. Vol. 1: *Theory of Molecular Fluids: Fundamentals*. 1. Ed. Oxford: Oxford University Press, 1984. – 626 p. – ISBN 0–198–55602–0
- [GH71a] GRAHAM, R.; HAKEN, H.: Fluctuations and stability of stationary non-equilibrium systems in detailed balance. In: *Zeitschrift für Physik* 245 (1971), April, No. 2, p. 141–153
- [GH71b] GRAHAM, R.; HAKEN, H.: Generalized thermodynamic potential for Markoff systems in detailed balance and far from thermal equilibrium. In: *Zeitschrift für Physik* 243 (1971), June, No. 3, p. 289–302
- [GKC04] GUHA, P.; KAR, S.; CHAUDHURI, S.: Direct synthesis of single crystalline In_2O_3 nanopyrramids and nanocolumns and their photoluminescence properties. In: *Applied Physics Letters* 85 (2004), October, No. 17, p. 3851
- [GL50] GINZBURG, V. L.; LANDAU, L. D.: On the theory of superconductivity. In: *Zhurnal Éksperimental'noi i Teoreticheskoi Fiziki* 20 (1950), p. 1064–1082
- [GL98] GRAF, H.; LÖWEN, H.: Density jumps across phase transitions in soft-matter systems. In: *Physical Review E* 57 (1998), May, No. 5, p. 5744–5753
- [GL99] GRAF, H.; LÖWEN, H.: Density functional theory for hard spherocylinders: phase transitions in the bulk and in the presence of external fields. In: *Journal of Physics: Condensed Matter* 11 (1999), February, No. 6, p. 1435–1452
- [GM84] GROOT, S. R. d.; MAZUR, P.: *Non-Equilibrium Thermodynamics*. 1. Ed. New York: Dover Publications, 1984 (Dover Books on Physics and Chemistry). – 544 p. – ISBN 0–486–64741–2
- [GP95] GENNES, P.-G. de; PROST, J.: *International Series of Monographs on Physics*. Vol. 83: *The Physics of Liquid Crystals*. 2. Ed. Oxford: Oxford University Press, 1995. – 597 p. – ISBN 0–198–51785–8
- [Gra74] GRAHAM, R.: Hydrodynamic fluctuations near the convection instability. In: *Physical Review A* 10 (1974), November, No. 5, p. 1762–1784
- [Gra77a] GRAHAM, R.: Covariant formulation of non-equilibrium statistical thermodynamics. In: *Zeitschrift für Physik B: Condensed Matter* 26 (1977), December, No. 4, p. 397–405

- [Gra77b] GRAHAM, R.: Path integral formulation of general diffusion processes. In: *Zeitschrift für Physik B: Condensed Matter* 26 (1977), September, No. 3, p. 281–290
- [Gra78] GRAHAM, R.: Path-integral methods in Nonequilibrium Thermodynamics and Statistics. In: GARRIDO, L. (ed.); SEGLAR, P. (ed.); SHEPHERD, P. J. (ed.): *Stochastic Processes in Nonequilibrium Systems*. Vol. 84. 1. Ed. Berlin: Springer, June 1978. – ISBN 3–540–08942–X, chapter 4, p. 82–138
- [Gri86] GRINFELD, M. A.: Instability of the interface between a nonhydrostatically stressed elastic body and a melt. In: *Akademiia Nauk SSSR Doklady* 290 (1986), January, No. 6, p. 1358–1363
- [Gro88] GROSSMANN, S.: *Funktionalanalysis im Hinblick auf Anwendungen in der Physik*. 4. Ed. Wiesbaden: AULA-Verlag, 1988 (Studien-Text). – 317 p. – ISBN 3–891–04479–8
- [GS06] GAUGER, E.; STARK, H.: Numerical study of a microscopic artificial swimmer. In: *Physical Review E* 74 (2006), August, No. 2, p. 021907
- [Gub80] GUBBINS, K. E.: Structure of non-uniform molecular fluids: integrodifferential equations for the density-orientation profile. In: *Chemical Physics Letters* 76 (1980), December, No. 2, p. 329–332
- [HAN⁺06] HAN, Y.; ALSAYED, A. M.; NOBILI, M.; ZHANG, J.; LUBENSKY, T. C.; YODH, A. G.: Brownian motion of an ellipsoid. In: *Science* 314 (2006), October, No. 5799, p. 626–630
- [Has07] HASSLER, U.: *Statistik und ihre Anwendungen*. Vol. 16: *Stochastische Integration und Zeitreihenmodellierung: Eine Einführung mit Anwendungen aus Finanzierung und Ökonometrie*. 1. Ed. Berlin: Springer, 2007. – 325 p. – ISBN 3–540–73567–4
- [HB91] HAPPEL, J.; BRENNER, H.: *Mechanics of Fluids and Transport Processes*. Vol. 1: *Low Reynolds Number Hydrodynamics: With Special Applications to Particulate Media*. 2. Ed. Dordrecht: Kluwer Academic Publishers, 1991. – 553 p. – ISBN 9–024–72877–0
- [HBL10] HÄRTEL, A.; BLAAK, R.; LÖWEN, H.: Towing, breathing, splitting, and overtaking in driven colloidal liquid crystals. In: *Physical Review E* 81 (2010), May, No. 5, p. 051703
- [HBRZ10] HOLZER, L.; BAMBERT, J.; RZEHAK, R.; ZIMMERMANN, W.: Dynamics of a trapped Brownian particle in shear flows. In: *Physical Review E* 81 (2010), April, No. 4, p. 041124

- [HCLG06] HONG, L.; CACCIUTO, A.; LUIJTEN, E.; GRANICK, S.: Clusters of charged Janus spheres. In: *Nano Letters* 6 (2006), November, No. 11, p. 2510–2514
- [HCS⁺08] HO, C.; CHEN, W.; SHIE, T.; LIN, J.; KUO, C.: Novel fabrication of Janus particles from the surfaces of electrospun polymer fibers. In: *Langmuir* 24 (2008), May, No. 11, p. 5663–5666
- [HE08] HUANG, Z.; ELDER, K. R.: Mesoscopic and microscopic modeling of island formation in strained film epitaxy. In: *Physical Review Letters* 101 (2008), October, No. 15, p. 158701
- [HEEW11] HUNTER, G. L.; EDMOND, K. V.; ELSESSER, M. T.; WEEKS, E. R.: Tracking rotational diffusion of colloidal clusters. In: *Optics Express* 19 (2011), August, No. 18, p. 17189–17202
- [HEK⁺09] HAJI-AKBARI, A.; ENGEL, M.; KEYS, A. S.; ZHENG, X.; PETSCHKE, R. G.; PALFFY-MUHORAY, P.; GLOTZER, S. C.: Disordered, quasicrystalline and crystalline phases of densely packed tetrahedra. In: *Nature* 462 (2009), December, No. 7274, p. 773–777
- [Hel05] HELSETH, L. E.: Self-assembly of colloidal pyramids in magnetic fields. In: *Langmuir* 21 (2005), August, No. 16, p. 7276–7279
- [HJL⁺09] HOSEIN, I. D.; JOHN, B. S.; LEE, S. H.; ESCOBEDO, F. A.; LIDDELL, C. M.: Rotator and crystalline films via self-assembly of short-bond-length colloidal dimers. In: *Journal of Materials Chemistry* 19 (2009), January, No. 3, p. 344–349
- [HJR⁺07] HOWSE, J. R.; JONES, R. A. L.; RYAN, A. J.; GOUGH, T.; VAFABAKHSH, R.; GOLESTANIAN, R.: Self-motile colloidal particles: from directed propulsion to random walk. In: *Physical Review Letters* 99 (2007), July, No. 4, p. 048102
- [HK64] HOHENBERG, P.; KOHN, W.: Inhomogeneous electron gas. In: *Physical Review* 136 (1964), November, No. 3B, p. 864–871
- [HLW06] HAIRER, E.; LUBICH, C.; WANNER, G.: *Geometric Numerical Integration: Structure-Preserving Algorithms for Ordinary Differential Equations*. Berlin: Springer, 2006 (Computational Mathematics). – 644 p. – ISBN 3–540–30663–3
- [HM06] HANSEN, J.-P.; McDONALD, I. R.: *Theory of Simple Liquids*. 3. Ed. Amsterdam: Elsevier Academic Press, 2006. – 416 p. – ISBN 0–12–370535–5

- [HM09] HANSEN-GOOS, H.; MECKE, K.: Fundamental measure theory for inhomogeneous fluids of nonspherical hard particles. In: *Physical Review Letters* 102 (2009), January, No. 1, p. 018302
- [HM10] HANSEN-GOOS, H.; MECKE, K.: Tensorial density functional theory for non-spherical hard-body fluids. In: *Journal of Physics: Condensed Matter* 22 (2010), August, No. 36, p. 364107
- [HØUZ09] HOLDEN, H.; ØKSENDAL, B. K.; UBOE, J.; ZHANG, T.: *Stochastic Partial Differential Equations: A Modeling, White Noise Approach*. 2. Ed. Berlin: Springer, 2009 (Universitext). – 305 p. – ISBN 978–0–387–89487–4
- [HRRS04] HATWALNE, Y.; RAMASWAMY, S.; RAO, M.; SIMHA, R. A.: Rheology of active-particle suspensions. In: *Physical Review Letters* 92 (2004), March, No. 11, p. 118101
- [HTL09] HAGEN, B. ten; TEEFFELEN, S. van; LÖWEN, H.: Non-Gaussian behaviour of a self-propelled particle on a substrate. In: *Condensed Matter Physics* 12 (2009), June, No. 4, p. 725–738
- [HTL11] HAGEN, B. ten; TEEFFELEN, S. van; LÖWEN, H.: Brownian motion of a self-propelled particle. In: *Journal of Physics: Condensed Matter* 23 (2011), April, No. 19, p. 194119
- [HW04] HINRICHSSEN, H.; WOLF, D. E.: *Nonlinear & Complex Systems*. Vol. 7: *The Physics of Granular Media*. 1. Ed. Weinheim: John Wiley & Sons, 2004. – 500 p. – ISBN 3–527–40373–6
- [HWHW09] HOFFMANN, M.; WAGNER, C. S.; HARNAU, L.; WITTEMANN, A.: 3D Brownian diffusion of submicron-sized particle clusters. In: *Nano* 3 (2009), September, No. 10, p. 3326–3334
- [HWL11] HAGEN, B. ten; WITTKOWSKI, R.; LÖWEN, H.: Brownian dynamics of a self-propelled particle in shear flow. In: *Physical Review E* 84 (2011), September, No. 3, p. 031105
- [IKK⁺03] IVLEV, A. V.; KHRAPAK, A. G.; KHRAPAK, S. A.; ANNARATONE, B. M.; MORFILL, G.; YOSHINO, K.: Rodlike particles in gas discharge plasmas: theoretical model. In: *Physical Review E* 68 (2003), August, No. 2, p. 026403
- [JA10] JAATINEN, A.; ALA-NISSILA, T.: Extended phase diagram of the three-dimensional phase field crystal model. In: *Journal of Physics: Condensed Matter* 22 (2010), May, No. 20, p. 205402

- [JAEAN09] JAATINEN, A.; ACHIM, C. V.; ELDER, K. R.; ALA-NISSILA, T.: Thermodynamics of bcc metals in phase-field-crystal models. In: *Physical Review E* 80 (2009), September, No. 3, p. 031602
- [Jef22] JEFFERY, G. B.: The motion of ellipsoidal particles immersed in a viscous fluid. In: *Proceedings of the Royal Society of London. Series A, Containing Papers of a Mathematical and Physical Character* 102 (1922), November, No. 715, p. 161–179
- [JIC⁺07] JEONG, U.; IM, S. H.; CAMARGO, P. H. C.; KIM, J. H.; XIA, Y.: Microscale fish bowls: a new class of latex particles with hollow interiors and engineered porous structures in their surfaces. In: *Langmuir* 23 (2007), October, No. 22, p. 10968–10975
- [JKB05] JOHNSON, P. M.; KATS, C. M. v.; BLAADEREN, A. van: Synthesis of colloidal silica dumbbells. In: *Langmuir* 21 (2005), October, No. 24, p. 11510–11517
- [JRDG03] JASZCZAK, J. A.; ROBINSON, G. W.; DIMOVSKI, S.; GOGOTSI, Y.: Naturally occurring graphite cones. In: *Carbon* 41 (2003), August, No. 11, p. 2085–2092
- [JV72] JAHN, T. L.; VOTTA, J. J.: Locomotion of protozoa. In: *Annual Review of Fluid Mechanics* 4 (1972), January, No. 1, p. 93–116
- [Kal10] KALIKMANOV, V. I.: *Theoretical and Mathematical Physics. Vol. 46: Statistical Physics of Fluids: Basic Concepts and Applications.* 2. Ed. Berlin: Springer, 2010. – 260 p. – ISBN 3–642–07511–8
- [KB04] KIM, M. J.; BREUER, K. S.: Enhanced diffusion due to motile bacteria. In: *Physics of Fluids* 16 (2004), September, No. 9, p. L78–L81
- [KBEP06] KEGEL, W. K.; BREED, D.; ELSESSER, M.; PINE, D. J.: Formation of anisotropic polymer colloids by disparate relaxation times. In: *Langmuir* 22 (2006), July, No. 17, p. 7135–7136
- [KBH10] KONDRAT, S.; BIER, M.; HARNAU, L.: Phase behavior of ionic liquid crystals. In: *Journal of Chemical Physics* 132 (2010), May, No. 18, p. 184901
- [KDT⁺97] KRISHNAN, A.; DUJARDIN, E.; TREACY, M. M. J.; HUGDAHL, J.; LYNUM, S.; EBBESEN, T. W.: Graphitic cones and the nucleation of curved carbon surfaces. In: *Nature* 388 (1997), July, No. 6641, p. 451–454
- [Kha89] KHALATNIKOV, I. M.: *Frontiers in Physics. Vol. 23: An Introduction to the Theory of Superfluidity.* 2. Ed. Redwood City: Addison Wesley, 1989. – 206 p. – ISBN 0–201–09505–X

- [Kit95] KITTEL, C.: *Introduction to Solid State Physics*. Vol. 1. 7. Ed. New York: John Wiley & Sons, 1995. – 688 p. – ISBN 0-471-11181-3
- [KJM04] KIOY, D.; JANNIN, J.; MATTOCK, N.: Focus: Human African trypanosomiasis. In: *Nature Reviews Microbiology* 2 (2004), March, No. 3, p. 186–187
- [Kle09] KLEINERT, H.: *Path Integrals in Quantum Mechanics, Statistics, Polymer Physics, and Financial Markets*. 5. Ed. Singapore: World Scientific Publishing, 2009. – 1579 p. – ISBN 9-814-27356-2
- [KLK96] KIRCHHOFF, Th.; LÖWEN, H.; KLEIN, R.: Dynamical correlations in suspensions of charged rodlike macromolecules. In: *Physical Review E* 53 (1996), May, No. 5, p. 5011–5022
- [KP06] KLOEDEN, P. E.; PLATEN, E.: *Applications of Mathematics: Stochastic Modelling and Applied Probability*. Vol. 23: *Numerical Solution of Stochastic Differential Equations*. 1. Ed. Berlin: Springer, 2006. – 636 p. – ISBN 3-540-54062-8
- [Krö97] KRÖNER, D.: *Numerical Schemes for Conservation Laws*. Chichester & Stuttgart: Wiley & Teubner, 1997. – 508 p. – ISBN 3-519-02720-8
- [KS65] KOHN, W.; SHAM, L. J.: Self-consistent equations including exchange and correlation effects. In: *Physical Review* 140 (1965), November, No. 4A, p. 1133–1138
- [KS11] KOCH, D. L.; SUBRAMANIAN, G.: Collective hydrodynamics of swimming microorganisms: living fluids. In: *Annual Review of Fluid Mechanics* 43 (2011), January, No. 1, p. 637–659
- [KVK⁺09] KRAFT, D. J.; VLUG, W. S.; KATS, C. M. v.; BLAADEREN, A. van; IMHOF, A.; KEGEL, W. K.: Self-assembly of colloids with liquid protrusions. In: *Journal of the American Chemical Society* 131 (2009), January, No. 3, p. 1182–1186
- [Lam93] LAMB, S. H.: *Cambridge Mathematical Library*. Vol. 6: *Hydrodynamics*. 6. Ed. New York: Cambridge University Press, 1993. – 768 p. – ISBN 978-0-521-45868-9
- [Lan08] LANGEVIN, P.: Sur la théorie du mouvement brownien. In: *Comptes Rendus de l'Académie des Sciences* 146 (1908), January, No. 1, p. 530–533
- [Lan86] LANGER, J. S.: Models of Pattern Formation in First-Order Phase Transitions. In: GRINSTEIN, G. (ed.); MAZENKO, G. (ed.): *Directions in Condensed Matter Physics*. Vol. 1. Singapore: World Scientific Publishing, 1986. – ISBN 9-971-97842-3, p. 165–186

- [LBLO01] LANÇON, P.; BATROUNI, G.; LOBRY, L.; OSTROWSKY, N.: Drift without flux: Brownian walker with a space-dependent diffusion coefficient. In: *Europhysics Letters* 54 (2001), April, No. 1, p. 28–34
- [LBLO02] LANÇON, P.; BATROUNI, G.; LOBRY, L.; OSTROWSKY, N.: Brownian walker in a confined geometry leading to a space-dependent diffusion coefficient. In: *Physica A: Statistical Mechanics and its Applications* 304 (2002), February, No. 1-2, p. 65–76
- [LBW89] LÖWEN, H.; BEIER, T.; WAGNER, H.: Van der Waals theory of surface melting. In: *Europhysics Letters* 9 (1989), August, No. 8, p. 791–796
- [LBW90] LÖWEN, H.; BEIER, T.; WAGNER, H.: Multiple order parameter theory of surface melting: a van der Waals approach. In: *Zeitschrift für Physik B: Condensed Matter* 79 (1990), February, No. 1, p. 109–118
- [Les66] LESLIE, F. M.: Some constitutive equations for anisotropic fluids. In: *The Quarterly Journal of Mechanics and Applied Mathematics* 19 (1966), April, No. 3, p. 357–370
- [LGG⁺09] LEPTOS, K. C.; GUASTO, J. S.; GOLLUB, J. P.; PESCI, A. I.; GOLDSTEIN, R. E.: Dynamics of enhanced tracer diffusion in suspensions of swimming eukaryotic microorganisms. In: *Physical Review Letters* 103 (2009), November, No. 19, p. 198103
- [LHMS10] LAPOINTE, C. P.; HOPKINS, S.; MASON, T. G.; SMALYUKH, I. I.: Electrically driven multiaxis rotational dynamics of colloidal platelets in nematic liquid crystals. In: *Physical Review Letters* 105 (2010), October, No. 17, p. 178301
- [LL91a] LANDAU, L. D.; LIFSCHITZ, E. M.: *Lehrbuch der theoretischen Physik*. Vol. 7: *Elastizitätstheorie*. 7. Ed. Frankfurt am Main: Verlag Harri Deutsch, 1991. – 223 p. – ISBN 3–817–11332–3
- [LL91b] LANDAU, L. D.; LIFSCHITZ, E. M.: *Lehrbuch der theoretischen Physik*. Vol. 6: *Hydrodynamik*. 5. Ed. Berlin: Akademie Verlag, 1991. – 683 p. – ISBN 3–055–00070–6
- [LL92] LANDAU, L. D.; LIFSCHITZ, E. M.: *Lehrbuch der theoretischen Physik*. Vol. 9: *Statistische Physik II*. 4. Ed. Frankfurt am Main: Verlag Harri Deutsch, 1992. – 404 p. – ISBN 3–817–11334–X
- [LL07] LAU, A. W. C.; LUBENSKY, T. C.: State-dependent diffusion: thermodynamic consistency and its path integral formulation. In: *Physical Review E* 76 (2007), July, No. 1, p. 011123

- [LL08] LANDAU, L. D.; LIFSCHITZ, E. M.: *Lehrbuch der theoretischen Physik*. Vol. 5: *Statistische Physik I*. 8. Ed. Frankfurt am Main: Verlag Harri Deutsch, 2008. – 517 p. – ISBN 978–3–817–11330–9
- [LLRC10] LÓPEZ, L. G.; LINARES, D. H.; RAMIREZ-PASTOR, A. J.; CANNAS, S. A.: Phase diagram of self-assembled rigid rods on two-dimensional lattices: theory and Monte Carlo simulations. In: *Journal of Chemical Physics* 133 (2010), September, No. 13, p. 134706
- [LLW00] LOMBA, E.; LADO, F.; WEIS, J. J.: Structure and thermodynamics of a ferrofluid monolayer. In: *Physical Review E* 61 (2000), April, No. 4, p. 3838–3849
- [LM97] LIU, C.; MUTHUKUMAR, M.: Annihilation kinetics of liquid crystal defects. In: *Journal of Chemical Physics* 106 (1997), May, No. 18, p. 7822–7828
- [LMB76] LOVETT, R.; MOU, C. Y.; BUFF, F. P.: The structure of the liquid-vapor interface. In: *Journal of Chemical Physics* 65 (1976), July, No. 2, p. 570–572
- [Löw94a] LÖWEN, H.: Brownian dynamics of hard spherocylinders. In: *Physical Review E* 50 (1994), August, No. 2, p. 1232–1242
- [Löw94b] LÖWEN, H.: Charged rodlike colloidal suspensions: an ab initio approach. In: *Journal of Chemical Physics* 100 (1994), May, p. 6738–6749
- [Löw94c] LÖWEN, H.: Interaction between charged rodlike colloidal particles. In: *Physical Review Letters* 72 (1994), January, No. 3, p. 424–427
- [Löw94d] LÖWEN, H.: Melting, freezing and colloidal suspensions. In: *Physics Reports* 237 (1994), February, No. 5, p. 249–324
- [Löw02] LÖWEN, H.: Density functional theory of inhomogeneous classical fluids: recent developments and new perspectives. In: *Journal of Physics: Condensed Matter* 14 (2002), November, No. 46, p. 11897–11905
- [Löw10a] LÖWEN, H.: A phase-field-crystal model for liquid crystals. In: *Journal of Physics: Condensed Matter* 22 (2010), March, No. 36, p. 364105
- [Löw10b] *Chapter 2: Applications of Density Functional Theory in Soft Condensed Matter*. In: LÖWEN, H.: *Series in Soft Condensed Matter*. Vol. 3: *Understanding Soft Condensed Matter via Modeling and Computation*. Singapore: World Scientific Publishing, 2010. – ISBN 9–814–29558–2, p. 9–45

- [LP09] LAUGA, E.; POWERS, T. R.: The hydrodynamics of swimming microorganisms. In: *Reports on Progress in Physics* 9 (2009), September, No. 72, p. 096601
- [LPB96] LAMMERT, P. E.; PROST, J.; BRUINSMA, R.: Ion drive for vesicles and cells. In: *Journal of Theoretical Biology* 178 (1996), February, No. 4, p. 387–391
- [LS03] LIDDELL, C. M.; SUMMERS, C. J.: Monodispersed ZnS dimers, trimers, and tetramers for lower symmetry photonic crystal lattices. In: *Advanced Materials* 15 (2003), October, No. 20, p. 1715–1719
- [LS05] LAUGA, E.; SQUIRES, T. M.: Brownian motion near a partial-slip boundary: a local probe of the no-slip condition. In: *Physics of Fluids* 17 (2005), October, No. 10, p. 103102
- [Lut06] LUTSKO, J. F.: First principles derivation of Ginzburg-Landau free energy models for crystalline systems. In: *Physica A* 366 (2006), July, No. 1, p. 229–242
- [Mar55] MARUYAMA, G.: Continuous Markov processes and stochastic equations. In: *Rendiconti del Circolo Matematico di Palermo* 4 (1955), January, No. 1, p. 48–90
- [MAS01] McDONALD, A. J.; ALLEN, M. P.; SCHMID, F.: Surface tension of the isotropic-nematic interface. In: *Physical Review E* 63 (2001), January, No. 1, p. 010701
- [MC99] MARTÍNEZ-RATÓN, Y.; CUESTA, J. A.: Fundamental measure theory for mixtures of parallel hard cubes: II. Phase behavior of the one-component fluid and of the binary mixture. In: *Journal of Chemical Physics* 111 (1999), July, No. 1, p. 317–327
- [MC09] MILLER, W. L.; CACCIUTO, A.: Hierarchical self-assembly of asymmetric amphiphatic spherical colloidal particles. In: *Physical Review E* 80 (2009), August, No. 2, p. 021404
- [McM71] McMILLAN, W. L.: Simple molecular model for the smectic A phase of liquid crystals. In: *Physical Review A* 4 (1971), September, No. 3, p. 1238–1246
- [MD04] MAKINO, M.; DOI, M.: Brownian motion of a particle of general shape in Newtonian fluid. In: *Journal of the Physical Society of Japan* 73 (2004), October, No. 10, p. 2739

- [MD08] MARECHAL, M.; DIJKSTRA, M.: Stability of orientationally disordered crystal structures of colloidal hard dumbbells. In: *Physical Review E* 77 (2008), June, No. 6, p. 061405
- [MD10] MARECHAL, M.; DIJKSTRA, M.: Phase behavior and structure of colloidal bowl-shaped particles: simulations. In: *Physical Review E* 82 (2010), September, No. 3, p. 031405
- [MDL⁺95] MOURCHID, A.; DELVILLE, A.; LAMBARD, J.; LÉCOLIER, E.; LEVITZ, P.: Phase diagram of colloidal dispersions of anisotropic charged particles: equilibrium properties, structure, and rheology of laponite suspensions. In: *Langmuir* 11 (1995), June, No. 6, p. 1942–1950
- [MEP03] MANOHARAN, V. N.; ELSESSER, M. T.; PINE, D. J.: Dense packing and symmetry in small clusters of microspheres. In: *Science* 301 (2003), July, No. 5632, p. 483–487
- [Mer79] MERMIN, N. D.: The topological theory of defects in ordered media. In: *Reviews of Modern Physics* 51 (1979), July, No. 3, p. 591–648
- [MGV09] MCKENNA, I. M.; GURURAJAN, M. P.; VOORHEES, P. W.: Phase field modeling of grain growth: effect of boundary thickness, triple junctions, misorientation, and anisotropy. In: *Journal of Materials Science* 44 (2009), January, p. 2206–2217
- [Mil75] MILSTEIN, G. N.: Approximate integration of stochastic differential equations. In: *Theory of Probability and Its Applications* 19 (1975), July, No. 3, p. 557–562
- [MK06] MITCHELL, J. G.; KOGURE, K.: Bacterial motility: links to the environment and a driving force for microbial physics. In: *FEMS Microbiology Ecology* 55 (2006), January, No. 1, p. 3–16
- [MKD⁺10] MARECHAL, M.; KORTSCHOT, R. J.; DEMIRÖRS, A. F.; IMHOF, A.; DIJKSTRA, M.: Phase behavior and structure of a new colloidal model system of bowl-shaped particles. In: *Nano Letters* 10 (2010), April, No. 5, p. 1907–1911
- [MKP08] MELLENTHIN, J.; KARMA, A.; PLAPP, M.: Phase-field crystal study of grain-boundary premelting. In: *Physical Review B* 78 (2008), November, No. 18, p. 184110
- [MM09] MARCONI, U. M. B.; MELCHIONNA, S.: Kinetic theory of correlated fluids: from dynamic density functional to Lattice Boltzmann methods. In: *Journal of Chemical Physics* 131 (2009), July, No. 1, p. 014105

- [MM10] MARCONI, U. M. B.; MELCHIONNA, S.: Dynamic density functional theory versus kinetic theory of simple fluids. In: *Journal of Physics: Condensed Matter* 22 (2010), September, No. 36, p. 364110
- [MN98] MATSUMOTO, M.; NISHIMURA, T.: Mersenne twister: a 623-dimensionally equidistributed uniform pseudorandom number generator. In: *ACM Transactions on Modeling and Computer Simulation* 8 (1998), January, No. 1, p. 3–30
- [MPB01] MUKHERJEE, P. K.; PLEINER, H.; BRAND, H. R.: Simple Landau model of the smectic-A-isotropic phase transition. In: *European Physical Journal E* 4 (2001), March, p. 293–297
- [MPB02] MUKHERJEE, P. K.; PLEINER, H.; BRAND, H. R.: Landau model of the smectic C-isotropic phase transition. In: *Journal of Chemical Physics* 117 (2002), October, No. 16, p. 7788–7792
- [MPB05] MUKHERJEE, P. K.; PLEINER, H.; BRAND, H. R.: A phenomenological theory of the isotropic to chiral smectic-C phase transition. In: *European Physical Journal E* 17 (2005), August, No. 4, p. 501–506
- [MPP72] MARTIN, P. C.; PARODI, O.; PERSHAN, P. S.: Unified hydrodynamic theory for crystals, liquid crystals, and normal fluids. In: *Physical Review A* 6 (1972), December, No. 6, p. 2401–2420
- [MPVL10] MOURAD, M. C. D.; PETUKHOV, A. V.; VROEGE, G. J.; LEKKERKERKER, H. N. W.: Lyotropic hexagonal columnar liquid crystals of large colloidal gibbsite platelets. In: *Langmuir* 26 (2010), August, No. 17, p. 14182–14187
- [MRBA96] MIGUEL, E. de; RIO, E. Martín del; BROWN, J. T.; ALLEN, M. P.: Effect of the attractive interactions on the phase behavior of the Gay-Berne liquid crystal model. In: *Journal of Chemical Physics* 105 (1996), September, No. 10, p. 4234–4249
- [MRR07] MUHURI, S.; RAO, M.; RAMASWAMY, S.: Shear-flow induced isotropic-to-nematic transition in a suspension of active filaments. In: *Europhysics Letters* 784 (2007), May, No. 4, p. 48002
- [MS58] MAIER, W.; SAUPE, A.: Eine einfache molekulare Theorie des nematischen kristallinflüssigen Zustandes. In: *Zeitschrift für Naturforschung Teil A* 13 (1958), July, p. 564–566
- [MS59] MAIER, W.; SAUPE, A.: Eine einfache molekularstatistische Theorie der nematischen kristallinflüssigen Phase. Teil I. In: *Zeitschrift für Naturforschung Teil A* 14 (1959), October, p. 882–889

- [MS60] MAIER, W.; SAUPE, A.: Eine einfache molekularstatistische Theorie der nematischen kristallinflüssigen Phase. Teil II. In: *Zeitschrift für Naturforschung Teil A* 15 (1960), April, p. 287–292
- [MT99] MARCONI, U. M. B.; TARAZONA, P.: Dynamic density functional theory of fluids. In: *Journal of Chemical Physics* 110 (1999), April, No. 16, p. 8032–8044
- [MT00] MARCONI, U. M. B.; TARAZONA, P.: Dynamic density functional theory of fluids. In: *Journal of Physics: Condensed Matter* 12 (2000), February, No. 8A, p. 413–418
- [MTCM08] MARCONI, U. M. B.; TARAZONA, P.; CECCONI, F.; MELCHIONNA, S.: Beyond dynamic density functional theory: the role of inertia. In: *Journal of Physics: Condensed Matter* 20 (2008), December, No. 49, p. 494233
- [MZ06] MUCCIOLI, L.; ZANNONI, C.: A deformable Gay Berne model for the simulation of liquid crystals and soft materials. In: *Chemical Physics Letters* 423 (2006), May, p. 1–6
- [NEHK09] NAESS, S. N.; ELGSAETER, A.; HELGESEN, G.; KNUDSEN, K. D.: Carbon nanocones: wall structure and morphology. In: *Science and Technology of Advanced Materials* 10 (2009), December, No. 6, p. 065002
- [NW07] NEWTON, M. C.; WARBURTON, P. A.: ZnO tetrapod nanocrystals. In: *Materials Today* 10 (2007), May, No. 5, p. 50–54
- [Øks03] ØKSENDAL, B. K.: *Stochastic Differential Equations: An Introduction with Applications*. 6. Ed. Berlin: Springer, 2003 (Universitext). – 374 p. – ISBN 978-3-540-04758-2
- [OLW91] OHNESORGE, R.; LÖWEN, H.; WAGNER, H.: Density-functional theory of surface melting. In: *Physical Review A* 43 (1991), March, No. 6, p. 2870–2878
- [Ons49] ONSAGER, L.: The effects of shape on the interaction of colloidal particles. In: *Annals of the New York Academy of Sciences* 51 (1949), May, No. 4, p. 627–659
- [Onu02] ONUKI, A.: *Phase Transition Dynamics*. 1. Ed. Cambridge: Cambridge University Press, 2002. – 726 p. – ISBN 0-521-57293-2
- [OO09] OHTA, T.; OHKUMA, T.: Deformable self-propelled particles. In: *Physical Review Letters* 102 (2009), April, No. 15, p. 154101
- [PB89] PLEINER, H.; BRAND, H. R.: Spontaneous splay phases in polar nematic liquid crystals. In: *Europhysics Letters* 9 (1989), June, No. 3, p. 243–249

- [PB96] PLEINER, H.; BRAND, H. R.: Hydrodynamics and Electrohydrodynamics of Liquid Crystals. In: BUKA, A. (ed.); KRAMER, L. (ed.): *Pattern Formation in Liquid Crystals*. Vol. 9. 1. Ed. New York: Springer, May 1996. – ISBN 0–387–94604–7, chapter 2, p. 15–67
- [PCYB10] PALACCI, J.; COTTIN-BIZONNE, C.; YBERT, C.; BOCQUET, L.: Sedimentation and effective temperature of active colloidal suspensions. In: *Physical Review Letters* 105 (2010), August, No. 8, p. 088304
- [PDB06] PERUANI, F.; DEUTSCH, A.; BÄR, M.: Nonequilibrium clustering of self-propelled rods. In: *Physical Review E* 74 (2006), September, No. 3, p. 030904R
- [PDO09] POPESCU, M. N.; DIETRICH, S.; OSHANIN, G.: Confinement effects on diffusiophoretic self-propellers. In: *Journal of Chemical Physics* 130 (2009), May, No. 19, p. 194702
- [PE10] PROVATAS, N.; ELDER, K.: *Phase-Field Methods in Materials Science and Engineering*. 1. Ed. Weinheim: WILEY-VCH Verlag GmbH & Co. KGaA, 2010. – 312 p. – ISBN 3–527–40747–2
- [PH88] PONIEWIERSKI, A.; HOLYST, R.: Density-functional theory for nematic and smectic-A ordering of hard spherocylinders. In: *Physical Review Letters* 61 (1988), November, No. 21, p. 2461–2464
- [PKO⁺04] PAXTON, W. F.; KISTLER, K. C.; OLMEDA, C. C.; SEN, A.; ST. ANGELO, S. K.; CAO, Y.; MALLOUK, T. E.; LAMMERT, P. E.; CRESPI, V. H.: Catalytic nanomotors: autonomous movement of striped nanorods. In: *Journal of the American Chemical Society* 126 (2004), September, No. 41, p. 13424–13431
- [PLB02] PLEINER, H.; LIU, M.; BRAND, H. R.: Convective nonlinearities for the orientational tensor order parameter in polymeric systems. In: *Rheologica Acta* 41 (2002), May, No. 4, p. 375–382
- [Ple94] *Chapter 20: Hydrodynamik komplexer Fluide*. In: PLEINER, H.: *IFF Spring School Lecture Notes*. Vol. 25: *Komplexe Systeme zwischen Atom und Festkörper: Vorlesungsmanuskripte des 25. IFF-Ferienkurses vom 28. Februar 1994 bis 11. März 1994 im Forschungszentrum Jülich*. 1. Ed. Jülich: Forschungszentrum Jülich, 1994. – ISBN 3–893–36128–6, p. 20.1–20.32
- [Ple97] *Chapter E1: Komplexe Fluide – ein Überblick*. In: PLEINER, H.: *IFF Spring School Lecture Notes*. Vol. 28: *Dynamik und Strukturbildung in kondensierter Materie: Vorlesungsmanuskripte des 28. IFF-Ferienkurses vom 3. März 1997 bis 14. März 1997 im Forschungszentrum Jülich*. 1.

- Ed. Jülich: Forschungszentrum Jülich, 1997. – ISBN 3–893–36204–5, p. E1.1–E1.22
- [PPT⁺09] POL, E. van d.; PETUKHOV, A. V.; THIES-WEESIE, D. M. E.; BYELOV, D. V.; VROEGE, G. J.: Experimental realization of biaxial liquid crystal phases in colloidal dispersions of boardlike particles. In: *Physical Review Letters* 103 (2009), December, No. 25, p. 258301
- [Pro10] PROTTER, P. E.: *Stochastic Modelling and Applied Probability*. Vol. 21: *Stochastic Integration and Differential Equations*. 2. Ed. Berlin: Springer, 2010. – 419 p. – ISBN 978–3–642–05560–7
- [PTVF92] PRESS, W. H.; TEUKOLSKY, S. A.; VETTERLING, W. T.; FLANNERY, B. P.: *Numerical Recipes in C: The Art of Scientific Computing*. 2. Ed. Cambridge: Cambridge University Press, 1992. – 994 p. – ISBN 0–521–43108–5
- [Pur77] PURCELL, E. M.: Life at low Reynolds number. In: *American Journal of Physics* 45 (1977), January, No. 1, p. 3–11
- [QBX⁺07] QIN, L.; BANHOLZER, M. J.; XU, X.; HUANG, L.; MIRKIN, C. A.: Rational design and synthesis of catalytically driven nanorotors. In: *Journal of the American Chemical Society* 129 (2007), November, No. 48, p. 14870–14871
- [QZR⁺08] QUILLIET, C.; ZOLDESI, C.; RIERA, C.; BLAADEREN, A. van; IMHOF, A.: Anisotropic colloids through non-trivial buckling. In: *European Physical Journal E* 27 (2008), September, No. 1, p. 13–20
- [Ram10] RAMASWAMY, S.: The mechanics and statistics of active matter. In: *Annual Review of Condensed Matter Physics* 1 (2010), August, No. 1, p. 323–345
- [Rau10] RAUSCHER, M.: DDFT for Brownian particles and hydrodynamics. In: *Journal of Physics: Condensed Matter* 22 (2010), September, No. 36, p. J4109
- [RBMF95] ROIJ, R. van; BOLHUIS, P.; MULDER, B.; FRENKEL, D.: Transverse interlayer order in lyotropic smectic liquid crystals. In: *Physical Review E* 52 (1995), August, No. 2, p. R1277–R1280
- [RDKP07] RAUSCHER, M.; DOMÍNGUEZ, A.; KRÜGER, M.; PENNA, F.: A dynamic density functional theory for particles in a flowing solvent. In: *Journal of Chemical Physics* 127 (2007), December, No. 24, p. 244906

- [RDP⁺04] ROORDA, S.; DILLEN, T. van; POLMAN, A.; GRAF, C.; BLAADEREN, A. van; KOOI, B. J.: Aligned gold nanorods in silica made by ion irradiation of core-shell colloidal particles. In: *Advanced Materials* 16 (2004), February, No. 3, p. 235–237
- [Rei98] REICHL, L. E.: *A Modern Course in Statistical Physics*. 2. Ed. New York: John Wiley & Sons, 1998. – 842 p. – ISBN 978-0-471-59520-5
- [RELK02] ROTH, R.; EVANS, R.; LANG, A.; KAHL, G.: Fundamental measure theory for hard-sphere mixtures revisited: the White Bear version. In: *Journal of Physics: Condensed Matter* 14 (2002), November, No. 46, p. 12063–12078
- [Ris72] RISKEN, H.: Solutions of the Fokker-Planck equation in detailed balance. In: *Zeitschrift für Physik* 251 (1972), June, No. 3, p. 231–243
- [Ris96] RISKEN, H.: *Springer Series in Synergetics*. Vol. 18: *The Fokker-Planck Equation: Methods of Solution and Applications*. 3. Ed. Berlin: Springer, 1996. – 474 p. – ISBN 3-540-61530-X
- [RJP10] RAFAÏ, S.; JIBUTI, L.; PEYLA, P.: Effective viscosity of microswimmer suspensions. In: *Physical Review Letters* 104 (2010), March, No. 9, p. 098102
- [RL08] REX, M.; LÖWEN, H.: Dynamical density functional theory with hydrodynamic interactions and colloids in unstable traps. In: *Physical Review Letters* 101 (2008), October, No. 14, p. 148302
- [RL09] REX, M.; LÖWEN, H.: Dynamical density functional theory for colloidal dispersions including hydrodynamic interactions. In: *European Physical Journal E* 28 (2009), February, No. 2, p. 139–146
- [RLB95] RENNER, C.; LÖWEN, H.; BARRAT, J.-L.: Orientational glass transition in a rotator model. In: *Physical Review E* 52 (1995), November, No. 5, p. 5091–5099
- [Ros89] ROSENFELD, Y.: Free-energy model for the inhomogeneous hard-sphere fluid mixture and density-functional theory of freezing. In: *Physical Review Letters* 63 (1989), August, No. 9, p. 980–983
- [Ros94] ROSENFELD, Y.: Density functional theory of molecular fluids: free-energy model for the inhomogeneous hard-body fluid. In: *Physical Review E* 50 (1994), November, No. 5, p. R3318–R3321
- [Rot10] ROTH, R.: Fundamental measure theory for hard-sphere mixtures: a review. In: *Journal of Physics: Condensed Matter* 22 (2010), February, No. 6, p. 063102

- [RSLT96] ROSENFELD, Y.; SCHMIDT, M.; LÖWEN, H.; TARAZONA, P.: Dimensional crossover and the freezing transition in density functional theory. In: *Journal of Physics: Condensed Matter* 8 (1996), September, No. 40, p. L577–L581
- [RSLT97] ROSENFELD, Y.; SCHMIDT, M.; LÖWEN, H.; TARAZONA, P.: Fundamental-measure free-energy density functional for hard spheres: dimensional crossover and freezing. In: *Physical Review E* 55 (1997), April, No. 4, p. 4245–4263
- [Ru09] RAVNIK, M.; ŽUMER, S.: Nematic colloids entangled by topological defects. In: *Soft Matter* 5 (2009), January, No. 2, p. 269–274
- [RWL07] REX, M.; WENSINK, H. H.; LÖWEN, H.: Dynamical density functional theory for anisotropic colloidal particles. In: *Physical Review E* 76 (2007), August, No. 2, p. 021403
- [RY79] RAMAKRISHNAN, T. V.; YUSSOUFF, M.: First-principles order-parameter theory of freezing. In: *Physical Review B* 19 (1979), March, No. 5, p. 2775–2794
- [Sat10] SATOH, A.: *Introduction to Practice of Molecular Simulation: Molecular Dynamics, Monte Carlo, Brownian Dynamics, Lattice Boltzmann and Dissipative Particle Dynamics*. 1. Ed. London: Elsevier, 2010 (Elsevier Insights). – 322 p. – ISBN 0–123–85148–3
- [SB97] SAKAGUCHI, H.; BRAND, H. R.: A modulation mediated hexagon-rectangle transition in pattern forming systems. In: *Physics Letters A* 227 (1997), February, No. 3-4, p. 209–215
- [Sch76] SCHUTTE, C. J. H.: *The Theory of Molecular Spectroscopy*. Vol. 1: *The Quantum Mechanics and Group Theory of Vibrating and Rotating Molecules*. 1. Ed. Amsterdam: North-Holland Publishing Company, 1976. – 512 p. – ISBN 0–720–40291–3
- [Sci08] SCIORTINO, F.: Gel-forming patchy colloids and network glass formers: thermodynamic and dynamic analogies. In: *European Physical Journal B* 64 (2008), August, No. 3-4, p. 505–509
- [SE77] SAAM, W. F.; EBNER, C.: Density-functional theory of classical systems. In: *Physical Review A* 15 (1977), June, No. 6, p. 2566–2568
- [SF04] SCHILLING, T.; FRENKEL, D.: Self-poisoning of crystal nuclei in hard-rod liquids. In: *Journal of Physics: Condensed Matter* 16 (2004), May, No. 19, p. 2029

- [SGM08] SEVONKAEV, I.; GOIA, D. V.; MATIJEVIĆ, E.: Formation and structure of cubic particles of sodium magnesium fluoride (neighborite). In: *Journal of Colloid and Interface Science* 317 (2008), January, No. 1, p. 130–136
- [SH77] SWIFT, J.; HOHENBERG, P. C.: Hydrodynamic fluctuations at the convective instability. In: *Physical Review A* 15 (1977), January, No. 1, p. 319–328
- [SHP06] STEFANOVIC, P.; HAATAJA, M.; PROVATAS, N.: Phase-field crystals with elastic interactions. In: *Physical Review Letters* 96 (2006), June, No. 22, p. 225504
- [SHP09] STEFANOVIC, P.; HAATAJA, M.; PROVATAS, N.: Phase field crystal study of deformation and plasticity in nanocrystalline materials. In: *Physical Review E* 80 (2009), October, No. 4, p. 046107
- [SICP10] SACANNA, S.; IRVINE, W. T. M.; CHAIKIN, P. M.; PINE, D. J.: Lock and key colloids. In: *Nature* 464 (2010), March, No. 7288, p. 575–578
- [SIGK99] SUZUKI, T.; IYAMA, T.; GUBBINS, K. E.; KANEKO, K.: Quasi-symmetry structure of CCl_4 molecular assemblies in a graphitic nanopore: a grand canonical Monte Carlo simulation. In: *Langmuir* 15 (1999), August, No. 18, p. 5870–5875
- [Sin91] SINGH, Y.: Density-functional theory of freezing and properties of the ordered phase. In: *Physics Reports* 207 (1991), September, No. 6, p. 351–444
- [SJ01] SCHULZ, H. N.; JØRGENSEN, B. B.: Big bacteria. In: *Annual Review of Microbiology* 55 (2001), October, No. 1, p. 105–137
- [SLW10] SIRCAR, S.; LI, J.; WANG, Q.: Biaxial phases of bent-core liquid crystal polymers in shear flows. In: *Communications in Mathematical Sciences* 8 (2010), September, No. 3, p. 697–720
- [Smo06] SMOLUCHOWSKI, M. von: Zur kinetischen Theorie der Brownschen Molekularbewegung und der Suspensionen. In: *Annalen der Physik* 326 (1906), November, No. 14, p. 756–780
- [Smo16] SMOLUCHOWSKI, M. von: Über Brownsche Molekularbewegung unter Einwirkung äußerer Kräfte und deren Zusammenhang mit der verallgemeinerten Diffusionsgleichung. In: *Annalen der Physik* 353 (1916), January, No. 24, p. 1103–1112
- [Som00] SOMOV, B. V.: *Astrophysics and Space Science Library*. Vol. 251: *Cosmic Plasma Physics*. 1. Ed. Dordrecht: Kluwer Academic Publishers, 2000. – 672 p. – ISBN 0–792–36512–7

- [SS08] SAINTILLAN, D.; SHELLEY, M. J.: Instabilities and pattern formation in active particle suspensions: kinetic theory and continuum simulations. In: *Physical Review Letters* 100 (2008), April, No. 17, p. 178103
- [Sta07] STARK, H.: Immer in Bewegung bleiben: Die sonderbare Welt der kleinen Reynolds-Zahlen. In: *Physik Journal* 6 (2007), November, No. 11, p. 31–37
- [Sta09] STARK, H.: Algentanz im Walzertakt: Zilien von Mikroorganismen erzeugen eine nichtlineare Dynamik in zäher Umgebung. In: *Physik Journal* 8 (2009), July, No. 7, p. 16–19
- [Sta10] STARK, H.: Zähe Schwimmer. In: *Physik Journal* 9 (2010), May, No. 5, p. 16–17
- [SZO⁺10] SOLOMON, M. J.; ZEITOUN, R.; ORTIZ, D.; SUNG, K. E.; DENG, D.; SHAH, A.; BURNS, M. A.; GLOTZER, S. C.; MILLUNCHICK, J. M.: Toward assembly of non-close-packed colloidal structures from anisotropic pentamer particles. In: *Macromolecular Rapid Communications* 31 (2010), January, No. 2, p. 196–201
- [TBVL09] TEEFFELEN, S. van; BACKOFEN, R.; VOIGT, A.; LÖWEN, H.: Derivation of the phase-field-crystal model for colloidal solidification. In: *Physical Review E* 79 (2009), May, No. 5, p. 051404
- [TDY02] TÓTH, G. I.; DENNISTON, C.; YEOMANS, J. M.: Hydrodynamics of topological defects in nematic liquid crystals. In: *Physical Review Letters* 88 (2002), March, No. 10, p. 105504
- [TGPS08] TIerno, P.; GOLESTANIAN, R.; PAGONABARRAGA, I.; SAGUÉS, F.: Magnetically actuated colloidal microswimmers. In: *Journal of Physical Chemistry B* 112 (2008), November, No. 51, p. 16525–16528
- [TGT⁺09] TEGZE, G.; GRÁNÁSY, L.; TÓTH, G. I.; PODMANICZKY, F.; JAATINEN, A.; ALA-NISSILA, T.; PUSZTAI, T.: Diffusion-controlled anisotropic growth of stable and metastable crystal polymorphs in the phase-field crystal model. In: *Physical Review Letters* 103 (2009), July, No. 3, p. 035702
- [Tha08] THAOKAR, R. M.: Brownian motion of a torus. In: *Colloids and Surfaces A: Physicochemical and Engineering Aspects* 317 (2008), March, No. 1-3, p. 650–657
- [THT09] TAVARES, J. M.; HOLDER, B.; TELO DA GAMA, M. M.: Structure and phase diagram of self-assembled rigid rods: equilibrium polydispersity and nematic ordering in two dimensions. In: *Physical Review E* 79 (2009), February, No. 2, p. 021505

- [TL08] TEEFFELEN, S. van; LÖWEN, H.: Dynamics of a Brownian circle swimmer. In: *Physical Review E* 78 (2008), August, No. 2, p. 020101
- [TLHL06] TEEFFELEN, S. van; LIKOS, C. N.; HOFFMANN, N.; LÖWEN, H.: Density functional theory of freezing for soft interactions in two dimensions. In: *Europhysics Letters* 75 (2006), August, No. 4, p. 583–589
- [TP10] TEMLEITNER, L.; PUSZTAI, L.: Local order and orientational correlations in liquid and crystalline phases of carbon tetrabromide from neutron powder diffraction measurements. In: *Physical Review B* 81 (2010), April, No. 13, p. 134101
- [TSPT02] TASINKEVYCH, M.; SILVESTRE, N. M.; PATRÍCIO, P.; TELO DA GAMA, M. M.: Colloidal interactions in two-dimensional nematics. In: *European Physical Journal E* 9 (2002), November, No. 4, p. 341–347
- [TT87] TOLEDANO, J.-C.; TOLEDANO, P.: *World Scientific Lecture Notes in Physics*. Vol. 3: *The Landau Theory of Phase Transitions: Application to Structural, Incommensurate, Magnetic, and Liquid Crystal Systems*. 1. Ed. Singapore: World Scientific Publishing, 1987. – 451 p. – ISBN 9–971–50025–6
- [TTR05] TONER, J.; TU, Y.; RAMASWAMY, S.: Hydrodynamics and phases of flocks. In: *Annals of Physics* 318 (2005), July, No. 1, p. 170–244
- [TYN⁺03] TABE, Y.; YAMAMOTO, T.; NISHIYAMA, I.; YONEYA, M.; YOKOYAMA, H.: Ferroelectric nematic monolayer. In: *Japanese Journal of Applied Physics* 42 (2003), April, No. 4B, p. L406–L409
- [TZL09] TEEFFELEN, S. van; ZIMMERMANN, U.; LÖWEN, H.: Clockwise-directional circle swimmer moves counter-clockwise in Petri dish- and ring-like confinements. In: *Soft Matter* 5 (2009), September, No. 22, p. 4510–4519
- [VBV⁺11] VOLPE, G.; BUTTINONI, I.; VOGT, D.; KÜMMERER, H.; BECHINGER, C.: Microswimmers in patterned environments. In: *Soft Matter* 7 (2011), August, No. 19, p. 8810–8815
- [Vin07] VINK, R. L. C.: Liquid crystals in two dimensions: first-order phase transitions and nonuniversal critical behavior. In: *Physical Review Letters* 98 (2007), May, No. 21, p. 217801
- [VL92] VROEGE, G. J.; LEKKERKERKER, H. N. W.: Phase transitions in lyotropic colloidal and polymer liquid crystals. In: *Reports on Progress in Physics* 55 (1992), August, No. 8, p. 1241–1309

- [VSB99] VERKHOVSKY, A. B.; SVITKINA, T. M.; BORISY, G. G.: Self-polarization and directional motility of cytoplasm. In: *Current Biology* 9 (1999), December, No. 1, p. 11–20
- [WCH01] WHITE, T. O.; CICCOTTI, G.; HANSEN, J.-P.: Brownian dynamics with constraints. In: *Molecular Physics* 99 (2001), December, No. 24, p. 2023–2036
- [WCH09] WU, H.; CHEN, C.; HUANG, M. H.: Seed-mediated synthesis of branched gold nanocrystals derived from the side growth of pentagonal bipyramids and the formation of gold nanostars. In: *Chemistry of Materials* 21 (2009), January, No. 1, p. 110–114
- [WDCK90] WEYERICH, B.; D'AGUANO, B.; CANESSA, E.; KLEIN, R.: Structure and dynamics of suspensions of charged rod-like particles. In: *Faraday Discussions of the Chemical Society* 90 (1990), July, No. 1, p. 245–259
- [We03] WALZ, G.; ET AL.: *Lexikon der Mathematik*. Vol. 1-6. Heidelberg: Spektrum Akademischer Verlag, 2003. – 2674 p. – ISBN 3–827–41159–9
- [Wei02] WEISSTEIN, E. W.: *CRC Concise Encyclopedia of Mathematics*. 2. Ed. Boca Raton, Florida: Chapman & Hall/CRC, 2002. – 3252 p. – ISBN 1–584–88347–2
- [WF03] WALECKA, J. D.; FETTER, A. L.: *Quantum Theory of Many-Particle Systems*. 1. Ed. Mineola: Dover Publications, 2003. – 640 p. – ISBN 0–486–42827–3
- [WJ09] WENSINK, H. H.; JACKSON, G.: Generalized van der Waals theory for the twist elastic modulus and helical pitch of cholesterics. In: *Journal of Chemical Physics* 130 (2009), June, No. 23, p. 234911
- [WL08] WENSINK, H. H.; LÖWEN, H.: Aggregation of self-propelled colloidal rods near confining walls. In: *Physical Review E* 78 (2008), September, No. 3, p. 031409
- [WL11] WITTKOWSKI, R.; LÖWEN, H.: Dynamical density functional theory for colloidal particles with arbitrary shape. In: *Molecular Physics* 109 (2011), December, No. 23-24, p. 2935–2943
- [WL12] WITTKOWSKI, R.; LÖWEN, H.: Self-propelled Brownian spinning top: dynamics of a biaxial swimmer at low Reynolds numbers. In: *Physical Review E* 85 (2012), February, No. 2, p. 021406
- [WLB10] WITTKOWSKI, R.; LÖWEN, H.; BRAND, H. R.: Derivation of a three-dimensional phase-field-crystal model for liquid crystals from density functional theory. In: *Physical Review E* 82 (2010), September, No. 3, p. 031708

- [WLB11a] WITTKOWSKI, R.; LÖWEN, H.; BRAND, H. R.: Microscopic and macroscopic theories for the dynamics of polar liquid crystals. In: *Physical Review E* 84 (2011), October, No. 4, p. 041708
- [WLB11b] WITTKOWSKI, R.; LÖWEN, H.; BRAND, H. R.: Polar liquid crystals in two spatial dimensions: the bridge from microscopic to macroscopic modeling. In: *Physical Review E* 83 (2011), June, No. 6, p. 061706
- [WLP98] WIERENGA, A. M.; LENSTRA, T. A. J.; PHILIPSE, A. P.: Aqueous dispersions of colloidal gibbsite platelets: synthesis, characterisation and intrinsic viscosity measurements. In: *Colloids and Surfaces A: Physicochemical and Engineering Aspects* 134 (1998), March, No. 3, p. 359–371
- [WM08] WALTHER, A.; MÜLLER, A. H. E.: Janus particles. In: *Soft Matter* 4 (2008), April, No. 4, p. 663–668
- [WT07] WATANABE, G.; TABE, Y.: Tilted and non-tilted liquid crystalline Langmuir monolayers: analogy to bulk smectic phases. In: *Journal of the Physical Society of Japan* 76 (2007), September, No. 9, p. 094602
- [WV09] WU, K.; VOORHEES, P. W.: Stress-induced morphological instabilities at the nanoscale examined using the phase field crystal approach. In: *Physical Review B* 80 (2009), September, No. 12, p. 125408
- [WWI⁺02] WATANABE, K.; WAKITA, J.-I.; ITOH, H.; SHIMADA, H.; KUROSU, S.; IKEDA, T.; YAMAZAKI, Y.; MATSUYAMA, T.; MATSUSHITA, M.: Dynamical properties of transient spatio-temporal patterns in bacterial colony of *Proteus mirabilis*. In: *Journal of the Physical Society of Japan* 71 (2002), February, No. 2, p. 650–656
- [YA11] YABUNAKA, S.; ARAKI, T.: Polydomain growth at isotropic-nematic transitions in liquid crystalline polymers. In: *Physical Review E* 83 (2011), June, No. 6, p. 061711
- [YFG76] YANG, A. J. M.; FLEMING, P. D.; GIBBS, J. H.: Molecular theory of surface tension. In: *Journal of Chemical Physics* 64 (1976), May, No. 9, p. 3732–3747
- [YLV09] YU, Y.; LIU, B.; VOIGT, A.: Phase-field modeling of anomalous spiral step growth on Si(001) surface. In: *Physical Review B* 79 (2009), June, No. 23, p. 235317
- [YLW⁺06] YAN, Q.; LIU, F.; WANG, L.; LEE, J. Y.; ZHAO, X. S.: Drilling nanoholes in colloidal spheres by selective etching. In: *Journal of Materials Chemistry* 16 (2006), May, No. 22, p. 2132–2134

- [YW97] YIN, J. S.; WANG, Z. L.: Ordered self-assembling of tetrahedral oxide nanocrystals. In: *Physical Review Letters* 79 (1997), September, No. 13, p. 2570–2573
- [ZBP⁺08] ZERROUKI, D.; BAUDRY, J.; PINE, D.; CHAIKIN, P.; BIBETTE, J.: Chiral colloidal clusters. In: *Nature* 455 (2008), September, No. 7211, p. 380–382
- [ZD06] ZHANG, Z. X.; DUIJNEVELDT, J. S.: Isotropic-nematic phase transition of nonaqueous suspensions of natural clay rods. In: *Journal of Chemical Physics* 124 (2006), April, No. 15, p. 154910
- [ZG04] ZHANG, Z.; GLOTZER, S. C.: Self-assembly of patchy particles. In: *Nano Letters* 4 (2004), July, No. 8, p. 1407–1413
- [ZLX⁺06] ZHOU, G.; LÜ, M.; XIU, Z.; WANG, S.; ZHANG, H.; ZHOU, Y.; WANG, S.: Controlled synthesis of high-quality PbS star-shaped dendrites, multipods, truncated nanocubes, and nanocubes and their shape evolution process. In: *Journal of Physical Chemistry B* 110 (2006), February, No. 13, p. 6543–6548
- [ZUP⁺11] ZABURDAEV, V.; UPPALURI, S.; PFOHL, T.; ENGSTLER, M.; FRIEDRICH, R.; STARK, H.: Langevin dynamics deciphers the motility pattern of swimming parasites. In: *Physical Review Letters* 106 (2011), May, No. 20, p. 208103

Index

A

- approximation
adiabatic 47, 63, 66
constant-mobility 74, 111, 113–115
Fourier 89, 91, 99
local equilibrium 80, 82
one-mode 73, 99, 104, 106
Ramakrishnan-Yussouff . . 61, 71, 89, 93
random-phase 61
virial 61
weighted-density 61
- average
ensemble 58, 87, 178
noise 18, 62, 178

B

- Bose-Einstein condensation 1
Brownian motion 1–127, 133

C

- center of hydrodynamic reaction 17, 22
- characteristic
collision time 80, 180
energy 97, 179
force 29, 179
length 97, 179
mean free path length 80, 179
time 29, 179
- chemical potential . . 54, 59, 62, 84, 119, 177
- Clebsch-Gordan coefficient 108, 175
- CMA *see* approximation, constant-mobility
- colloid *see* see particle, colloidal
- colloidal liquid crystal 1, 7, 53–126
lyotropic 53
thermotropic 53
- continuum hypothesis 80
- Cooper pair 57

- cosmological Kibble mechanism 121
- Couette flow *see* shear flow
- critical
exponent 77, 179
phenomenon 1
- current 84, 85, 112–115, 177
dissipative *see* current, irreversible
irreversible 1, 84, 86, 113, 177
quasi- 84, 85, 112–115, 177
reversible 1, 84, 85, 177

D

- DDFT . . *see* density functional theory, dyn.
- density functional theory . . 4, 53–66, 87–122
dynamical . 3, 5, 39–51, 62–66, 110–115
quantum mechanical 57
static 4, 5, 58–62, 87–109, 125
- DFT *see* density functional theory
- diffusion tensor 17, 44, 46, 48, 49, 176
- drift vector 18, 19, 22, 176
- dynamical DFT *see* DDFT

E

- entropy
current 49
density 55, 83, 86, 177
production 48, 85, 86
- equation
balance 49, 73, 84
conservation 73, 84
continuity 42, 45, 49
DDFT 45–47, 73, 111, 115, 126
Fokker-Planck 3, 13, 14
Langevin . 3, 6, 13–38, 63, 123–129, 133
Smoluchowski 4, 13, 42–45, 64
stochastic differential . . . 6, 24, 133–137
- Eulerian angles 2, 10, 16, 175

expansion
 amplitude 73
 Fourier 92, 94, 105
 functional Taylor 60, 61, 89, 94
 gradient 5, 55, 67–86, 93, 129–132
 Itô-Taylor 135
 Landau 96, 109
 stochastic Taylor 135
 Stratonovich-Taylor 135
 Taylor .. 70, 71, 76, 77, 88, 91, 131, 135

F

fluid
 complex 54, 57
 molecular 1
 Stockmayer 89
 Frank
 constants 108, 117, 118, 179
 free-energy density 108, 117
 function
 dissipation 48, 114, 115, 120, 177
 Onsager-Machlup 49
 functional
 density . *see* functional, grand canonical
 dissipation ... 4, 48–50, 75, 86, 114–115
 generalized thermodynamic .. 77, 79, 83
 grand canonical 55, 59, 181
 Helmholtz free-energy ... 59–74, 87–115
 Ljapunov 49
 Onsager 61

G

generalized hydrodynamics . 80–86, 115–122
 generalized hydrostatics 5, 83, 117–119
 Gibbs relation 84, 120
 Ginzburg-Landau theory ... 75–80, 115–123
 dynamic 79–80, 119
 quantum mechanical 57, 75
 static 76–79, 116–117
 GL theory *see* Ginzburg-Landau theory
 granular material 1

H

Hamiltonian 77, 81, 83
 hierarchy
 BBGKY 46, 65

YBG 46, 66
 hydrodynamic 80
 description 80
 interactions 41, 44, 51, 62
 limit 81
 mode 80
 range 80
 variable 81, 84, 118, 177

I

integral
 functional *see* integral, path
 path 3, 14
 stochastic 134

L

Langmuir monolayer 4
 laning 12, 50, 126
 LE *see* equation, Langevin
 linear irreversible thermodynamics .. 55, 86

M

MD simulation *see* molecular dyn. sim.
 method
 Euler-Maruyama 24, 133, 135
 extrapolation 137
 Milstein 24, 133, 135
 Newton 100
 steepest-descent 99
 stochastic Runge-Kutta . 6, 24, 133–137
 microorganism . 2, 3, 10–12, 15, 37–38, 125
 microswimmer . 3, 8, 10–12, 37–38, 125, 126
 model
 generalized macroscopic 56, 82
 McMillan's 53
 Onsager's 53
 phase field 4, 67–68
 phase field crystal *see* PFC model
 Swift-Hohenberg 69
 Yukawa-segment 106, 121
 molecular dynamics simulation 67, 74

O

Onsager
 model *see* model, Onsager's
 principle 17, 55, 85

reciprocity relation 85
operator
angular derivation 16, 178
angular momentum 16, 178
projection 66, 110, 112
rotational gradient 16, 178
Smoluchowski 45, 64, 178
trace 107, 178
translational-angular derivation 18, 178
translational derivation . *see* op., tr. gr.
translational gradient 16, 178

P

particle
active 2, 7, 10–51, 122–127
anisotropic 1–31, 37–127
apolar 4, 8, 53, 97–109
biaxial 2, 7–86, 123–127
colloidal 1–127
isotropic 2, 8, 32–36
Janus 8, 10, 12, 90
orthotropic 3, 22–24, 29–31, 48, 123
passive 2, 7–10, 123, 124
polar 4, 8, 53, 90–97, 110–115, 122
self-propelled *see* particle, active
uniaxial 2, 4, 8, 48, 87–122, 124, 125
PFC model . . . *see* phase field crystal model
PF model *see* phase field model
phase field crystal model 67–74, 87–122
dynamic 73–74, 110–115
static 68–73, 87–109
traditional 70–72, 74, 93, 96, 108, 109
plasma
complex *see* plasma, dusty
cosmic 1
dusty 1, 121
potential 20–23, 40–47, 58–66, 72, 90, 177

R

Rayleigh-Bénard convection 69
Riemannian manifold 127

S

Schur complement 45
SDE . . . *see* equation, stochastic differential
self-organization 1, 12, 50

shear flow 3, 32–36, 124
SH model *see* model, Swift-Hohenberg
spherical harmonic 108, 177
stochastic calculus 133
Itô 18, 24, 133
Klimontovich 18, 133
Stratonovich 18, 133, 134
superconductivity 75
superfluidity 1
symbol
Kronecker 78, 181
Levy-Civita 78, 181

T

tensor
coupling 17, 22, 47, 176
damping *see* diffusion tensor
diffusion *see* diffusion tensor
friction 44, 176
inverse friction *see* diffusion tensor
rotation 17, 22, 176
translation 17, 22, 176
theory
Bardeen-Cooper-Schrieffer 57
BCS . *see* theory, Bardeen-Cooper-Schr.
density functional *see* DFT
elasticity 82
Ericksen-Leslie 53
fundamental measure 61, 88
Ginzburg-Landau *see* GL theory
Landau 75, 76
Landau-de Gennes 53, 105
linear-response 62, 63
Maier-Saupe 53
mean-field 4, 5, 53–86, 125
thermodynamic
conjugate 49, 83, 85, 119, 180
force 85, 86, 180
topological
defect 5, 103, 121, 125, 126
winding number 103, 125, 179
transformation
Fourier 71, 131, 132
Legendre 59, 84
turbulence 12, 50, 126

V

variable

hydrodynamic .. *see* hydrodyn. variable

macroscopic 82, 84, 118

non-hydrodynamic 82

symmetry 81
vector, drift *see* drift vector**W**

Wiener process 134

List of symbols

Coefficients:

$\alpha_n, \alpha_n(\dots)$	expansion coefficients
$B_T^{\parallel}, B_T^{\perp}$	translational drift coefficients
B_R	rotational drift coefficient
$C(l_1, l_2, l, m_1, m_2, m)$	Clebsch-Gordan coefficient
D_1, D_2, D_3	translational diffusion coefficients of an arbitrary particle
$D_C^{\parallel}, D_C^{\perp}$	coupling coefficients of an arbitrary particle
D_T	translational diffusion coefficient of an isotropic particle
D_R	rotational diffusion coefficient of a uniaxial particle
ξ	friction coefficient

Coordinates and velocities:

x_1, x_2, x_3	Cartesian coordinates
$\hat{e}_1, \hat{e}_2, \hat{e}_3$	Cartesian unit vectors
\vec{r}	position vector
$\vec{r}^N = (\vec{r}_1, \dots, \vec{r}_N)$	N -particle position vector
\hat{u}	normalized orientation vector
\hat{u}_{\parallel}	parallel orientation vector
\hat{u}_{\perp}	perpendicular orientation vector
φ	polar angle in polar coordinates or auxiliary angle
ϕ	azimuthal angle in spherical coordinates
θ	polar angle in spherical coordinates
χ	third Eulerian angle
$\vec{\omega} = (\phi, \theta, \chi)$	Eulerian angles
$\vec{\omega}^N = (\vec{\omega}_1, \dots, \vec{\omega}_N)$	N -particle Eulerian orientation vector

ω	angular frequency
$\vec{\omega}$	angular velocity
$\vec{\omega}^N = (\vec{\omega}_1, \dots, \vec{\omega}_N)$	N -particle angular velocity vector
t	time
$\vec{\mathfrak{r}} = (\vec{r}, \vec{\omega})$	position-orientation vector
$\vec{\mathfrak{r}}^N = (\vec{r}^N, \vec{\omega}^N)$	N -particle position-orientation vector
$\vec{\mathfrak{v}} = (\dot{\vec{r}}, \vec{\omega})$	translational-angular velocity vector
$\vec{\mathfrak{v}}^N = (\dot{\vec{r}}^N, \vec{\omega}^N)$	N -particle translational-angular velocity vector

Drift, diffusion, and friction tensors:

$\vec{B}_T(\phi)$	two-dimensional translational drift vector
$\vec{B}_R(\vec{\omega})$	three-dimensional rotational drift vector
$\vec{B}(\vec{\mathfrak{r}})$	six-dimensional translational-rotational drift vector
C_S	coupling tensor
$\vec{D}_C(\phi)$	coupling vector
$D_T(\phi)$	translational diffusion tensor
$\mathcal{D}(\vec{\mathfrak{r}})$	total 6×6 -dimensional diffusion tensor
$\mathcal{D}_N(\vec{\mathfrak{r}}^N)$	total $6N \times 6N$ -dimensional N -particle diffusion tensor
$\mathcal{H}, \tilde{\mathcal{H}}$	hydrodynamic coefficient matrices
K	translation tensor
Ω_S	rotation tensor
$\Upsilon_N(\vec{\mathfrak{r}}^N)$	$6N \times 6N$ -dimensional N -particle friction tensor

Functions and distributions:

$c^{(n)}(\vec{\mathfrak{r}}_1, \dots, \vec{\mathfrak{r}}_n)$	n -particle direct correlation function
$\delta(x)$	Dirac's delta distribution
$E(T, \psi)$	general thermodynamic potential
$\varepsilon(\vec{r}, t)$	generalized energy density
$\mathfrak{F}[f(\vec{x})](\vec{k}), \tilde{f}(\vec{k})$	Fourier transform of the function $f(\vec{x})$
$\mathfrak{F}^{-1}[\tilde{f}(\vec{k})](\vec{x}), f(\vec{x})$	inverse Fourier transform of the function $\tilde{f}(\vec{k})$

$P(\vec{\mathbf{x}}_1, \dots, \vec{\mathbf{x}}_n, t)$	n -particle probability density
$\mathbf{r}(\vec{r}, t)$	dissipation function
$\rho^{(n)}(\vec{\mathbf{x}}_1, \dots, \vec{\mathbf{x}}_n, t)$	n -particle number density
$U(\vec{\mathbf{x}}_1, \dots, \vec{\mathbf{x}}_N, t)$	total N -particle potential
$U_{\text{ext}}(\vec{\mathbf{x}}_1, \dots, \vec{\mathbf{x}}_N, t)$	total external potential
$U_{\text{int}}(\vec{\mathbf{x}}_1, \dots, \vec{\mathbf{x}}_N)$	total particle interaction potential
$U_1(\vec{\mathbf{x}}, t)$	one-particle external potential
$\bar{U}_1(\vec{\mathbf{x}})$	“substitute” one-particle external potential
$U_n(\vec{\mathbf{x}}_1, \dots, \vec{\mathbf{x}}_n)$	n -particle interaction potential
$Y_{lm}(\hat{u})$	spherical harmonic with indices l and m

Hydrodynamic currents and variables:

$c(\vec{r}, t)$	concentration
$\vec{g}(\vec{r}, t)$	density of translational momentum
$\vec{J}^{X_c}(\vec{r}, t)$	current associated with X_c
$\vec{J}_D^{X_c}(\vec{r}, t)$	dissipative current associated with X_c
$\vec{J}_R^{X_c}(\vec{r}, t)$	reversible current associated with X_c
$\mu(\vec{r}, t)$	chemical potential
$\mu_c(\vec{r}, t)$	relative chemical potential
$\Phi^{X_n}(\vec{r}, t)$	quasi-current associated with X_n
$\Phi_D^{X_n}(\vec{r}, t)$	dissipative quasi-current associated with X_n
$\Phi_R^{X_n}(\vec{r}, t)$	reversible quasi-current associated with X_n
$\rho(\vec{r}, t) \equiv \rho^{(1)}(\vec{r}, t)$	one-particle number density
$\sigma(\vec{r}, t)$	entropy density
$u(\vec{r}, t)$	scalar layer displacement
$\vec{v}(\vec{r}, t)$	velocity field
$X(\vec{r}, t)$	general hydrodynamic variable
$X_c(\vec{r}, t)$	general density of a conserved quantity
$X_n(\vec{r}, t)$	general density of a non-conserved quantity
$\delta X = X - X_0$	deviation of X from its equilibrium value X_0

Operators:

$\partial_i \equiv \frac{\partial}{\partial x_i}$	partial differentiation with respect to x_i
$\partial_{\vec{r}} = (\partial_1, \dots, \partial_d)$	translational derivation operator
$\partial_t \equiv \frac{\partial}{\partial t}$	partial differentiation with respect to t
$\partial_\phi \equiv \frac{\partial}{\partial \phi}, \partial_\theta \equiv \frac{\partial}{\partial \theta}, \partial_\chi \equiv \frac{\partial}{\partial \chi}$	partial angular differentiation
$\partial_{\vec{\omega}} = (\partial_\phi, \partial_\theta, \partial_\chi)$	angular derivation operator
$\partial_{\mathbf{r}_i} \equiv \frac{\partial}{\partial \mathbf{r}_i}$	partial differentiation with respect to \mathbf{r}_i
$\partial_{\vec{r}} = (\partial_{\vec{r}}, \partial_{\vec{\omega}})$	translational-angular derivation operator
\mathfrak{d}_i	i th element of $\vec{\nabla}_{\vec{r}}$
$\frac{\delta}{\delta f(x)}$	functional differentiation with respect to $f(x)$
$\vec{\nabla}_{\vec{r}} \equiv \partial_{\vec{r}}$	translational gradient operator
$\vec{\nabla}_{\vec{r}^N}$	N -particle translational gradient operator
$\vec{\nabla}_{\vec{\omega}} = i\hat{L}$	rotational gradient operator
$\vec{\nabla}_{\vec{\omega}^N}$	N -particle rotational gradient operator
$\vec{\nabla}_{\vec{r}} = (\vec{\nabla}_{\vec{r}}, \vec{\nabla}_{\vec{\omega}})$	translational-rotational gradient operator
$\vec{\nabla}_{\vec{r}^N} = (\vec{\nabla}_{\vec{r}^N}, \vec{\nabla}_{\vec{\omega}^N})$	N -particle translational-rotational gradient operator
$\Delta_{\vec{r}}$	translational Laplace operator
\hat{L}	angular momentum operator
$\hat{\mathcal{L}}$	Smoluchowski operator
$\int_{\mathcal{V}} dV$	spatial integration
$\int_{\mathcal{S}} d\Omega$	angular integration
$\int_{\mathcal{G}} d\mathfrak{X} = \int_{\mathcal{V}} dV \int_{\mathcal{S}} d\Omega$	spatial-angular integration
$\lambda_{\max}(\cdot)$	biggest eigenvalue
$\text{tr}(\cdot)$	trace
$\langle \cdot \rangle$	ensemble average or noise average
$ \cdot $	absolute value
$\ \cdot\ $	Euclidean norm

Order-parameter fields:

$\psi(\vec{r}, t)$	reduced translational density or arbitrary phase field
$\vec{P}(\vec{r}, t)$	local polarization

$S(\vec{r}, t)$	nematic order parameter
$\hat{n}(\vec{r}, t)$	nematic director
$Q(\vec{r}, t)$	nematic tensor

Parameters and constants:

α_c	critical exponent
A	surface of the two-dimensional domain \mathcal{A}
$\beta = 1/(k_B T)$	absolute or effective inverse thermal energy
d	number of spatial dimensions
e	elementary charge
E_c	characteristic energy
η	dynamic (shear) viscosity
F_c	characteristic force
$G \in \{A, V\}$	measure of the general domain \mathcal{G}
$\dot{\gamma}$	shear rate
Γ_c, Γ_n	mobility parameters
k	wave number
k_B	Boltzmann's constant
K_0	scalar parameter in a phase field model
K_1, K_2, K_3	Frank constants
l_c	characteristic length
λ_c	characteristic mean free path length
Λ	thermal de Broglie wavelength
m	topological winding number
Pe_r	rotational Péclet number
q	charge
$q_0, \varepsilon_0, \alpha_0$	parameters in the traditional PFC model
$\bar{\rho}$	reference particle number density
S	reference point
t_c	characteristic time
T	absolute or effective temperature

T_c	critical temperature
τ_c	characteristic collision time
V	volume of the three-dimensional domain \mathcal{V}

Rotation matrices:

$R_i(\varphi)$	i th elementary rotation matrix
$R(\vec{\omega})$	3×3 -dimensional rotation matrix
$\mathcal{R}(\vec{\omega})$	6×6 -dimensional block diagonal rotation matrix
$\mathcal{R}_N(\vec{\omega}^N)$	$6N \times 6N$ -dimensional block diagonal rotation matrix

Sets:

\mathcal{A}	two-dimensional spatial domain
$\mathcal{G} \in \{\mathcal{A}, \mathcal{V}\}$	general spatial domain
$\mathcal{G} = \mathcal{V} \times \mathcal{S}$	spatial-orientational domain
\mathcal{S}	domain for angular integration
\mathcal{S}_{d-1}	d -dimensional unit sphere
\mathcal{V}	three-dimensional spatial domain

Superscripts and overscripts:

M^{-1}	inverse of M
M^T	transpose of M
\dot{x}	time derivative of x
x'	rescaled or dimensionless form of x
\bar{x}	complex conjugate or substitute of x
\vec{x}	vector
\hat{x}	unit vector or operator
X^\natural	thermodynamic conjugate of X
X^\sharp	thermodynamic force associated with X

Thermodynamic functionals:

\mathcal{E}	general thermodynamic functional
\mathcal{F}	Helmholtz free-energy functional
\mathcal{F}_{id}	ideal gas free-energy functional
\mathcal{F}_{exc}	excess free-energy functional
\mathcal{F}_{ext}	external free-energy functional
Ω	grand canonical functional
\mathfrak{R}	dissipation functional

Further symbols:

\cdot	matrix product or scalar product
\times	cross product
\otimes	dyadic product
$*$	convolution
$\underline{\vee}$	exclusive OR
i	imaginary unit
$\mathbb{1}$	unit matrix
δ_{ij}	Kronecker delta symbol
ϵ_{ijk}	Levy-Civita symbol
$\text{diag}(\dots)$	diagonal matrix